# Evaluation of Novel Efflux Transport Inhibitor for the improvement of drug delivery through epithelial cell monolayer

Amit SONAWANE

Submitted for the Degree of

Doctor of Philosophy

Faculty of Life Sciences

University of Bradford

2015

# Abstract

Amit Sonawane

Evaluation of Novel Efflux Transport Inhibitor for the improvement of drug delivery through epithelial cell monolayer

**Keywords:** Galaxolide, P-Glycoprotein inhibition, permeability study, Blood-Brain Barrier, TEER, MDR

Blood-brain barrier (BBB) is a unique membranous barrier, which segregates brain from the circulating blood. It works as a physical and metabolic barrier between the central nervous system (CNS) and periphery. In mammals, endothelial cells were shown to be of BBB and are characterized by the tight junctions along with efflux system which are responsible for the restriction of movement of molecules within the cells. Efflux system consists of multidrug resistance proteins such as P-glycoprotein (P-gp). P-gp removes substances out back from the brain to the blood before they reach to the brain. So the barrier is impermeable to many compounds such as amino acids, ions, small peptides and proteins, making it the most challenging factor for the development of new drugs for targeting CNS.

Curcumin is a bioactive compound that has a number of health promoting benefits such as anti-inflammatory, anticancer, anti-oxidant agent; as well as a role in neurodegenerative diseases, but low oral bioavailability is the major limiting factor. Low water solubility and rapid metabolism are the two important factors responsible for poor bioavailability of curcumin. Galaxolide is a musk

compound and previously known for the bioaccumulation of toxic components in the aquatic animals by interference with the activity of multidrug/multixenobiotic resistance efflux transporters (MDR/MXR). The bioavailability of curcumin can be enhanced when administered with galaxolide.

This study was carried out to investigate the effect of galaxolide on the permeation of curcumin through the epithelial cell monolayers. MDCKII-MDR1 cell monolayer is used an *in vitro* blood-brain barrier model while Caco-2 monolayer is used as an *in vitro* intestinal model, which also expresses the P-glycoprotein. The curcumin and galaxolide were separately solubilised in the DMSO and used in combination to perform permeation study, to determine the effect of galaxolide on curcumin permeation through epithelial cell monolayers.

The galaxolide shows an efflux protein inhibition activity and this activity was used to enhance permeation of curcumin through the Caco-2 monolayer. In summary, galaxolide is a novel permeation enhancer molecule, which can be used for the improvement of drug delivery of other bioactive compounds in future.

# DEDICATED TO MY BELOVED MOTHER

## Who lived this dream with me...

# *Acknowledgement*

Finally, most awaited moment has arrived, where I am moving further toward completion of my PhD thesis and getting step closer to my dream which I've seen long ago. On the verge of completion of my PhD thesis, I now look back fondly towards all the hardship that has been a learning experience for me and have made me stronger and clear in thoughts. I would like to take an opportunity to humbly acknowledge and appreciate the efforts of all the people who have contributed in my research.

First of all, I take the foremost opportunity to express my gratitude to my respected supervisors ***Dr. Roger Phillips, Dr. Sriharsha Kantamneni and Prof. Anant Paradkar,*** who always boosted my morale with their excellent supervision, valuable guidance and encouragement and also in believing me throughout the course. I consider myself privileged to have worked under their guidance, as they always shared their vast experience generously and patiently in spite of their busy schedule. They also kept me motivating throughout my research work and their motivations helped me to overcome ups and downs I faced during work.

I would like to thanks my sponsor ***Department of Social Welfare, Govt. of Maharashtra (India)***, who supported me with providing funds to cover my tuition fees and personal expenses. Without their support, this journey would not be easy going.

I would specially like to thanks ***Dr. Simon Allison,*** who have helped me in my work unconditionally and made himself available for me whenever I needed

him. He has shared his vast experience of research with me and which has helped me a lot to improve my work.

It gives me immense pleasure to express my sincere gratitude towards ***Ratnadeep, Rohan, Hrushi, Rishi and CPES members*** as well as all ***ICT members*** for their all support. I also would like to thank my dearest friend ***Shrikant*** for his support on every stage.

I specially want to acknowledge and express my feelings for my ***MOTHER*** who lived this dream with me and blessed me with her good wishes and enthusiasm to see this work complete. She is the only person who supported me to complete my education and this PhD is a result of her support only and without her support, it would not be possible at all. I am gratified for her eternal love, trust and support which always has a positive influence on my performance and is a driving force towards my success.

I also would like to thanks all my family members, my brother ***Sumit*** who handled my family in my absence, my three sisters ***Bhramanti. Shital*** and ***Priya*** and their sweet naughty kids, for shading their unconditional love towards me, which gives me deep ecstasy and keeps me motivated towards my work. I also want to express my deep gratitude towards ***Prafulla*** and ***Apsari*** for being my family away from home and making me comfortable in absence of my loved ones.

Finally, who I have missed to acknowledge here, I want to thank all those for their direct or indirect contribution in my journey to achieve this goal.

# Table of Contents

# List of Figures

# List of Tables

# Glossary

| | | |
|---|---|---|
| µg | : | microgram |
| µl | : | microliter |
| µM | : | micro molar |
| ABC protein family | : | ATP-binding cassette superfamily |
| AD | : | Alzheimer’s disease |
| ADP | : | Adenosine diphosphate |
| ATP | : | Adenosine triphosphate |
| Aβ peptide | : | beta-amyloid peptide |
| BBB | : | Blood brain barrier |
| BBMEC | : | Bovine brain microvessel endothelial cells |
| BCRP | : | Breast cancer resistance protein |
| BD-Cur | : | Bisdemethoxycurcumin |
| BMVEC | : | Brain microvessel endothelial cells |
| BRCA1 | : | Breast cancer type 1 susceptibility protein |
| BSA | : | Bovine Serum Albumin |
| CAA | : | Cerebral amyloid angiopathy or Congophilic angiopathy |
| CNS | : | Central nervous system |
| CsA | : | Cyclosporine A |
| Cur | : | Curcumin |
| D-Cur | : | Demethoxycurcumin |
| DMEM | : | Dulbecco's Modified Eagle's medium |
| DMSO | : | Dimethyl sulfoxide |

| | | |
|---|---|---|
| DNA | : | Deoxyribose nucleic acid |
| ECM | : | Extracellular matrix |
| EMEM | : | Eagle's minimum essential medium |
| EMT | : | Epithelial-mesenchymal transition |
| FACS | : | Fluorescent activated cell sorting |
| FBA | : | Fetal Bovine Serum |
| FDA | : | U.S. Food and Drug Administration |
| Gal | : | Galaxolide |
| GLUT1 | : | Glucose transporter 1 |
| GUK | : | Guanyl kinase-like domain |
| HBSS | : | Hank's Balanced Salt Solution |
| HEPES | : | 2-[4-(2-hydroxyethyl) piperazin-1-yl]ethanesulfonic acid |
| HHCB | : | 1,3,4,6,7,8-hexahydro-4,6,6,7,8,8-hexamethylcyclopenta[g]-2-benzopyran |
| HPLC | : | High performance liquid chromatography |
| HRP | : | Horseradish peroxidase |
| HUVEC | : | Human umbilical vein endothelial cells |
| $IC_{50}$ | : | dose required to inhibit half the population of a tested cells *in vitro* after a specified test duration |
| IS | : | Internal standard |
| JAM | : | Junctional adhesion molecules |
| M'gel | : | Matrigel™ |
| MAGUK | : | Membrane-associated guanylate kinase-like proteins |
| MDCK | : | Madin-Darby canine kidney |

| | | |
|---|---|---|
| MDR | : | Multidrug resistance |
| mg | | milligram |
| Mini-Pgp | : | Mini P-glycoprotein |
| ml | | millilitre |
| MRP | : | Multidrug resistance-associated protein |
| MTT dye | : | Thiazolyl Blue Tetrazolium Bromide |
| MXR | : | Multixenobiotic resistance |
| NBD | : | Nucleotide binding domain |
| OD | : | Optical density |
| $P_{app}$ | : | Apparent permeability |
| PBMEC | : | Porcine brain microvessel endothelial cells |
| PBS | : | Phosphate Buffer Saline |
| PBST | : | PBS with o.1% Tween 20 |
| P-gp | : | P-glycoprotein |
| Pi | : | Inorganic phosphate |
| PI3K | : | Phosphatidylinositol 3-kinase |
| PIC | : | Protease Inhibitor Cocktail |
| PTEN | : | Phosphatase and tensin homolog |
| Rb | : | Retinoblastoma protein |
| Rh123 | : | Rhodamine 123 |
| RIPA buffer | : | Radio-immunoprecipitation assay buffer |
| RNA | : | Ribose nucleic acid |
| RPMI 1640 | : | Roswell Park Memorial Institute1640 |
| RT | : | Retention time |

| | | |
|---|---|---|
| Spgp | : | Sister P-glycoprotein |
| TCA cycle | : | Tricarboxylic acid cycle/ Citric acid cycle |
| TEER | : | Transendothelial electrical resistance |
| Temo | : | Temozolomide |
| TFA | : | Trifluoroacetic acid |
| TJ | : | Tight junction |
| TM | : | Transmembrane |
| TMD | : | Transmembrane domains |
| VEGF-A | : | Vascular endothelial growth factor-A |
| Ver | : | Verapamil |
| Vin | : | Vinblastine sulfate salt |
| WB | : | Western Blot |
| ZO | : | Zonula occludens proteins |

# 1 : Introduction

A number of mechanisms are available in a biological system to protect it from exposure to almost any foreign substance with exception to nutrient uptake. The physiological arrangement and the chemical and biochemical barriers associated with the physiological structures form the first line of defence. Any drug, delivered by any route, will almost certainly face some of these barriers before reaching their target site. The physicochemical and biochemical properties of the drug molecule determine its interaction with these barriers.

The body is protected against external invaders and toxins through number of biological barriers which are present in body. The blood-brain barrier (BBB) is one of such barrier that forms the tightest membrane and limits the entry of molecules from the bloodstream to the brain. Similarly, for the drug molecules to be orally bioavailable, another barrier is there called epithelial layers of gastrointestinal tract. It is necessary to breach these barriers for the successful delivery of drugs through the intestinal mucosa or the BBB. The hurdles to drug delivery can be categorized as physiological, biochemical, and chemical barriers. The physiological barrier in the intestinal mucosa or the blood-brain barrier protects the body from various molecules such as toxins, by inhibiting their passage through the barriers. Next obstacle is biochemical barrier that must be overcome by drug, which consists metabolizing enzymes that can degrade the drug molecules before reaching to its target site. Finally, the drug should have optimal physiochemical properties for its permeation across the biological barriers. Thus, these various factors have to be taken into account when designing drugs with improved absorption characteristics.

In order to achieve efficient treatments of central nervous system (CNS) cancers, it is necessary to transport therapeutic agents across the specialized

vascular system of the brain, the BBB. Transport across BBB presents challenges especially in case of brain tumours due to undefined nature of cerebrovascular system associated with cancer progression and development of biomarkers which can be coupled to therapeutic agents for targeted delivery but bypassing the resistance mechanism. A great deal of effort, therefore, is presently focused on improving CNS bioavailability, and tumours thereof, of therapeutic drugs that can be specifically targeted to diseased tissue, improving therapeutic opportunities, efficiency, and patient survival, while decreasing side-effects to normal cells. Various pharmacological agents have been used to open the BBB and direct invasive methods can introduce therapeutic agents into the brain substance. It is important to consider not only the net delivery of the agent to the CNS, but also the ability of the agent to access the relevant target site within the CNS. Major challenge in drug delivery is strong efflux mechanisms present at BBB as well as in cancer tissue. Drug permeation can be improved across BBB and in cancer tissues by suppression of these efflux transport systems.

Sufficient concentrations of therapeutic agents or xenobiotic compounds are needed at the site of action to show their pharmacological and toxicological actions. These compounds when in desired concentration can bind to the targeted receptor or enzymes and show their response. To achieve the desired response against the site of action, drug molecule need to cross the biological membranes which is an important determinant for absorption, distribution, elimination and therapeutic or toxic effects of drug molecules. Biological membranes are not just a lipid bilayer, but lipid bilayers with number of embedded proteins including various transporters. These transporters play an

important role to pass drug molecules through biological membranes along with physicochemical characteristics of drug. Numerous transporters are present in the biological membranes; amongst them a group is present called an efflux transporter. The group of efflux transporters includes mainly P-glycoprotein (Pgp, MDR1), multidrug resistance-associated proteins (MRPs) and breast cancer resistance proteins (BCRP). These proteins mainly involved in removal of wide range of molecules, which are structurally and functionally different, from the cells against a concentration gradient. These efflux proteins show their transport activity against number of anticancer agents which are clinically important, and prevent their intracellular accumulation which can lead to inappropriate cell killing and poor treatment, and this phenomenon known as “multidrug resistance” (MDR) and MDR is one of the major hurdle to achieve successful cancer chemotherapy (David R. Hipfner[1], 1999; Ira and Pastan, 1988; Pastan, 1993; T. Litmana et al., 2001). In reverse of this, these transporters could be beneficial and can improve the therapeutic efficacy of a particular drug molecule by improving poor bioavailability of some anticancer agents with inhibition of P-glycoprotein and other efflux proteins (Johan W. Jonker and Beijnen, 2000; Kimura et al., 2002; Kruijtzer et al., 2002). So if P-glycoprotein is inhibited by using various inhibitors, reversers or modulators; then it may increase the absorption of drug into the intestine and result into the high oral availability of particular drug molecule, which then lead to the successful chemotherapy (Robert and Jarry, 2003).

Cell based assays are necessary in pharmaceutical research to study the tissue permeability ability of lead drug molecules. These assays are widely used after primary screening of drug molecules with desired pharmacological properties

to identify drug properties with regards to the tissue permeability. These approaches with cell based assays are not only cost effective but it also minimizes use of animal sources. Various different cell lines and cell based assays are used in this study in order to achieve the desired outcome of study.

### 1.1 Galaxolide

Galaxolide or HHCB (1,3,4,6,7,8-hexahydro-4,6,6,7,8,8-hexamethylcyclopenta[g]-2-benzopyran) is an artificial polycyclic musk compound with a clean sweet musky floral woody odour used as fragrancing agent in huge extent for the preparation of number of personal care products such as cosmetics, perfumes, detergents, air freshener, cleaning agents, body lotions etc (Kannan et al., 2005) . Amongst all polycyclic musk compounds, galaxolide is one of the most widely used musk compound (Rimkus, 1999). According to some reports, it is cleared that the musk compounds accumulates in the aquatic animals including fish, mussels etc (Kannan et al., 2005), while some reports shown that the musk compounds were found in the human milk, human adipose tissues and blood plasma (Rimkus and Wolf, 1996). Excess use and bioaccumulation of these compounds raised the issues of toxicity on human and wild life.

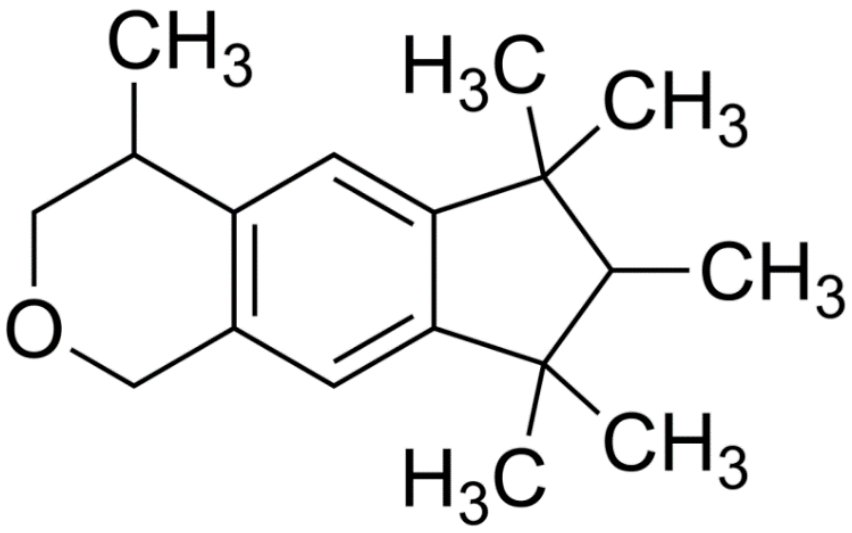


***Figure 1.1:Chemical Structure of HHCB (Galaxolide)***

The musk compounds are also responsible for the interference with activity of multidrug/multixenobiotic resistance efflux transporters (MDR/MXR) and it shows dominant activity against P-glycoprotein like transporters. The study on marine mussel *Mytilus californianus* shows that these musk compounds are responsible for inhibition of activity of efflux transporters and inhibitory effects of them lasts for about 24-48 hrs even after termination of exposure to these musks (Luckenbach and Epel, 2005). The MDR efflux transporters are referred as the first line of defense mechanism as they prevent bioaccumulation of toxic compounds inside the cells. So if these efflux transporters are inhibited, the sensitivity to toxic compounds which are normally excluded by cells increases and allow them to enter cells and accumulate (Epel, 1998). This property of the galaxolide can be useful in the drug therapy against the cells which show MDR; especially cancer cells which shows poor response to drugs.

## 1.2 Curcumin

Curcumin is the phenolic compound andprimarycurcuminoid of the Indian spice turmeric (*Curcuma longa*), found along with other two curcumionoids named demethoxycurcumin (D-Cur) and bisdemethoxycurcumin (BD-Cur) in the rhizome of plant.It is used as food additive in many Indian recipes. In addition to this, Curcumin has number of therapeutic effects as it acts as anti-inflammatory, anticancer, antioxidation, antimicrobial agent;along with these properties, curcumin also acts against neurodegenerative, cardiovascular, pulmonary, metabolic, autoimmune and neoplastic diseases (Aggarwal and Harikumar, 2009).

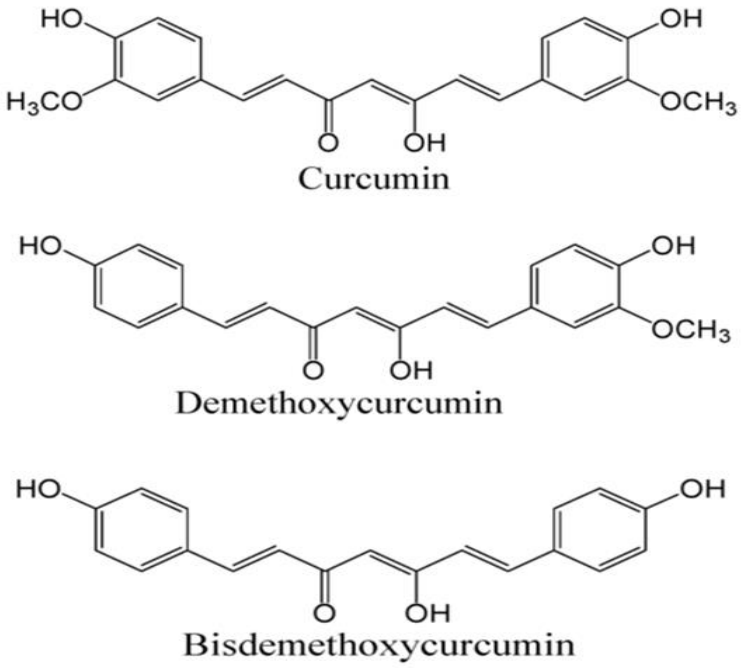


***Figure 1.2: Chemical structures of the three major curcuminoids***

*Curcumin, demethoxycurcumin (D-Cur) and bisdemethoxycurcumin (BD-Cur)*

The clinical trials on human have proved that it is safe to consume up to 8000mg curcumin per day, as it is well tolerated and have less adverse effect. Also *in vitro* studies shown that the curcumin has beneficial effects for humans in chemoprevention against colon cancer (Johnson and Mukhtar, 2007). Cancer is not a single disease as it is a combination of number of neoplastic disease; that is why it is hard to apply targeted drug therapies against it, so it needs combination of different targeted therapies. Curcumin is a compound which can act as anti-carcinogenic, antiangiogenic, immunomodulatory, proapoptotic and antioxidant agent which is effective against cancer as a potential drug (Hasima and Aggarwal, 2012). In addition with all these therapeutic effects curcumin has beneficial activity in Alzheimer's disease as it is the compound which has anti-amyloidogenic property (Ono et al., 2004). Alzheimer's disease is one of the growing disease worldwide in recent days and patients with it are increasing at high rate i.e. more than 35 million peoples are affected worldwide with Alzheimer's. The beta-amyloid (Aβ) peptide is one of the major marker of Alzheimer's disease which aggregates in the brain to form amyloid plaques (Selkoe, 2001). The Aβ peptide is responsible for the neurotoxicity by affecting membrane receptors and intracellular signalling (Behl and Moosmann, 2002).

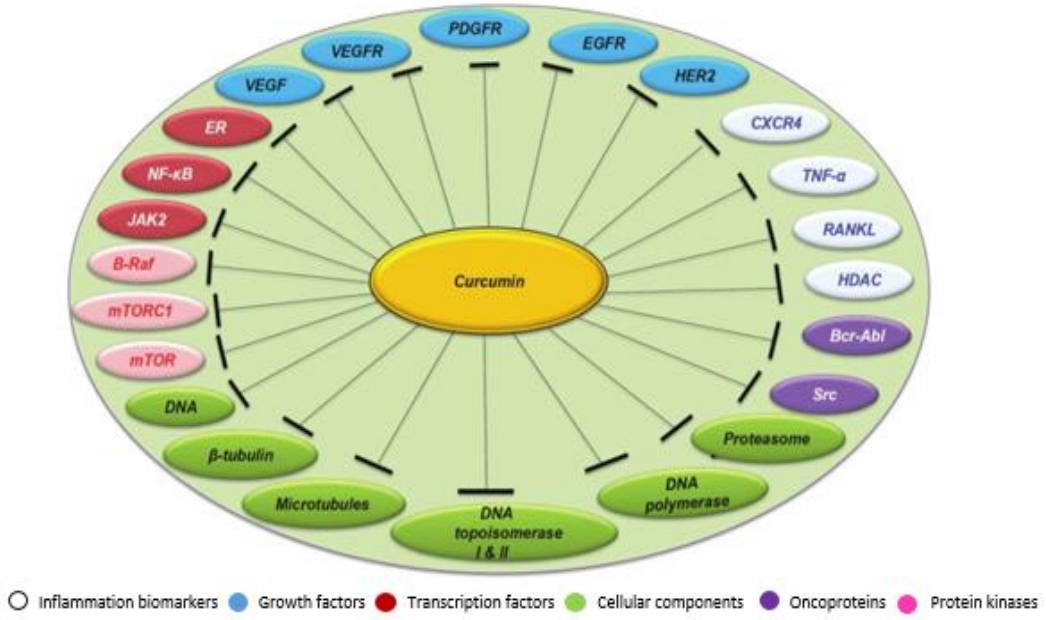


***Figure 1.3: Cancer targets with FDA approved drugs***

*Curcumin has therapeutic action against all those cancer targets, against which FDA has approved drugs (Hasima and Aggarwal, 2012)*

## 1.3 Outline of thesis

This thesis investigates the characteristics of galaxolide as a novel efflux inhibitor molecule. Galaxolide is a musk compound, widely used in the personal care products to add musk smell. Galaxolide is used as novel P-glycoprotein (P-gp) inhibitor throughout the study and administered in combination with drug molecules. The approach is to enhance the drug therapy to the cells which shows multidrug resistance, for example cancer cells and to pass the drug through biological membranes which expresses efflux proteins like P-gp and other proteins from efflux transporter protein family. The chapter-1 of thesis introduces the drug delivery approaches through intestinal barrier and blood-brain barrier (BBB) and then followed by the chapter-2 which describes

background, and focuses on brief introduction to the cancer physiology, Alzheimer's disease, structure of blood-brain barrier and *in vitro* models of blood-brain barrier. Chapter-3 describes aims and objectives of the study. Chapter-4 describes materials and methods used for this study. Chapter-5 focuses on the galaxolide toxicity on cells, P-gp expression and inhibition studies, while chapter-6 explains the results for development of HPLC methods and the permeability study of curcumin and effect of galaxolide on curcumin permeation. Chapter-7 explains the results and discussions for the histology studies and trans-epithelial electrical resistance (TEER). Also the chapter explains the effect of matrigel on histology of membranes. Finally, chapter-8 focusses on conclusions and future works and chapter-9 bibliography.

# 2 : Background

This chapter briefly introduces cancer disease, along with its hallmarks and also focuses on the Alzheimer's disease. The BBB and efflux system present within is the major obstacle during the treatment of brain cancer and Alzheimer's. This chapter later describes the structure of BBB and P-glycoprotein (P-gp). The P-gp is one of the key proteins present in BBB and responsible for the drug efflux from the brain to blood stream.

## 2.1 Cancer

Cancer is a condition where cells in a specific part of the body grow and reproduce uncontrollably. Unlike other diseases, cancer is not a result of single gene defect, so it is not a single disease; it is a group of number of neoplastic diseases, which is result of the misbehaviour of multiple cell signalling pathways (Vogelstein and Kinzler, 2004). Cancer is most harmful disease and is one of the most leading cause of mortality in all over the world (Kong et al., 2000). Now a days there are many advances in oncology; however, as per the World Health Organization within next two decades the chances of cancer incidence will be double than today.

Cancer is a disease of cell growth and division, where cells continue to grow and divide in an uncontrolled and indefinite manner. Normal cells have a wide number of internal defence mechanisms against becoming a cancerous cell, and so many changes need to occur before cell start to grow uncontrollably to form cancer. Douglas Hanahan and Robert Weinberg have been mentioned the six hallmarks of cancer which include sustaining proliferative signalling, evading growth suppressors, resisting cell death, enabling replicative immortality, inducing angiogenesis and activating invasion and metastasis (Hanahan and

Weinberg, 2000) later two more hallmarks mentioned by them as the result of conceptual progress in last few years, which are reprogramming of energy metabolism and evading immune destruction. The following Figure 2.1 shows the total 10 established hallmarks of cancer including six previous and two new emerging hallmarks with two enabling factors: inflammation and genomic instability (Hanahan and Weinberg, 2011).These hallmarks can provide useful framework of concept to understand the complex cancer biology.

### 2.1.1 Hallmarks of cancer

The earlier six hallmarks of cancer proposed by Hanahan and Weinberg are sustaining proliferative signaling, evading growth suppressors, resisting cell death, enabling replicative immortality, inducing angiogenesis and activating invasion and metastasis.


***Figure 2.1: Hallmarks of Cancer***

*The figure describes the total 10 hallmarks of cancer. Out of which six hallmarks are originally proposed in 2000 which includes sustaining proliferative signalling, evading growth suppressors, resisting cell death, enabling replicative immortality, inducing angiogenesis and activating invasion and metastasis; and recently two additional hallmarks are proposed; known as emerging hallmarks; which are reprogramming of energy metabolism and evading immune destruction; along with two enabling factors: inflammation and genetic instability (Hanahan and Weinberg, 2011)*

#### 2.1.1.1 Sustaining Proliferative Signalling

Growth signalling in normal cells is a highly regulated process wherein proliferative signals are activated whenever necessary and deactivated when no longer necessary; this tight regulation ensures cell homeostasis. However, in cancer cells this regulation is compromised. As a disease of uncontrolled cell division, cells must acquire the ability to continually grow in order to become cancerous. Cancer cells constitutively activate signalling pathways to become self-sufficient in providing their own growth signals, so that they are no longer dependent on external signals to prompt them to progress through the cell cycle. Cancers also become resistant to anti-growth signals, meaning they can ignore normal signalling that limits the growth of cells to prevent abnormal division. This ability to sustain chronic proliferation is one of the fundamental trait of cancer cells (Hanahan and Weinberg, 2000; Hanahan and Weinberg, 2011).There are several alternative ways through which cancer cells can sustain proliferative signalling which includes production of growth factor ligands by themselves so they can respond with expression of cognate receptors which then leads to autocrine proliferative stimulation. On the other hand cancer cells have ability to pass signals to stimulate normal cells which are present within the tumour associated stroma to reciprocate various growth factors to cancer cells (Bhowmick et al., 2004; Cheng et al., 2008). Along with these ways cancer cell can use other phenomenon as well to maintain its proliferative signalling like increasing the number of receptors on the cell surface, structurally altering receptors to facilitate cancer cell signalling, and activating proteins in the downstream signalling pathway (Hanahan and

Weinberg, 2011).Recent studies also highlight the ability of cancer cells to disrupt negative feedback loops that constitute a safety mechanism to dampen a signalling pathway whenever a mitogenic signal is hyper-activated. One key example of this is the RAS oncoprotein. Oncogenic activity of RAS is not the result of overactive RAS signalling but rather the disruption of normal negative feedback mechanisms operated by the oncogenic GTPase (Bardeesy and Sharpless, 2006). Other examples of this process include loss-of-function mutations in phosphatase and tensin homolog (PTEN), which amplify phosphatidylinositol 3-kinase (PI3K) signalling(Jiang and Liu, 2009; Yuan and Cantley, 2008).These are several ways through which cancer cells can sustain its proliferative signalling property.

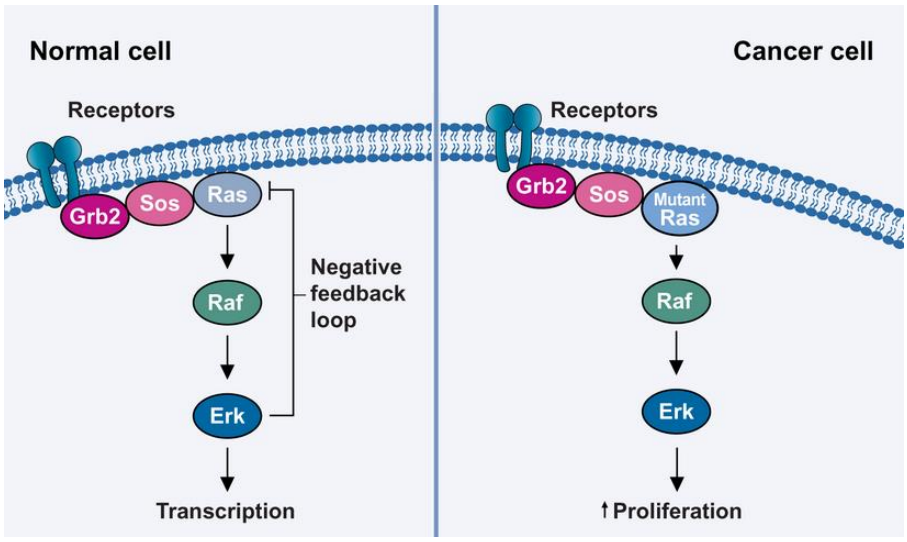


***Figure 2.2: RAS Signalling Pathway***

*Tumour cells disrupt negative feedback loops in the oncogenic RAS signaling pathway, leading to sustained proliferative signaling in tumour cells (Bardeesy and Sharpless, 2006)*

### 2.1.1.2 Evading Growth Suppressors

Cell proliferation in normal cells is a tightly controlled process wherein the pro- and anti-proliferation signals coordinate their activities at the cell cycle level. Particularly, the $G_1$phase of the cell cycle is a vital checkpoint wherein the antigrowth signals exert their influence to block cell proliferation (Ringshausen et al., 2006)

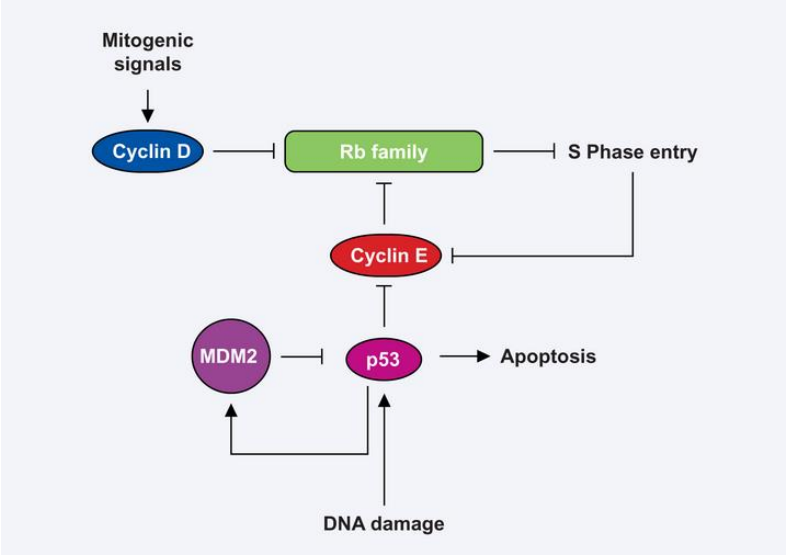


***Figure 2.3:RB and p53 Regulate Cell Cycle Checkpoint Controls***

*Rb and p53 are 2 common tumor suppressors that are inactivated in tumor cells, leading to uncontrolled growth and proliferation (Sherr, 2004)*

The two tumour suppressors most commonly dysregulated in cancer cells are retinoblastoma protein (Rb) and p53 and as a result of which cancer cell keeps proliferating without limits. In normal tissue, these proteins are part of a large network that controls the cell cycle. Rb actively inhibits cell passage through the restriction point in the $G_1$ cell cycle phase, while cancer cells with mutated Rb remove this gatekeeper and allow for ongoing cell proliferation. The p53

functions as a central regulator of apoptosis because it arrests the cell cycle in cells with DNA damage. Dysregulation of p53 allows for cell cycle progression despite DNA damage and cellular stresses.(Hanahan and Weinberg, 2011; Ringshausen et al., 2006).

#### 2.1.1.3 Resisting Cell Death

In case of aberrant and potentially cancerous growth signalling, normal cells activate programmed cell death called apoptosis. Apoptosis also activated in the situations like DNA damage and other cellular stresses, which can also be features of cancerous cells, and so apoptosis represents a crucial mechanism to avoid accumulation of damage and mutations that can culminate in cancer formation. Cancer cells acquire the ability to evade this induction of cell death, which is crucial for both maintaining tumour growth and allowing cancerous cells to form in the first stage of disease development. Cancer cells circumvent normal growth suppressors in order to continue proliferating. Apoptosis or programmed cell death is considered as the natural barrier for the cancer development (Adams and Cory, 2007). Apoptosis occurs through two pathways named the intrinsic and the extrinsic pathways. Intrinsic pathway or mitochondrial pathway is initiated by intracellular stresses, while the extrinsic or death-receptor pathway is initiated by engagement of cell surface receptors with specific ligands. Both pathways lead to the activation of proteases, caspases 8 and 9 respectively. These proteases then start proteolysis with the initiation of cascade and finally lead to the apoptosis. A cell then disassembles and engulfed by the neighbour cells and phagocytic cells. The intrinsic pathway may be important in cancer, as many of the cellular stresses encountered by

cancer cells are activators of the intrinsic pathway (Hanahan and Weinberg, 2011).The intrinsic pathway is tightly regulated by a group of related proteins called the BCL-2 family which consists. The BCL-2 family of proteins are known as important gatekeepers to the apoptotic response. This group of structurally related proteins consists pro-apoptotic (Bax and Bak) and anti-apoptotic (Bcl-xL, Bcl-w, Mcl-1, A1) members that interact with one another (Adams and Cory, 2007; Hanahan and Weinberg, 2011). Many cancers resist the apoptotic pathway with dysregulation of BCL-2 family members. Cancer cells are thought to achieve this through two main mechanisms: by a down-regulation of pro-apoptotic proteins, or by an increase in BCL-2 expression (Letai, 2008).

#### 2.1.1.4 Enabling Replicative Immortality

The cells growing in a culture generally have a finite potential of replication. Such cells after particular number of doublings, stop their growth and this stage is termed as senescence. This senescence can be reversed by disabling the tumour suppressor proteins like p53 and pRb, and cells are allowed to grow further for multiple generations until they reach to second phase called crisis. This stage is characterised by large number of cell deaths, karyotypic disarray which is associated with end-to-end fusion of chromosomes and occasionally emergence of variant cells, which has ability to multiply limitlessly, and the trait is termed as immortalization (Wright et al., 1989).Recently molecular cancer research has uncovered some additional functions of telomerase which are independent of telomere normal functions and may responsible for the tumour growth. These additional functions are Enhancement of cell proliferation and/or resistance to apoptosis (Kang et al., 2004), DNA damage repair

(Masutomi et al., 2005), RNA-dependent RNA polymerase function (Maida et al., 2009) and Association with chromatin (Masutomi et al., 2005; Park et al., 2009).

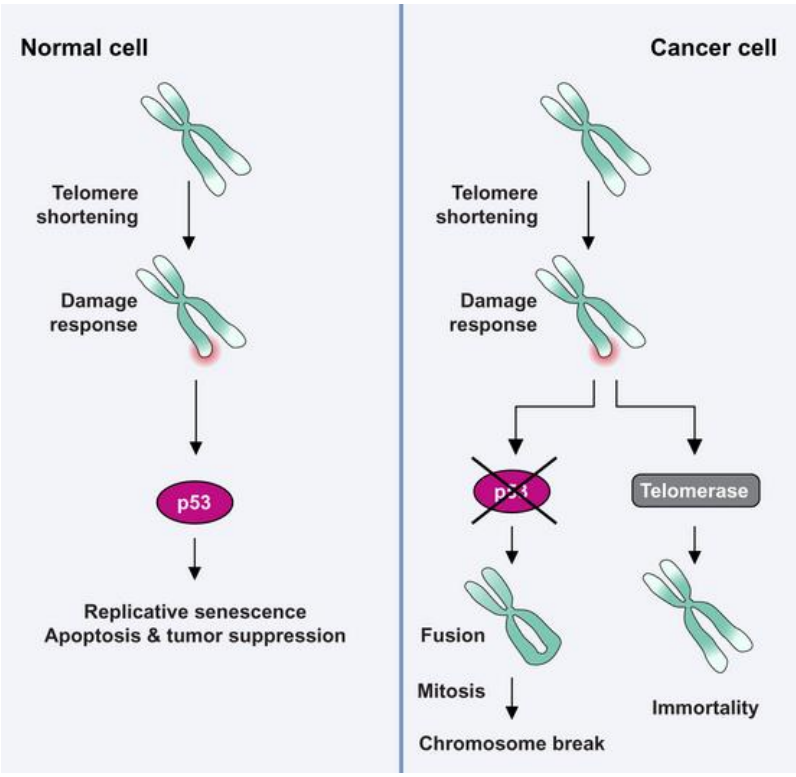


***Figure 2.4: Enabling replicative immortality***

*A shortening of telomere length activates replicative senescence in normal cells; however, tumour cells overcome the finite replicative ability by overexpressing telomerase, an enzyme that maintains telomere length (Artandi and DePinho, 2010)*

### 2.1.1.5 Inducing Angiogenesis

Like normal tissue, a tumour mass requires a blood supply. For a tumour to be able to grow it must induce the creation of its own blood supply. This process by which the host's normal blood supply is extended and grows into the tumour is called angiogenesis. In tumour cells, the process of angiogenesis, or the

formation of new blood vessels, is important for sustained tumour growth and metastasis. Tumour angiogenesis is a multistep process and involves signalling input from several pro-angiogenic growth factors (Bergers and Benjamin, 2003; Hicklin and Ellis, 2005).The tumour vasculature induction; the moment at which a tumour begins to overexpress pro-angiogenic factors like vascular endothelial growth factor-A (VEGF-A), is known as the “angiogenic switch (Bergers and Benjamin, 2003; Hanahan and Weinberg, 2011). Angiogenesis results in the delivery of oxygen and nutrients, and production of growth factors that benefit tumour cells which finally leads to the tumour expansion and local invasion. Recent studies also revealed that the two additional components have important roles in tumour neovasculature. First is pericytes, which are supporting cells associated in normal tissue vasculature. These pericytes, in recent studies have found that they are important for the tumour angiogenesis (Raza et al., 2010). Second component is bone marrow; the research also indicates that bone marrow derived cells may help to initiate the angiogenic switch (Hanahan and Weinberg, 2011).

#### 2.1.1.6 Activating Invasion and Metastasis

The mechanism of invasion and metastasis is not fully understood and it remained an unsolved mystery till date. Tissue invasion and metastasis are integral components in how tumour cells escape from the primary site and spreads into distant organs. In general, process of invasion and metastasis involves changes in the cell-cell/matrix attachment by alteration in gene expressions encoded for corresponding proteins like E-cadherin. The progression of invasion and metastasis is inversely proportional to E-cadherin

expression (Hanahan and Weinberg, 2011).Invasion and metastasis is basically a complex process. This process of invasion and metastasis has several steps like Local tissue invasion, Intravasation, Transition through the blood and lymphatic system and Colonization of foreign tissue. This multistep process of invasion and metastasis is often termed as invasion-metastasis cascade (Fidler, 2003; Talmadge and Fidler, 2010). This cascade begins with the changes in the biology of cells occurred due to the 'invasion' which then followed with the 'intravasation' by cancer cell into the blood and lymph vessels located in the vicinity of cancer cells. These cells then transported through lymphatic and hematogenous systems to the various parts located apart and finally these cells were escaped from these vessels and the process is reverse to the intravasation and named as 'extravasation'. After escape from the lumina of the vessels, these cells forms small cancerous nodules termed as 'micro-metastasis', and finally these micrometastatic lesions grown into the macroscopic tumours and this step is known as the 'colonization' (Hanahan and Weinberg, 2011).

### 2.1.2 Emerging hallmarks and enabling characteristics

Apart from these earlier six hallmarks, the recent research studies reveals two new emerging hallmarks; reprogramming of energy metabolism and evading immune destruction; which are responsible for the progression of cancer pathogenesis in almost all types of cancer. Along with new emerging hallmarks, two enabling characteristics of cancer are also revealed; inflammation and genomic instability; which were described below.

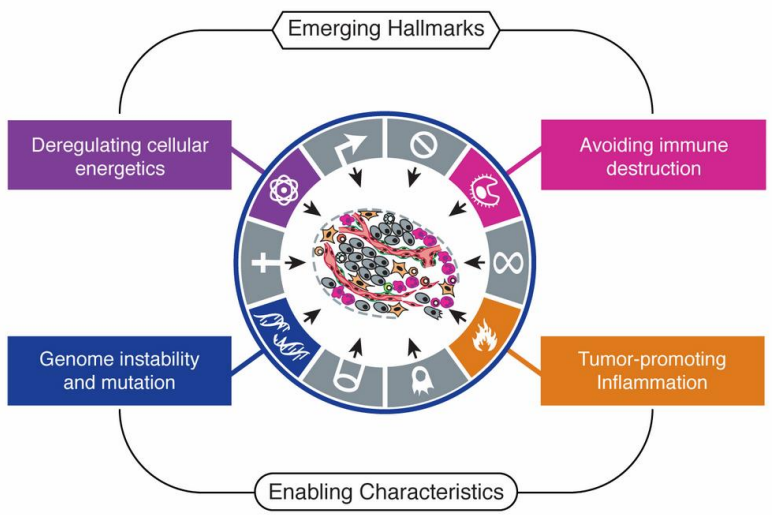


***Figure 2.5: Emerging hallmarks and enabling characters***

*Image present two new hallmarks of cancer – reprogramming of energy metabolism and evasion of immune destruction – that have emerged as critical capabilities of cancer cells and two "enabling characteristics" - properties of neoplastic cells that facilitate acquisition of hallmark capabilities - that include genome instability/mutation and tumour-promoting inflammation (Hanahan and Weinberg, 2011)*

#### 2.1.2.1 Emerging Hallmark-1: Reprogramming of energy metabolism

Reprogramming energy metabolism has been identified as an emerging hallmark of cancer. To maintain uncontrolled cell division and proliferation, cancer cells needs more energy and to get that required energy cancer cells make alterations in energy production programme as per their need. These alterations were done in various means like, reprogramming their glucose metabolism, upregulating glucose transporters such as glucose transporter 1 (GLUT1) and Depending on alternate metabolic pathways. Normal cells, in aerobic conditions metabolise glucose first to the pyruvate and this process takes place in cytosol, and then formed pyruvate transported to the mitochondria to follow TCA cycle to generate energy, while in anaerobic conditions cells prefer glycolysis for energy production. But cancer cells behave in strange way to produce their energy, as they re-programme their glucose metabolism for energy production and remains depend on glycolysis even in presence of oxygen. This kind of glycolysis is termed as ‘aerobic glycolysis. This reprogramming of energy metabolism by cancer cells is low efficient process as compared to the mitochondrial phosphorylation, and is supported by the glycolysis. Cancer cells does this by increasing the glucose intake to the cancer cells and the glucose intake is increased by upregulation of glucose transporter 1 (GLUT 1). Cancer cells splits available glucose to lactate irrespective of the availability of oxygen (the Warburg effect), and diverts glucose metabolites to useful anabolic processes that accelerate cell proliferation (DeBerardinis et al., 2008; Hanahan and Weinberg, 2011; Hsu and Sabatini, 2008; Jones and Thompson, 2009; Marie and Shinjo, 2011).

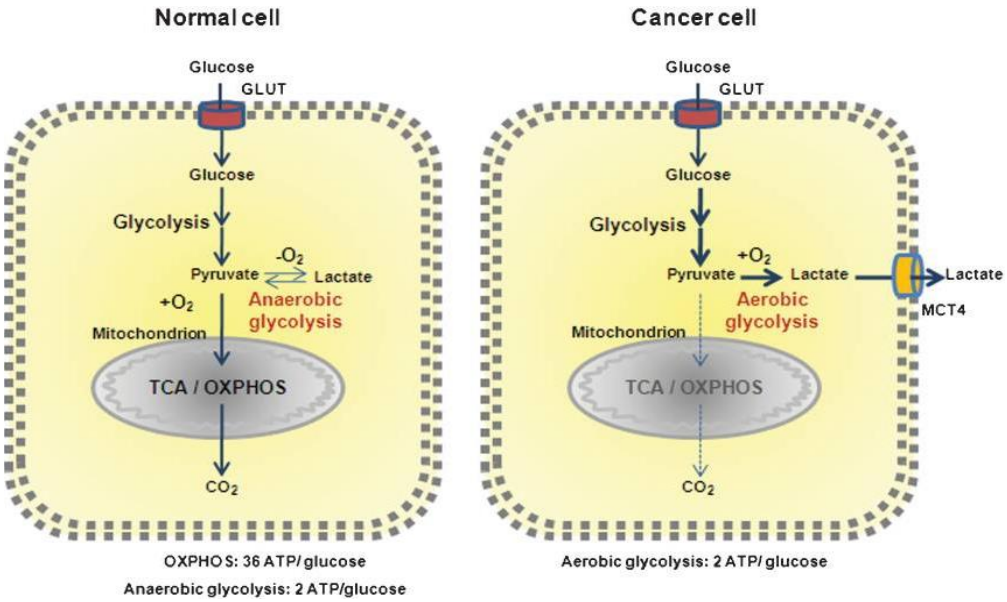


***Figure 2.6: The Warburg effect***

*Cancer cells convert available glucose to lactate irrespective of the availability of oxygen (the Warburg effect), thereby diverting glucose metabolites to useful anabolic processes that accelerate cell proliferation (Marie and Shinjo, 2011)*

#### 2.1.2.2 Emerging Hallmark-2: Evading Immune Destruction

Cells have immune system to protect themselves from almost all types of external harms. Immune surveillance is an essential cellular process that actively prevents tumour formation in the human body. Preclinical studies have suggested that an active immune system continuously recognizes and eliminates the vast majority of cancer cells before they establish themselves and form a tumour mass. The process is known as immunoediting. However, cancer immunoediting includes 3 key phases: elimination, equilibrium, and escape.

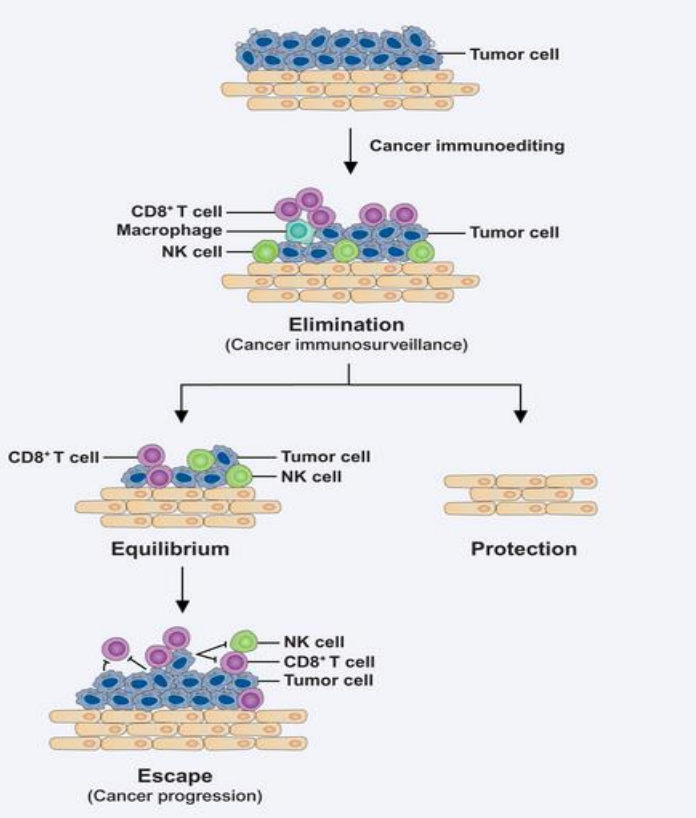


***Figure 2.7: Cancer Immunoediting: Elimination, Equilibrium and Escape***

*Cancer immunoediting, an emerging hallmark, comprises 3 key phases elimination, equilibrium, and escape. Cancer cells that successfully navigate these phases acquire the ability to evade immune destruction (Prendergast, 2008)*

The immune system successfully recognizes and eliminates cancer cells, a process often described as the elimination phase. During the elimination phase, some weakly immunogenic cells remain un-eliminated and eventually turns into solid tumours and such tumour cells, remained un-eliminated by the immune system proceed to the equilibrium phase, in which the immune system controls cancer cell growth but does not completely eliminate the transformed cells. Tumour cells not susceptible to immune destruction enters into the escape

phase. In this phase, the “escaped” tumour clones; cells which are not effectively detected and destroyed by the immune system; continue to divide and grow (Hanahan and Weinberg, 2011; Prendergast, 2008; Teng et al., 2008).

#### 2.1.2.3 Enabling characteristics-1: Genome Instability and Mutation

All above mentioned hallmarks are acquired by the tumour cells and are somewhere interlinked and depended on the genome alterations. Multiple alterations in the genomes of cancer cells serve as the platform for many oncogenic processes. Cancer cells take advantage of increased rates of mutations in order to accumulate several mutations needed to boost tumorigenesis. Cancer cells does this with several ways including; increased sensitivity to mutagenic agents, breakdown in one or more of the cell’s DNA repair mechanisms mediated by genes such as p53 or breast cancer type 1 susceptibility protein (*BRCA1*) and/or a combination of these factors. Accumulation of these mutations is accelerated by altering DNA-maintenance machinery-termed as “caretaker” of genomes (Kinzler and Vogelstein, 1997). These caretakers were involved in the processes like detecting DNA damage and activating repair machinery, directly repairing damaged DNA, inactivating or intercepting mutagenic molecules. Tumour cells can inactivate or suppress these caretaker genes and increase the rate of mutations and tumorigenesis. Studies on cancer cell genome also explores that that the genetic instability increases tumour progression (Hanahan and Weinberg, 2011).

#### 2.1.2.4 Enabling characteristics-2: Tumour promoting inflammation

The tumour microenvironment is densely infiltrated by innate and adaptive immune system cells that enable tumours to mimic inflammatory conditions seen in normal tissues (Dvorak, 1986). Current studies in molecular cancer research reveals that this tumour-associated inflammation might have role in tumour growth. Studies also indicates that tumour-associated inflammation may play role in tumour growth by supplying the tumour microenvironment with various components like growth factors, survival factors, pro-angiogenic factors, extracellular matrix (ECM)–modifying enzymes that promote angiogenesis, invasion, and metastasis and inductive signals that activate epithelial-mesenchymal transition (EMT) and other hallmark-facilitating mechanisms (DeNardo et al., 2010; Grivennikov et al., 2010; Qian and Pollard, 2010). Above all, inflammation is seen in early stages of neoplastic disease. Early inflammation can release chemicals into the tumour microenvironment and may lead to genetic mutations that enable and accelerate the formation of a tumour (Hanahan and Weinberg, 2011).

Cancer is caused by many more dysregulated genes which occur over a long period before emerging its symptoms. So targeting any single gene is not of any use while developing drug against cancer. However some targeted drugs and chemotherapies are developed which are effective against these gene products or pathways. But there are also some limitations like drug resistance and ineffective targeting which effects on efficacy of these therapies (Vogelstein and Kinzler, 2004). So an approach of combination chemotherapy should be the next paradigm against cancer. It includes targeting multiple gene targets by

the combination of several drugs or the single drug which can modulate multiple targets (Aschele et al., 2002). For the treatment of various types of cancer U.S. Food and Drug Administration (FDA) have been approved many different drugs which can able to modulate multiple targets. However these drugs have higher costs and number of undesirable side effects and even though they are not effective enough (Hasima and Aggarwal, 2012). The major problem associated with failure of chemotherapy in cancer is MDR caused by the membrane transporter P-gp molecules. In humans P-gp is encoded by the MDR1 genes and is expressed at high level in cancer cells. So MDR is the most accepted reason responsible for the chemo resistance in cancer treatment (El-Readi et al., 2010; Huang et al., 2012; Sui et al., 2012; Thomas and Coley, 2003).

Before the modern era of chemotherapy the natural sources of drugs were used for the treatment and prevention of cancer for the centuries. The drugs derived from natural sources are not fully understood for their mechanism of action against particular target, however according to some estimates about 80% of today's anticancer drugs have roots from natural products (Hasima and Aggarwal, 2012).

## 2.2 Alzheimer's disease

Alzheimer's disease (AD) is a chronic neurodegenerative disease which leads to progressive loss of memory and other cognitive functions. Alzheimer's accounts for 60-70% of cases of dementia. Alzheimer's is a progressive condition that means the symptoms develop gradually and becomes more severe over the time. Alzheimer's disease is one of the growing diseases worldwide and in recent days number of patients diagnosed is increasing due to increased aging population. Alzheimer's has a higher risk in older age, as severity of symptoms doubles every 5 years after age of 65 (Hirtz et al., 2007). The most common symptoms of Alzheimer's are difficulty in remembering recent events i.e short term memory loss, problems with language, disorientation, mood swing loss of motivation etc. The symptoms lead to death after 3 to 9 years of diagnosis of Alzheimer's.

The beta-amyloid (Aβ) peptide is one of the major marker of Alzheimer's disease which aggregates in the brain to form amyloid plaques (Figure 2.8). The Aβ peptide is responsible for the neurotoxicity by affecting membrane receptors and intracellular signalling (Behl and Moosmann, 2002; Selkoe, 2001). Aβ peptides are the natural metabolites consists 36-43 amino acids in their structure. These peptides spontaneously aggregate and form a deposits of amyloid plaques in brain parenchyma and cerebral blood vessels. These plaques are termed as congophilic angiopathy or cerebral amyloid angiopathy (CAA). The Aβ peptide self-aggregates in various physiological structures; some aggregates as small oligomers which consists 2 to 6 peptides, while some forms fibril structure and arrange themselves in β-pleated sheets. The β-pleated

sheets are advance form of amyloid plaques and are insoluble fibres. Besides this, other symptoms are also occurred in Alzheimer's like loss of neurons and white matter, inflammation and oxidative damage (Anand et al., 2014; Querfurth and LaFerla, 2010).

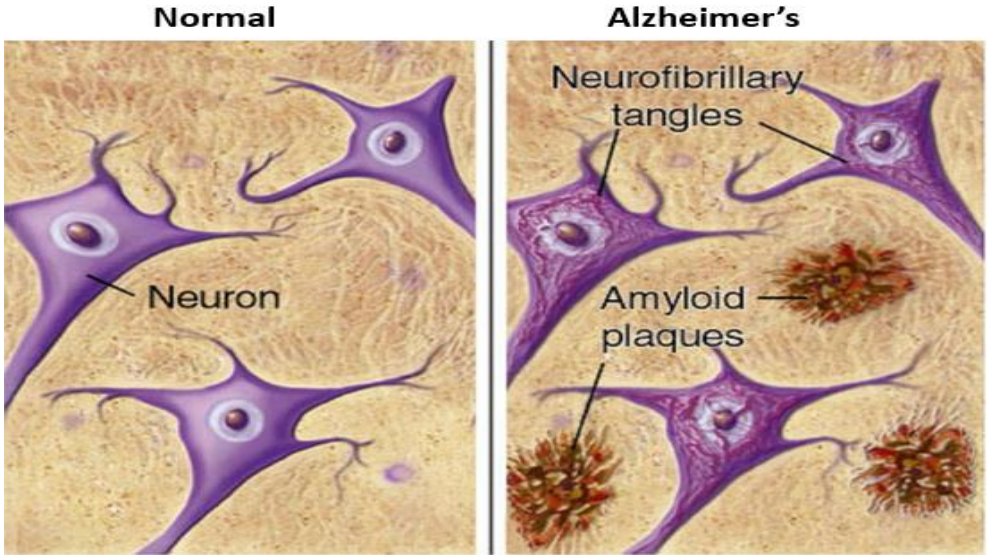


***Figure 2.8: Plaques and Tangles in Alzheimer's***

*Image showing the pathological characteristics of Alzheimer's disease: beta-amyloid (Aβ) peptide; which aggregates in the brain to form amyloid plaques and Neurofibrillary tangles (Image courtesy : http://www.brightfocus.org/alzheimers)*

Neurofibrillary tangles (Figure 2.8) are another major marker of Alzheimer's. These tangles are occurred in Alzheimer's disease and other neurodegenerative diseases. These are filamentous inclusions present in the pyramidal neurons and termed as the tauopathies (Lee et al., 2001). The tangles serve as the pathologic markers of the severity of disease, as the high number of tangles represents the more severe the disease. These tangles are formed by the hyper-phosphorylated 'Tau' proteins aggregates (Figure 2.9).

‘Tau’ proteins are present in high numbers in the neurons and are less common in other parts of the body. These proteins have a role to stabilize microtubules. The ‘Tau’ protein, due to several mutations in genes goes under hyper-phosphorylation. These hyper-phosphorylated proteins lack the affinity towards the microtubules and self-associate to form double helix structures (Iqbal et al., 2005). Like Aβ peptide, aggregated tangles of ‘Tau’ proteins are also cytotoxic and can impair cognition (Khlistunova et al., 2006; Querfurth and LaFerla, 2010; Santacruz et al., 2005).

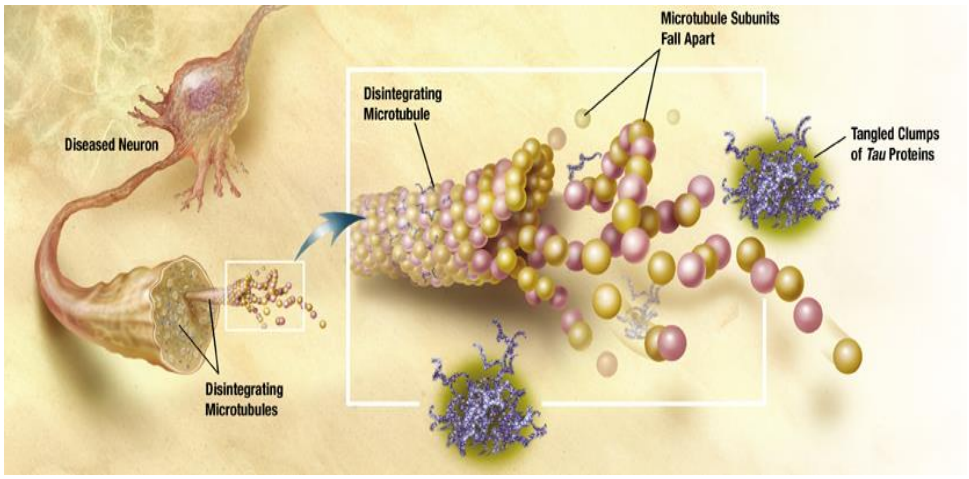


***Figure 2.9: Tau Protein Tangles***

*In Alzheimer’s disease, changes in tau protein lead to the disintegration of microtubules in brain cells (Rodgers, Anne B. 2002).*

FDA currently approved the drugs for the treatment of the Alzheimer’s diseases which includes acetylcholine esterase inhibitors. The drug inhibits the enzyme acetylcholine esterase and increases the level of neurotransmitter acetylcholine, which seems to have depleted in the Alzheimer’s brain. Besides these, there are several other targeting sites for the treatment of Alzheimer’s disease which includes the targeting of Aβ peptide targeting of ‘tau’ proteins,

as these are the major biomarkers of Alzheimer's and causes the cellular deaths in brain which results in the neurotoxicity. Along with these clinical targets, several other targets are also taken into consideration to treat Alzheimer's like targeting ApoE4, other approaches like application of antioxidants, anti-inflammatory drugs or mitochondrial protectors, because there are several evidences available in Alzheimer's like oxidative damage, inflammation and mitochondrial impairment (Cummings, 2004; Huang and Mucke, 2012).

## 2.3 Blood-Brain Barrier (BBB)

The Brain is separated from the blood circulation by the membranous barrier; this physiological barrier is known as the Blood-brain barrier (BBB). The BBB plays the dual function as barrier and carrier. The barrier can protect brain from the harmful toxic substances which can be present in blood circulation by preventing their entry to the brain and the carrier function allows the useful substances like nutrients to enter inside the brain and removal of metabolites (Sloan et al., 2012; Wilhelm et al., 2011). The BBB is the major obstacle in drug development as it provides poor permeability for drug candidates by preventing them to penetrate into the brain and it is the main problem faced by pharmaceutical industries (Terasaki et al., 2003).

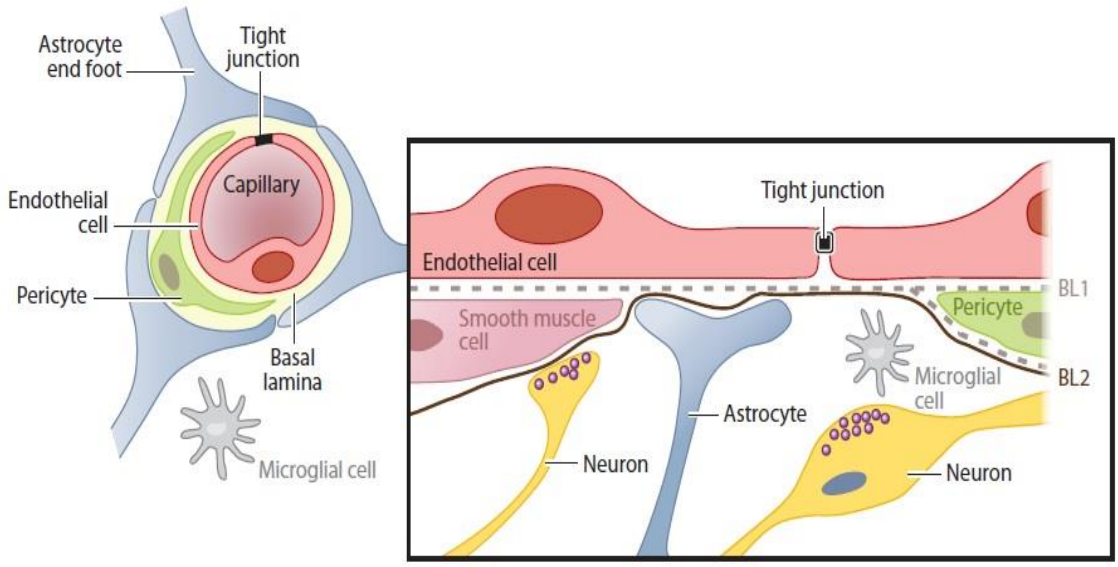


***Figure 2.10:The three cell model of blood-brain barrier***

*The cells; endothelial cell, pericyte and astrocyte end foot; that are involved in structure of blood-brain barrier (Sloan et al., 2012)*

### 2.3.1 Structure of Blood Brain Barrier

The BBB is mainly composed of endothelial cells, astrocytes and pericytes. Other cell components like neurons and microglia are also important elements in the function of BBB (Hawkins and Davis, 2005). The Figure 2.10 shows the three cell model of the brain vasculature. The endothelial cell located at the centre and regulates the BBB permeability. It shares close relationship with other two cells; pericyte and astrocyte end foot. Pericyte shares the common basement membrane with the endothelial cell. The pericyte is phagocytic cell and there is approximately one pericyte for every three endothelial cells. About 99% of the brain surface of the capillary basement membrane is covered by the astrocyte end foots (Pardridge, 1999).

Brain microvessel endothelial cells (BMVEC) are the major components of the BBB. These endothelial cells are tightly connected to each other, and this junction is known as Tight junction (TJ) (Liu et al., 2012). The tight junctions are made up of with combination of transmembrane proteins and cytoplasmic accessory proteins. Specialized transmembrane proteins like claudin, occluding, cadherins and junctional adhesion molecules (JAM) which hold endothelial cells together. Cytoplasmic accessory proteins like ZO-1, ZO-2, ZO-3, cingulin and others form a bonding with actin-membrane protein, which provides the primary cytoskeleton to endothelial cells for their structural and functional integrity (Ballabh et al., 2004; Liu et al., 2012). Measurement of trans endothelial electrical resistance (TEER) can be used for the evaluation of the tightness of these junctions (Sloan et al., 2012).

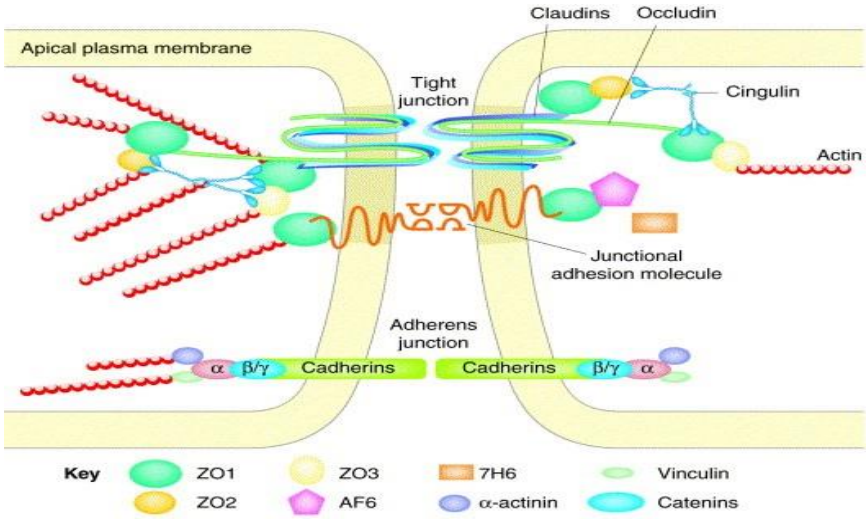


***Figure 2.11: Schematic representation of proteins involved in tight junction (TJ) formation in blood-brain barrier***

*Interaction of proteins associated with the tight junction in blood-brain barrier. Occludin, claudin, junctional adhesion molecules and cadherins are transmembrane proteins while others; ZOs, 7H6; are cytoplasmic proteins. Actin is membrane protein which forms a primary cytoskeleton of cells (Huber et al., 2001)*

The Figure 2.11 shows an interaction of proteins associated with the tight junction in BBB. Occludin, claudin, junctional adhesion molecules and cadherins are transmembrane proteins while others are cytoplasmic proteins. Actin is membrane protein which forms a primary cytoskeleton of cells.

### 2.3.2 Tight Junction (TJ) Proteins

Tight junctions are complex combination of the transmembrane proteins and cytoplasmic accessory proteins. These proteins links to actin-based cytoskeleton to form seal between two cells. These tight junctions are mainly formed with three integral proteins; claudin, occludin and junctional adhesion

molecules (JAM) (Gonzalez-Mariscal et al., 2003; Huber et al., 2001; Liu et al., 2012)

#### 2.3.2.1 Occludin

Amongst all these transmembrane proteins, Occludin is the first identified protein in the TJ having molecular weight about 60-65kDa. Occludin has both the terminus; N-terminus and C-terminus located intracellular and it consists of four transmembrane domains, two extracellular domains and three cytoplasmic domains (Feldman et al., 2005). Two occluding molecules from adjacent cells form a dimer by binding with each other. Occludin shows a unique characteristic compared to other transmembrane proteins that it binds 150 amino acid sequence in the C-terminus to F-actin. The C-terminus of occludin is also binds to the cytoskeleton localized in cell membrane through the cytoplasmic proteins like zona occludens (ZOs). The GK domain of ZOs involved in this binding with C-terminus of occludin (Gonzalez-Mariscal et al., 2003).

#### 2.3.2.2 Claudins

Claudins are a protein family having 24 different proteins with molecular weight ranging from about 20 to 24 kDa. Like occludins claudins also has four transmembrane domain, two extracellular domains and a short intracellular carboxyl chain (Gonzalez-Mariscal et al., 2003). Similar to occludins; claudins extracellular domains form homotypical dimmer with adjacent endothelial cells and forms backbone of TJ (Huber et al., 2001). Claudins binds to the PDZ domain of ZOs with the help of C-terminus of their intracellular domains. However claudins and occludin has many similar characters, claudins are not homologous to occludin in sequence (Liu et al., 2012). There are various

claudins found in brain endothelial cells like Claudin-1, claudin-2, claudin-3, claudin-5, claudin-11 and claudin-12 (Huber et al., 2001; Romanitan et al., 2010; Sandoval and Witt, 2008). Claudin-5 is considered as hallmark of BBB, and in CNS angiogenesis it plays an important role in earlier stages (Tam and Watts, 2010). Claudin-5 is expressed in almost all segments of brain endothelial cells, also in the blood vessels of kidney and lungs (Liu et al., 2012).

#### 2.3.2.3 Junctional Adhesion Molecules (JAM)

The junctional adhesion molecules (JAM) are the recently identified protein amongst transmembrane proteins involved in the tight junctions. JAM is glycosylated protein with molecular weight 45kDa, which found in epithelial cells and endothelial cells. JAM has three different structural domains which consists extracellular region having 215 amino acid sequence with two variable type Ig domains, one transmembrane domain and a single intracellular tail having 45 amino acids in it; the tail links with the type-II PDZ binding motif (Gonzalez-Mariscal et al., 2003; Martin-Padura et al., 1998). JAM belongs to the immunoglobulin superfamily which has the single transmembrane domain with two immunoglobulin like loops and these loops are formed by disulfide bonds (Ballabh et al., 2004). Besides tight junctions, JAM shows several other cellular functions like leukocyte transmigration, platelet activation, angiogenesis and virus binding (Bradfield et al., 2007; Mandell and Parkos, 2005).

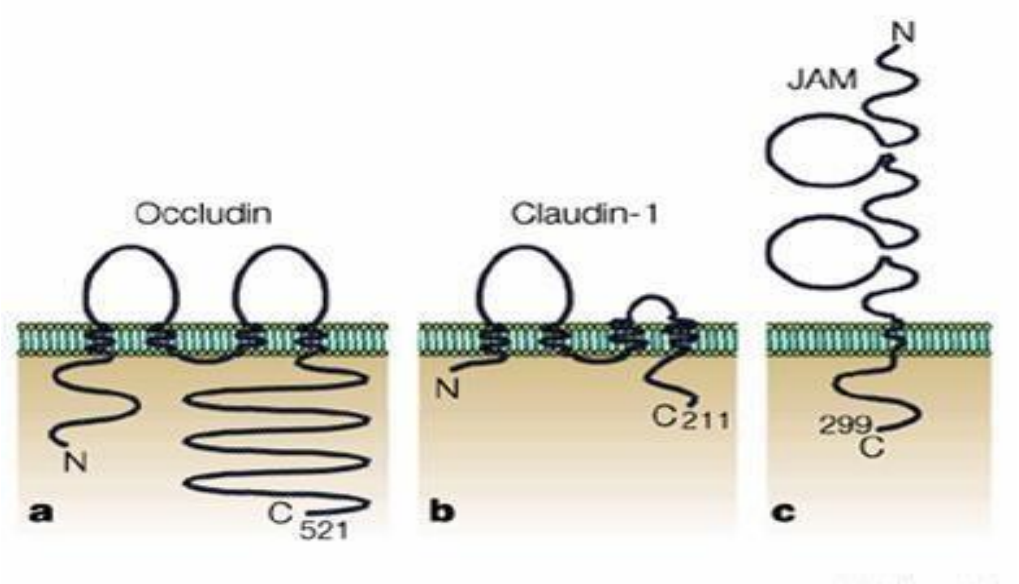


***Figure 2.12:Schematic representation of Structural arrangement of transmembrane proteins present in TJ***

***a) Occludin b) Claudin-1 and c) JAM***

*a )Occludin has four transmembrane domains with two extracellular loops. b) Claudin-1 also has four transmembrane domains, but shows no sequence similarity to occludin. Note that the cytoplasmic tail of claudin-1 is shorter than that of occludin. c) Junctional adhesion molecule (JAM) has a single transmembrane domain, and its extracellular portion bears two immunoglobulin-like loops that are formed by disulphide bonds (Tsukita et al., 2001).*

### 2.3.2.4 Cytoplasmic Accessory Proteins

Cytoplasmic accessory proteins including Zonula Occludins proteins (ZO-1, ZO-2 and ZO-3), Cingulin, 7H6 and several others are involved in the formation of TJ. The ZOs are belongs to the membrane-associated guanylate kinase-like proteins (MAGUKs) family having sequence similarity with each other. The molecular weights of ZOs are like ZO-1 220kDa, ZO-2 160kDa and ZO-3 130kDa. The ZOs contains three PDZ domains includes PDZ1, PDZ2 and

PDZ3, one SH3 domain and one guanyl kinase-like (GUK) domain. The domains are act as protein binding molecules and help to organize proteins at the plasma membrane (Ballabh et al., 2004). PDZ-1 domain of ZOs directly binds to claudins through COOH-terminal (Itoh et al., 1999) and occludins are linked through GUK domain of ZO-1 (Mitic et al., 2000) while JAM binds directly to ZO-1 and other PDZ containing proteins (Ebnet et al., 2000). Actin, the primary skeleton protein is also binds to the ZO-1 and ZO-2 through their COOH-terminal forming a complex cross-links transmembrane elements which gives structural support to the endothelial cells (Haskins et al., 1998).

### 2.3.3 Blood Brain Barrier Transport Mechanism

The endothelial cells present in BBB are very different from the one which are present in peripheral blood vessels. As described earlier the endothelial cells present in BBB contains TJ which allow the entry to very few small hydrophilic molecules such as ethanol or mannitol and restrict large number of compounds to enter inside the brain. The membrane has highly negative charge, so generally anionic compounds are removed from the site (Abbott et al., 2008; Sloan et al., 2012).

However there are number of restrictions to enter the BBB, most molecules could transported through the BBB by using one of the mechanisms described below (Abbott et al., 2008).

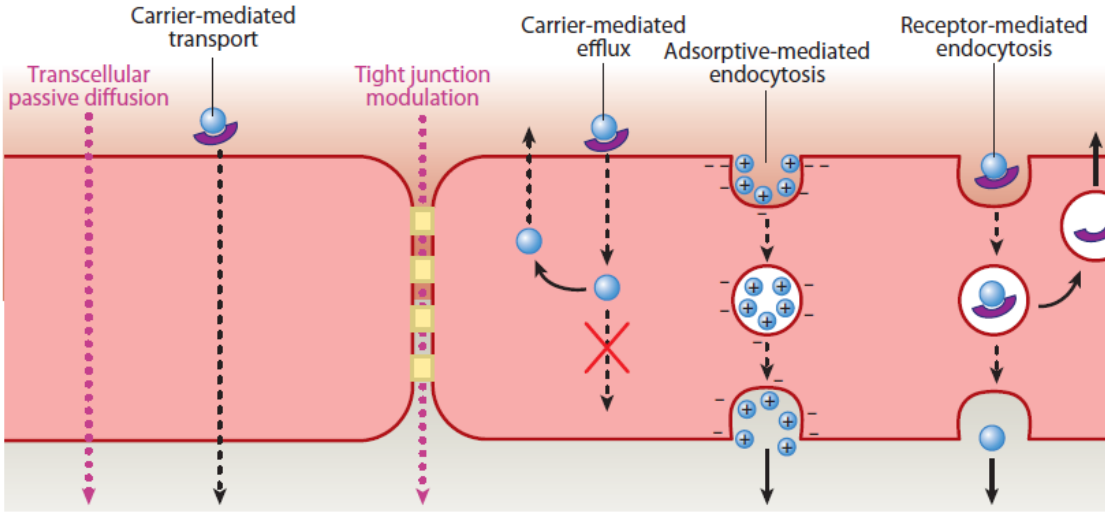


***Figure 2.13:Blood brain barrier transport mechanism***

*Schematic representation of blood-brain transport mechanisms available for the molecules to cross the barrier. Small, lipid-soluble substrates are able to diffuse across the membrane passively (transcellular passive diffusion) but active efflux system may remove back some of them into the circulation (carrier mediated efflux). Small hydrophilic substances may pass through the tight junctions either by experimental manipulation or by opening paracellular pathways (tight junction modulation). Small endogenous molecules, including amino acids, nucleosides, and glucose, are transported across the blood-brain barrier by transport proteins (carrier-mediated transport). Endogenous large plasma proteins, including albumin, are transported across the blood-brain barrier by adsorptive-mediated endocytosis. Larger molecules, including insulin and transferrin, are recognized by receptors on the luminal side of the endothelium and are transported across the cell for release into the brain parenchyma (receptor-mediated endocytosis) (Abbott et al., 2008; Sloan et al., 2012).*

#### 2.3.3.1 Transcellular Passive Diffusion

This transport mechanism can include the passive diffusion of small sized lipophilic compounds across the endothelial membrane. More the compound is lipophilic, greater the ability for permeation and vice versa. Acetaminophen and fluoxetine are the examples of the compounds which are transported by this mechanism (Abbott et al., 2008; Sloan et al., 2012).

#### 2.3.3.2 Carrier-Mediated Transport

Numbers of carrier transporters are used to transport the molecules across the BBB. Generally essential polar molecules such as amino acids, nucleoside, peptide, vitamin and glucose transporters are transported into the brain by this mechanism. Some neurotransmitters like dopamine and serotonin are unable to cross the barrier, so in such case precursors of them levodopa and tryptophan can be transported into the brain by this mechanism (Abbott et al., 2008; Sloan et al., 2012).

#### 2.3.3.3 Receptor-Mediated Endocytosis

This is the most common method and generally used for transport of large molecules like peptides and proteins. The molecules are bind to the receptors present on membrane and then entered into the membrane by the process of endocytosis. Insulin, transferring, cytokines and other large peptides are the examples of the molecules transported by this approach (Abbott et al., 2008; Sloan et al., 2012).

#### 2.3.3.4 Adsorptive-Mediated Endocytosis

The BBB is highly anionic in character so the cationic molecules are adsorbed to it non-specifically. Once the molecules adsorbed to the membrane they undergo endocytosis. This type of transport mechanism has higher capacity as compared to the receptor-mediated endocytosis. The example of the molecules transported by this type of transport mechanism includes the highly positively charged molecules like histones, cationized albumin, and arginine-containing peptides (Abbott et al., 2008; Sloan et al., 2012).

#### 2.3.3.5 Transport by TJ Modulation

Generally, TJs present in the endothelial cells at the BBB are very protective against transport of molecules. They restrict the entry of even highly hydrophilic compounds through BBB via paracellular diffusion. However, if the TJs are disrupted, the molecules which would be excluded normally can make the entry across the BBB. Such changes in the resistance of the TJs are usually occurred by the disease or the drug administration, which can disrupt the protein which are involved in the TJ formation. Experimentally, the administration of hyperosmolar solutions like 25% mannitol can disrupt the TJs. The cells undergo shrinking which may open the TJs due to the high ionic strength when such solution is applied. For brain tumour treatment, this method is employed clinically. TJs can also modified by the leukocytes and immune cells to cross the BBB via transcellular mechanism. In case of ischemia or brain trauma the TJs can also change their properties.

Along with all these transport mechanisms present at the BBB which transports the substances from blood to brain, there is efflux mechanism located which

removes the substances back in to the blood from the endothelial cells before they reach to the brain. In case of attempting drug delivery to the brain, these carrier-mediated efflux mechanisms provide a great challenge to the scientists working in pharmaceutical area. The carrier-mediated efflux system at the BBB includes the multidrug resistance proteins such as P-glycoprotein (P-gp) (Abbott et al., 2008; Sloan et al., 2012).

When it comes to drug permeability, efflux transporter proteins play an important role in permeation of drugs through the blood-brain barrier. This is because large number of drug molecules are substrates of the ABC transporters (efflux transporters) and because of that drug molecules get interacted with these efflux transporters and cannot reach to their targets in required concentrations (Wilhelm et al., 2011).

## 2.4 In vitro Blood-Brain Barrier Models

As seen in section (2.3.1), blood-brain barrier is a very tight membrane which allows only specific components to pass through it depending on their different biochemical characteristics. This property of blood-brain barrier is very important and can be taken into consideration during the drug delivery to the CNS through blood-brain barrier. Besides the drug delivery, some scientific and industrial interests towards the blood-brain barrier with regards to its physiology and pathology results in the development of number of *in vitro* blood-brain barrier. Some widely used *in vitro* BBB models are described below. Cell culture models are widely used as primary screening tools for the BBB drug permeability (Sloan et al., 2012).

To mimic *in vitro* blood-brain barrier, there are few basic characteristics and requirements and any *in vitro* model need to achieve maximum of these characteristics and requirements to get acceptable *in vitro* blood-brain barrier model. These characteristics and requirements are described in following Table 2.1 (Reichel et al., 2003)

***Table 2.1: Basic Characteristics and Requirements in vitro BBB model*** *(Reichel et al., 2003)*

| **Characteristics** | **Specific requirement for *in vitro* blood-brain barrier** |
|---|---|
| Restricted paracellular Pathway | TEER ≥ 2KΩ $cm^2$(despite this ideal TEER value, TEER value minimum of more than 150-200 Ω $cm^2$ accepted for permeability studies through *in vitro* BBB)<br>Low paracellular permeability |
| Brain capillary endothelial cell characteristics | Morphology, endothelial cell and BBB markers, enzyme expression |
| Functional expression of BBB-specific transport mechanisms | Nutrient transfer (glucose and L-amino acid ), efflux pumps (P-gp, BCRP), receptors (insulin), low leukocyte adherence |
| *In vivo* like modulation | Permeability altered by bradykinin, interleukins, glial factors, dexamethasone |
| Practicality | Availability, convenience, predictability and reproducibility |

### 2.4.1 *In vitro* Blood-brain barrier models from cells of non-cerebral origin

Number of publications are available which shows that the cells from non-cerebral origin have been used as an *in vitro* blood-brain barrier. Cells like MDCK (Madin-Darby Canine Kidney) are one of the most widely used cell line as an *in vitro* model to carry out permeability studies across blood-brain barrier. This cell line have relatively faster growth and may form cell monolayer in shorter time to mimic blood-brain barrier. These cells shows similarities with TJ present in the brain endothelial cells and forms the intact cell membrane. Despite this, there are some differences in TJ proteins of MDCK cells and brain endothelial cells. Claudine-1 is prominent protein in MDCK cells while Claudine-5 is major in brain endothelial cells, also brain endothelial cells lack the ZO-3 proteins, as it does not express it (Wilhelm et al., 2011). Blood-brain barrier shows the presence of efflux transporter proteins in its structure. The transfected MDCK cells with MDR1 genes; the genes encoding for the efflux protein, P-glycoprotein (P-gp overexpressing MDCK cells) are widely used as *in vitro* blood-brain barrier for permeability screening (Wang et al., 2005). The disadvantage over this cells is, these are from canine origin and not from the human. Even though the cell lines is not from human origin, the P-gp overexpressing MDCK cells (MDCK-MDR1) are considered as one of the best *in vitro* blood-brain barrier for the permeability studies from non-cerebral origin (Nicolazzo et al., 2006; Wang et al., 2005).

Human umbilical vein endothelial cells (HUVECs) is another cell line from non-cerebral origin, which is used as *in vitro* blood-brain barrier. This cell line is derived from the human origin (Langford et al., 2005). In some studies. Caco-2

cells are also used as an *in vitro* blood-brain barrier for the estimation of permeability studies. But recent studies shown that the Caco-2 forms a poor blood-brain barrier model (Lundquist et al., 2002; Nicolazzo et al., 2006)

### 2.4.2 *In vitro* Blood-brain barrier models from origin of cerebral endothelial cells

Primary brain capillary endothelial cells are used as *in vitro* blood-brain barrier models. These cells provides the close resemblance with the *in vivo* blood-brain barrier phenotype (Lundquist et al., 2002). To obtain these brain capillary endothelial cells, sources like bovine, porcine, rat or humans are generally used. Bovine brain microvessel endothelial cells (BBMECs) and porcine brain microvessel endothelial cells (PBMECs) are most commonly used models for the blood-brain barrier transport studies by the researchers as a primary cell models (Gumbleton and Audus, 2001). These endothelial cell culture models have characteristics of blood-brain barrier to express efflux transporter proteins such as P-glycoprotein, which is one of the common hurdle during the treatment of anticancer drugs in brain cancers (Sloan et al., 2012).

Other endothelial cell lines used as an *in vitro* blood-brain barrier is RBE4 cell line, which is obtained from the rat brain endothelial cells and transfected with the plasmid having E1A genes (Roux et al., 1994). RBE4 cell lines shows characteristics of blood-brain barrier like expression of P-glycoproteins, gamma-glutamyl transpeptidase activity and high alkaline phosphatase activity. The cell line is used to study signalling characteristics of brain endothelial cell and also used to study P-glycoprotein regulation (Wilhelm et al., 2011). hCMEC/D3 is another cell line and is one of the best characterised human cell

line used as an *in vitro* blood-brain barrier. The cell line shows the expression of junctional proteins as well as expression of efflux transporter proteins (Weksler et al., 2005).

Brain endothelial cells play the central role in the formation of blood-brain barrier and is a major component of the barrier as well. Along with endothelial cells, other cells such as pericytes, glial cells and neurons have regulatory roles to maintain blood-brain barrier (Deli et al., 2005). Co-culture of these cells with endothelial cells are used to form *in vitro* blood-brain barrier. The co-culture of glial cells and endothelial cells are used to obtain *in vitro* blood-brain barrier. The endothelial cells used to co-culture are the primary cultures of rat, bovine or mouse origin, or sometimes cell lines are also used. Similarly, the glial cells obtained from the primary cells or in some cases C6 cell lines are also used. The blood-brain barrier obtained from co-culture of endothelial cells and glial cells is one of the widely accepted *in vitro* blood-brain barrier (Wilhelm et al., 2011).

Co-culture of endothelial cells with pericytes are also used to obtain *in vitro* blood-brain barrier. Pericytes remain in close contact with the endothelial cells, because of that they are used to get co-culture models for the *in vitro* blood-brain barrier. These co-culture models shows the high trans epithelial electric resistance (TEER) and also they shows the expression efflux transporters. Other cells like neurons are also used to co-culture with endothelial cells to get blood-brain barrier models. To achieve blood-brain barrier properties in endothelial cells, either differentiating embryonic neural progenitor cells or mature neurons are used (Weidenfeller et al., 2007; Wilhelm et al., 2011).

## 2.5 P-Glycoprotein (P-gp)

P-glycoprotein is a transporter protein and belongs to the ATP-binding cassette (ABC) superfamily which has been described as a as sensitive tissues protected by it from toxic substances and at same time, on the other hand in cancer cells it shows MDR which prevent effective chemotherapy (Sharom, 2008). P-glycoprotein (Pgp, ABCB1) is a membrane protein plays an important role in the removal of toxic compounds from the cells by its efflux mechanism, which confers the multidrug resistance (MDR) to the cells (Loo et al., 2012). The ATP-binding cassette (ABC) family of transport proteins is one of the biggest protein families found in the living organisms (Dean and Annilo, 2005; Dean et al., 2001). The ABC protein family consists large number of membrane proteins which transports wide variety of substrates like sugars, amino acids, drugs, antibiotic, toxins, peptides, nucleotides, ions across the plasma membrane and this transport is energy driven as ABC protein binds to ATP molecule to carry out transport (Dean et al., 2001; Sharom, 2008).

### 2.5.1 Structure of P-Glycoprotein (Pgp)

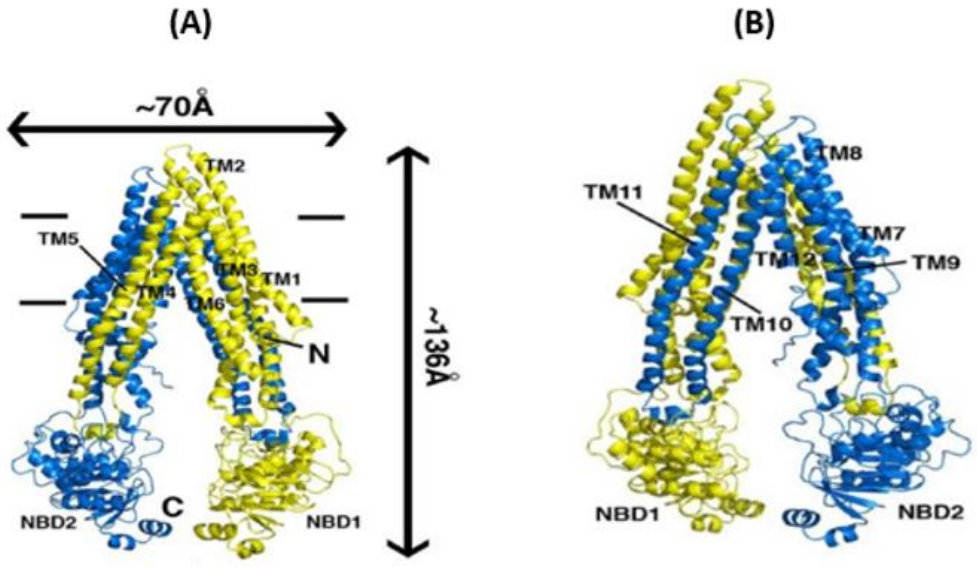


***Figure 2.14: Stereo structure of P-Glycoprotein***

*(A) Front View(B) Back View*

*The N- and C-terminal half of the molecule is coloured yellow and blue respectively. TMs 4 and 5 and TMs 10 and 11 crossover to form intertwined interfaces that stabilize the inward-facing conformation. Horizontal bars represents the approximate positioning of the lipid bilayer. The N- and C- termini are labelled in (A). Transmembrane (TM) domains and nucleotide binding domain (NBDs) are also labelled (Aller et al., 2009).*

The Figure 2.14 shows the stereo structures of Pgp from both front and back view. The Pgp consists of two membrane bound domains, each made up of six transmembrane (TM) helices and two cytoplasmic nucleotide binding (NB) domains. The Pgp structure has inward facing conformation and is achieved by the two bundles of transmembrane (TM) helices, forming the large cavity open to the cytoplasm. The cytoplasmic nucleotide binding domains are separated by ~30$A^0$ and are involved in the binding and hydrolysis of ATP (Aller et al.,

2009). There are three highly conserved sequence motifs; Walker A, Walker B and signature C motifs; present in nucleotide binding domains (NBDs) of all ABC proteins which play an important role in the process of ATP binding and hydrolysis. Signature C motif is unique to the ABC superfamily while Walker A and Walker B motifs are present in most of the protein molecules. The Walker A and Walker B motifs of one NBD and the LSGGQ Signature C motif from the partner NBD subunit together form the ATP binding site. So at the dimer interface of NBD, two molecules of ATP are bound and the structure is known to be a “sandwich dimer” (Sharom, 2008). This “sandwich dimer” is able to form a stable structure when inactivation of ATPase activity of the protein conferred by mutation (Hanekop et al., 2006; Smith et al., 2002). So it seems that in the catalytic cycle of ABC proteins these NBD dimerization process has important role (Sharom, 2008).

### 2.5.2 Cellular localization of P-glycoprotein (Pgp)

Studies on human and rodents have been shown that the P-glycoprotein is expressed in most of the cells at the very low level but the epithelial cells of colon, small intestine, bile and kidney tubules, adrenal glands shows the higher expression of Pgp at their apical region, it means the epithelial cells which play role in the excretory function generally express the Pgp (Croop et al., 1989; Thiebaut et al., 1987). The Pgp transporter is also expressed at the endothelial cells of blood-brain barrier (Beaulieu et al., 1997), blood-testes barrier (Melaine et al., 2002), blood-mammary tissue barrier (Edwards et al., 2005) and in the endothelial cells of the cochlea and vestibule in the blood-inner ear barrier (Saito et al., 1997). So the Pgp plays an important role of protection in human

physiology as it protects susceptible organs like brain, testes, inner ear from the toxic compounds. Pgp has a broad range of substrates and is recognizes the compounds having smallest size 330Da up to the larger molecules with 4000Da (Lam et al., 2001; Ramachandra et al., 1998). Most of the Pgp substrate molecules are hydrophobic in nature, and that is why Pgp is considered as “molecular hydrophobic vacuum cleaner” which removes substrates from the membrane and expels them out to confer MDR (Aller et al., 2009; Raviv et al., 1990). The Pgp has been considered as “double-edged sword” as it protects sensitive tissues from the toxic substances and on the other hand at the same time it causes MDR to prevent chemotherapy treatment in tumours (Sharom, 2008).

### 2.5.3 Mechanism of action of P-glycoprotein (Pgp)

The mechanism of action of P-gp in not revealed fully yet. Many important aspects like stoichiometric coupling between movement of drug molecule and the hydrolysis of ATP are still remains as a mystery. However some studies on the transport mechanism of P-gp shows that the drug transport is carried out by the two cycles, which are interconnected to each other (Callaghan et al., 2006). The first is catalytic cycle, which involves the hydrolysis of ATP which is useful for driving the transport. And the second cycle is substrate transport cycle, which carries the translocation of the drug molecule to the extracellular side of the membrane from the cytoplasmic side (Sharom, 2008).

### 2.5.3.1 The transport cycle of P-glycoprotein

Transport cycle of P-gp consists the hydrolysis of ATP molecule by catalytic cycle and the movement of drug-substrate molecule to the extracellular side. Assumption by Higgins and Linton says that the affinity for the ATP molecule has been increased by the drug-substrate binding, as drug binding lowers the activation energy required for the formation of closed NBD dimer (Ambudkar et al., 2006). In the catalytic cycle ATP molecules are bound with low affinity to the both NBDs (Sharom, 2008). Each NBD contains Walker A, Walker B and Signature C motif. Binding of ATP leads to the formation of 'sandwich dimer' between two NBDs (Janas et al., 2003), in which walker A and Walker B motif of one NBD binds with the signature C motif of partner NBD and vice versa. Due to the close association of NBDs and the formation of dimer, the two catalytic sites are formed within the dimer, to which two ATP molecules were bound. There are two mechanisms were proposed for the study of catalytic cycle of ATP as 'processive clamp' mechanism and 'alternating catalytic' site mechanism.

#### 2.5.3.1.1 Processive Clamp Mechanism

The 'processive clamp mechanism' model is shown in Figure 2.15, which proposes that the hydrolysis of both the ATP molecules were takes place in a succession which leads to formation and release of ADP and Pi. As shown in given diagrammatic model, in *step-1* two ATP molecules are bound to both NBDs which lead to the formation of the dimer complex as shown *step-2*. After the formation of dimer, ATP hydrolysis starts by the first NBD shown in *step-3*, which either release the first Pi followed by the hydrolysis of second ATP on the

other NBD to release second Pi shown in *step-4,5 and 8*; or as shown in *step-6,7,and 8*, the second ATP is hydrolysed before release of Pi and then both phosphates are released. Once the both ATP molecules were hydrolysed to ADP and Pi, both phosphates are released from the dimer, which leads to the dissociation of dimer complex and as a result of which, ADP molecules are released as shown in *step-9 and 10*. The both NBDs are now free again to start new catalytic cycle on binding with ATPs (Janas et al., 2003).

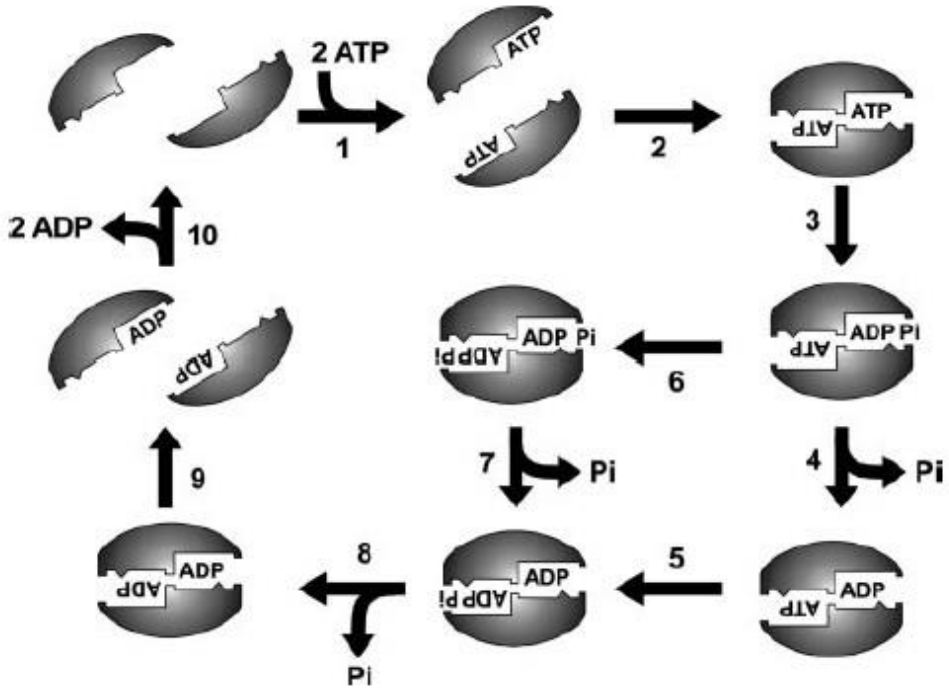


***Figure 2.15:Processive clamp model for the ATPase cycle of the NBD of ABC transporter***

*Step-1 two ATP molecules are bound to both NBDs which lead to the formation of the dimer complex as shown step-2. After the formation of dimer, ATP hydrolysis starts by the first NBD shown in step-3, which either release the first Pi followed by the hydrolysis of second ATP on the other NBD to release second Pi shown in step-4,5 and 8; or as shown in step-6,7,and 8, the second ATP is hydrolysed before release of Pi and then both phosphates are released. Once the both ATP molecules were hydrolyzed to ADP and Pi, both phosphates are released from the dimer, which leads to the dissociation of dimer complex and as a result of which, ADP molecules are released as shown in step-9 and 10. The both NBDs are now free again to start new catalytic cycle on binding with ATPs (Janas et al., 2003)*

### 2.5.3.1.2 Alternating catalytic site mechanism

The diagrammatic model (Figure 2.16) shows the alternating catalytic site cycle of ATP hydrolysis. Two P-gp transmembrane domains (TMDs) represented by the rectangles, while circle, square and the hexagon represents the different conformational structures of N- and C-catalytic sites.

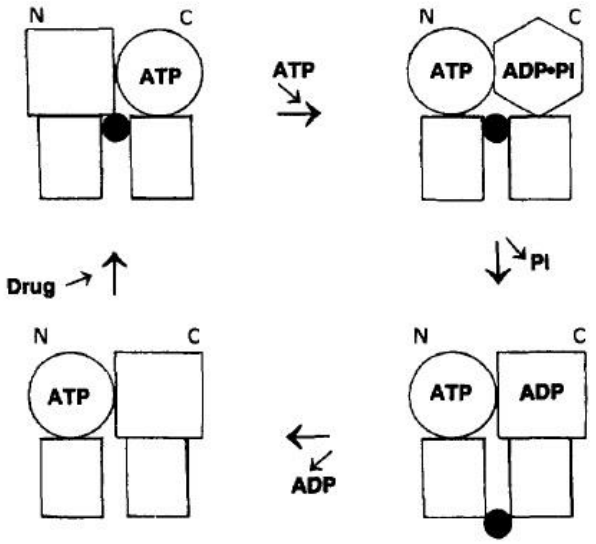


***Figure 2.16:Alternating site mechanism for the ATPase cycle of the NBD of ABC transporter***

*Two P-gp transmembrane domains (TMDs) represented by the rectangles, while circle, square and the hexagon represents the different conformational structures of N- and C-catalytic sites (Senior et al., 1995)*

The structure at top left side shows that the ATP molecule is bound to the C-catalytic site, while N-catalytic site is empty. And the drug molecule is also bound at the inside-facing transport site. As shown in the structure at the top right, the ATP hydrolysis takes place at the C-catalytic site, which is induced by the ATP binding at the N-catalytic site. The hydrolysis of ATP at C-catalytic site

leads to the conformational change within the C-catalytic site, which then prohibits the hydrolysis of ATP at the N-catalytic site. The conformation of C-catalytic site immediately after bond cleavage is shown by hexagon in the structure, and this conformation with bound ADP.Pi is a high chemical potential state. The bottom right structure shows the release of the Pi and the relaxed conformation of C-catalytic site. This relaxed conformation of C-catalytic site allows the movement of drug molecule from the higher affinity inside-facing to the lower affinity outside-facing. And the last structure at the bottom left shows the complete dissociation of the drug molecule and the ADP. The next cycle now starts at the N-catalytic site, in the same way on binding of the new drug molecule at the inside-facing transport site as shown in top left structure (Senior et al., 1995).

### 2.5.4 P-Glycoprotein Modulation

P-gp is responsible for the MDR and is the major reason to cause failure of chemotherapy treatment to cure cancers. Still it is controversial that the extent of P-gp involved in the MDR in cancers and the survival rate of patients on modulation of P-gp (Sharom, 2008). P-gp inhibition can show dramatic effect on drug accumulation within the cells, as blockage of P-gp couldn't able to eliminate the drug molecules from the intestine. Initially P-gp inhibition was focused to improve the efficacy of cancer chemotherapy by using the P-gp modulators with the anti-cancer drugs, but afterwards it's been realized that the modulators could be useful to improve the delivery of anticancer drugs by altering their pharmacological behaviour (Sikic et al., 1997). An addition of effective P-gp modulators may increase the absorption of drugs into the

intestine and also the penetration through the protective barriers like blood-brain barrier which is useful to treat brain diseases. This study has been carried in a mouse model using PSC833 modulator (Mayer et al., 1997). So development of effective P-gp modulator may improve the drug delivery to the brain.

The first generation P-gp modulators including verapamil, cyclosporine A, tamoxifen and calmodulin antagonists were identified in 1980s (Krishna and Mayer, 2000). The first generation modulators were generally used clinically for the treatment of medical conditions. But the problem associated with these modulators is high toxicity and low efficacy. Because of the low binding affinity, they need to be administered in higher dose and as a result of which these modulators have been shown adverse pharmacological results like unacceptable toxicity (Krishna and Mayer, 2000; Sharom, 2008).

Second generation modulators are more potent and less toxic than the first generation P-gp modulators, these includes dexverapamil, dexniguledipine, valspodar (PSC833) and biricodar (VX-710) (Krishna and Mayer, 2000). When the both modulators and the treatment drugs were the substrate for the cytochrome P450 3A, serious pharmacological effects were observed (Sharom, 2008). The second generation modulators have some limitations as these compounds do not able to metabolize and excrete the cytotoxic compounds results into the unuseful toxic effect which may impact on the chemotherapy dose (Krishna and Mayer, 2000).

To overcome the limitations of the second generation modulators, the new modulators were developed using the structure-activity relationships and

combinational chemistry known as third generation P-gp modulators. The third generation P-gp modulators show the low toxicity and increased selectivity with high potency, which includes LY335979 (zosuquidar), XR9576 (anthranilamide derivative tariquidar) and OC144-09 (ontogen). As these third generation modulators have different origin and chemical structures, they have common characteristics like high potency and specificity for the P-gp transporter (Krishna and Mayer, 2000; Sharom, 2008).

The best and most promising example for the third generation P-gp modulator is tariquidar as it binds with high affinity and noncompetitively to the P-gp and inhibits its activity. On the other hand second generation modulators compete with cytotoxic agent as a substrate to bind with the P-gp transporter (Krishna and Mayer, 2000; Roe et al., 1999).

# 3 : Aims and Objectives

## 3.1 Aim

The aim of this study is to evaluate galaxolide as novel efflux transporter inhibitor to improve the drug delivery through epithelial cell layers such as intestinal barrier and blood-brain barrier.

## 3.2 Objectives

- To determine cytotoxicity of galaxolide on various cell lines (Caco-2, SH-SY5Y, LN229, U87MG, MDCK, MDCKII, MDCKII-MDR1, MDCKII-BCRP and MDCKII-MRP1). To study effect of galaxolide on drug toxicity. To study P-glycoprotein expression and inhibition.
- To develop HPLC method for curcumin quantification. To study curcumin permeability through cell membranes. To study effect of galaxolide on curcumin permeation through *in vitro* intestinal and blood-brain barrier models.
- To perform histological study to assess the integrity of membrane and ability of various cells to form membrane. To study effect of matrigel on membrane formation by various cells.

# 4 : Materials and Methods

This chapter will provide details about materials used for this study and the methods followed to complete objectives

## 4.1 Materials

All materials used including media, cell lines, chemicals, lab consumables and instruments were listed in following tables with their product/catalogue numbers and source/manufactures.

***Table 4.1: Media and Chemicals***

| Sr. No. | Media and Chemicals | Catalog no. | Source |
|---|---|---|---|
| **1.** | EMEM Media | 30-2003 | ATCC |
| **2.** | McCoy's 5A Media | 30-2007 | ATCC |
| **3.** | DMEM Media | 61965-026 | Gibco/Life Technologies |
| **4.** | RPMI 1640 | R5886 | Sigma |
| **5.** | Hank's Balanced Salt Solution | H9269 | Sigma |
| **6.** | Trypsin-EDTA | T4049 | Sigma |
| **7.** | L-Glutamine | 25030 | Gibco/Life Technologies |
| **8.** | Sodium Pyruvate | 11360 | Gibco/Life Technologies |
| **9.** | Penicillin/Streptomycin | P4333 | Sigma |
| **10.** | Fetal Bovine Serum | 10500-064 | Gibco/Life Technologies |
| **11.** | Doxorubicin Hydrochloride | D1515 | Sigma |
| **12.** | Matrigel™ | 734-1100 | VWR/BD |
| **13.** | Bouin's Solution | HT10132 | Sigma |
| **14.** | Trifluoroacetic acid | T6508 | Sigma |

| | | | |
|---|---|---|---|
| **15.** | Emodin | E7881 | Sigma |
| **16.** | Bovine Serum Albumin | A7030 | Sigma |
| **17.** | HEPES | H0891 | Sigma |
| **18.** | Phosphate Buffer Saline (PBS) | 20-741-05 | Severn Biotech Ltd. |
| **19.** | Thiazolyl Blue Tetrazolium Bromide (MTT dye) | M5655 | Sigma |
| **20.** | Curcumin | 00003927 | ChromaDex™ |
| **21.** | Galaxolide® | 00070290 | International Flavours and Fragrances |
| **22.** | Verapamil | V4629 | Sigma |
| **23.** | Cyclosporine A | C3662 | Sigma |
| **24.** | Rhodamine 123 | R8004 | Sigma |
| **25.** | Temozolomide | T2577 | Sigma |
| **26.** | Vinblastine sulfate salt | V1377 | Sigma |
| **27.** | Anti-ABCB1/MDR1 Antibody | LS-C178472 | Source BioScience |
| **28.** | Anti P-glycoprotein Mouse Antibody (C219) | 517310 | Merck |
| **29.** | Mouse IgG1 Negative control Antibody | CBL610 | Merck |
| **30.** | Anti-Actin Antibody | MAB1501 | Merck |
| **31.** | Protease Inhibitor Cocktail | P8340 | Sigma |
| **32.** | Phosphatase Inhibitor Cocktail | P5726 | Sigma |
| **33.** | Page ruler plus pre-stained protein (Protein Marker) | 26619 | Fermentas/Thermo Scientific |

| | | | |
|---|---|---|---|
| **34.** | RIPA Buffer | R0278 | Sigma |
| **35.** | Tween 20 | P1379 | Sigma |
| **36.** | Histoclear II | 12954900 | Fischer Scientific/National Diagnostics |
| **37.** | DPX Mounting Medium | - | Raymond A Lamb |
| **38.** | Harris Hematoxilin | HHS32 | Sigma |
| **39.** | Paper Developer (Ilford Multigrade) | 1155073 | Harman Technologies |
| **40.** | Fixer Solution (Ilford Rapid Fixer) | 1984262 | Harman Technologies |
| **41.** | Acetonitrile (HPLC Grade) | - | Fischer Scientific |
| **42.** | Ethanol | - | Fischer Scientific |
| **43.** | Xylene | - | Fischer Scientific |
| **44.** | DMSO | - | Fischer Scientific |

***Table 4.2: Consumables***

| **Sr. No.** | **Consumable** | **Catalog no.** | **Source** |
|---|---|---|---|
| **1.** | Hybond ECL Membrane | RPN2020D | GE Healthcare |
| **2.** | Symmetry C18 Column | WAT054275 | Waters Ltd. |
| **3.** | HPLC Vials | 186000847C | Waters Ltd. |
| **4.** | Collagen coated Transwells | 3496 | Corning |
| **5.** | Black bottom sterile 96 well plates | 732-2699 | VWR |
| **6.** | 96 well MTT plates | 3799 | Corning |
| **7.** | 24 well plates | 3524 | Corning |
| **8.** | BCA Protein Kit | 23227 | Thermo Scientific |

| | | | |
|---|---|---|---|
| **9.** | Cell Scraper | 3010 | Corning |

***Table 4.3: Instruments***

| **Sr.No.** | **Instrument** | **Manufacturer** |
|---|---|---|
| **1.** | MTT Plate Reader | Thermo Scientific |
| **2.** | Fluoroscent Plate Reader | Thermo Scientific |
| **3.** | BCA Assay Plate Reader | Thermo Scientific |
| **4.** | Western Blot Assembly | Bio-Rad |
| **5.** | FACS Machine | BD Biosciences |
| **6.** | FACS Software | Cell Quest Pro |
| **7.** | HPLC System (Waters e2695) | Waters Ltd. |
| **8.** | HPLC Software | Empower3 |
| **9.** | Microcentrifuge (Labofuge 400R) | Heraeus |
| **10.** | Heating Block | Grant/Clifton |
| **11.** | Water bath | Grant |
| **12.** | Lab Water Purifier | Elga (Purelab Option) |
| **13.** | Homogeniser | Scientific Laboratory Suppliers |
| **14.** | Vortex (Vortex Genie 2) | Scientific Industries |
| **15.** | Magnetic Stirrer | Stuart Scientific |
| **16.** | Slide Drying Bench | Raymond A Lamb |
| **17.** | Water Bath_Histology | Raymond A Lamb |
| **18.** | Tissue Embedding Unit | Raymond A Lamb |
| **19.** | Microtome | Leica |

| | | |
|---|---|---|
| **20.** | Magnetic Stirrer (Permeability study) | Amicon |
| **21.** | TEER Machine (Epithelial Volt-ohmmeter) | World Precision Instruments |
| **22.** | TEER Measuring Probe | World Precision Instruments |

## 4.2 Methods

### 4.2.1 Cell Culture

Cells were grown in T25/T75 flask containing corresponding Media for the particular cell line supplemented with 10% or 20% of Foetal Bovine Serum (FBS) as per requirement. The flasks inoculated with cells were maintained at controlled conditions in humidified incubator temperature maintained at $37^0$C and supplemented with 5% $CO_2$. The medium was replaced with fresh medium at an interval of every 3-4 days depending on cell growth rate as some cells grow faster or some have slow growth rate. At the time of medium change the old media was removed and discarded and cells were washed twice with Hank's Balanced Salt Solution (HBSS) solution. Cells remain attached to the surface of the flask. Once cells were washed, HBSS solution was removed and fresh media was added to the flasks containing cells and returned back to the incubator. Cells were routinely passaged when they reached to approximately 70 to 80% confluence. To passage cells, the old media from flasks were removed and cells are washed twice with HBSS. After washing, flasks were treated with the 0.25% trypsin/EDTA; 2ml/T25 or 3ml/T75 flask; for about 5-10 mins to detach cells from the surface of flask. Flasks treated with trypsin were kept for incubation for about 5-10 min at $37^0$C. After incubation detached cells were resuspended in the 10ml of fresh growth media. These cells were then centrifuged at 2000 rpm at room temperature. The supernatant (medium containing trypsin) was discarded and cell pellet was resuspended in 10ml of fresh growth media. Cell count was taken and 0.5 to 1ml of cell suspension were transferred to the new non vented flasks containing 10ml of fresh growth

medium. Flasks were placed in incubator and followed the same maintenance procedure (protocol followed from ICT lab manuals).

Same procedure was applied to maintain all other cell lines mentioned in following Table 4.4. Only the medium was changed as per the requirement of particular cell line

***Table 4.4: Cell Lines and Media Used***

| **Sr. No.** | **Cell Lines** | **Media Used** | **Source** |
|---|---|---|---|
| **1.** | Caco-2 | EMEM Media with 20% FBS | ICT, University of Bradford, Bradford |
| **2.** | MDCK (NBL-2) | EMEM Media with 10% FBS | ATCC (CCL-34) |
| **3.** | MDCKII | DMEM Media with 10% FBS | Netherlands Cancer Institute, Amsterdam |
| **4.** | MDCKII-MDR1 | DMEM Media with 10% FBS | Netherlands Cancer Institute, Amsterdam |
| **5.** | MDCKII-BCRP1 | DMEM Media with 10% FBS | Netherlands Cancer Institute, Amsterdam |
| **6.** | MDCKII-MRP1 | DMEM Media with 10% FBS | Netherlands Cancer Institute, Amsterdam |
| **7.** | PANC-1 | DMEM Media with 10% FBS + Glutamine | ICT, University of Bradford, Bradford |
| **8.** | SiHa | EMEM Media with 10% FBS | ICT, University of Bradford, Bradford |

| | | | |
|---|---|---|---|
| **9.** | DLD-1 | RPMI 1640 Media with 10% FBS | ICT, University of Bradford, Bradford |
| **10.** | MCF-7 | EMEM Media with 10% FBS | ICT, University of Bradford, Bradford |
| **11.** | MCF-7/adr | RPMI 1640 Media with 10% FBS + Doxorubicin (8 µg/ml) | ICT, University of Bradford, Bradford |
| **12.** | U87MG | RPMI 1640 Media with 10% FBS | ICT, University of Bradford, Bradford |
| **13.** | LN229 | DMEM Media with 10% FBS + Glutamine | ICT, University of Bradford, Bradford |
| **14.** | H460 | RPMI 1640 Media with 10% FBS | ICT, University of Bradford, Bradford |
| **15.** | SH-SY5Y | RPMI 1640 Media with 10% FBS | ICT, University of Bradford, Bradford |
| **16.** | HCT 116 | McCoy's 5A Medium with 10% FBS | ICT, University of Bradford, Bradford |
| **17.** | HT 29 | McCoy's 5A Medium with 10% FBS | ICT, University of Bradford, Bradford |

### 4.2.2 Cell Count

Once cells were detached from the flask after 0.25% trypsin/EDTA treatment, fresh media was added to flask and cells were collected in suspension. To get rid of trypsin from media, collected cell suspension were centrifuged at 2000

rpm at room temperature and supernatant was discarded gently without disturbing pellet. Pellet then resuspended in the fresh growth media. Approx. 20µl of cell suspension was collected using micropipette and transferred it to the haemocytometer. 5 grids of the haemocytometer was used to count cells and finally mean of the 5 grids was taken to calculate the cell number per ml present in the collected suspension (protocol followed from ICT lab manuals).

The final cell count expressed as: mean cell count × $10^4$ cells/ml of medium.

### 4.2.3 Galaxolide cytotoxicity (MTT Assay)

MTT assay was performed to study toxicity of galaxolide on different cell lines (protocol followed from ICT lab manuals). To carry out this study concentration range of galaxolide with 500µM was used as a highest concentration and was diluted double fold to achieve serially lesser range of drug concentrations for the treatment on cells; it means next drug concentration is half the previous one and vice versa. Cells were treated and incubated with drug concentrations for 72hrs.

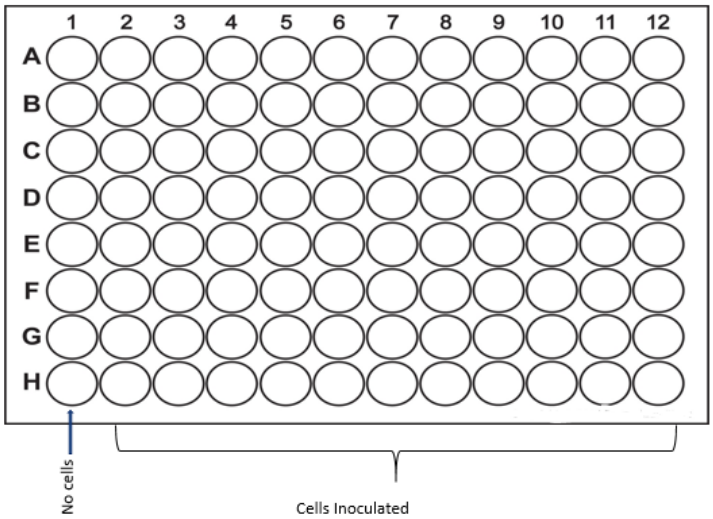


***Figure 4.1: Template of MTT plate_ Inoculation of cells***

On the Day-1 of assay, required cells were trypsinised, centrifuged and were resuspended in fresh media to get cell suspension. Cell count was done and cell suspension was prepared having approx. $1\times10^4$ cells per ml. 200µl cell suspension containing $2\times10^3$cells were inoculated per well in 96 well plate using multichannel pipette. Except the first row of well, cells were inoculated in all remaining rows (Figure 4.1), leaving first row as a blank control. Plates were placed for incubation at $37^0$ C supplemented with 5% $CO_2$ for 24 hrs.

Once 24 hrs incubation done, plates were removed from the incubator and old media present in wells was removed with multichannel pipette. Empty well were then replaced with the freshly prepared drug concentrations. Row 1 and 2 added with growth media without the drug while row 3 to 12 were replaced with lowest to highest galaxolide concentrations respectively obtained by the double fold serial dilution (Figure 4.2). Once drug solutions added to the respective wells, plates were returned to the incubator at $37^0$ C supplemented with 5% $CO_2$ for 72 hrs.

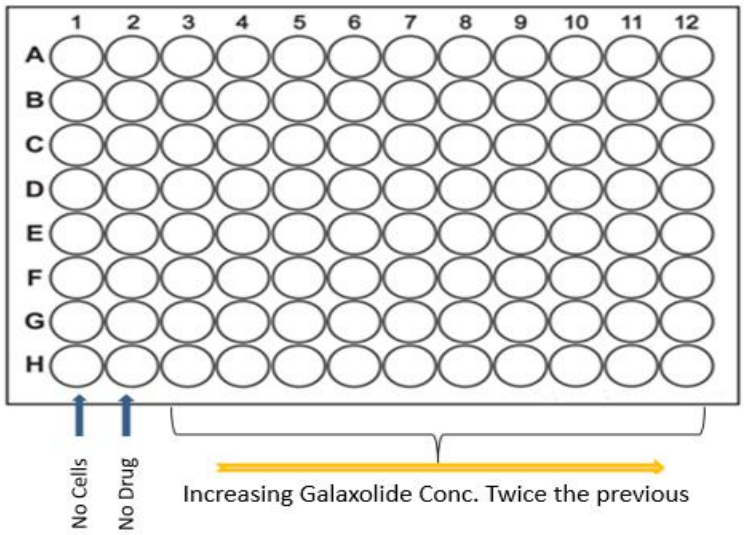


***Figure 4.2: Galaxolide cytotoxicity_MTT assay***

After 72hr treatment, plates were taken out from the incubator and 20 µl MTT (Stock=5mg/ml; 100µg/well) dye was added to each well. Plated then followed by 4hr incubation. When incubation time over, plates were taken out and all media containing MTT was removed and replaced with 150 µl DMSO. Wells were mixed to dissolve the violet crystals formed. Plate count was taken at 540nm using plate reader (Figure 4.3) and $IC_{50}$ value was obtained from the graph plotted. The Figure 4.4 shows the flow chart for the protocol.

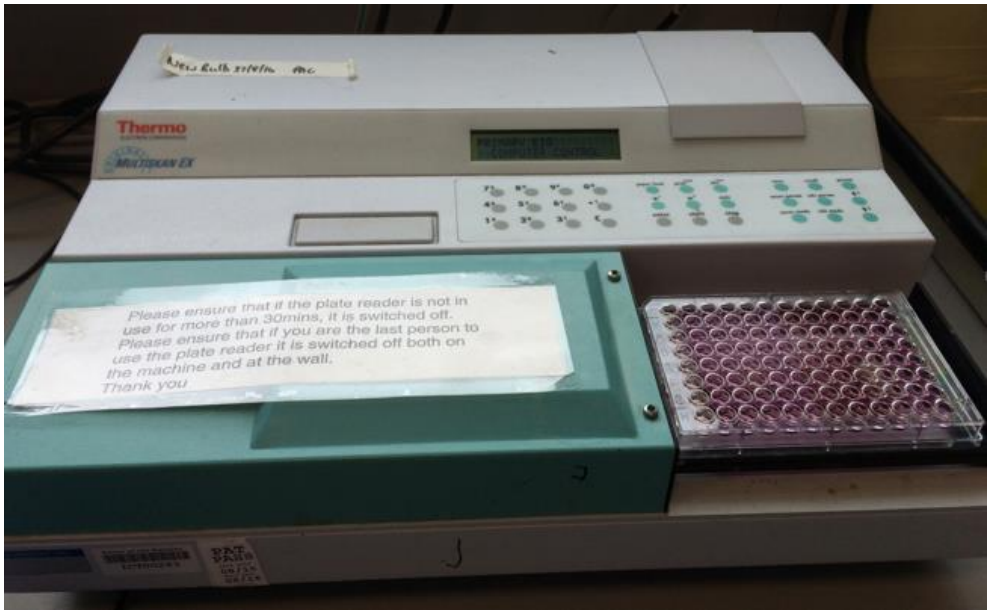


***Figure 4.3: MTT Plate reader***

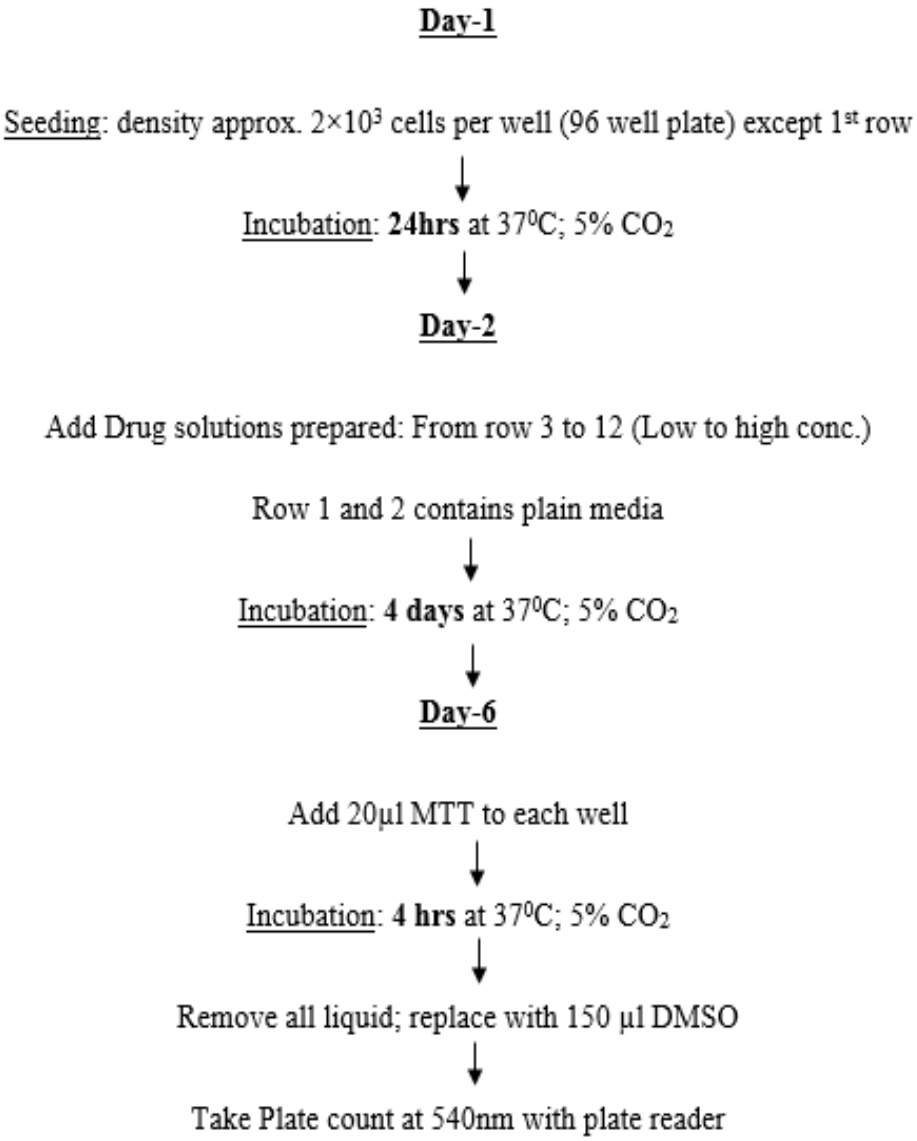


***Figure 4.4: MTT Assay_ Flow Chart***

### 4.2.4 Effect of Galaxolide on drug toxicity

**Step 1:** Seeding

Cells were grown in a T75 cell culture flask until the cell density reaches approximately 80% of the flask surface area. Medium was discarded; cells were washed with Hank's balanced salt solution (HBSS) and then trypsinised in order to get freely floating cell suspension. Cells were counted and a suspension was prepared in complete tissue culture medium such that the cell density would be $1\times10^4$ cells per ml. 200 µl of this suspension was seeded in each well except 1st column of the 96 well plate leading to cell density of $2\times10^3$ cells per well. Cells were allowed to grow for 24 hours at $37^0$ C supplemented with 5% $CO_2$, so that they also stick to the bottom of the plate.

**Step 2:** Drug exposure

After 24 hours of growth, each well was emptied of the old medium and fed with 200 µl of fresh medium containing serially increasing concentrations of drug. To explain with the help of following Figure 4.5, Column 1 was left empty; column 2 was fed with blank medium containing no drug. Column 3 to 12, were fed tissue culture medium containing concentrations of drugs (curcumin and temozolomide) ranging up to 500µM as a highest concentration, where each column in numeric order from 3 to 12 was exposed to twice the concentration of the drug than previous. Plates were further incubated for 24 hours. Similar procedure was repeated with drug concentrations supplemented with the known P-gp inhibitors verapamil (5µM) and cyclosporine-A (5 µM) along with galaxolide (1 µM).

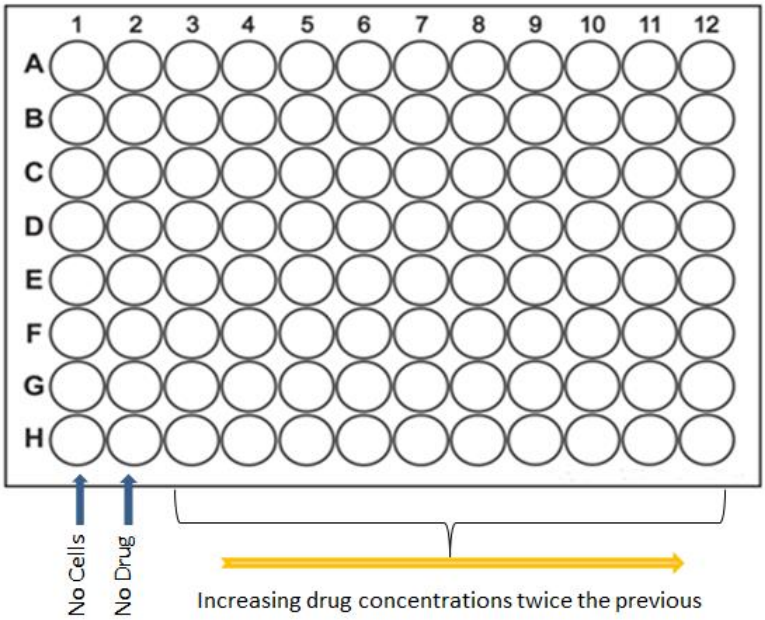


***Figure 4.5: MTT assay plate template_drug treatment***

**Step 3:** MTT assay

Finally, 5 mg/ml solution of MTT was prepared in distilled water and 20 µl of it was added in each well. Plates were incubated for 4 hours and then medium was discarded. 150 µl of DMSO was added to each well and mixed to dissolve purple coloured crystals formed with MTT at the bottom of each well. The absorbance of each well was determined at 540 nm using plate reader. $IC_{50}$ value was obtained from the graphs plotted.

### 4.2.5 Inoculation and Growth of cells on Transwells

Collagen-coated transwells having pore size of 3.0µm was used throughout the studies. Various cells were grown on transwells with different cell number during inoculation as per the experimental requirement, but inoculation procedure is same for all.

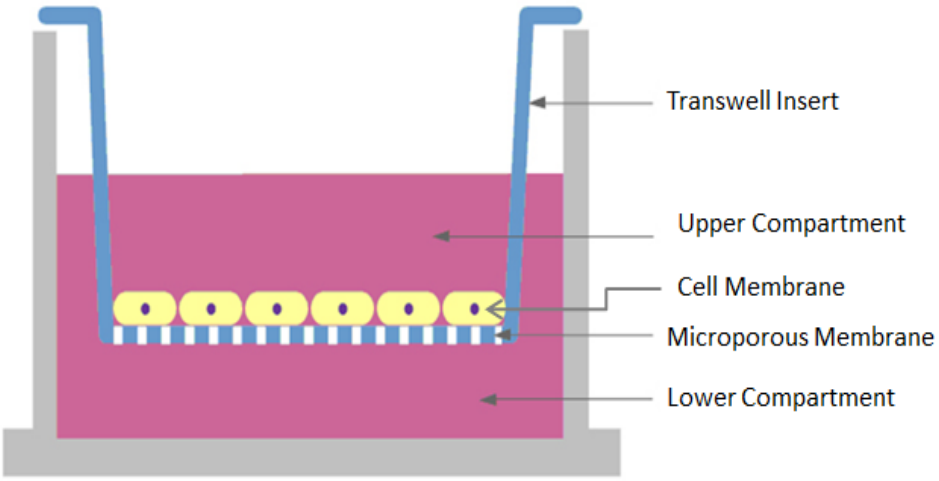


***Figure 4.6: Transwell***

Cells when reach approx. 80% or more confluence was used for experimental set up. Cells were washed and trypsinised as per above mentioned procedure and cell suspension was prepared after centrifugation using fresh media. Cells then counted using haemocytometer and cell suspension having cell density 1 × $10^6$ cells/ml was prepared. Each transwell inoculated with the 100µl cell suspension, it means 1 × $10^5$ cells/transwell was seeded. Transwells were placed in well plates and moved to incubator for 2-4hrs incubation without addition of any media to the top or bottom chamber of transwells. This step is done to allow cells to attach to the transwell membrane. After incubation plates were removed and 200µl media to top chamber and 1.5ml media to bottom chamber were added and plates were returned to the incubator set to the temp. $37^0$ C supplemented with 5% $CO_2$. Medium was changed every three days of interval. The sequence of media removal and replacement is critical to success any assay that requires the cells to adhere to the membrane surface. When feeding the transwells it is important to maintain the net positive hydrostatic

pressure above the cells to prevent the cells from being pushed off the membrane. Therefore, the sequence of media removal and addition is always the same as:

1. Remove media from the receiver or bottom chamber
2. Remove media from the top/upper chamber
3. Add media to the top/upper chamber
4. Add media to receiver or bottom chamber.

### 4.2.6 Inoculation and Growth of cells on Transwells with addition of Matrigel

Cells were inoculated in presence of matrigel, to study its effect on cell growth and membrane forming ability of cell. Various cell lines were used as per requirement to carry this study. Cells when reached at approx. 80% confluence, flasks were removed from incubator and cells were washed and treated with trypsin. After trypsinisation cell suspension was prepared and cell count was taken. Cell suspension with $1 \times 10^6$ cells/ml cell density was prepared according to cell count. 1 ml of this cell suspension was taken and centrifuged. Pellet was collected and re-suspended in pre-cooled media containing ice cold matrigel (different concentrations as per requirement) in it. The suspension was mixed well and 100µl of it was inoculated per transwell. Transwells then incubated for 4-6 hrs without adding media to the bottom chamber to allow cells to attach the membrane of transwells. After incubation 200µl media to top chamber and 1.5ml media to bottom chamber was added and plated were placed in incubator at $37^0$ C supplemented with 5% $CO_2$. Medium change and other maintenance

procedure were followed as described above. The Figure 4.7 shows the brief procedure for inoculation of cells on transwells with and without matrigel.

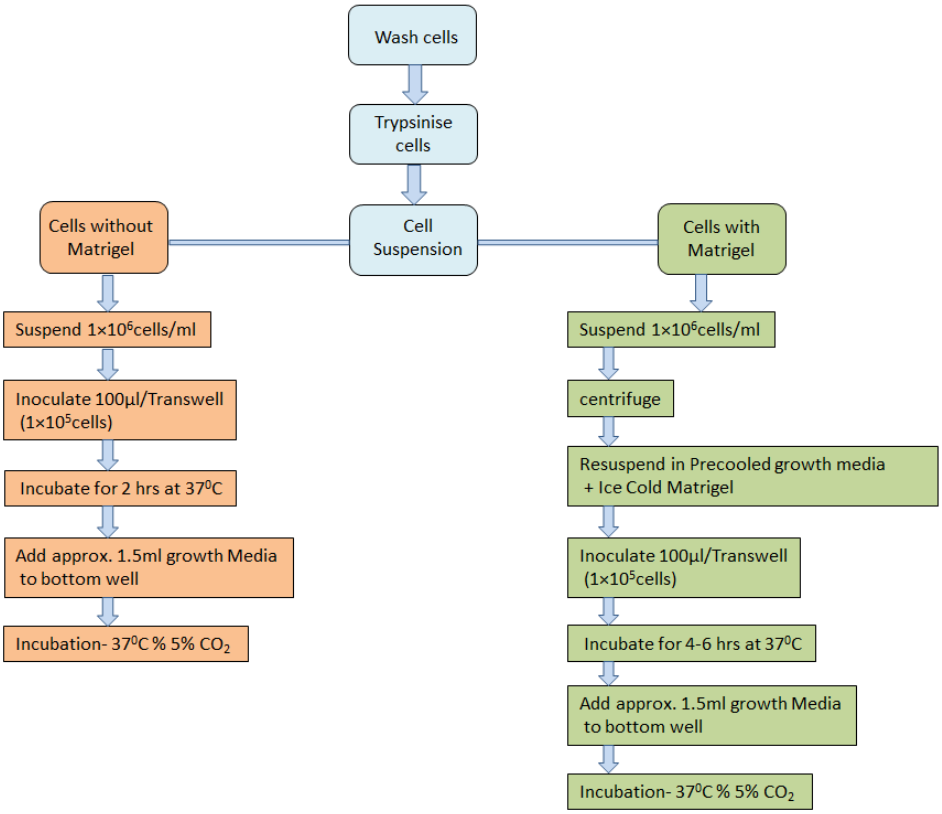


***Figure 4.7: Flow chart of cell inoculation on transwell with and without matrigel***

### 4.2.7 Transepithelial electrical resistance (TEER) measurement

TEER is the resistance across the membrane or it measures the resistance to pass current across the cell monolayer. The TEER value was calculated by using following formula (Yu and Huang, 2011):

$$\textbf{TEER } (\Omega.cm^2) = [TEER_{(m)} (\Omega) - TEER_{(b)} (\Omega)] \times A\ (cm^2)$$

Where,

TEER : Trans epithelial electrical resistance

$TEER_{(m)}$ : Resistance reading obtained for cell monolayer

$TEER_{(b)}$ : Resistance reading obtained for the blank insert

A : Surface area of insert filter membrane

To perform TEER measurement, plates previously inoculated with cells were taken out from the incubator at the certain time point as per requirement and transwell was transferred to new plate. Medium from upper and lower chamber was removed and replaced with fresh medium with 200µl at upper and 700µl in lower chamber. Along with this, one blank insert (transwell without cells) also prepared in same way containing 200µl media in upper and 700µl in bottom chamber. This blank was prepared to measure blank reading. The electrode (STX2 electrode) was kept in medium to equilibrate with media for about 10-15 min prior to carry out readings.

The electrode has two unequal arms with different lengths. During the time of TEER measurement, the short probe was placed in upper chamber while long one was in basal chamber as shown in Figure 4.8 and the readings were

recorded for blank insert as well as for insert having cells by using EVOM$^2$ epithelial volt-ohmmeter Figure 4.9.

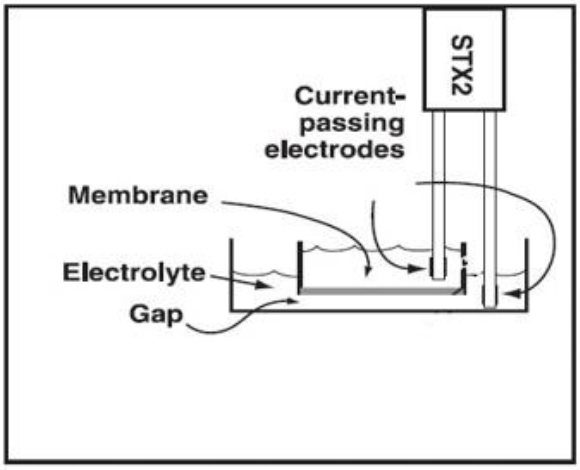


***Figure 4.8: Placement of electrode in transwell during TEER measurement***

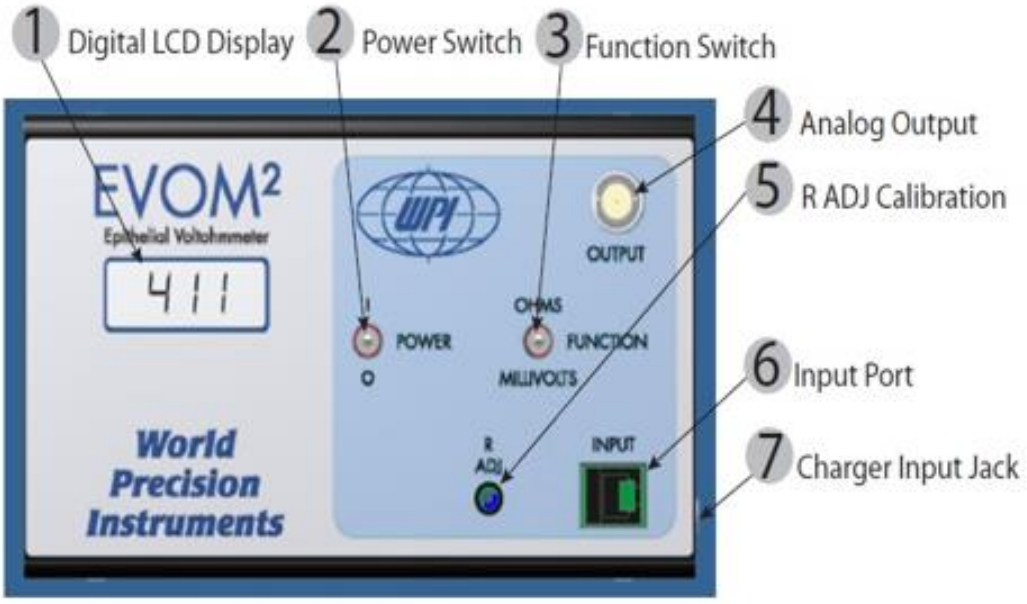


***Figure 4.9: EVOM$^2$ Meter***

## 4.3 Histology Study

To study histology of cell membranes, various steps were followed from seeding of cells on transwell to prepare stained slides. All these steps are described in detail in following section. (Histology procedures were adapted from corning protocols for transwell and staining procedure followed from ICT lab manuals)

### 4.3.1 Inoculation and growth of cells on transwells

The cells were maintained in their respective medium with required supplements as per need at $37^0$C with 5% $CO_2$. To follow histology, cells when reached to approx. 80% confluence, were removed from incubator. Flasks were then washed with HBSS and trypsin was added to detach the cells from the surface. Cells with trypsin was incubated for 5-10 mins and then flasks were removed from incubator and a manual shake was given to flask to get the free floating cells. Once all cells were detached from the surface and free floating cells were observed, fresh media was added to flask and cell suspension was collected in tube and centrifuged to get trypsin free pellet. Pellet then resuspended in fresh growth media and cell count was taken using haemocytometer. Cell suspension was prepared as per the requirement. Transwells having 6.5mm diameter and 3.0µ pore size were placed on the wells of 24 well plate. Each transwell then inoculated with the 100µl of cell suspension (which may contains $1\times10^5$, $2\times10^5$ or $3\times10^5$ cells per transwells). Once cells were inoculated at required density, transwells were incubated for 2 hrs without addition of medium to lower compartment (basolateral or bottom well) to allow cells to attach the membrane. After 2 hrs well plates were removed from

incubator and 200 µl of growth medium to top well and 1.5 ml to the bottom well was added and plates were placed for incubation at $37^0$C with 5% $CO_2$. Medium was changed after every 3 days. Every time point plates were removed from incubator, one well was taken to new well plate and media was replaced with fresh media for the one well which have been removed. Top chamber replaced with 200 µl while bottom chamber was replaced with 700 µl media. TEER was measured and recorded for this well along with blank well which does not have cells grown on it.

### 4.3.2 Fixation

After TEER reading, media from well was removed and transwell having cells on it was transferred gently to the universal tube. Approx. 5 ml Bouin's solution was added to universal tube ensuring transwell was completely covered under Bouin's solution. Transwell was incubated for 1 hr with Bouin's solution. After incubation Bouin's solution was poured off and 70% ethanol was added to wash wells. Transwell was then washed gently with ethanol. This step was repeated until no more yellow colour of Bouin's solution was removed. Once all yellow traces washed out, transwell was stored at room temperature in universal tube having 70% ethanol until all transwells got ready.

### 4.3.3 Dehydration and cleaning

Dehydration and cleaning was generally done by using automated tissue processor (Figure 4.11) for most of the tissues. Tissues were placed in the tissue processor cassettes (Figure 4.10) after fixation and then placed in the automated tissue processor and required programme was selected. Cassettes containing tissue was automatically passed through the different increasing

concentrations of ethanol to dehydrate tissue and then through histoclear or xylene solution to clean the tissue.

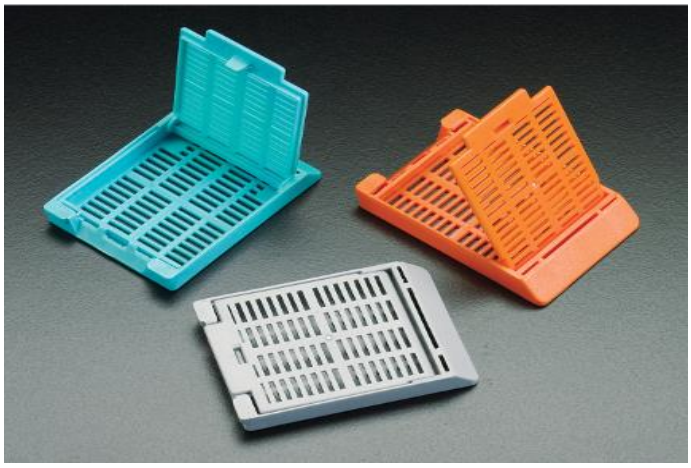

***Figure 4.10: Tissue processor cassette***

***Figure 4.11: Automated Tissue processor***

In case of this study, cells were grown on and fixed with the transwell membrane, and intact transwells with cells grown on it were directly used for further processing. Transwells were large in size to fit in the tissue processing cassettes. So to overcome this, above mentioned steps for dehydration and cleaning was done manually.

Once all transwells were fixed, they were ready to go further for histology study. The next step was dehydration, which usually carried out by transferring transwells through solutions of increasing ethanol concentrations. After fixation, transwells were stored in 70% ethanol. The 70% ethanol then replaced with 95% ethanol and incubated for 10 mins. Incubation then followed with removal of 95% ethanol and addition of 100% ethanol for 10 mins and this step with absolute ethanol was repeated twice.

Once dehydration process was done, cell layer on transwells was needed to clean and this was done by addition was histoclear. Xylene was also used normally to clean the tissue, but here in this case with transwells, xylene reacted with polymer used to make transwells and dissolved the transwells in it. So in case of study with transwells, histoclear was used strictly. Incubation with histoclear was done for 10 mins.

### 4.3.4 Embedding

Embedding was done on the tissue embedding station (Figure 4.12). Before starting dehydration process, tissue embedding station was switched on; this will melt the paraffin wax in the meantime. Oven was also set to $58^0$C.

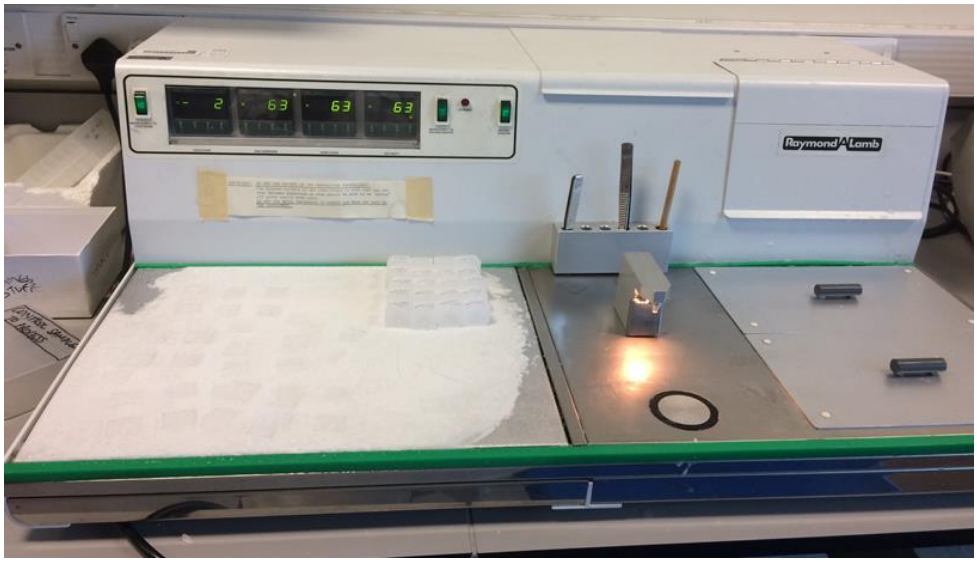


***Figure 4.12: Tissue embedding station***

Once incubation with histoclear was done, it was removed and transwells were moved to 24 well plates and liquid paraffin was added over it ensuring that transwells were completely embedded in paraffin wax. Plates were then transferred to the oven set at $58^0$C. Transwells were incubated in liquid paraffin for 1hr. After 1 hr incubation plated were removed from the oven and replaced with fresh liquid paraffin and returned back to oven for another 1 hr. Plates were then removed from the oven, transwells were half emptied with paraffin, and moved to new 24 well plate and placed at room temperature for approx. 1 hr and then for 30 mins in the freeze. Plates then removed and membrane was gently cut off from each of the transwells with sharp blade. The harvested

membranes were then transferred to the plastic moulds (Figure 4.13). These moulds then used to prepare wax blocks by filling liquid paraffin to these moulds. The membranes were set at the bottom and each wax block was labelled with respective cells. Block then allowed cool and solidify for 1 hr on the cooling plate associated with the tissue embedding station. After 1 hr tissue embedding station was switched off and blocks were placed for overnight at room temperature. Next day, plastic moulds was removed and entire blocks were harvested (Figure 4.14) and stored in freezer until sections were taken.

***Figure 4.13: Plastic moulds***

***Figure 4.14: Paraffin blocks with tissues***

### 4.3.5 Sectioning

Before beginning to sections, water bath was switched on and was set to $50^0$ C. Blocks formed earlier were placed in deep freezer for 30 mins. This may harden the blocks and would give clean and sharp sections as wax was better to cut when it was cooled.


***Figure 4.15: Microtome***

Microtome was switched on keeping lock on ensuring that lever was not moving and blade was replaced with new sharp blade. Once all settings were done, blocks were removed one by one from the freezer and were fixed on the block holder on microtome (Figure 4.15). Lock was removed and lever was pulled outwards and moved in circular motion to take sections. Sections with 5µm thickness were obtained. The sections then moved to water bath (Figure 4.16) set to $50^0$C for 1 min. Sections then transferred to the clean glass slide and slide was labelled with respective information. Slides then placed on slide drying hot plate (Figure 4.17) set at $50^0$ C for 30 min to attach paraffin embedded sections firmly on glass slides. Once slides were dried and sections were attached firmly on the glass slides, slides were stored at room temperature until staining.


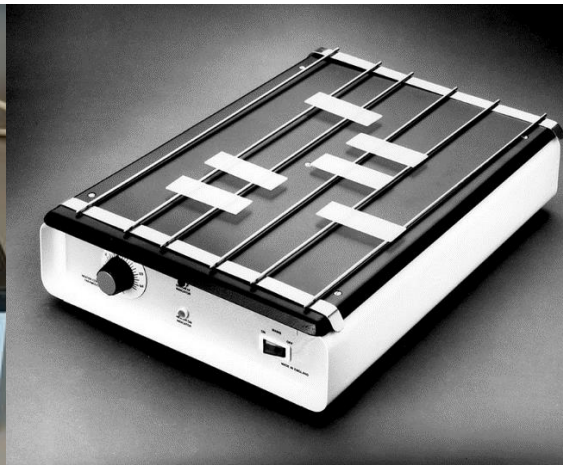

***Figure 4.16: Water bath***

***Figure 4.17: Slide drying hot plate***

### 4.3.6 H and E Staining

Staining of sections can be done by using different stains. Here we used Hematoxylin-Eosin (H and E) staining method, which is most commonly used method. Hematoxylin is an active staining component which stains the nuclear component of cells a dark blue, while eosin stains the cytoplasmic organelles varying shades of pink, red or orange. The combination of hematoxylin and eosin provides a broad range of morphological information about the sections.

#### 4.3.6.1 De-waxing and rehydrating sections

Slides prepared with sections were placed in a slide staining rack (Figure 4.18). The rack then was passed through the xylene and diluting ethanol solutions to de-waxing and rehydrating sections. Sections were first transferred to the pure xylene (Xylene-1) for 5 min, then transferred to another container containing pure xylene (Xylene-2) for 5 mins. After that sections were placed in container having 50% xylene/ethanol mixture for 5 mins and then moved to the Absolute

ethanol (Ethanol-1) for 5 min. Then again moved to Absolute ethanol (Ethanol-2) followed with 90% ethanol and then finally in 70% ethanol for 2 min each.

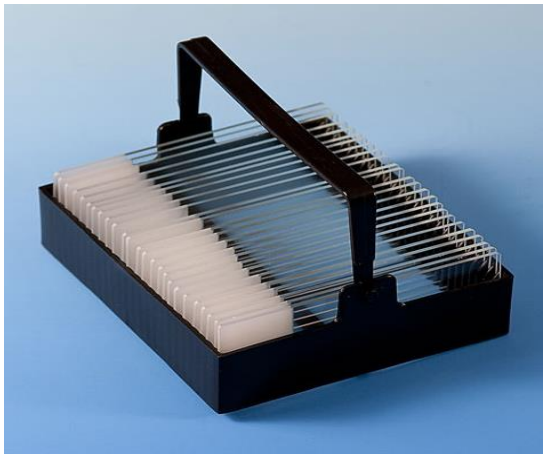

***Figure 4.18: Slide staining rack***

#### 4.3.6.2 Staining

Once de-waxed and rehydrated, sections were stained in Hematoxylin for 10 mins. After staining, sections were washed in slow running tap water and then placed in acid-alcohol (0.5% HCL in 70% Ethanol) solution for 5 sec to get rid of excess hematoxylin. Then washed briefly in tap water and moved to container having Scott's tap water for 2 mins. Sections then counterstained in 1% aqueous eosin for 1 min and finally washed under tap water. Sections then drained for 1 mins to run out excess water.

#### 4.3.6.3 Dehydrating, cleaning and Mounting

When sections drained off excess water, they were dehydrated passing them through absolute ethanol-2 for 1 min, absolute ethanol-1 for 3 mins, 50% xylene/ethanol for 3 mins, xylene-2 for 3 mins and finally in clear xylene for 5 mins. Clear xylene was used to clean the sections before mounting. Once every

step was done, sections were mounted in DPX medium. During mounting, coverslip was flooded with DPX medium and was placed gently over the slide containing sections. Any bubbles formed were removed using needle point and finally mounted slides were placed to dry at room temperature. Once dried, slides were observed under microscope and results were noted. The Figure 4.19 shows the flow chart for H and E staining.

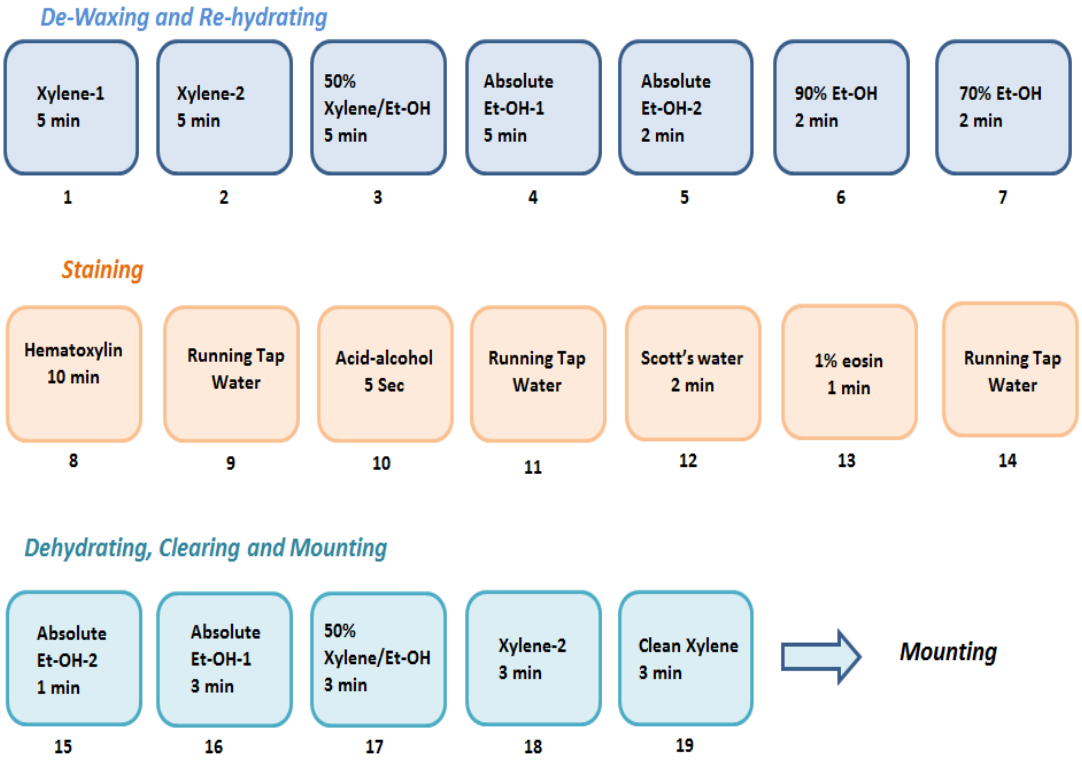


***Figure 4.19: Histology procedure flow chart***

## 4.4 Western blotting

Western blot analysis was done to study the expression of P-gp in cells (Procedure adapted from Dr. Simon Allison). Steps involved in western blot analysis are described as follow:

### 4.4.1 Cell Harvesting and Lysis

Cells were grown and harvested at the several time points to analyse the protein expression. At the time of cell harvesting, flasks were taken out from incubator and washed twice with the PBS. After wash cells were treated with trypsin and followed by addition of media to get cell suspension. To get rid of trypsin, cell suspension was centrifuged and pellet was collected. Pellet then washed twice with 5ml PBS to get rid of traces of media. After PBS wash, 200µl lysis buffer was added to the pellet and mixed by pipetting. Lysis buffer was prepared by mixture of RIPA lysis buffer, Protease inhibitor cocktail (PIC) and phosphatase inhibitor cocktail. 1ml of lysis buffer prepared with 965µl RIPA lysis buffer, 25µl Protease inhibitor cocktail and 10µl phosphatase inhibitor cocktail. Every time, lysis buffer was prepared fresh. Once pellet was mixed with lysis buffer, it was transferred to the chilled eppendorf tube and placed on wet ice for 15 min. and then stored at $-20^0$C until all samples were ready.

### 4.4.2 Sample preparation to load on gel

Once all samples were harvested, cell lysates removed from the -20 freezer and placed on wet ice for 15 min to defrost it. Cell lysates were then followed to the homogenisation using homogenizer (Figure 4.20) to get uniform samples. During this step, homogenizer probe was positioned carefully at the middle of

the sample to avoid bubble formation (Figure 4.21). Each sample was sonicated thrice having 30 sec lag time between two sonication cycles. To avoid mixing of two samples during homogenisation, 2 eppendorf tubes containing distilled water was homogenised after and before each sample. After homogenisation all samples were places on wet ice and mixed with pipetting. 100µl of each homogenised sample was transferred to the new eppendorf tube and 50µl of Laemmli's dye was added to each sample. Samples were stirred well and stored at -20$^0$C until they were loaded on the gel. The remaining lysate samples were used to carry BSA assay to quantify total protein concentration in the lysate.

***Figure 4.20: Homogenizer***

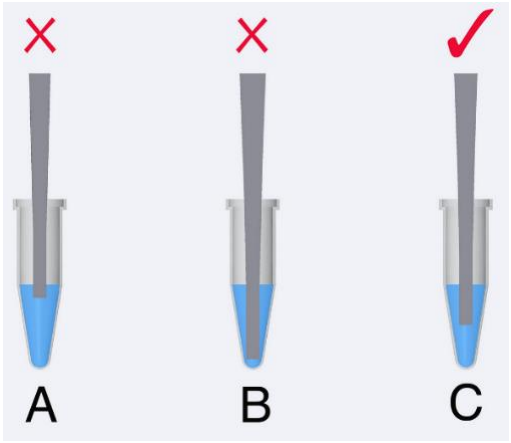


***Figure 4.21: Position of probe during homogenisation***

### 4.4.3 BSA Assay

BSA assay is done to determine the total protein concentration present in the cell lysates harvested for the western blot analysis.

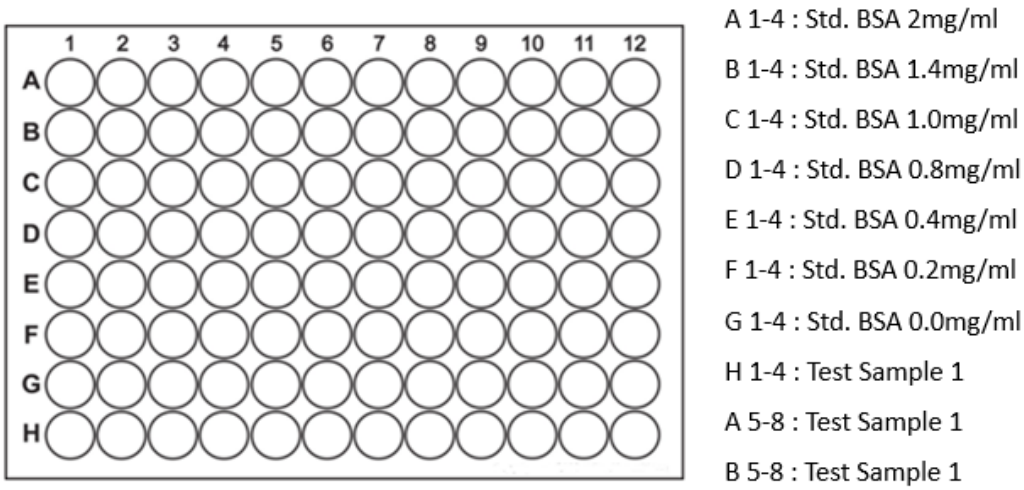


***Figure 4.22: BSA assay template***

BSA Assay was performed using 96 well plate. Different concentrations of BSA were used as standard with a range of 2.0mg/ml, 1.4mg/ml, 1.0mg/ml, 0.8mg/ml, 0.4mg/ml, 0.2mg/ml and 0.0mg/ml. To perform assay, 10µl of standard sample was used for each well and for each samples four well were used. Same criteria were used for test samples; 4µl of test samples was added to each well and four wells were used for each sample. Once all standard and test samples were added to corresponding wells, addition of 200µl BSA reagent was done to each well. To add this reagent multichannel pipette was used to get uniform colour intensity. The BSA reagent is a mixture of Reagent A and Reagent B (Reagent A-25ml + Reagent B-0.5ml). Plate was incubated for 30 min at room temperature and after incubation readings were taken using plate reader (Figure 4.23). Graph plotted using readings obtained and total protein concentration was calculated for each sample. Figure 4.22 shows the template of samples loaded on plate.


***Figure 4.23: BSA assay plate reader***

### 4.4.4 Gel Preparation

Two different gels with 7.5% and 15% concentrations were prepared. P-glycoprotein molecule has larger molecular weight; 170KD, so it needs 7.5% gel to run while 15% gel prepared for the actin. These gels prepared using the gel making glass cassette (Figure 4.24). After preparation gels were allowed to solidify for 1 hr. 10% SDS solution was overlaid above the gel to avoid drying from the top edge. After 1hr, liquid SDS which was overlaid was drained off. Stacking gel with 4% concentration was prepared and overlaid it to previous gel and comb was inserted above it to form wells to load the samples. Stack gel allowed to solidify for 30 mins. When gel solidified, comb was removed gently and gel along with glass cassettes was ready to load the samples. Then gel was assembled in the electrophoresis assembly and flooded with the running buffer. The electrophoresis assembly then connected to the power unit.

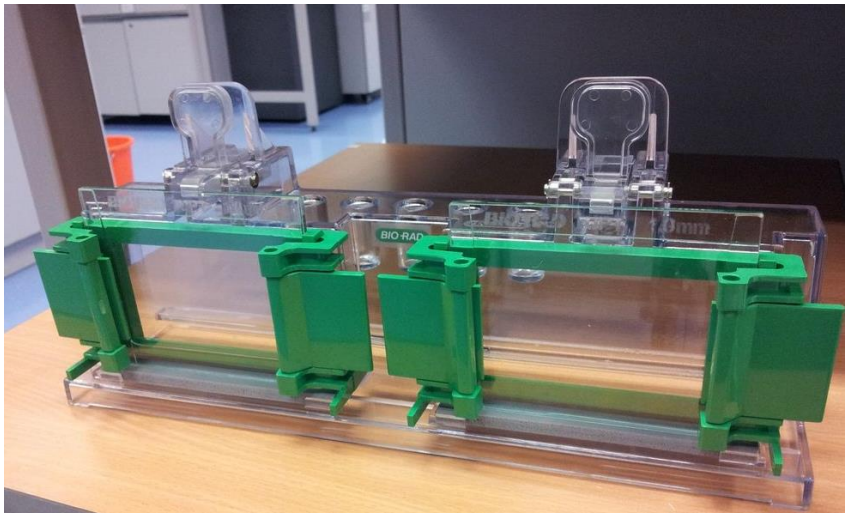


***Figure 4.24: Gel making glass cassette***

### 4.4.5 Loading and running samples on Gel

The harvested samples after homogenisation and mixed with the Laemmli's dye was removed from freezer. Samples and protein marker were defrosted in $37^0$C water bath. Using heating blocks (Figure 4.25), the samples were boiled at $100^0$C for 5 mins. After boiling samples were centrifuged to get down evaporated liquid and then vortexed.

***Figure 4.25: Heating block***

Samples now ready to load on gel, was loaded considering equal amount of total protein (35µg) per well. First well was loaded with 8µg protein marker and last with 4µg protein marker to get an idea about direction of gel. In between two markers different test samples were loaded. Once all samples were loaded, lid was placed onto the chamber and power unit (Figure 4.26) was switched on to run at 70 volts for 1hr and after an hour power increased to 120 volts. The electrophoresis run until blue dye moved to the bottom of the gel and eventually gets out of the gel. In the meantime transfer buffer was prepared and nitrocellulose membrane was soaked into it.

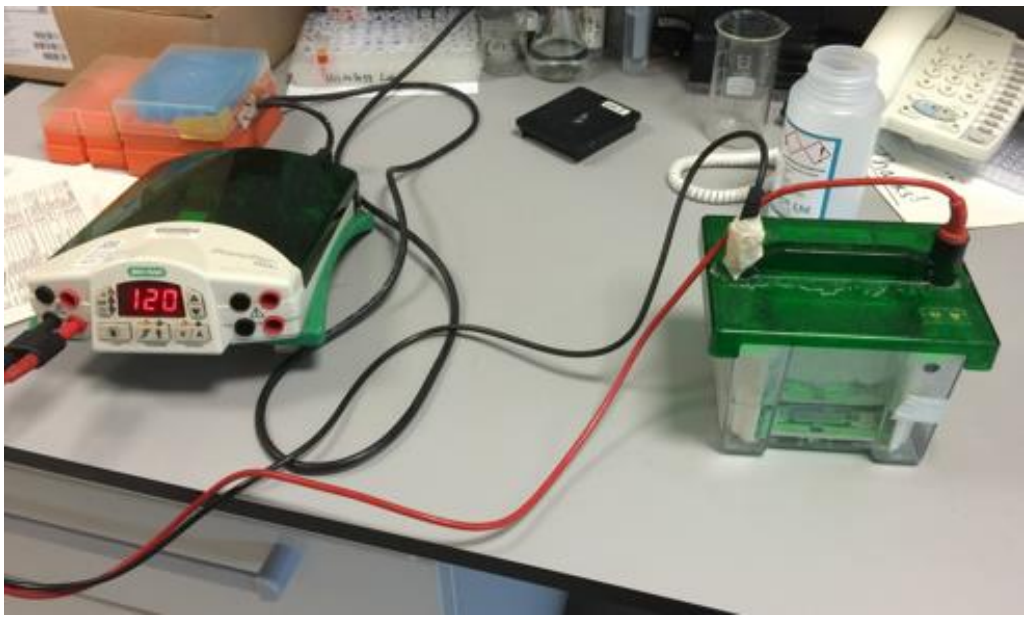


***Figure 4.26: Gel running chamber and power unit***

### 4.4.6 Transferring the protein from the gel to the membrane

When gel finished running, removed it from the electrophoresis assembly and then removed gently from the plastic tray using the green key. Well area was cut off with the spatula to make the gel smaller and gel was placed in the tray containing transfer buffer to avoid it from drying. Nitrocellulose membrane was

used to transfer proteins from gel was soaked already in transfer buffer. The transfer sandwich was prepared in a tray containing transfer buffer in a following order from white holder to black holder as sponge, 2 pieces of blotting paper, nitrocellulose membrane, gel, 2 pieces of blotting paper and sponge as shown in the Figure 4.27. When applying the nitrocellulose membrane over the gel, 10 ml stripette was rolled over it gently to ensure there was no any air bubbles between two layers.

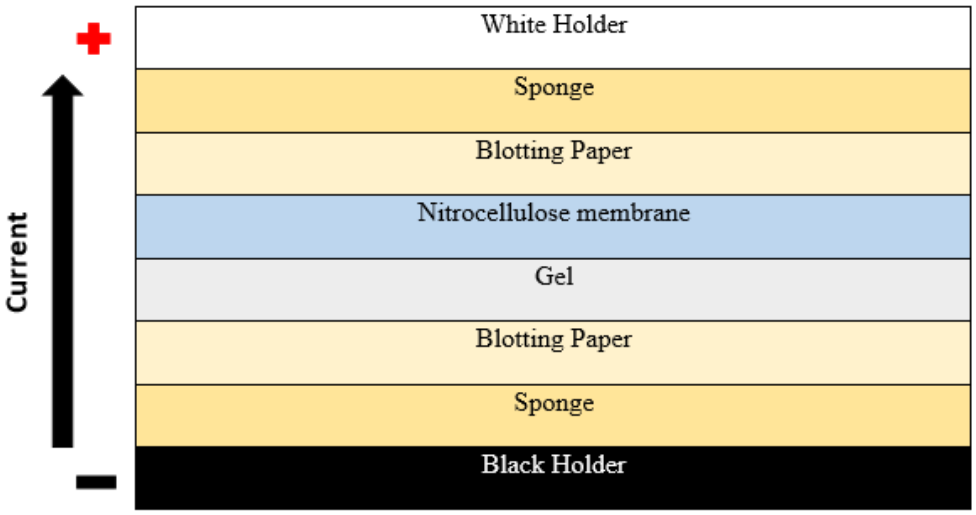


***Figure 4.27: Transfer sandwich***

When transfer sandwich was prepared, it was transferred to the tank containing transfer buffer ensuring black side of cassette fits towards the black side of the tank (Figure 4.28). Tank then connected to the power unit and was run on 35 mA for approx. 16 hrs. After run membrane with transferred proteins was removed and dried for about 1hr and then stored at -20$^0$C in sealed polythene bag until ready for next work.

***Figure 4.28: Transfer cassette and tank with power supply***

### 4.4.7 Antibody staining

Membranes were removed from storage and allowed to thaw at room temperature for 15 min. After thawing membranes were transferred to the container containing PBS with 0.1% Tween 20 (PBST) and incubated for 15 min at room temperature with shaking on orbital shaker (Figure 4.29). PBST then poured off and replaced with the blocking solutions (5% Milk Powder-Marvel) and incubated at room temperature for 1 hr. In mean time primary antibody solution was prepared in blocking solution as per the data sheet. 1 hr incubation then followed with removal of blocking solution and then addition of primary antibody. Membranes treated with primary antibody incubated overnight on shaking condition at $4^0$C.


***Figure 4.29: Orbital shaker***

Once incubation done, primary antibody solution was removed from container and blots were replaced with PBST and incubated at room temperature for 5 mins with shaking. The process was repeated thrice to remove unbound primary antibody traces. When washing done blots were incubated with secondary antibody prepared in blocking solution. Blots then incubated for 1 hr on shaking at room temperature. After incubation with secondary antibody, blots were washed thrice with PBST for 5 mins each time at room temperature with shaking condition. After washing, blots were drained on tissue paper and fixed on the developing box. Blots then flooded with the ECL solution for 1 min and then covered with the photocopy paper and then moved to dark room to develop the films.

### 4.4.8 Developing Films

Film developing was completely done in the dark room. Blots were immediately proceed for photo film development once treated with the ECL reagent. In dark room three separate trays containing developer solution, distilled water and

fixer solution respectively was arranged as shown in the Figure 4.30. Films were exposed to the blots fixed in developing box with various exposure times. After exposure films were transferred to the tray-1 containing developer solution for 2 mins, then moved to the tray-2 for 1 min containing distilled water to get rid of developer solution from the film. Finally films were transferred to the tray-3 containing fixer solution for at least of 2 mins and then at the end films were moved back to the tray-2 having distilled water. All developed films then removed from the distilled water and air dried and then marked according to the protein marker and labelled.

Developer and fixer solution was prepared in dark room. Developer solution was prepared with 50 ml developer diluted to 500 ml using distilled water while same volume of fixer solution was prepared with 75 ml fixer diluted to 500 ml using distilled water.

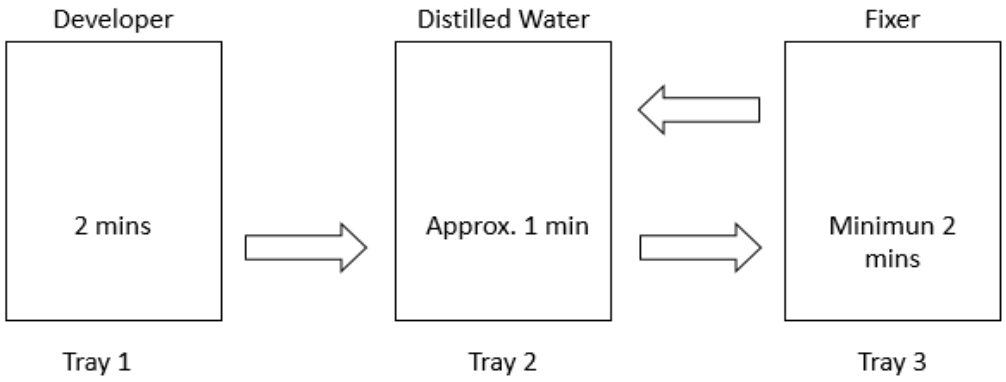


***Figure 4.30: Film developing set-up***

## 4.5 Fluorescence activated cell sorting (FACS)

Fluorescence activated cell sorting (FACS) is a technique which can be used to study protein expression (Procedure adapted from Dr. Simon Allison). P-gp expression was analysed by this method as well. Following are the steps involved in FACS analysis.

### 4.5.1 Cell Treatment

Cells were seeded in T75 flasks (2 flasks per cell line) and grown to confluence. Medium changed every three days. When appropriate confluence was acquired, cells were trypsinised and collected in suspension and centrifuged at 1000 rcf for 5 minutes. Supernatant was discarded and pellet was collected.

### 4.5.2 Fixation

Before fixation, collected pellet was washed twice with PBS. During washing pellet was transferred to the 15ml Falcon tube. After PBS wash pellet was resuspended in 1ml ice-cold (-20) methanol in PBS (90:10).

To avoid clumps of cells during resuspension; pellet was initially resuspended in 100µl PBS and then 900µl of ice-cold methanol was added drop wise with continuous vortex. This suspension then incubated on ice for 30 min and then transferred to $-20^0$ C until required for analysis.

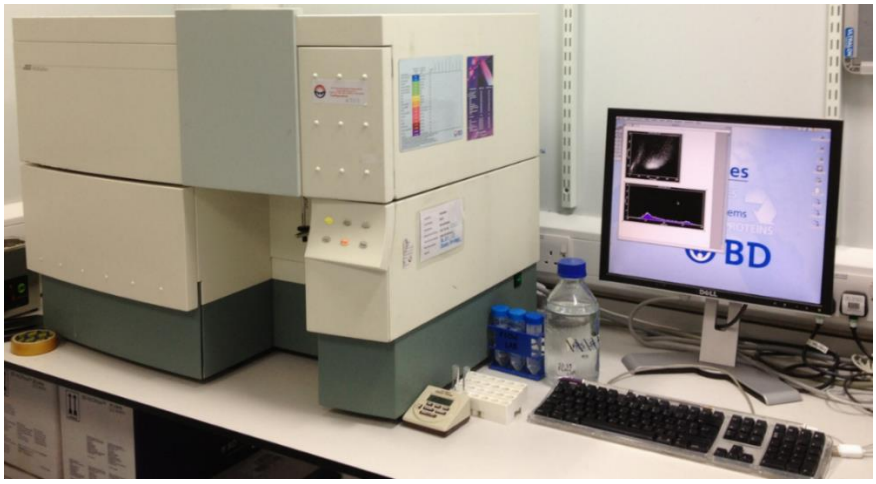


***Figure 4.31: FACS machine (BD Biosciences)***

### 4.5.3 Staining with Antibody

#### 4.5.3.1 Staining with specific primary and secondary antibody

Fixed samples removed from -20$^0$ C storage, and centrifuged to get sell pellet. Obtained cell pellet was washed twice with incubation buffer (PBS containing 0.5% BSA). This washing step was done to get rid of methanol. After washing and centrifugation, pellet was obtained, which was resuspended in 200μl incubation buffer.

Suspended pellet incubated for 10min at room temperature and 4μl of primary antibody (final concentration 1:50) per vial containing 200μl of cell suspension in incubation buffer was added. The suspension then kept for incubation at room temperature for about 1hr.

1hr incubation followed by centrifugation to collect cell pellet. Pellet was washed twice with incubation buffer and finally resuspended in 200μl incubation buffer containing secondary antibody having final concentration 1:1000 (1μl antiboby

diluted to 1000μl incubation buffer). Cells with secondary antibody were incubated for 30min in dark condition at room temperature. Once incubation done, volume of samples was matched to 1ml by addition of 800μl of incubation buffer (200μl initial volume) and samples were analysed by FACS (Figure 4.31).

Each cell line having two vials as one treated with primary and secondary antibody and other one treated with secondary antibody alone. Each sample analysed three times

#### 4.5.3.2 Staining with positive and negative control antibodies

Same like above, in second set of study each cell sample were equally divided in two vials to get equal protein concentration. Antibody staining protocol was used same as above. Cells were treated with Positive and negative control primary antibodies and incubated for 1hr at room temperature. Once incubation with primary antibodies done, then cells were centrifuged and pellet was washed twice with incubation buffer and followed by the corresponding secondary antibody treatment as mentioned in above protocol. Once all treatments and incubations with both primary and secondary antibodies were done, volume of sample matched to 1ml by adding required amount of incubation buffer, and finally samples were analysed with FACS taking three reads per sample.

## 4.6 Rhodamine efflux Assay

Rhodamine efflux assay protocol was adapted from previously developed method. Procedure to study rhodamine efflux assay was used with several modifications in it to achieve better results. Black bottom 96 well plates were used to carry this assay.

1. Protocol-1:

Day-1

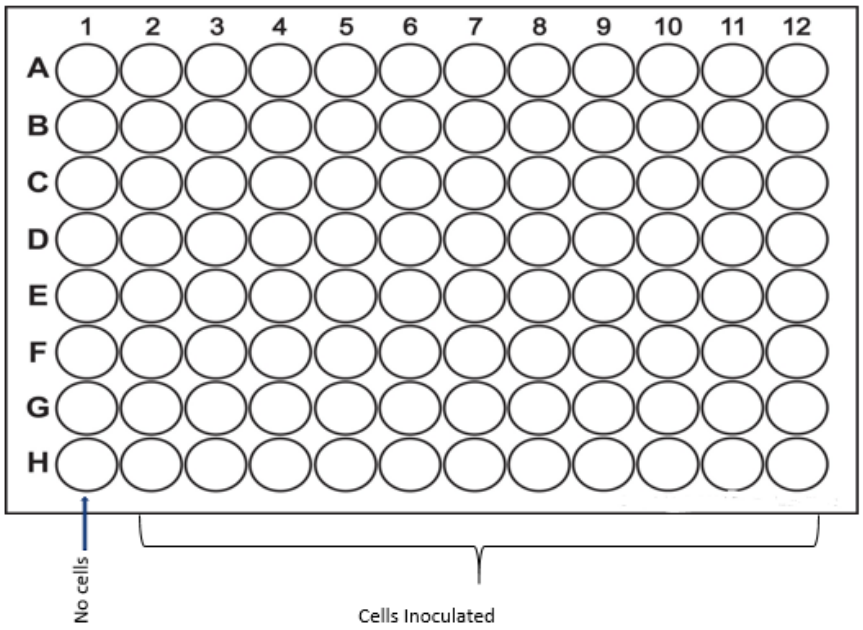


***Figure 4.32: Rh123 assay_ cells inoculation***

Cells were grown to approx. 80% confluence, and then used to carry out study. Flask with grown cells was removed from incubator and cells were washed twice with PBS and then trypsinised. After addition of trypsin cells were incubated for about 5 mins and then media was added once cells were detached from the surface of the flask. Trypsinised cells were then centrifuged to get rid of media containing trypsin and pellet was collected which then

resuspended in the fresh growth medium, Cell count was taken and cell suspension with $1\times10^5$ cells/ml was prepared. With multichannel pipette, 200µl cell suspension to each well was inoculated except 1st row (Figure 4.32); which means $2\times10^4$ cells/well was inoculated. Plated then placed for the incubation at $37^0$ C with 5% $CO_2$ and incubated for 24 hrs.

Day-2

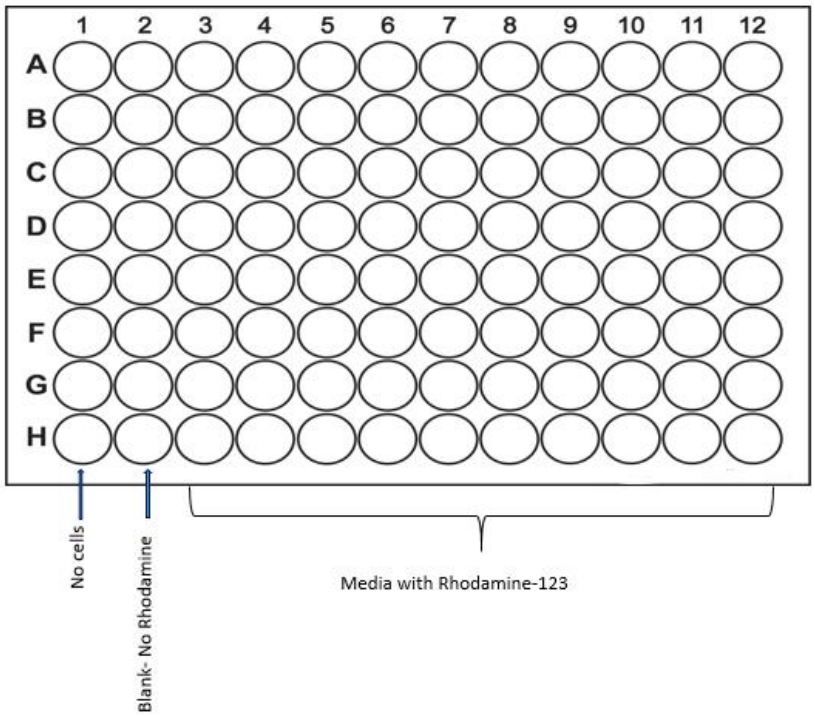


***Figure 4.33: Rh123 assay_Rhodamine 123 treatment***

Next day when 24 hrs incubation done, plates were removed from incubator and placed in laminar. Old media from each well was removed and replaced with fresh media containing 8µM rhodamine-123 in it. Rhodamine containing media was replaced in all wells except 1st and 2nd row as shown in the Figure 4.33 Cells then placed back for 1 hr incubation with rhodamine-123.

After 1hr incubation, rhodamine containing media was removed from all the wells and each well was replaced with the fresh media or corresponding inhibitor solutions as shown in the Figure 4.34 below. Once all wells were replaced with their corresponding solutions; plates then moved to plate reader which was set to continuous reading mode with 37$^0$C incubation temperature to incubate plates throughout readings. Readings were taken started from zero time reading and followed with every hr reading up to 24 hrs. After 24 hrs, viability of cells was tested using tryphan blue cell count method to ensure the cell viability after 24 hrs reading.

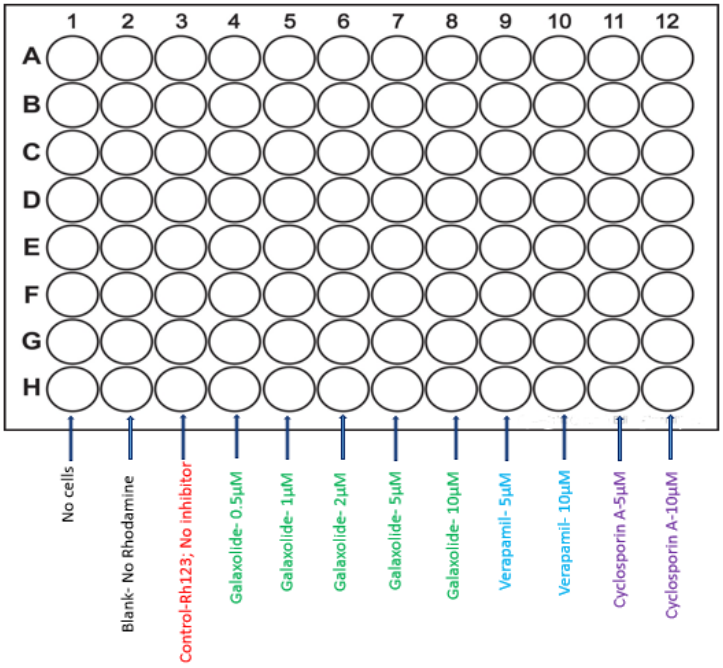


***Figure 4.34: Rh123 assay_Pgp inhibitor treatment***

2. Protocol-2:

This protocol is slight modification of above protocol-1.All changes were done on Day-2 procedure; while Day-1 procedure is unchanged throughout. Day-1 procedure was same; while there was one step added in Day-2 procedure. After

incubation with rh123 for 1hr, instead of replacing fresh media or corresponding inhibitor solutions directly, cells were washed thrice with fresh media after Rh123 incubation was removed, and then replaced with media solutions containing respective inhibitors with different concentrations. This step is done to get rid of excess rh123, which is not penetrated in cells. Finally well plates were moved to the plate reader to measure readings as mentioned above in Protocol-1.

3. Protocol-3

Like protocol-2, this protocol is modification as well derived from protocol-1. On Day-2, Cells were incubated with Rhodamine-123 solution for 1hr. Unlike of protocol-1 and 2; Rhodamine-123 solution was prepared in respective inhibitor solution, and rhodamine-123 was treated in presence of P-gp inhibitors. After 1hr incubation, rhodamine-123 solution was removed and cells were washed thrice with fresh media as done in protocol-1. After washing wells were replaced with corresponding inhibitor solutions. Plates then taken to the plate reader and readings were taken as mentioned above.

4. Protocol-4

In this protocol, on Day-2 wells were removed from incubator and old media was taken out. Before Rhodamine-123 treatment, cells were pre-incubated for 1 hr with respective inhibitor solutions. After 1 hr incubation, inhibitor solutions were replaced with the rhodamine-123 solution prepared again in inhibitor solutions and plates were placed back for incubation for 1hr. After 1hr incubation plates were removed from incubator and rhodamine-123 solution was taken out and plates were washed thrice with the fresh media and replaced with corresponding inhibitor solutions prepared in growth media. Plates then

moved to plate reader (Figure 4.35) and readings were recorded as per previously mentioned.

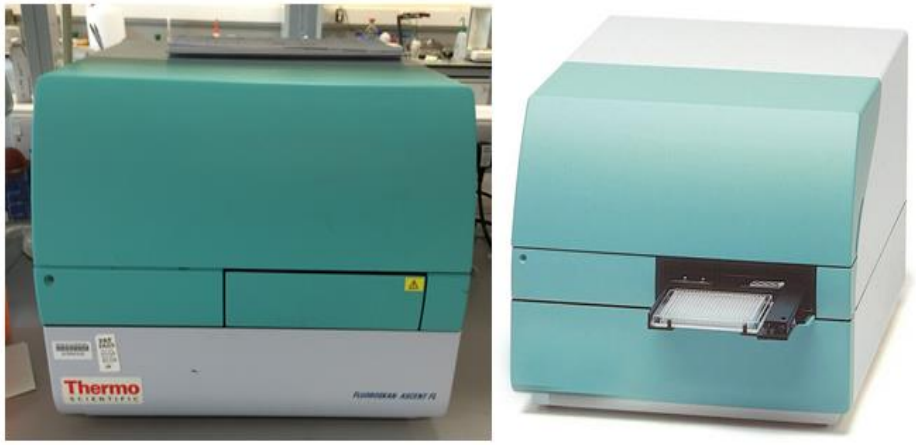


***Figure 4.35: Fluorescence plate reader***

## 4.7 HPLC Method development for Curcumin Quantification

To study curcumin permeability, it is necessary to develop analytical method to quantify the amount of curcumin permeated through the cell monolayers. HPLC method is developed for curcumin analysis from previously reported method (Li et al., 2009).

### 4.7.1 Method development without use of internal standard

Two different HPLC methods were developed with and without use of internal standard. To develop these methods, the solvent preparation and HPLC conditions are explained below.

#### 4.7.1.1 Preparation of curcumin solutions

Curcumin solutions were prepared in growth media to analyse with the HPLC. Curcumin is water insoluble so DMSO is used to dissolve it for the preparation

of desired concentrations. Initially solution with 10mM was prepared in 1ml of DMSO which was considered as a stock solution, and then it is diluted to 100 µM in the growth medium which is considered as a working solution/concentration. To prepare the working concentration with 100µM, 10 µl of stock solution was taken and diluted it to the 10ml with the growth medium. This curcumin solution was further diluted with growth media to achieve desired concentrations.

Once desired concentrations was prepared in the media, the prepared samples then followed with the extraction method. During extraction, equal volume of acetonitrile was added to the samples prepared. Mixed well and incubated for 10-15 mins at room temperature to precipitate proteins present in the media. After incubation samples were centrifuged at 13000 rcf for 15 mins at $4^0$C. Supernatant was collected gently and transferred to the HPLC vial and then analysed with the HPLC.

#### 4.7.1.2 Preparation of mobile phase-0.1% trifluoroacetic acid:Acetonitrile (40:60)

Isocratic mobile phase was used for the analysis of curcumin. At first 0.1% trifluoroacetic acid was prepared at a volume of 1L. 1L of distilled water was taken and 1ml of distilled water replaced with trifluoroacetic acid, which gives 0.1% triflouroacetic acid. 400ml of trifluoroacetic acid was taken and 600 ml of acetonitrile was added to it to make total volume 1L, which gives mobile phase having both solvents; 0.1% triflouroacetic acid and acetonitrile in a ratio of 40:60.

#### 4.7.1.3 HPLC System

Quantification of curcumin was done by using Waters e2695 HPLC system with Waters 2998 Photodiode Array Detector. The peaks were analysed by using Empower software. Column used was Waters Symmetry C18 5µ and 4.6×250mm. Isocratic mobile phase was used. Mobile phase solvents were 0.1% trifluoroacetic acid and Acetonitrile mixed in ratio of 40:60. All the solvents used were HPLC grade. All samples were analysed using flow rate 1ml/min with an injection volume 20µl. During analysis the samples were stored at $10^0$C while column was stored at $25^0$C. The run time for per sample was 15 min and the detection of analytes was made at the wavelength of 420nm. The following Table 4.5 describes the HPLC system and conditions.

***Table 4.5: HPLC method for curcumin without internal standard***

| |
|---|
| Run Time: **15min** |
| Mobile Phase: **0.1% Trifluoroacetic acid: Acetonitrile (ACN)** [40:60] - Isocratic |
| Column: **Waters Symmetry C18; 5µ; 4.6 X 250mm** |
| Wavelength: **420nm** |
| Flow Rate: **1ml/min** |
| Column Temp.: **$25^0$C** |
| Sample Temp.:**$10^0$C** |
| Detector: **Waters 2998 Photodiode Array Detector** |
| Software: **Empower 3** |
| HPLC System: **Waters e2695** |

### 4.7.2 Method development with internal standard

In this method emodin is used as an internal standard for the curcumin. Internal standard can be useful to minimize the error occurred by injection volumes.

#### 4.7.2.1 Preparation of curcumin and Emodin (Internal Standard) solutions

Curcumin solutions were prepared similarly as described in above procedure (4.7.1.1). Emodin was used as internal standard for curcumin. As emodin is water insoluble, it was dissolved in DMSO and stock solution of 0.5mM was prepared in DMSO. 20µM emodin was used throughout the studies, so to get this working concentration, stock solution was diluted accordingly in acetonitrile. During extraction step this emodin containing acetonitrile was mixed to curcumin samples instead of plain acetonitrile. Samples then mixed well and incubated for 10-15 mins at room temperature and then centrifuged at 13000 rcf for 15 mins at $4^0$ C. Supernatant then collected gently and transferred to the HPLC vials. Pellet was discarded. Supernatant was analysed then with HPLC.

***Table 4.6: HPLC method for curcumin with internal standard***

| |
|---|
| Run Time: **15min** |
| Mobile Phase: **0.1% Trifluoroacetic acid: Acetonitrile (ACN)** [40:60] - Isocratic |
| Column: **Waters Symmetry C18; 5µ; 4.6 X 250mm** |
| Wavelength: **420nm** |
| Flow Rate: **1.5ml/min** |
| Column Temp.: **$25^0$C** |
| Sample Temp.:**$10^0$C** |
| Detector: **Waters 2998 Photodiode Array Detector** |
| Software: **Empower 3** |
| HPLC System: **Warers e2695** |

Similar HPLC system was used as above with only change in flow rate. Flow rate was changed to 1.5ml/min; while all other conditions were kept unchanged. The Table 4.6 will describes the HPLC system and conditions used.

### 4.7.3 Curcumin analysis in Serum containing and Serum free media with 1:1 and 1:2 extraction methods:

This study was carried out to understand amount of curcumin yield in different media using different extraction methods. The experiment was set in two different groups; of which one having curcumin solutions prepared in serum containing media that means regular growth media while other group had

curcumin solutions prepared in serum free media. Each of the group was followed with the two different extraction methods of which one contain extraction with equal amount of acetonitrile that means acetonitrile was added to sample during extraction was having equal amount as that of sample so called as 1:1 extraction method. The other extraction method was having one part of sample volume and two parts of the acetonitrile during extraction which is named as 1:2 extraction method. These extraction methods were applied to both the above groups. Once respective volume of acetonitrile was added, samples were incubated for 10-15 mins at room temperature and after incubation centrifuged at 13000 rcf for 15 mi at $4^0$ C. Supernatant was collected gently and transferred to the HPLC vials and analysis were done. Peak areas were recorded and graphs were plotted accordingly.

### 4.7.4 Extraction Efficiency in Serum Media

From the results obtained in previous study, serum media with 1:1 extraction method was selected for the further studies. The extraction efficiency of curcumin in selected serum media was studied. To study extraction efficiency, two sets of curcumin samples were prepared separately, one in serum media and other in pure acetonitrile. 1:1 Extraction method was applied that is equal volume of acetonitrile was added to the samples prepared in serum media and acetonitrile. Then incubated for 10-15 min and followed with centrifugation at 13000 rcf for 15 mins at $4^0$ C. Only samples prepared in serum media gave supernatant and pellet, so supernatant from media samples were collected gently and transferred to the HPLC vials. Samples prepared in acetonitrile did not yield two fractions like supernatant and pellet so they were transferred to

HPLC vials straight away. All the samples then analysed by the HPLC and peak areas were recorded. Obtained peak areas of both the samples were used to compare them together and calculate extraction efficiency. Extraction efficiency was calculated by using following formula.

$$\boldsymbol{Extraction\ Efficiency}(\%) = \frac{\boldsymbol{PA_{EXT}}}{\boldsymbol{PA_{Not}EXT}} \times \mathbf{100}$$

Where,

PA_EXT= Peak Area after Extraction

PA_Not EXT= Peak Area without extraction (sample in pure solvent)

### 4.7.5 Curcumin Analysis in 4% BSA Media

4% BSA media was used for the later permeation studies. The BSA media was prepared with addition of 4% BSA in Hank's Balanced Salt Solution (HBSS) with $P^H$ 7.0. The media was used as receiver media in permeation study, so it needs to study curcumin yield in above mentioned media. So curcumin samples were prepared using 4% BSA media and analysed with HPLC. To study the difference in yield, the curcumin samples were prepared in three different solvents as curcumin in pure acetonitrile, curcumin in HBSS without BSA and curcumin in 4% BSA, internal standard was directly added to these samples during curcumin formulation. Of these three samples, pure acetonitrile and HBSS without BSA prepared samples were directly analysed with HPLC. While samples prepared in 4% BSA media were extracted with two different extraction methods as 1:1 and 1:2. After extraction these two samples were analysed by HPLC. Peak areas were recorded for all samples and yield of curcumin in form

of extraction efficiency was calculated with comparing peak areas of acetonitrile with rest of the samples.

### 4.7.6 Curcumin Extraction Efficiency in 4% BSA Media

Further to previous study, extraction efficiency of curcumin was studied in 4% BSA media with 1:1 extraction method. As these mentioned conditions gave high curcumin yield in previous study, the media was used for the permeation study. To calculate extraction efficiency, two sets of curcumin concentrations were prepared. One set was prepared in acetonitrile with curcumin concentrations 6.25µM, 12.5µM, 25µM and 50µM and another set was prepared in 4% BSA media with same curcumin concentrations. Once all samples were prepared, acetonitrile with 20µM emodin was prepared. This acetonitrile with emodin was used for the extraction and added to all the prepared sampled in equal volume of samples. All samples were then incubated at room temperature for 10-15 mins and then centrifuged at 13000 rcf for 15 mins at $4^0$ C. Samples then removed after centrifugation and supernatant was collected gently and transferred to the HPLC vials. All samples were then analysed with HPLC and peak areas for all samples were recorded and compared to calculate the extraction efficiency. Same formula as above was used to calculate the extraction efficiency.

## 4.8 Permeability Study

To study permeability study, it is necessary to form the uniform and intact cell membrane on the transwell. Once membrane is formed drug samples were applied to the apical side of membrane and permeation was monitored. Processes involved in this study are described as follow.

### 4.8.1 Generation of Cell membrane on transwells

Cells when reached to approx. 80% or more confluence was used for experimental set up. Flasks were taken out from incubator, cells were washed and trypsinised as per above mentioned procedure and cell suspension was prepared. Cell count was taken using haemocytometer and cell suspension having cell density $1 \times 10^6$ cells/ml was prepared. Each transwell inoculated with the 100µl cell suspension, it means $1 \times 10^5$ cells/transwell was seeded. Transwells were placed in well plates and moved to incubator for 2 hrs incubation without addition of any media to the bottom chamber of transwells. This step is done to allow cells to attach to the transwell membrane. After incubation plates were removed and 200µl media to top chamber and 1.5ml media to bottom chamber were added and plates were returned for the incubation at $37^0$ C supplemented with 5% $CO_2$. Medium was changed every three days of interval until cell membranes were ready for permeability study. TEER value was measured before and after the permeation to assess the confluence of cell monolayer.

### 4.8.2 Preparation of donor and receiver media

Curcumin is used as a drug sample while galaxolide as a permeation enhancer in this study.

To carry out permeability study through the cell membranes grown on transwells, donor and receiver media were needed. Donor media was prepared with drug concentrations while receiver media was the media without any drug concentration. Several donor and receiver media was prepared to carry out permeability study. Curcumin was the drug used to carry out permeability along

with the addition of galaxolide which was supposed to be the permeability enhancer. According to the need of experiment various donor and receiver media was prepared.

In initial studies, donor media was prepared in the growth medium. 50µM and 100µM curcumin solution was prepared in growth media. Curcumin is water insoluble compound, so it was initially dissolved in the DMSO solution and then further diluted with the assay media to get required working concentration making sure that DMSO concentration in donor media was not more than 1%. To study effect of galaxolide on permeability of curcumin, donor media was supplemented with 1µM or 5µM galaxolide in addition with above mentioned curcumin solutions. Galaxolide as well insoluble in water, so same as like curcumin, it was initially dissolved in DMSO and then further diluted with assay media to get working concentrations. The pH of this donor media was 7.4 throughout the studies. This donor media was supported with the receiver media which is nothing but regular growth media having pH 7.4. These donor and receiver media was used to study permeability of curcumin through several cell lines.

The other donor and receiver mediums were prepared in the HBSS solutions. To prepare donor media HBSS was supplemented with 20mM HEPES buffer having pH 6.5. The drug solutions were prepared in this donor media and drug solutions are curcumin, curcumin + galaxolide and curcumin + verapamil. Curcumin was used at concentration of 50µM while concentrations of galaxolide and verapamil were used 5µM each. All drug solutions were prepared as mentioned above. Unlike curcumin and galaxolide, verapamil is

water soluble, so it was directly dissolved in distilled water to get stock solution and further diluted with assay media in order to get working solution. The receiver media contain 4% BSA prepared in HBSS with addition of 20mM HEPES buffer. The pH of receiver media was set to the 7.0.

The donor media was applied to the upper compartment while receiver media was added in the lower compartment to study the permeability of curcumin through cell membrane.

Following figures; Figure 4.36, Figure 4.37 and Figure 4.38 describes the different experimental set ups with different donor and receiver media.

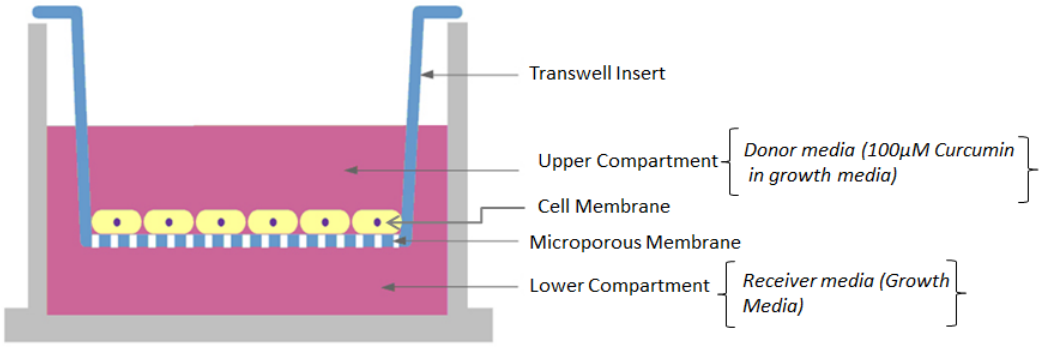


***Figure 4.36: Permeability study_100µM curcumin in media***

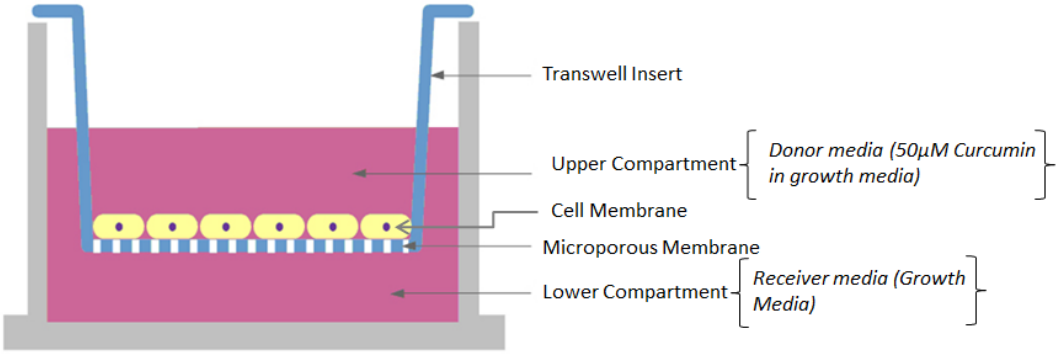


***Figure 4.37: Permeability study_50µM curcumin in media***

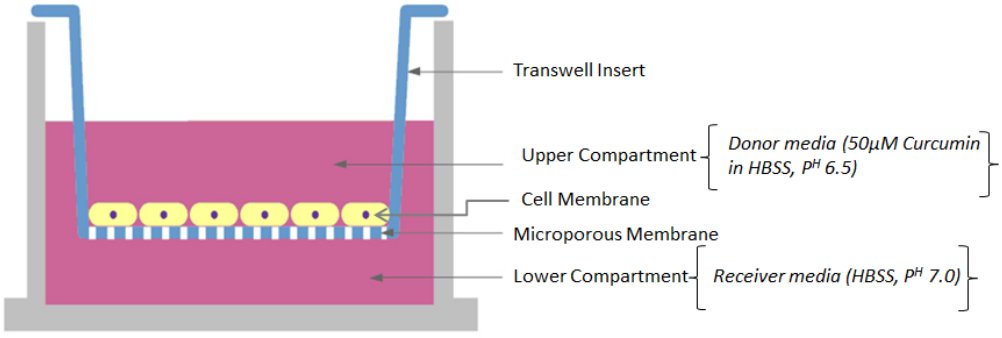


***Figure 4.38: Permeability study_50µM curcumin in HBSS***

### 4.8.3 Permeability Study

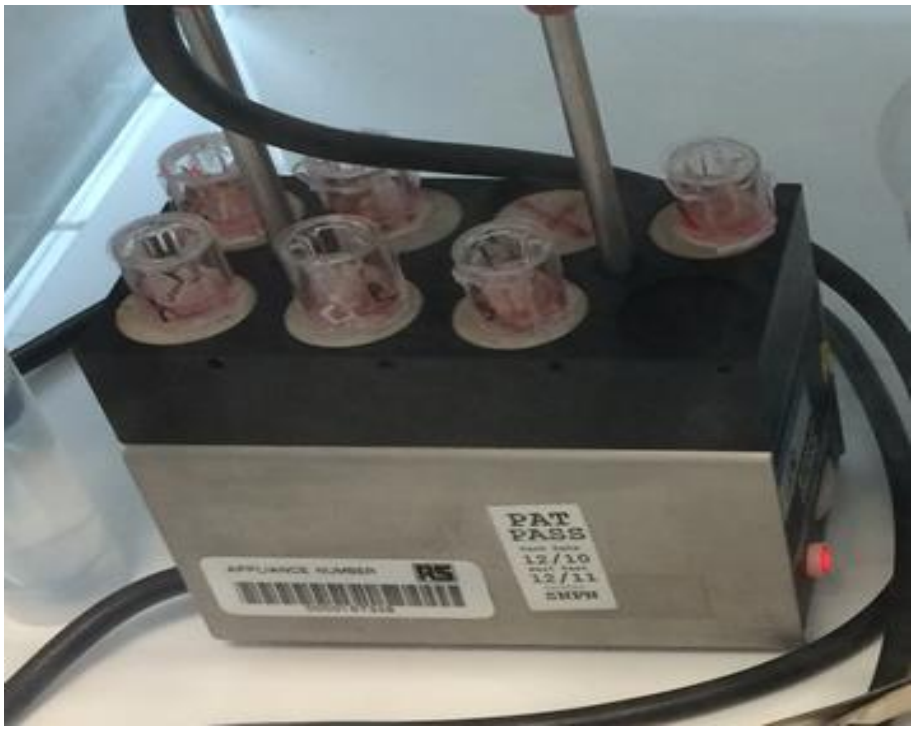


***Figure 4.39: Magnetic stirrer***

Cells were grown on the transwells until get intact cell membrane. The growth time on transwells was different for different cell lines, so cells were grown as per their individual requirements. Once cell membrane was intact and ready to carry out permeation study, transwells were removed from the incubator. Old media was removed from transwells using micropipette and replaced with the fresh media. Medium change order was same as described earlier. In the meantime, TEER measurement assembly was made ready, and TEER measuring probe was placed for calibration in media. Once media was changed for each transwell, TEER value was measured for each transwell along with the one blank transwell. TEER values were recorded. Transwells which were planned to treat with curcumin+galaxolide drug combination were pre-treated

with respective galaxolide concentration. Plates were placed in incubator for 1hr. After 1hr pre-treatment of galaxolide, plates were removed from incubator; transwells were allocated as per need. 200µl donor media with drug solutions was added to each transwell and transwells were placed in receiver compartment containing 1.2ml receiver media in it and a piece of stirrer wire. The permeation assembly was immedietly moved to the magnetic stirrer (Figure 4.39) fitted in the incubator. The permeation study was carried out at $37^0$C supplemented with 5% $CO_2$. Sample was collected at each time point.

During sample collection, 600µl solution from receiver media was collected and replaced with same amount of fresh receiver media. The solution from upper compartment (donor media) was remained unchanged till end of the study. In earlier studies, during sample collection, solutions from both the compartments were replaced every time. The samples were collected on various time points and finally analysed by HPLC. Once all samples were collected and study was done, TEER was measured once again and histology study of cell membranes was carried to check integrity of cell membranes.

### 4.8.4 HPLC Analysis

Samples collected were then analysed with HPLC method to detect amount of curcumin permeated at different time points. 600µl sample was collected at each time point. These samples were then extracted with HPLC grade acetonitrile. For extraction of samples, same amount of acetonitrile was added to the samples and samples were mixed well with vortex and incubated for 15min at room temperature. Once precipitate was appeared, samples were

centrifuged at 13000rcf, for 15 mins at $4^0$C. Supernatant was collected in and analysed with HPLC method described as above.

Quantification of curcumin was done by HPLC, using Waters e2695 HPLC system with Waters 2998 Photodiode Array Detector. The peaks were analysed by using Empower software. Column used as Waters Symmetry C18 5µ and 4.6×250mm. Mobile phase solvents were 0.1% trifluoro-acetic acid and Acetonitrile mixed in ratio of 40:60. Isocratic mobile phase was used. All the solvents used were HPLC grade. All samples were analysed using flow rate 1ml/min with an injection volume 20µl. Samples which were prepared with internal standard, were analysed using flow rate 1.5ml/min. During analysis the samples were stored at $10^0$C while column was stored at $25^0$C. The run time for per sample was 15 min and the detection of analytes was made at the wavelength of 420nm.

The samples analysed using internal standard, were extracted using acetonitrile containing 20µM emodin in it. Other procedures were followed as same. HPLC data was recorded and analysed. The apparent permeation rate was calculated using formula (Yu and Huang, 2011):

$$\boldsymbol{P_{app}} = \left(\frac{\boldsymbol{dQ}}{\boldsymbol{dt}}\right)\left(\frac{\mathbf{1}}{\boldsymbol{AC_0}}\right)$$

Where,

*dQ/dt* = rate of curcumin permeation

*A* = surface area of the transwell insert

$C_0$= initial concentration of curcumin

### 4.8.5 Histology study of cell membranes after permeability

Transwell membranes after permeability study were removed from magnetic stirrer and placed in well plates. Drug solutions were removed and transwells were washed twice with fresh media and finally 200µl in top chamber and 700µl in bottom chamber was flooded with fresh media. TEER readings were taken as mentioned earlier along with blank transwell. Transwells then fixed in Bouin's solution for 1 hr and then washed and stored in 70% ethanol. Histology study was carried when all transwells were ready.

# 5 : P-glycoprotein expression and inhibition

## 5.1 Introduction

The main objective in this chapter is to determine the safe concentration of galaxolide to use in cell based assays. Another objective is to study the P-gp expression in various cell lines, and later use these P-gp expressing cells to study P-gp inhibition assay and to determine the ability of galaxolide to inhibit P-gp.

## 5.2 Galaxolide Cytotoxicity

This research is focused to explore the P-gp inhibitory activity of galaxolide, and to use this characteristic of galaxolide for the improvement of drug permeation through the biological membranes. Galaxolide is key compound in experiment and used as novel efflux inhibitor molecule in this research and that is why it was necessary to study its toxicity on cell lines. So to determine safe concentration of galaxolide, toxicity study was done on various cell lines using MTT assay.

The general purpose of the MTT (3-[4,5-dimethylthiazol-2-yl]-2,5diphenyl tetrazolium bromide) assay is to measure viable cells in relatively high throughput 96-well plates, without the need of cell counting. The assay is based on the conversion of MTT into formazan crystals by living cells, which determines mitochondrial activity. For most cells, the total mitochondrial activity is related to the number of viable cells. The MTT assay is mainly used to measure the *in vitro* cytotoxic effects of drugs on cell lines.

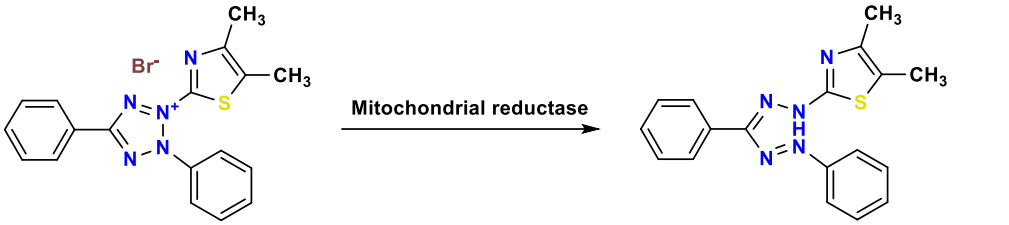


3-(4,5-dimethylthiazol-2-yl)-2,5-diphenyltetrazolium bromide (MTT)

(E,Z)-5-(4,5-dimethylthiazol-2-yl)-1,3-diphenylformazan (Formazan)

***Figure 5.1: Conversion of the tetrazolium salt MTT into formazan crystals***

*(Mosmann, 1983)*

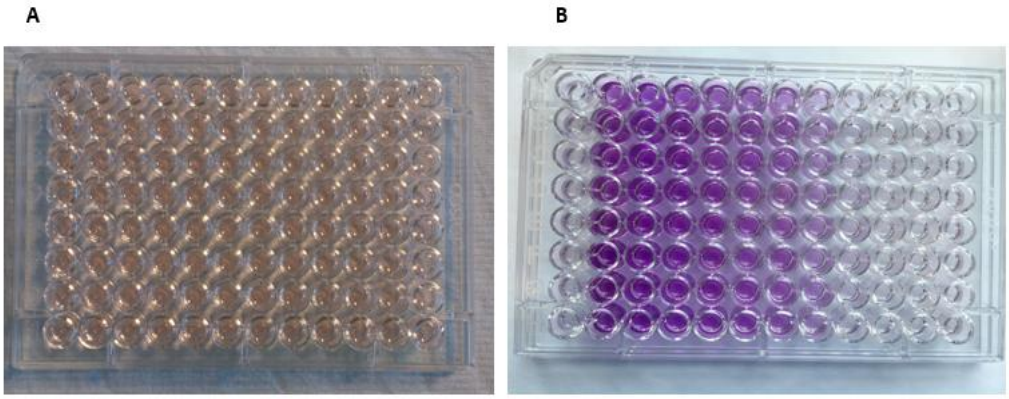


***Figure 5.2: MTT well plates A) before B) after addition of MTT dye***

*The colour formation is proportional to the number of living cells. Figure (B) shows the colour intensity goes on reducing on higher drug concentration side (right hand side). This is because of the more cell death at high drug concentration.*

The principle of the MTT assay is based on the mitochondrial activity of viable cells and for most of the cells it is constant; so any increase or decrease in the number of viable cells is directly proportional to change in mitochondrial activity. As mentioned earlier the mitochondrial activity is reflected by the formation of formazan crystals, which can be solubilised using DMSO for homogenous measurement. The optical density (OD) of formazan can be detected at 540nm. So any increase or decrease in viable cell number can be detected by measuring formazan concentration reflected in optical density.

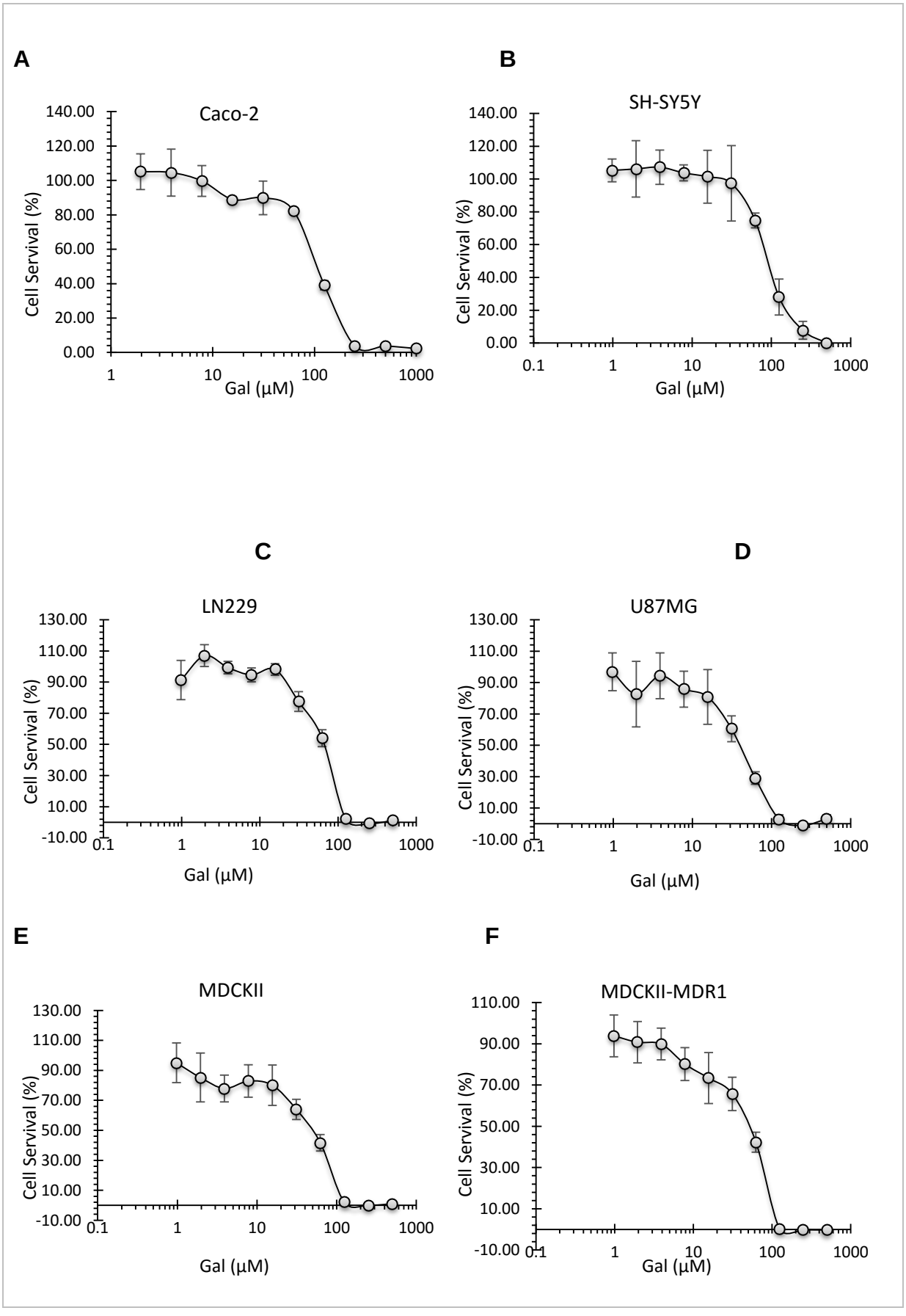
A
Caco-2
Cell Servival (%)
Gal (μM)
B
SH-SY5Y
Cell Servival (%)
Gal (μM)
C
LN229
Cell Servival (%)
Gal (μM)
D
U87MG
Cell Servival (%)
Gal (μM)
E
MDCKII
Cell Servival (%)
Gal (μM)
F
MDCKII-MDR1
Cell Servival (%)
Gal (μM)

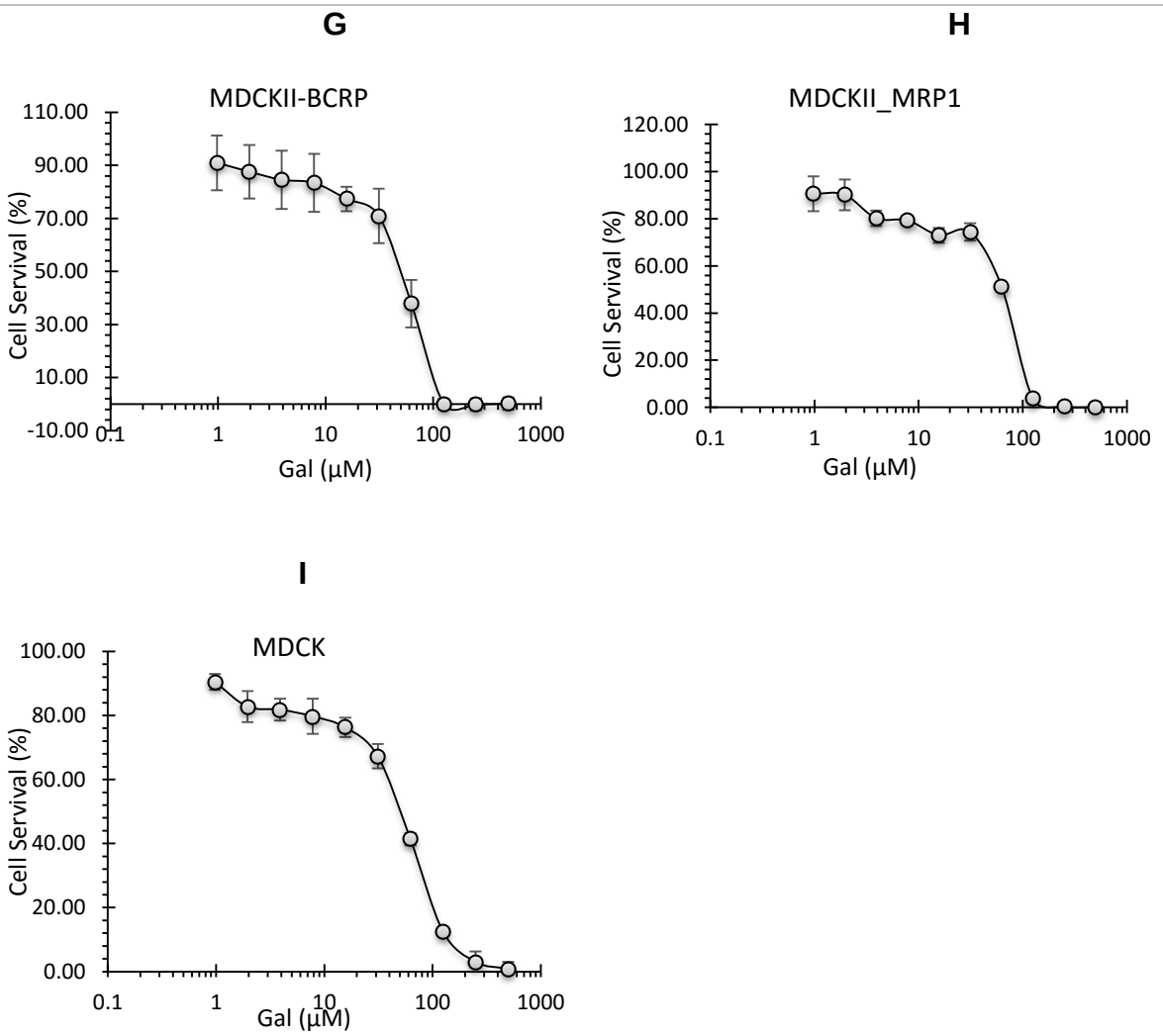


***Figure 5.3: MTT Assay_ Dose response curves for various cell lines***

*(A) Caco-2, (B) SH-SY5Y, (C)LN-229, (D) U87MG, (E) MDCKII, (F) MDCKII-MDR1, (G) MDCKII-BCRP, (H) MDCKII-MRP1 and (I) MDCK*

The Figure 5.3 shows the dose responsive curve for the various cell lines which contains values plotted on X and Y-axis as concentration (µM) vs cell survival (%) respectively. The dose response curves are steady at the initial stage which means more number of cell survival is there at lower drug concentration range and as concentration is increasing, the survival rate dropped exponentially and after that once again graph shows steady phase, and which has very few or no

cell survival at these stage, and this is because of the very high concentration of the drug exposure to the cells. Different cell lines were treated with galaxolide concentrations prepared with two fold dilution along with blank wells and untreated cells as a control of an experiment. When plates were measured with plate reader, the readings are used to plot dose responsive curves. To achieve these dose responsive curves, untreated cells are set as 100% survival and various concentrations of galaxolide were used against these untreated cells to calculate the percent survival of cells at given concentration of the galaxolide. By using these dose responsive curves $IC_{50}$ value (The value of $IC_{50}$ for a drug, is the dose required to inhibit half the population of a tested cells *in vitro* after a specified test duration) of galaxolide for each given cell line is calculated (Table 5.1).

***Table 5.1: Various cell lines with corresponding $IC_{50}$ values of Galaxolide***

| **Cell line** | **Galaxolide_$IC_{50}$ (µM) ± SD (n=3)** |
|---|---|
| Caco2 | 109.27 ± 2.99 |
| SH-SY5Y | 96.82 ± 7.19 |
| LN229 | 66.92 ± 6.41 |
| U87MG | 41.08 ± 7.32 |
| MDCK | 51.98 ± 2.32 |
| MDCKII | 50.51 ± 7.62 |
| MDCKII-MDR1 | 51.51 ± 6.98 |
| MDCKII-BCRP | 50.77 ± 9.30 |
| MDCKII-MRP1 | 64.19± 0.61 |

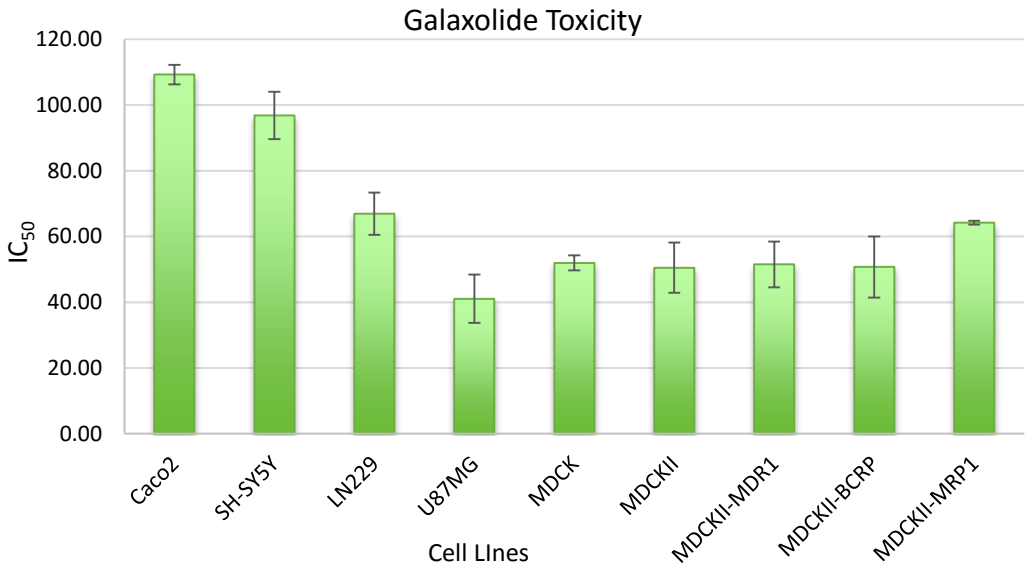


***Figure 5.4: Various cell lines with corresponding $IC_{50}$ values of Galaxolide***

Total nine different cell lines were used to study galaxolide toxicity. Some cells were cancer cell lines (LN229 and U87MG) while some were normal cells (Caco-2, SH-SY5Y, MDCK, MDCKII, MDCKII-MDR1, MDCKII-BCRP and MDCKII-MRP1. Amongst the tested cells against galaxolide, Caco-2 cell line shows highest $IC_{50}$ value which is about 98.87 µM while U87MG cell line shows lowest $IC_{50}$ value; 40.45µM. All other tested cells; SH-SY5Y (95.03µM), LN229 (66.90µM), MDCK (52.29µM) have shown different $IC_{50}$ values when tested for galaxolide toxicity. The derivatives of MDCK cell lines such as MDCKII cell line, MDCKII-MDR1 (MDR1/P-gp overexpressing cell lines), MDCKII-BCRP (BCRP overexpressing cell line) and MDCKII-MRP1 (MRP1 overexpressing cell line) have $IC_{50}$ values 55.02µM, 51.76µM, 49.56µM, and 64.19µM respectively. Data observed in above experiments shows that, Caco-2 cells are more resistive against galaxolide compared to all other cell lines. Also no cell line amongst the

tested cells have $IC_{50}$ value below 40µM, that means it is safer to use galaxolide below this concentration to carry out further experiments to evaluate galaxolide.

### 5.3 Effect of Galaxolide on drug toxicity

Use of galaxolide in this research was to evaluate it as an efflux protein inhibitor molecule such as P-glycoprotein inhibitor and to suppress the multidrug resistance conferred by the target cell, and as a result of which the drug molecule treated in combination with galaxolide should show higher activity against the targeted cells. This could be achieved by the suppression of the multi drug resistance with galaxolide in cells and allow accumulation of the drug inside the targeted cell. The drug toxicity assay/MTT assay was carried to study this hypothesis. Curcumin and Temozolomide were used as the drug candidates and was administered to the cells with and without the galaxolide. Drug candidates were applied in combination with known P-glycoprotein inhibitors such as Cyclosporine A and Verapamil as a positive control to track down the galaxolide activity. Dose response curves were obtained from the measurements observed (Figure 5.5, Figure 5.6 and Figure 5.7) and $IC_{50}$ values were obtained and compared to study the effect of galaxolide. U87MG and LN229 cell lines were used for this study. Both these cells are derived from the glioblastoma cells, and one of research objective was to improve drug delivery to brain cancer, so these cell models were used to study effect of galaxolide on drugs toxicity with respect to glioblastoma cells.

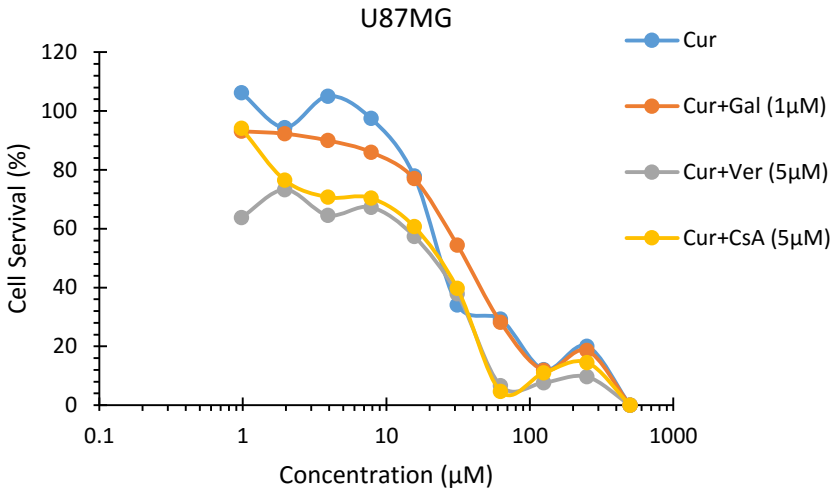


***Figure 5.5: Dose Responsive Curve of U87MG cells***

*with curcumin and Curcumin+ P-gp inhibitors (galaxolide, verapamil and cyclosporine A)*

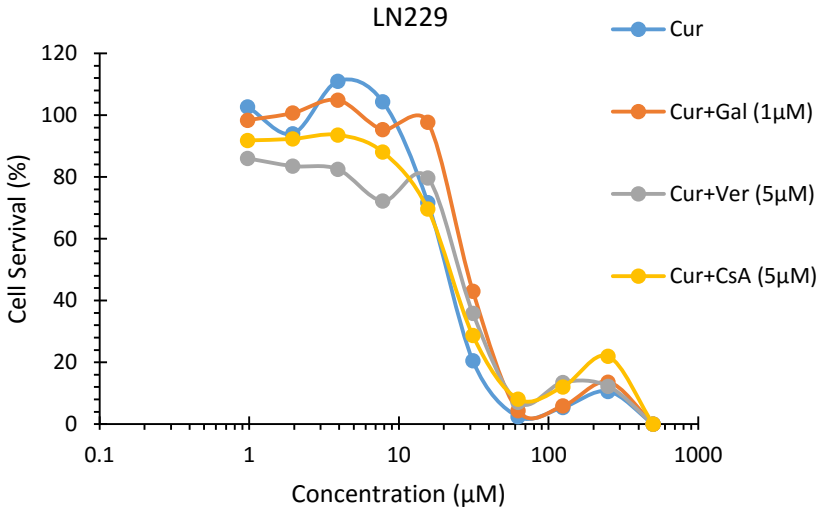


***Figure 5.6: Dose Responsive Curve of LN229 cells***

*with curcumin and Curcumin+ P-gp inhibitors (galaxolide, verapamil and cyclosporine A)*

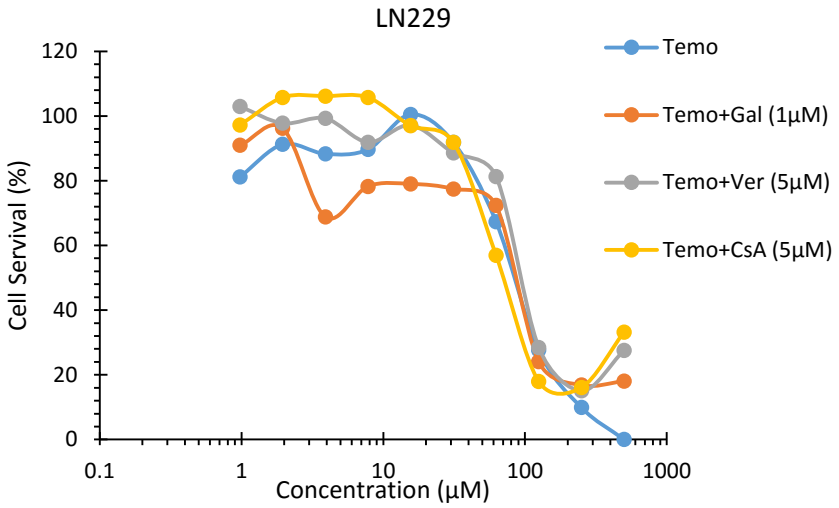


***Figure 5.7: Dose Responsive Curve of LN229 cells***

*with Temozolomide and Temozolomide+ P-gp inhibitors (galaxolide, verapamil and cyclosporine A)*

Curcumin and Temozolomide were treated with and without galaxolide and known P-gp inhibitor compounds. The dose responsive curves were obtained for each of the drug combinations as observed in the Figure 5.5, Figure 5.6 and Figure 5.7. For each curve, the graph line started with steady line at the lower concentration range (approx. 0.97 µM to 15 µM) and it felt down as concentration goes on increasing (approx. from 15 µM to 125 µM) and again it was appeared to be steady at the higher concentrations (125 µM to 500 µM). There was some rise in graph line which have been observed at the end of the curve line (near 250 µM concentration), and it was not the reading measured because of the mitochondrial activity of living cells and these might be the false positive results. These rise were possibly because of the readings observed due to pellets formed by the drugs at higher concentrations. Both drug molecules were water insoluble, or having very less water solubility and

because of that, drugs were prepared in the DMSO solutions and then final concentrations were prepared in the growth media. As media have water as a base components, drugs with higher concentration during preparation of dilutions formed precipitate and did not shown clear solution. So there was possibility that these precipitates formed might have been interfered with the optical density during the reading measurement, and as a result of which false positive results observed here. These curve lines and readings were used to calculate corresponding $IC_{50}$ value for each of the drug combinations.

***Table 5.2: $IC_{50}$ values of Curcumin and Curumin+inhibitors on U87MG cells***

| Drugs | $IC_{50}$ (µM) ± SD (n=3) |
|---|---|
| Cur | 25.78 ± 1.96 |
| Cur+Gal | 37.77 ± 4.32 |
| Cur+Ver | 21.72 ± 2.79 |
| Cur+CsA | 23.92 ± 2.41 |

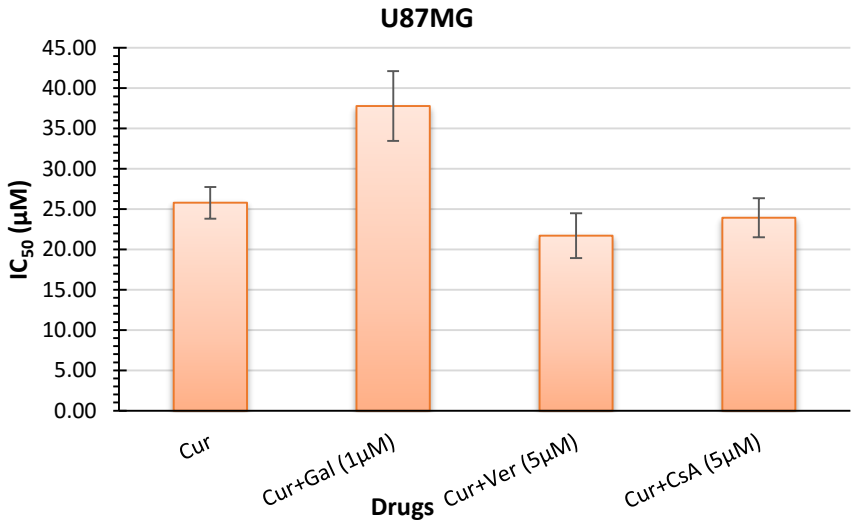


***Figure 5.8: $IC_{50}$ values of Curcumin and Curumin+inhibitors on U87MG cells***

Cell line U87MG treated with curcumin with and without co-administration of galaxolide and P-gp inhibitor molecules. Table 5.2 and Figure 5.8 shows the results obtained after the assay. Co-administration of curcumin and galaxolide shows the highest $IC_{50}$ value than other drug combinations. Actually we expected lowest $IC_{50}$with curcumin+galaxolide combination than curcumin only, because if galaxolide has P-gp inhibition avtivity, then it could stop efflux of drugs from the cells and eventually accumulation of drug would kill more cells at lower concentration. Positive controls, curcumin+ verapamil and curcumin+CsA shows lower $IC_{50}$ than curcumin.

***Table 5.3: $IC_{50}$ values of Curcumin and Curumin+inhibitors on LN229 cells***

| Drugs | $IC_{50}$ (µM) ± SD (n=3) |
|---|---|
| Cur | 22.29 ± 1.02 |
| Cur+Gal | 29.40 ± 1.08 |
| Cur+Ver | 26.08 ± 0.69 |
| Cur+CsA | 23.30 ± 2.26 |

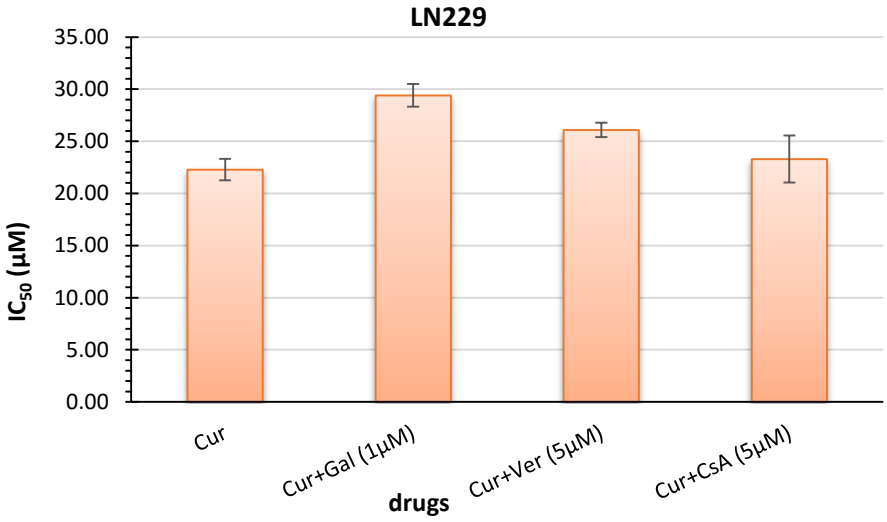


***Figure 5.9: $IC_{50}$ values of Curcumin and Curumin+inhibitors on LN229 cells***

As like with U87Mg cell lines, LN229 cells shown higher $IC_{50}$ for the curcumin+galaxolide dose (29.27 µM) than the curcumin only (22.25 µM) and other drug combinations. Here in LN229 cell lines, unlike U87MG, even curcumin+verapamil and curcumin+CsA doses shown higher $IC_{50}$ as well, than curcumin dose which were 26.22µM and 23.12µM respectively (Table 5.3 and Figure 5.9). From the results obtained with both of the cell lines, it seems that curcumin is possibly the poor substrate of the P-gp, and because of that even

in presence of the inhibitor molecules it did not shown any major difference in the $IC_{50}$ values and also shown the lower $IC_{50}$ than the curcumin+inhibitor doses.

***Table 5.4: $IC_{50}$ values of Temozolomide and Temozolomide+inhibitors on LN229 cells***

| Drug | $IC_{50}$ (µM) ± SD (n=3) |
|---|---|
| Temo | 85.05 ± 8.26 |
| Temo+Gal | 92.14 ± 5.19 |
| Temo+Ver | 97.77 ± 1.80 |
| Temo+CsA | 75.17 ± 5.43 |

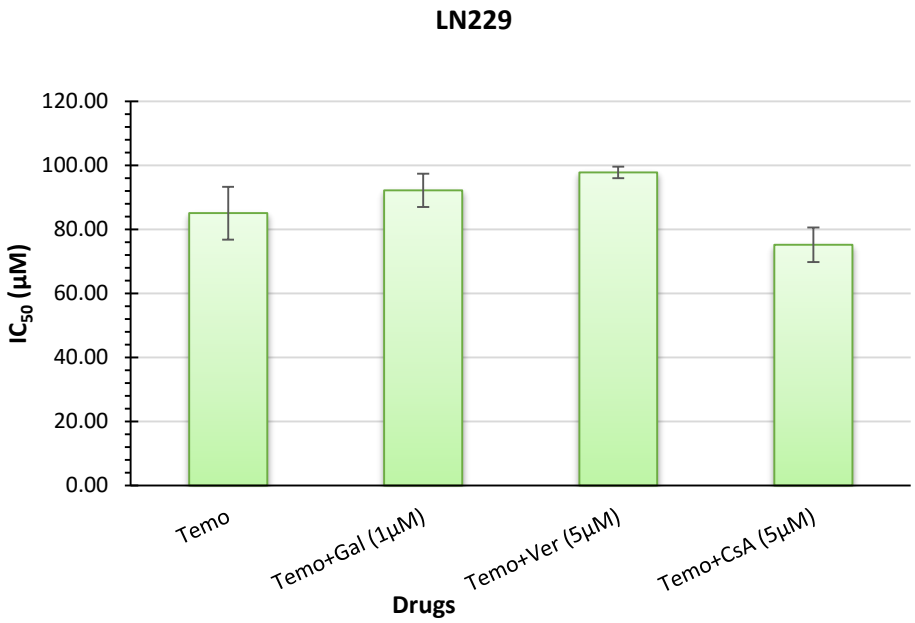


***Figure 5.10: $IC_{50}$ values of Temozolomide and Temozolomide+inhibitors on LN229 cells***

Studies with curcumin does not gave any clear idea about the effect of inhibitor molecules on toxicity of drug when administered in combination, so the curcumin was replaced with other drug; temozolomide. Study done with LN229 cell line which is derived from glioblastoma and temozolomide is a known drug used against glioblastoma. Temozolomide also shown similar results to curcumin, as there were no differences in $IC_{50}$ values. Temozolomide with and without galaxolide had almost same $IC_{50}$ values, 89.75 µM and 91.42µM respectively. Temozolomide+verapamil (99.55µM) dose shown highest while temozolomide+CsA (73.65µM) shown lowest $IC_{50}$ amongst these doses.

## 5.4 P-glycoprotein expression study

These experiments were performed to study characteristics of galaxolide to inhibit P-glycoprotein activity, and eventually to develop galaxolide as an *in vitro* P-glycoprotein inhibitor. To carry out the study, it was first necessary to confirm the expression of P-glycoprotein in cell lines which we were using in experiments. Caco-2 and MDCK cell lines were used to study P-glycoprotein expression as these cell lines later used to carry out permeability studies. Protein expression was analysed using two techniques; Western blotting and flow cytometry (FACS).

### 5.4.1 P-glycoprotein expression by western blot

Western blot (WB) also called immunoblot is an analytical method to detect protein, which is widely used to detect specific proteins in a given sample of tissue homogenate or extract. Identification of protein of interest is based on two distinguishing properties; a) molecular weight and b) antibody binding specificity. Western blot is highly sensitive technique.

Antibodies bind to specific sequences of amino acids, known as the epitope. Because amino acid sequences are different from protein to protein, antibodies can recognize specific proteins among a group of many. Therefore, a single protein can be identified in a cell lysate that contains thousands of different proteins and its abundance quantified through western blot analysis. First, proteins are separated from each other based on their size. Second, antibodies are used to detect the protein of interest. Finally, a substrate that reacts with an enzyme is used to view the antibody/protein complex.

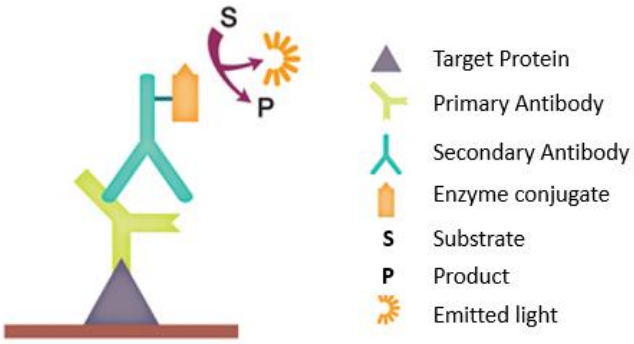


***Figure 5.11: Chemiluminescence detection***

Most proteins do not absorb visible wavelengths of light, and hence will not be visible during the course of electrophoresis. To ensure that the proteins are not eluted from the gel into the lower buffer reservoir, a small molecular weight, anionic dye, bromophenol blue is added to the protein before it is placed on the gel. The electrophoresis is halted when the dye reaches near the end of the running gel. The gel assembly is removed from the electrophoresis chamber, the glass plates separated, and the gel washed into buffer (transfer buffer). After a standard SDS-slab electrophoresis experiment is run, the gel is overlaid

with a piece of nitrocellulose filter paper. The sandwich of gel and filter paper is placed back into an electrophoresis chamber, such that the proteins migrate from the gel into the nitrocellulose, where they irreversibly bind. The filter paper can be removed and soaked in a solution containing a specific antibody to a protein of interest on the nitrocellulose. Enzyme linked secondary antibody is then added to this protein- antibody complex. The detection method used is dependent upon the enzyme to which the secondary antibody is conjugated. The most common enzyme used in Western Blotting is horseradish peroxidase (HRP), and the substrate used for detection is known as chemiluminescent substrate. The secondary antibody, which binds the antibody specific for the protein of interest, is conjugated to an enzyme; when it acts on the substrate, light is emitted (Figure 5.11).The produced light then gathered on X-ray film and used to develop the films. Films then analysed for the bands appeared on it.

#### 5.4.1.1 Quantification of total protein from cell lysates

BSA protein assay was done to study the total protein concentration present in the cell lysates harvested for the WB analysis. To carry out successful WB, it was necessary to load equal amount of protein on gel for every sample, so BSA protein assay helped to calculate total protein present in cell lysates.

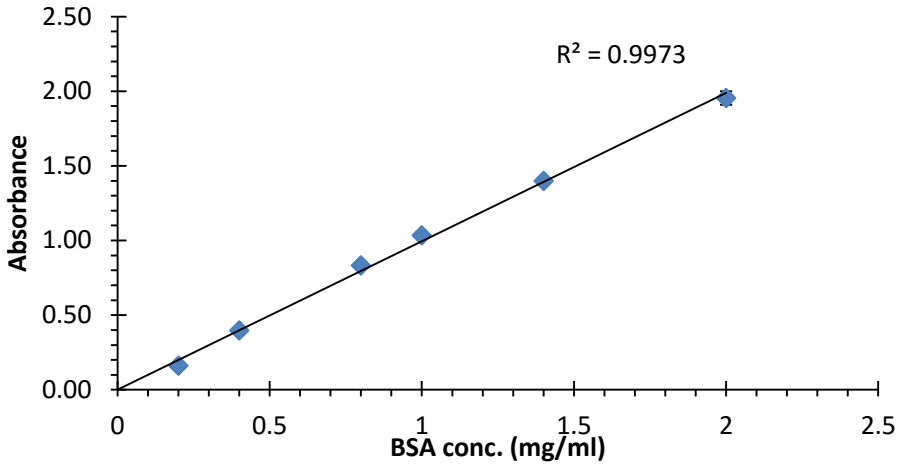


***Figure 5.12: BSA Protein Assay linearity curve***

BSA assay was done with known BSA concentration to get linear calibration curve (Figure 5.12). Cell samples were analysed along with standards. The colorimetric reading was plotted against the calibration curve to evaluate total protein concentrations present in the lysate. From obtained data, equal amount of proteins were loaded on the gel and other processes as mentioned above in methods were done to get final blots (Figure 5.13 and Figure 5.14).

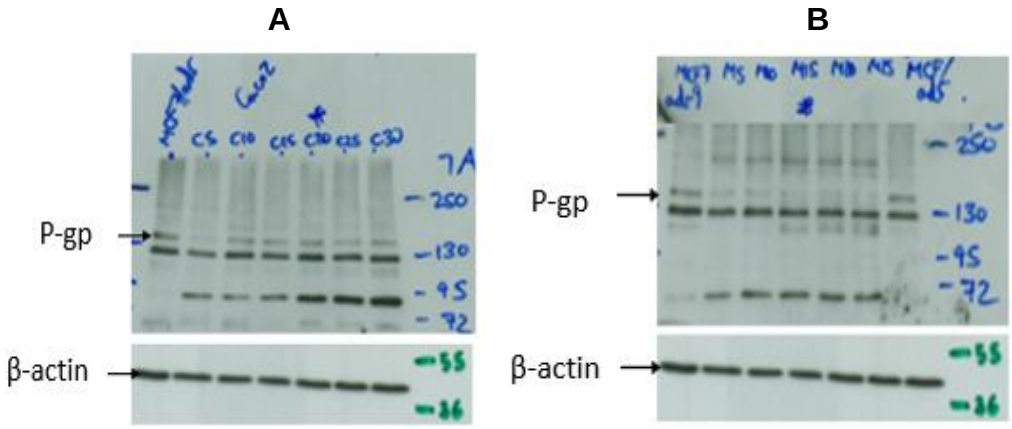


***Figure 5.13: Western blot analysis of P-glycoprotein***

*A) Caco-2 and B) MDCK*

P-glycoprotein is a large protein molecule with the molecular weight 170kD. Several bands were appeared in above blots. Figure 5.13 shows the blots A and B which were analysed for the P-glycoprotein expression in Caco-2 and MDCK cell lines respectively. Both blots shown similar expression bands. First column of both blots shows the bands for positive control for the P-glycoprotein and MCF-7/adr cell line was used as positive control as this cell line overexpress the P-glycoprotein. In blot A, column 2 to column 8 are the various Caco-2 samples harvested at different time points, such as every 5 days from day 5 to day 30, and this was done to check the differences in expression level of P-glycoprotein on different incubation time point. Similar samples were harvested for MDCK cell lines, and they were located in column 2 to column 7, while column 8 again contains positive control.

As mentioned above, P-glycoprotein is a 170kD protein molecule. Figure 5.13 showing blots A and B, where very light bands were appeared around 170kD region. Blot for Caco-2 shown dark bands around 130kD and 95kD; while blot for MDCK shown darks band around 130kD, which was similar like Caco-2 and other appeared near 72kD. The bands appeared in Caco-2 near 95kD and in MDCK near 72kd did not show its presence in a column where the positive control was present. This means these were not the bands for P-glycoproteins and were non-specific and unknown proteins. The bands near 170kD; though they were very light in appearance; shown the presence of P-glycoprotein expression in both the cell lines. In Caco-2 this band with 170kD located slightly above the band of 130kD. This band clearly shows expression of P-glycoprotein in abundance in positive control as compared to the different Caco-2 test

samples. Also it shown very low expression in samples which was harvested at day-5 and expression seems increasing with the increase in sample harvesting time. The band which appeared near 130kD, was probably for the sister P-glycoprotein (spgp); which is generally 140kD-150kD protein molecule. The spgp have high similarities in sequence with the P-glycoprotein; but this spgp is not a member of multigene family of P-glycoprotein (Childs et al., 1995; Gerloff et al., 1998).

The lower bands around 95kD in Caco-2 and near 72kD in MDCK were probably the bands of mini-Pgp protein molecules. These mini-Pgp are having molecular weights between 65kD to 96kD and have studied in some aquatic animals as well as it found to be expressed in natural killer cells instead of expression of regular 170kD P-glycoprotein (Kawai et al., 1994; Trambas et al., 2001; Valton et al., 2015). So there is possibility that these bands in above blots were possibly the mini-Pgp and they shown expression in Caco-2 and MDCK cells but not in positive control cells MCF-7/adr. The study performed without negative control and more ever the primary antibody used in this study, did not have any published review till now, so these results couldn't be robust. So repeated the western blot study with new antibody C219 (Anti P-glycoprotein Mouse Antibody - Merck-517310) and previous antibody (Anti-ABCB1/MDR1 Antibody-LS-C178472) as well. This new antibody have publication support as it was used in number of studies. In this study positive and negative controls were used along with the cell samples to support the results obtained.

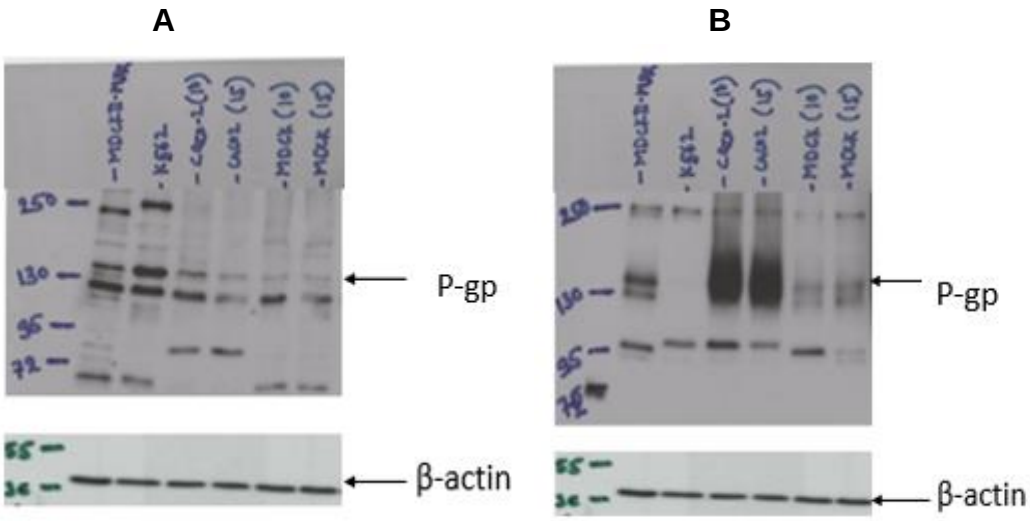


***Figure 5.14: Western blot for analysis of P-glycoprotein A) Anti ABCB1 antibody B) C219 Antibody***

*[Lane-1: Positive control. Lane-2: Negative control, Lane 3 and 4- Caco-2 samples (Day-10 and 15 respectively) and Lane 5 and 6- MDCK samples (Day 10 and 15 respectively)]*

Both blots in above Figure 5.14 were prepared to study P-glycoprotein expression with two different antibodies as mentioned above. Blot A treated with Anti ABCB1 antibody; which did not have any publication support while blot B is treated with C219 antibody; which was used in several published work. In both blots, first column is for positive control sample and MDCKII-MDR1 cell lines which overexpress P-glycoprotein was used as positive control, row second contains negative control; K562 cell line was used as negative control which did not express or shows very little expression of P-glycoprotein. Column 3 and 4 was loaded with Caco-2 samples (harvested on day 10 and 15 respectively) while column 5 and 6 contains MDCK cell samples (harvested on day 10 and 15 respectively).

Blot A treated with anti ABCB1 antibody; same antibody used in previous study. Purpose to do this repeated study was to analyse expression with both positive and negative controls. Bands in this blot appeared was to be non-specific and unknown. Bands near 250 kD were present in both positive and negative control, while they were completely absent in Caco-2 and MDCK cell samples. These bands should not be P-glycoprotein as it shows much higher molecular weight around 250 kD and were present in negative control as well. Next bands appeared around 150kD and 130kD, and these were present in all samples including positive and negative control as well, so this indicateed that these bands were also not P-glycoprotein. As mentioned above, these bands could be spgp according to molecular weight, but this possibility also raises questions, because it shown presence in negative control as well. But if the case is like, negative control cells; K562 have expression of spgp and not regular P-gp then these bands should be of spgp, but we didn't have any supporting data to confirm these assumptions for expression of spgp in these cell lines. Next bands seems near 85 kD approximately. This bands were present in positive control cells, absent in negative control cells, again present in both Caco-2 test samples and absent in MDCK test samples. The band in positive control was slightly lighter than bands present in Caco-2 samples. These bands probably the mini-Pgp, because mini-Pgp have molecular weight between 65kD to 96kD as explained above, and this mini-Pgp should have expressed in Caco-2 cells only and in lower quantity in positive control cells MDCKII-MDR1 while MDCK cells and negative control cells; K562 did not show expression of this mini-Pgp and because of that there were no appearance of bands on the blots developed.

Blot B have prepared with same samples as the previous one (blot A) and was treated with primary antibody C219.This film shows clear bands at the various molecular weight region. Bands appeared near 250kD and 95kD region were completely non-specific and unknown bands as they appeared in all samples including controls as well. Bands around 150kD and 130kD were present in all test samples and positive control and were absent in negative control. This indicates these were the bands of P-glycoprotein and spgp as this antibody was able to detect both these proteins from the samples. This study had confirmed that the cell lines Caco-2 and MDCK were able to express P-glycoprotein, and were able to play a good *in vitro* cell model to carry out further studies related to P-glycoprotein inhibition.

### 5.4.2 P-glycoprotein analysis by fluorescence activated cell sorting (FACS) method

Fluorescence-activated cell sorting (FACS) is a specialized type of flow cytometry. It provides a method for sorting a heterogeneous mixture of biological cells, one cell at a time, based upon the specific light scattering and fluorescent characteristics of each cell. It is a useful scientific instrument, as it provides fast, objective and quantitative recording of fluorescent signals from individual cells as well as physical separation of cells of particular interest.

The process begins by placing the cells into a flask and forcing the cells to enter a small nozzle one at a time (Figure 5.15). The cells travel down the nozzle which is vibrated at an optimal frequency to produce drops at fixed distance from the nozzle. As the cells flow down the stream of liquid, they are scanned

by a laser. Some of the laser light is scattered by the cells and this is used to count the cells. This scattered light can also be used to measure the size of the cells.

If we wanted to study the detection of specific protein, we could do so by tagging those proteins of interest with an antibody linked to a fluorescent dye. The laser light excites the dye which emits a colour of light that is detected by the photomultiplier tube, or light detector. By collecting the information from the light (scatter and fluorescence) a computer can determine the expression levels of the desired proteins.

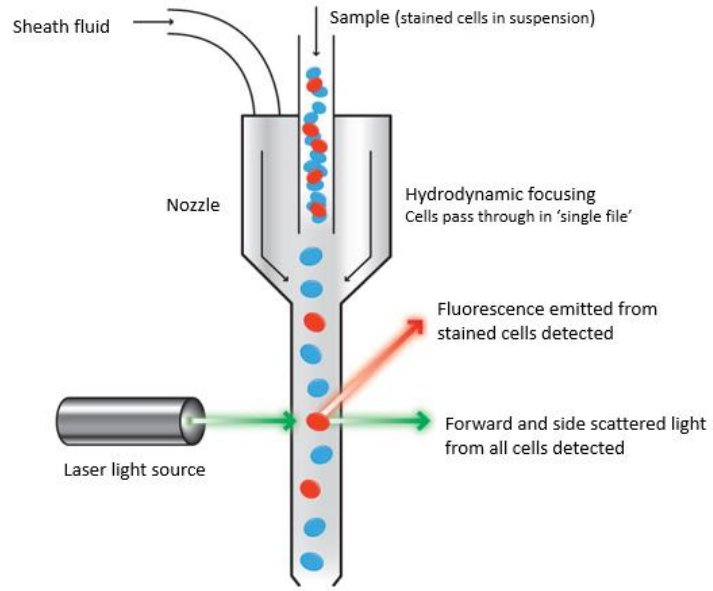


***Figure 5.15: FACS- how it works***

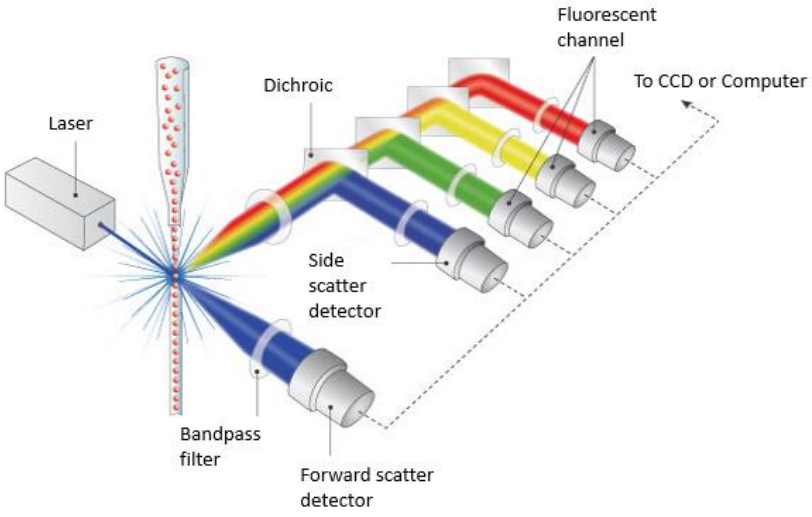


***Figure 5.16: FACS detection mechanism***

The Figure 5.16 shows the primary systems of the flow cytometry schematically. These are diplomatic systems which presents samples to the interrogation point and takes away the waist. The lasers, which are the light source for the scatter and fluorescence, the optics (dichroic) which gathers and

direct the light, the detectors which receive the lights and the electronics and peripheral computer system which converts the signals from detectors into digital data and perform the necessary analysis. The interrogation point is the heart of the system. This is where the laser and the sample intersects, and the optics collects the resulting scatter in fluorescence.

One of the most common ways to study cellular characteristics using flow cytometry involves the use of fluorescent molecule such as labelled antibodies. When laser light of the right wavelength strikes to these molecules, a fluorescent signal emitted and detected by the flow cytometer. How is this fluorescence information collected? The fluorescence light coming from labelled cells as they pass through the laser travels along the same path as the side scatter signal. As the light travels along this path, it is directed to the series of filters and mirrors, so that particular wavelength ranges are delivered to the appropriate detectors. Fluorescent data is generally collected in a way as forward and side scatter data. In a population of labelled cells some will be brighter than others. As each cell crosses the path of the laser a fluorescence signal is generated. The fluorescent light is then directed to the appropriate detector where it is translated into a voltage pulse proportional to the amount of fluorescence emitted. All of the voltage pulses are recorded and can be represented graphically.

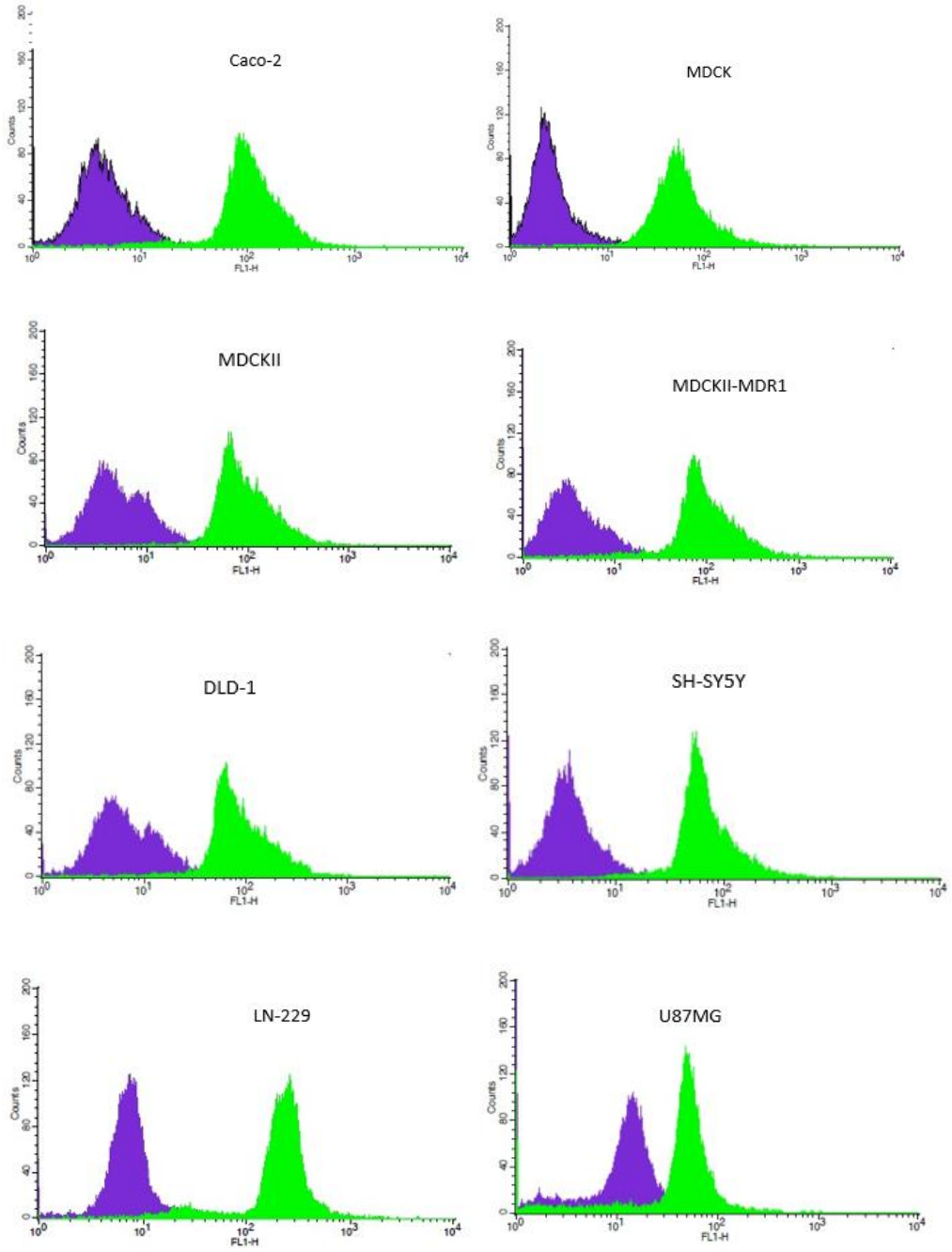


***Figure 5.17: Cytometric events displays the P-glycoprotein expression***

*peaks for P-glycoprotein expression (green Peaks) (Purple peaks denotes negative control)*

FACS analysis was done for various cell lines (Figure 5.17) to study P-glycoprotein expression. In above mentioned analysis Anti-ABCB1 antibody was used as primary antibody to detect P-glycoprotein. Each samples were analysed in two sets as one set treated with primary and secondary antibody to detect P-gp specifically while set two was treated with secondary antibody which act as negative control in this study. Green coloured histogram in above figure determines the signal for P-glycoprotein while violet coloured histogram determines the signal for control. The graph displays a relative fluorescence or light scatter intensity on X-axis against number of events (cell count) on Y-axis.

Histograms were achieved for cell lines mentioned above. In every graph, histograms for P-gp were more positively differentiated from the negative control histograms. These positive histograms clearly shown the expression of P-glycoprotein in analysed cell lines. The cell line U87MG shown comparatively less expression of P-glycoprotein as graph obtained for this cell line seems with lesser differentiation in P-gp positive histogram and negative control histogram. Both histograms seems to slightly overlapping at the base region. The cell line LN229 shown two histograms completely departed from each other, and P-gp positive histogram seemed to appear on more positive side. This could clearly show higher expression of P-glycoprotein in LN229 as compared to other cell lines analysed along with. The remaining cell lines such as Caco-2, MDCK. MDCKII, MDCKII-MDR1, DLD-1 and SH-SY5Y shown the cells treated with positive antibody have histogram at the more positive region than the negative control histogram. Both histograms were well separated without any overlaps, and confirms that these cell lines as well shown the P-glycoprotein expression.

To get more accurate data with this study, same experiment was repeated with two different antibodies for P-glycoprotein (C219 and Anti-ABCB1) and for negative control, isotype antibodies of these positive antibodies were used. The repeated study carried with Caco-2cell line and MDCKII-MDR1 cell line which is P-glycoprotein overexpressing cell line. The isotype antibodies (negative control antibody) was used to minimize the false result and to interpret data more specifically. The results observed in this study were mentioned below (Figure 5.18)

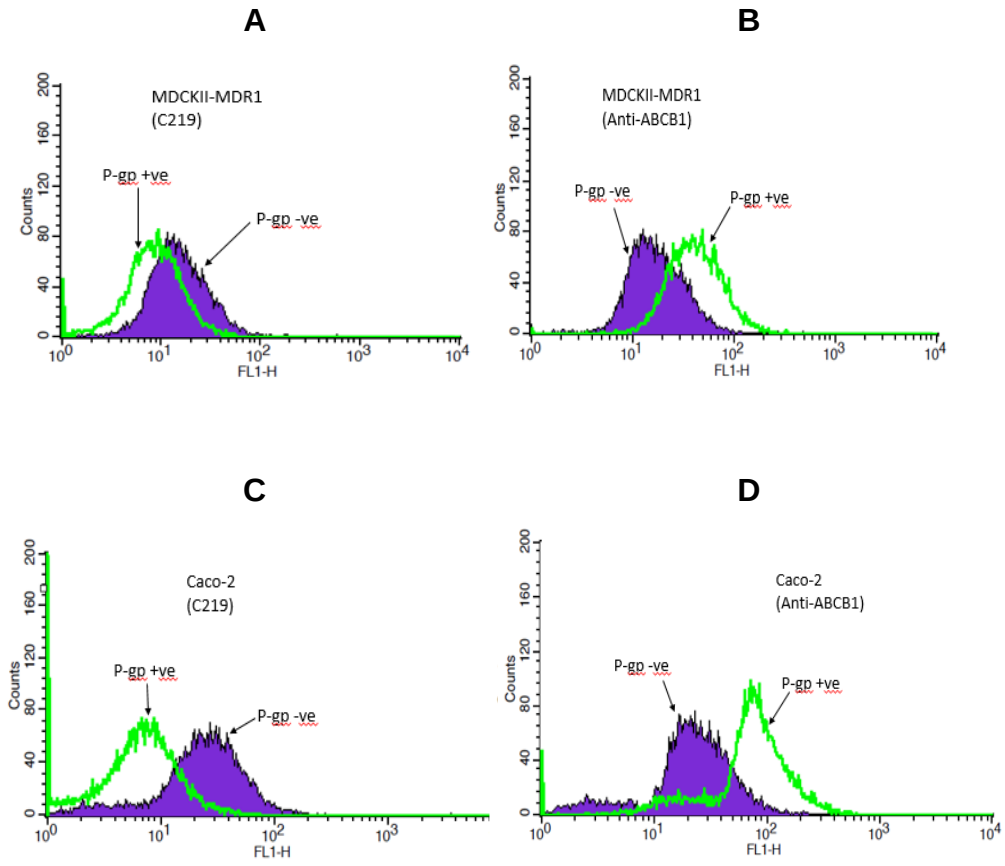


***Figure 5.18: Flow cytometry analysis of P-glycoprotein***

*with different antibodies; C219 (A,C) and Anti-ABCB1 (B,D)*

The graph above shows the histograms obtained with two different antibodies for P-glycoprotein and their isotype antibodies. The histograms obtained with positive antibody were plotted with green line while histograms with negative control isotype antibody were plotted with violet coloured solid plot. The Figure 5.18(A and C) shows the histograms with the C219 antibody for both cell lines MDCKII-MDR1 and Caco-2. The histograms with the P-gp positive antibody shown very low fluorescence intensity than the negative control histogram. These histograms shown dominance of negative control peaks over the positive peaks. So according to observations with C219 antibody, the above mentioned cell lines did not show presence of P-glycoprotein. But on the other hand similar samples were analysed with another antibody; Anti-ABCB1; and surprisingly results seemed completely reverse (Figure 5.18; B and D). The positive antibody samples shown histograms with higher fluorescence intensity. Though both the positive peak and negative control peaks were overlapping, positive peaks were clearly seems with higher fluorescence than negative control.

The C219 antibody in above experiment shown the negative results for the P-glycoprotein, while other antibody; Anti-ABCB-1; shown positive results in both the instances with or without isotype antibody. According to results obtained in above studies, it seems that C219 antibody was not suitable for the FACS studies. Because this antibody shows the negative results even in the MDCKII-MDR1 cell lines, and this cell line is known to overexpress P-glycoprotein.

## 5.5 P-glycoprotein inhibition study

Rh123 assay was used to study the P-glycoprotein inhibition with galaxolide as a novel P-gp inhibitor molecule and with known P-gp inhibitor compounds; verapamil and cyclosporine A.

The phenomenon of resistance of tumours to chemically unrelated anticancer drugs, termed multidrug resistance, represents a major challenge to the field of oncology. Multidrug resistance can be present at the time of diagnosis, or can be acquired after initial treatment of a cancer. Although multiple mechanisms mediate multidrug resistance, the first mediator of multidrug resistance to be characterized at the molecular level was MDR1 (Multi-drug resistance gene), also known as P-glycoprotein (P-gp) and ABCB1. MDR1 mediates resistance to various classes of chemotherapeutic agents by actively pumping the drugs from the cytosol and plasma membrane into the extracellular space. At least nine proteins related to MDR1 have been characterized to date and shown to mediate efflux of small molecules from cells. Two of these MDR1 relatives, multidrug-resistance-associated protein 1 (MRP1, or ABCC1) and breast cancer resistance protein (BCRP, or ABCG2), have also been demonstrated to mediate multidrug resistance in tumour cells. These proteins belong to a larger family of ABC proteins that function as transporters of ions, nutrients, and peptides. Multiple efforts have been made to standardize methods for MDR1 detection using flow cytometry, immunohistochemistry and immunoblotting. It has been estimated that at least 50% of human cancers express the MDR1 phenotype.MDR1 activity is also observed in various cell types in normal tissues. Brain microvascular endothelial cells express MDR1, which contributes

to the blood-brain barrier. It was proposed that expression of MDR1 in hematopoietic stem cells, intestine, and reproductive tissues (testicular endothelium and placental syncytiotrophoblast) protects these cells from the fatal effects of xenobiotics (Beck et al., 1996; Gottesman et al., 2002). Assessment of activity of MDR1, MRP1 and BCRP in cultured cells has been facilitated by the observation that several fluorescent small molecules, such as DiOC2(3), rhodamine 123, and calcein AM, which serve as substrates for MDR1 and its relatives. When these dyes added to the cells, it penetrates and emits fluorescence. As these dyes are the substrates of efflux proteins, they are pumped out from the cells interior to extracellular space. The efflux can be reversed by addition of efflux inhibitor molecules. This phenomenon is used to carry the Rh123 efflux assay in this study. Rh123 readily pass through cell membranes via both active and passive transport mechanisms and accumulate in mitochondria. Fluorescence is produced by accumulation of dye in the mitochondria (Altenberg et al., 1994; Forster et al., 2012).

### 5.5.1 Rhodamine 123 Assay

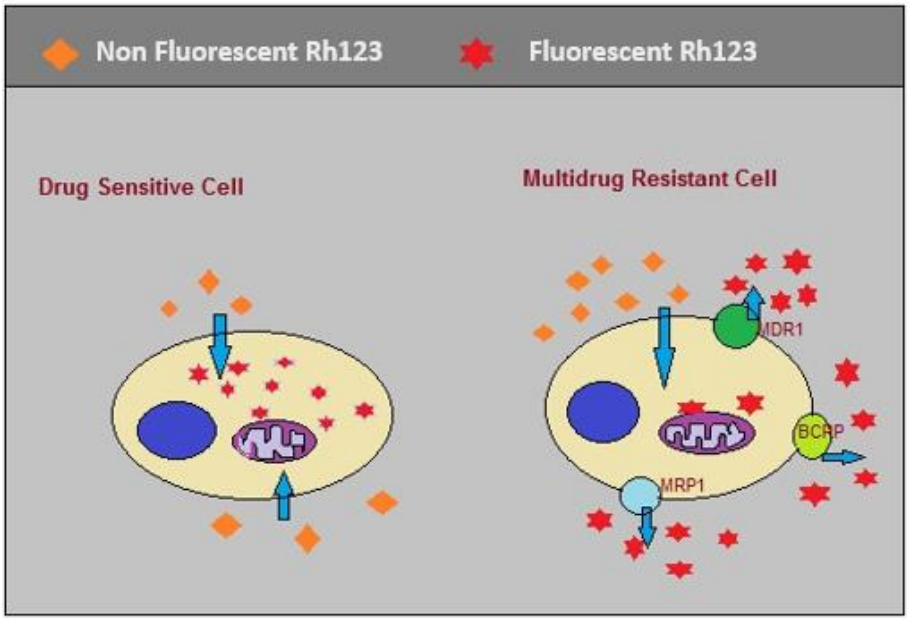


***Figure 5.19: Basic principle of Rh123 assay***

*In drug sensitive cells, non-fluorescent rh123 (orange diamonds) rapidly penetrates and accumulates in mitochondria and converts in fluorescent rh123 (red stars), and this accumulated rh123 emits high fluorescence. In multi-drug resistant cells, efflux proteins are present and they exclude rh123 (both fluorescent and non-fluorescent rh123) rapidly from the cells, and thus rh123 does not accumulates in the cells and eventually emits less fluorescence [adapted from: (Altenberg et al., 1994; Forster et al., 2012)].*

Rhodamine 123 dye is a substrate for the ABC transporter proteins. When cells are incubated with Rh123, the dye penetrates into the cells and produce fluorescence due to mitochondrial activity. But on the other hand the cells with efflux proteins can efflux the dye outside the cells and reduce the fluorescence. So if these efflux proteins were blocked with inhibitor molecules, the dye will retain inside the cell and will emit fluorescence. The fluorescence is then measured and percentage is calculated against the fluorescence obtained with

blank wells. So this principle is used in this assay to evaluate the characteristic of galaxolide to inhibit the P-gp and other efflux proteins (BCRP/MRP1). Verapamil and Cyclosporine-A are known P-gp inhibitors and used as positive controls in this study. As mentioned in methods section, assay was carried with different modifications in procedures to study the effect of inhibitors with different exposure times. Following are the results obtained for the assay.

A

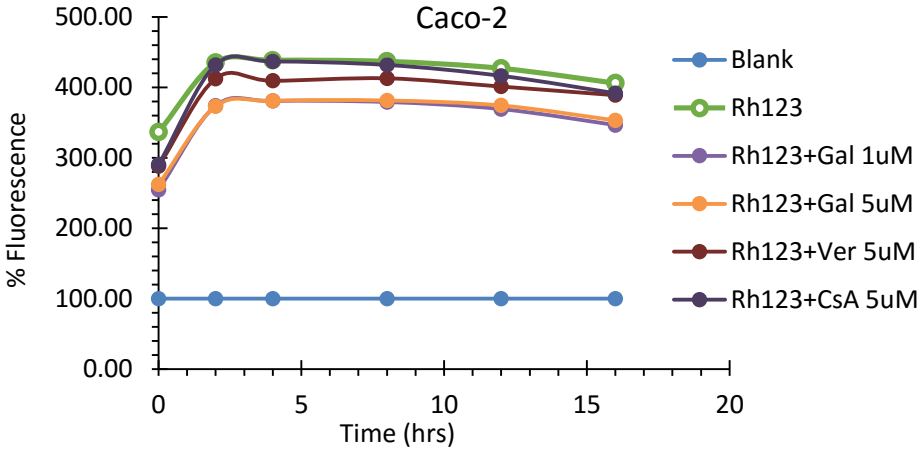


B

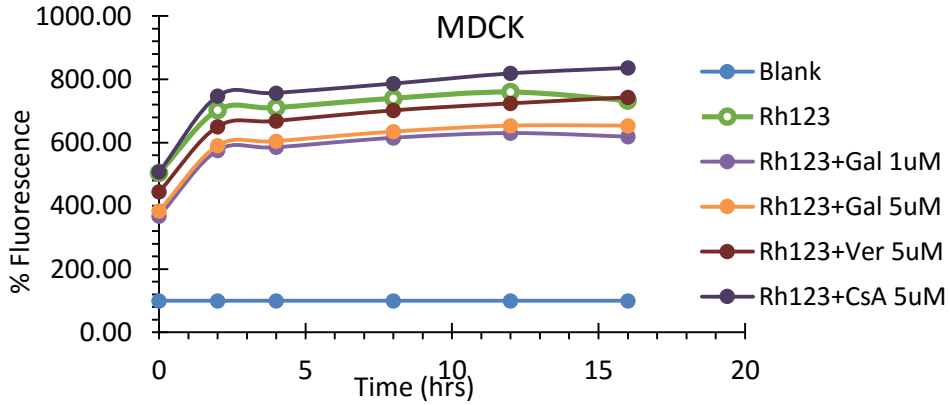


C)

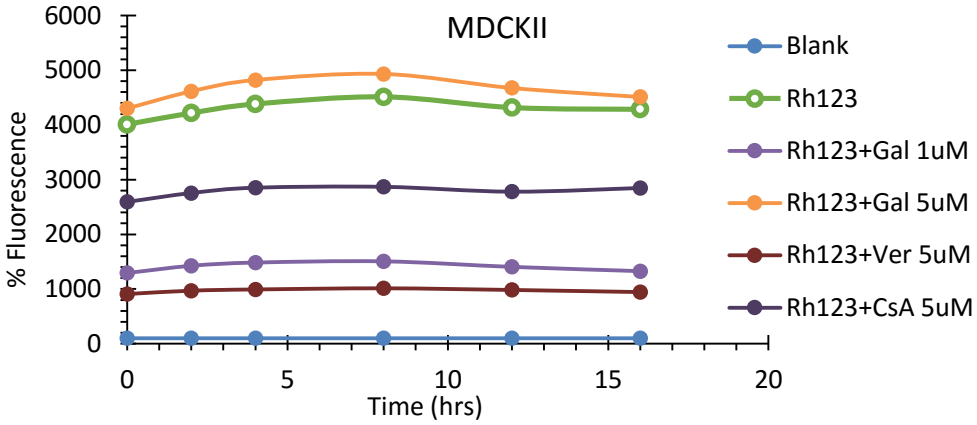


***Figure 5.20: % Fluorescence in Rh123 assay with different inhibitors***

*A) Caco-2, B) MDCK and C) MDCKII cells (4.6, 1)*

**D)**

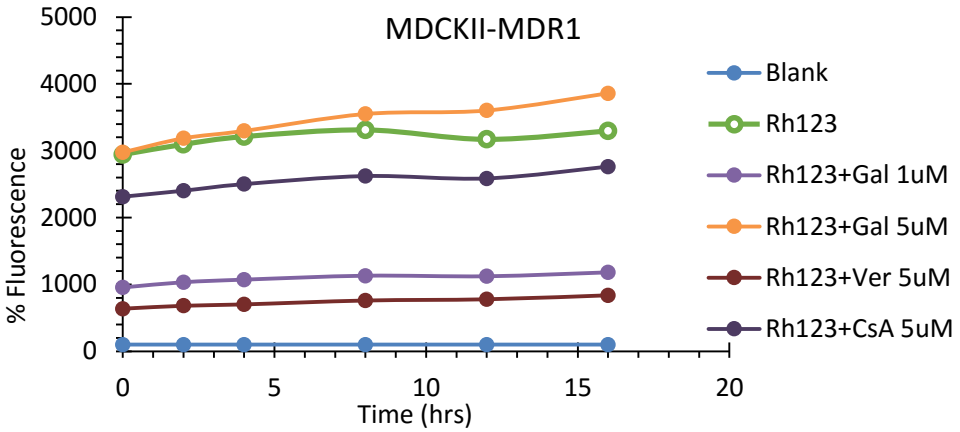


**E)**

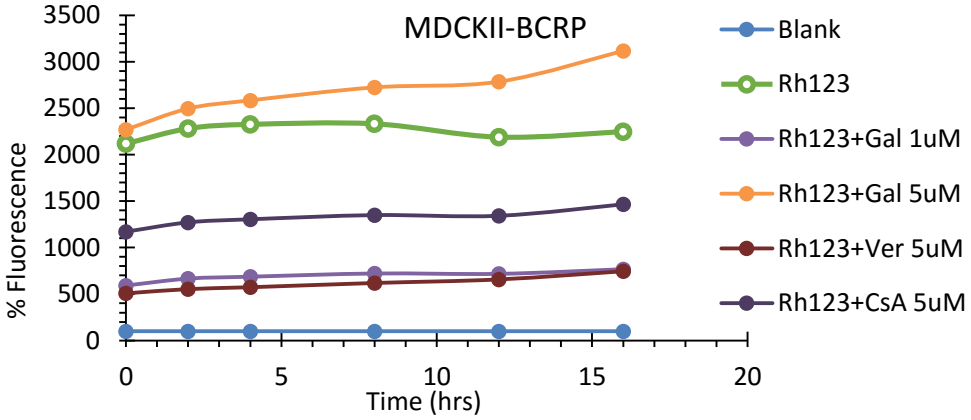


**F)**

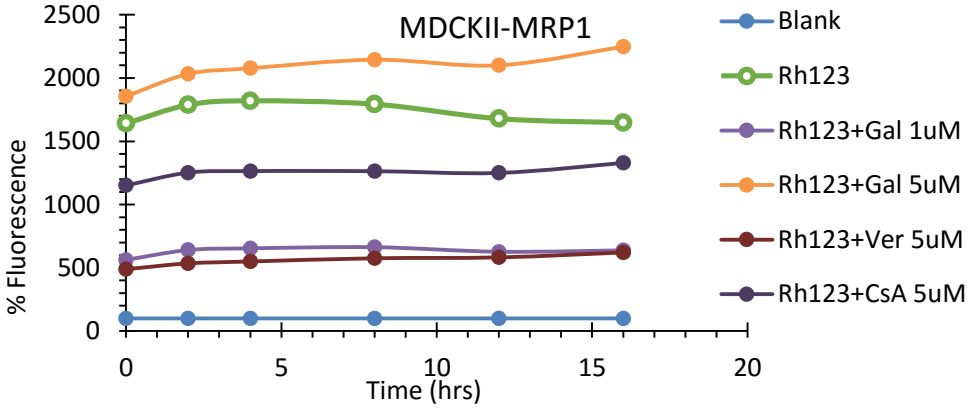


***Figure 5.21: % Fluorescence in Rh123 assay with different inhibitors***

*D) MDCKII-MDR1, E) MDCKII-BCRP and F) MDCKII-MRP1 cells (4.6, 1)*

The fluorescent dye rh123 was used as an indicator of efflux transport activity and fluorescence obtained from it used as a measure of inhibition by each compound at the specified concentration. Assay was carried using various cell lines like Caco-2 and MDCK in which expression of P-glycoprotein was studied. Other cells used were MDCKII cells which is derivative of MDCK cell line and efflux protein overexpressing MDCKII cells; MDCKII-MDR1 (Overexpressing P-gp protein). MDCKII-BCRP (over expressing BCRP protein) and MDCKII-MRP1 (overexpressing MRP1 protein). The results obtained in above Figure 5.20(A, B and C) and Figure 5.21 (D, E and F) shown the fluorescence pattern of rhodamine 123 in presence and absence of various inhibitor molecules. These results were obtained with protocol (4.6, 1) described earlier in methods section. Inhibitors were used in various range of concentrations to see the effect of concentration on the efflux pattern of Rh123. Galaxolide was used in range like 0.5μM, 1μM, 2μM, 5μM and 10μM; Verapamil and CsA, both are known P-gp inhibitors and used with two concentrations (5μM and 10μM). Results shown here describes only selected concentration at which activity observed higher and this was done for the ease of understanding graph.

Fluorescence obtained with blank samples; cells without treatment of Rh123 were set to the 100% and fluorescence for cells treated with Rh123 were calculated against blank samples and fluorescence pattern is observed as a function of time for the differences in various samples. Caco-2 and MDCK (Figure 5.20, A and B) cells shown similar fluorescence pattern, in which blank sample shown straight line at the bottom around 100% fluorescence. Positive control sample; cells treated with rh123 and not applied any inhibitor molecule

shown incline in first 2hr and from next reading taken at 4hr shown a slight decline and the decline is till the last reading taken at the 16hr time. In Caco-2 this decline was not so sudden but in MDCK cells after 12 hrs fluorescence shown the sudden decline. This fluorescence pattern of rh123 without any inhibitor shown the efflux of rh123 from the cells. On the other hand, samples treated with rh123 and various inhibitor molecules (Gal 1μM and 5μM; Ver 5μM, CsA 5μM) shown the same fluorescence pattern like the control sample. There was no any remarkable difference in fluorescent patterns observed with and without application of inhibitor molecules to the rh123 treated cell samples. As mentioned above, this experiment carried with procedure (4.6, 1) in which cells were not washed after incubation with rh123. So it is possibility that, we did not see any different in rh123 decay patterns in control sample and samples with inhibitors as well. It might be possible that the rh123 is wiped out from the cells in control set, but because of cells were not washed after incubation, they shown fluorescence with that excess rh123 even after they were excluded from the cells, and because of that there was no any differences in fluorescence obtained by control samples and samples treated with inhibitor molecules.

Same method was applied to the MDCKII cells and its derivatives, MDCKII-MDR1, MDCKII-BCRP and MDCKII-MRP1. These cells were modified to express specific efflux proteins, and so used to perform this assay and it was useful for comparative assessment of the ability of galaxolide to inhibit these specific efflux proteins. As shown in figures above (Figure 5.20, C and Figure 5.21, D, E, F), MDCKII cell line and its derivatives did not show clear results for the inhibition activity of galaxolide, as there was mixed population of graphs

were obtained for the fluorescent activity. Galaxolide at 5μM concentration shown highest activity against all three efflux proteins, while galaxolide at 1μM and other known inhibitors, Ver and CsA did not show any inhibitory activity. They shown fluorescence even less than the control cells where we did not applied inhibitors. This data did not interpret anything as it gives mixed results, and as mentioned above, this might be due to the excess rh123 remained. To overcome this issue the protocol was modified, in which cells were washed after rh123 incubation step. And results for that experiment Are plotted below.

**A)**

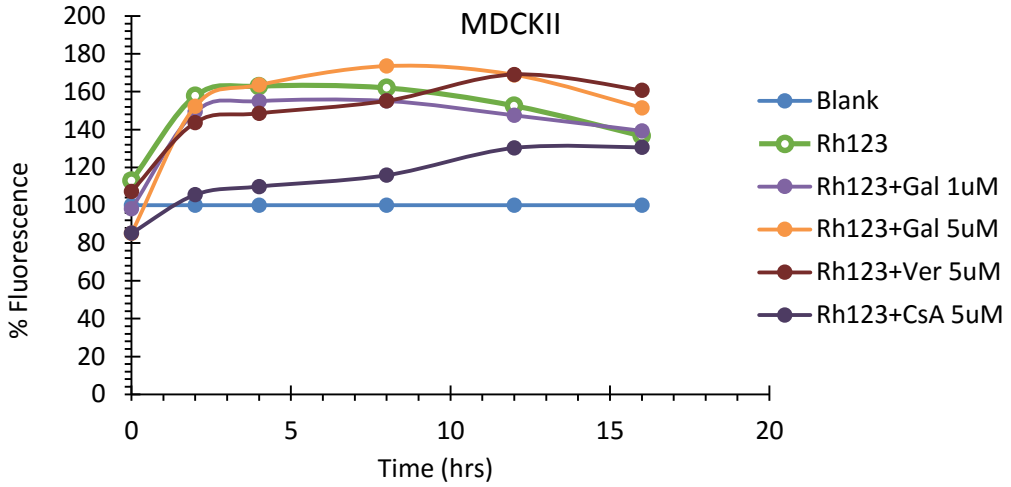
MDCKII
% Fluorescence
Time (hrs)
Blank
Rh123
Rh123+Gal 1uM
Rh123+Gal 5uM
Rh123+Ver 5uM
Rh123+CsA 5uM

**B)**

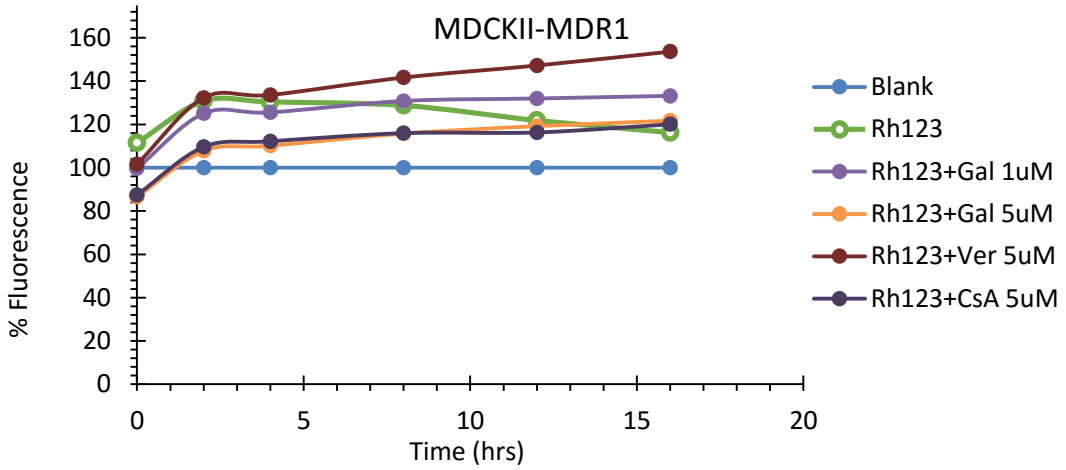
MDCKII-MDR1
% Fluorescence
Time (hrs)
Blank
Rh123
Rh123+Gal 1uM
Rh123+Gal 5uM
Rh123+Ver 5uM
Rh123+CsA 5uM

**C)**

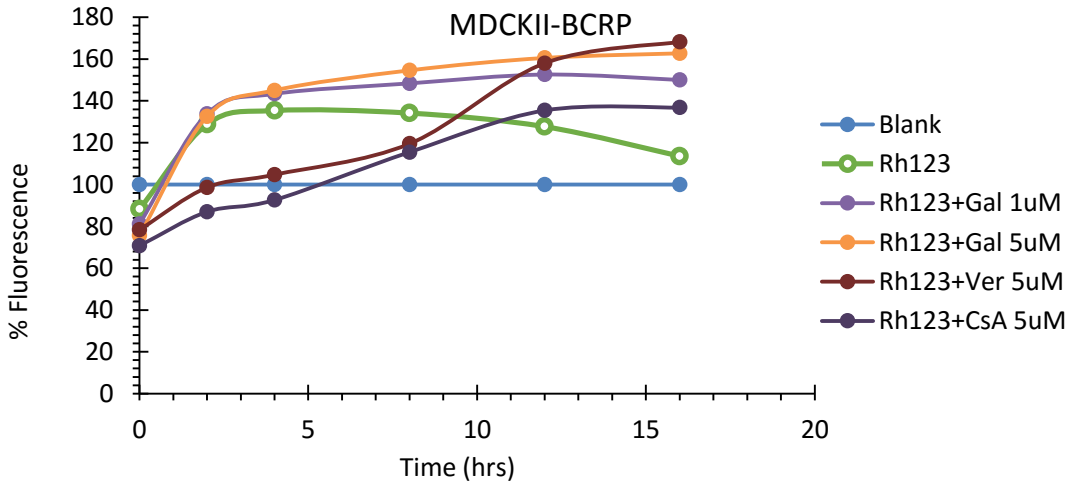
MDCKII-BCRP
% Fluorescence
Time (hrs)
Blank
Rh123
Rh123+Gal 1uM
Rh123+Gal 5uM
Rh123+Ver 5uM
Rh123+CsA 5uM

**D)**

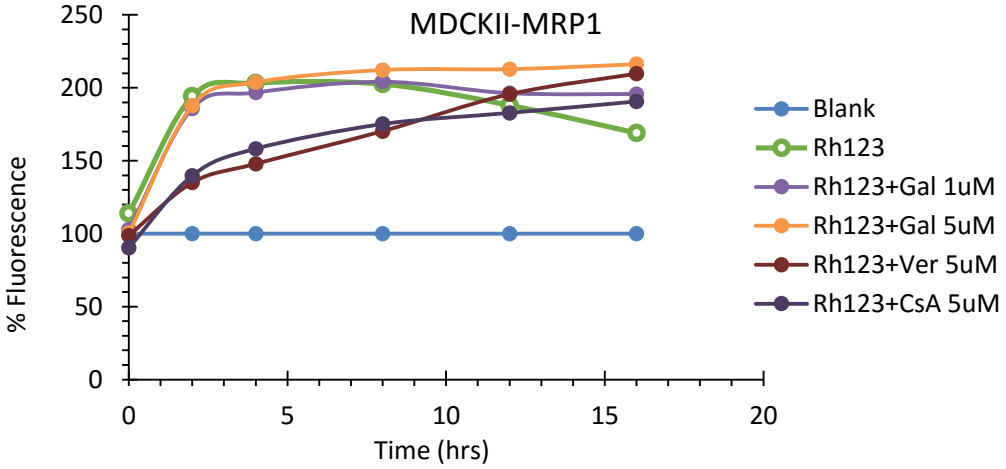


***Figure 5.22: % Fluorescence in Rh123 assay with different inhibitors***

*A)MDCKII, B) MDCKII-MDR1, C) MDCKII-BCRP and D) MDCKII-MRP1 cells (4.6, 2)*

Figure 5.22 (A, B, C, D) shows the results for rh123 assay performed with method (4.6, 2) in which slight modifications were done than previous method. Cells were washed after rh123 incubation before addition of corresponding inhibitor solutions to the respective wells. The step was done to get rid of excess rh123 present in the sample wells and to avoid the false results obtained in previous experiment.

In this repeated experiment promising results were obtained which can define the inhibitory activity of galaxolide along with known inhibitors; verapamil and cyclosporine A; against all three efflux proteins. The graphs (Figure 5.22) shown the increased fluorescence in all samples which had inhibitor solutions in it, while control sample which was treated with only rh123 show the decay of fluorescence as a function of time. The graph with rh123 decay shown the similar path in all four cell lines. The fluorescence with rh123 observed higher

in initial 2 hrs and after that the fluorescence declined gradually over the time. This data shown that efflux proteins were active and were responsible for the efflux of rh123 from the cells. On the other hand fluorescence intensity for samples treated with galaxolide and known inhibitor molecules seemed increasing gradually as the time increases. This kind of results were expected only when efflux proteins were inhibited or other strong substrate was added to the assay. The addition of strong substrate or inhibitor molecules could engage or block the efflux proteins like P-gp and other ABC protein family members. Such blocked or inhibited efflux proteins are not able to efflux rh123 from the cells and as a result of which rh123 accumulates in the cells and in presence of mitochondria it gives fluorescence. This fluorescence lasts without decay until and unless inhibitor molecules are removed, and that is why there was no any decline in the fluorescence with inhibitor molecules and galaxolide.

In case of MDCKII-MDR1 cell line which overexpresses MDR1 protein i.e. P-glycoprotein, Verapamil shown highest inhibitory activity against P-gp as compared to galaxolide and cyclosporine A. Galaxolide at 1μM concentration shown better inhibitory activity against P-gp as compared to galaxolide at 5μM and cyclosporine A. Cyclosporine A shows least P-gp inhibition activity and was approximately similar with galaxolide at 5μM. Even cyclosporine A shown least inhibitory activity, it did not shown any decay in the fluorescence as like the control. These results suggest that galaxolide has an ability to inhibit P-glycoprotein and it seems better P-gp inhibitor than the known inhibitor cyclosporine A.

Observations with MDCKII-BCRP shown similar decline with rh123 fluorescence as like MDCKII and MDCKII-MDR1. Galaxolide at both concentrations (1μM and 5μM) shown higher fluorescence which means highest inhibitory activity against BCRP as compared to other inhibitors, like verapamil and cyclosporine A. Cyclosporine A again shown least activity against BCRP as well. Galaxolide shows strong activity against BCRP as it shown higher fluorescence intensity immediately after 2 hrs and fluorescent intensity keeps increasing as per time. But in verapamil and cyclosporine A, the fluorescent intensity is very low till 6 hrs and which was near to blank readings and after that fluorescence intensity goes on increasing and with verapamil it reached to the maximum level even higher than the galaxolide. The data suggests that the verapamil and cyclosporine A had a poor inhibitory activity against the BCRP in initial time of assay but, as a function of time the activity increases. So it seems these two inhibitors need more time to react with BCRP and once reacted they show their inhibitory effect on BCRP for longer time. So at the end it could be stated that galaxolide have an inhibitory activity against BCRP as well along with the MDR1/P-gp protein.

MDCKII-MRP1 data shown fluorescence pattern similar to BCRP cells. Here also galaxolide showing highest inhibitory activity against MRP1 proteins as it shows higher fluorescence intensity since beginning of the assay. Verapamil and cyclosporine A shown least fluorescence in the beginning and then fluorescence keeps increasing as time increases. As per data obtained it seems that like BCRP, verapamil and cyclosporine A were also poor substrates of MRP1. Galaxolide seemed to be a better inhibitor of MRP1 as well than

verapamil and cyclosporine A. So now it was clear that galaxolide had an activity against all three efflux proteins, and it seemed to be a broad range efflux protein inhibitor. It shown advantage over known inhibitors verapamil and cyclosporine A, as these two inhibitors had good activity only against MDR1 while they show poor activity against BCRP and MRP1 unlike the galaxolide.

As seen in BCRP and MRP1 overexpressing cells, verapamil and cyclosporine A inhibition activity is less than the galaxolide and as a result of which these inhibitors shown very low fluorescence intensity in the beginning of assay which then gradually increased approximately after 4-6 hrs. To reduce this lag, protocol was modified. Cells were incubated with rh123 which was prepared in solutions with corresponding inhibitor concentrations (refer 4.6, 3). The idea behind this was just to reduce the lag phase acquired by verapamil and cyclosporine A while inhibition of BCRP and MRP1.

**A)**

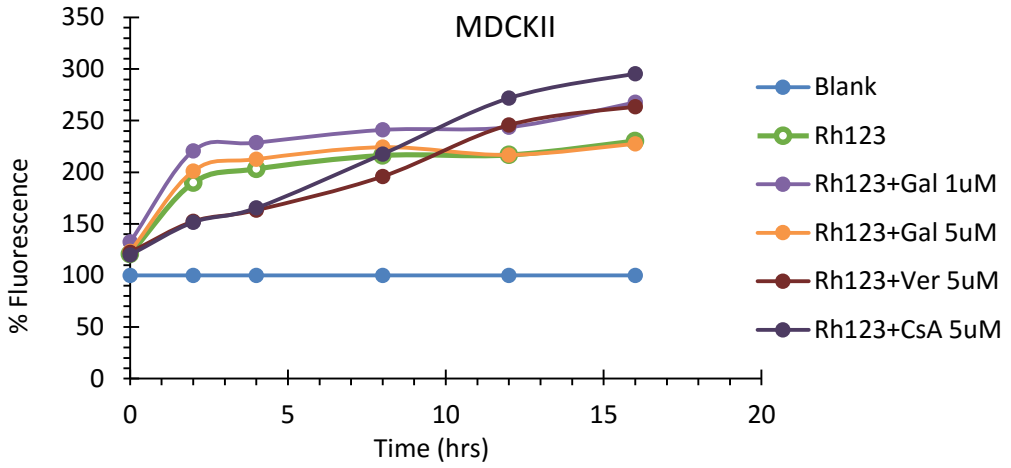
MDCKII
% Fluorescence
Time (hrs)
Blank
Rh123
Rh123+Gal 1uM
Rh123+Gal 5uM
Rh123+Ver 5uM
Rh123+CsA 5uM

**B)**

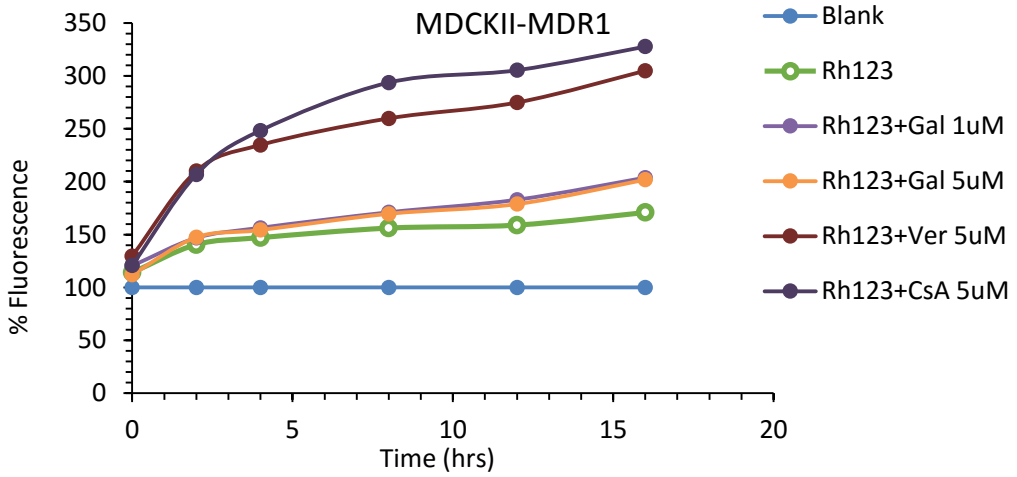
MDCKII-MDR1
% Fluorescence
Time (hrs)
Blank
Rh123
Rh123+Gal 1uM
Rh123+Gal 5uM
Rh123+Ver 5uM
Rh123+CsA 5uM

**C)**

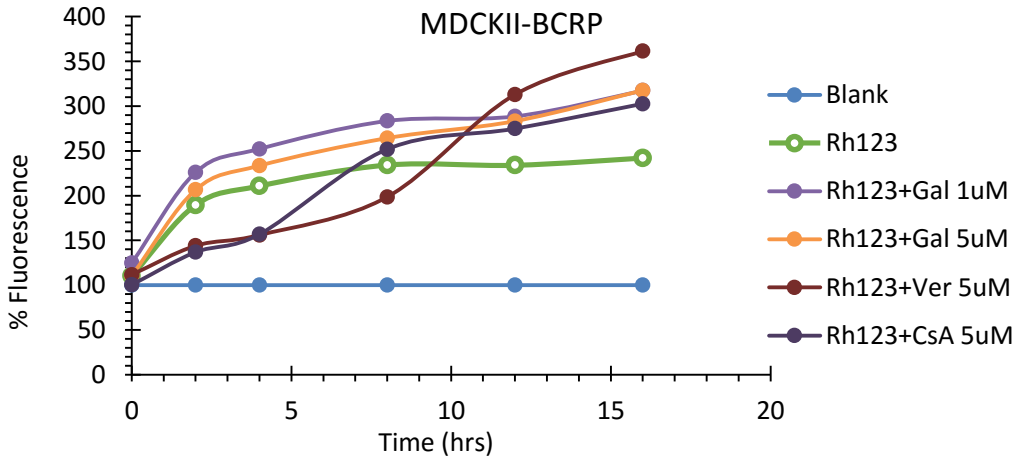
MDCKII-BCRP
% Fluorescence
Time (hrs)
Blank
Rh123
Rh123+Gal 1uM
Rh123+Gal 5uM
Rh123+Ver 5uM
Rh123+CsA 5uM

**D**

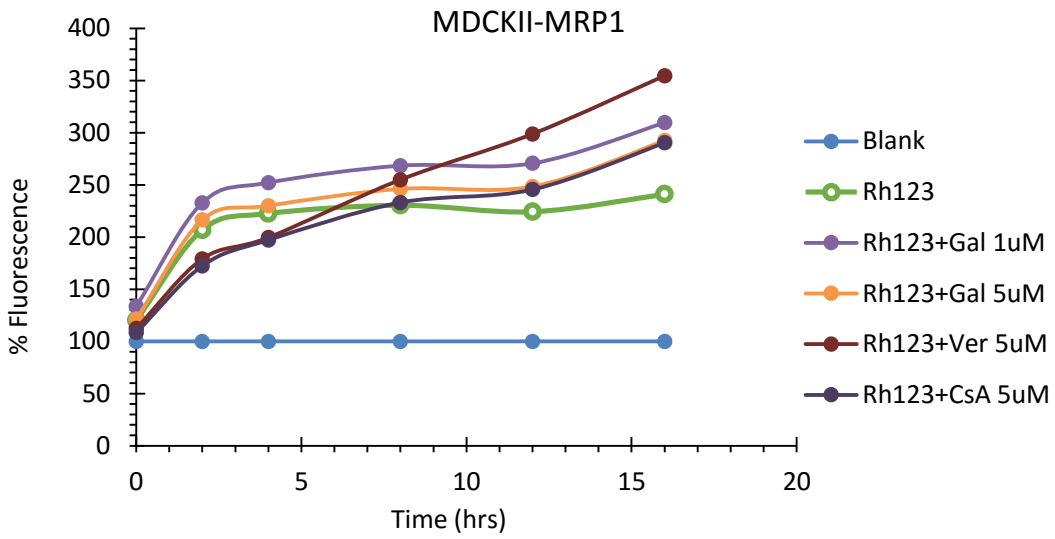


***Figure 5.23: % Fluorescence in Rh123 assay with different inhibitors***

*A)MDCKII, B) MDCKII-MDR1, C) MDCKII-BCRP and D) MDCKII-MRP1 cells (4.6,3)*

As mentioned above, this assay was modified with procedure (4.6, 3) described above, to reduce the lag phase acquired by verapamil and cyclosporine A to inhibit the BCRP and MRP1. To achieve this goal to reduce lag phase, cells were incubated in rh123 prepared in corresponding inhibitor concentrations. Here in Figure 5.23 it is seen that the modification in protocol was successful in some extent to reduce the lag phase of verapamil and cyclosporine A to inhibit BCRP and MRP1 proteins. In previous experiment it was seen that verapamil shown highest activity against MDR1 while cyclosporine A shown least activity as compared to galaxolide. Here, with this modified procedure huge difference in activities of verapamil and cyclosporine A against MDR1 was observed. Cyclosporine A unlike previous activity shown the highest fluorescence intensity than both verapamil and the galaxolide. Galaxolide did not show any

difference in activity as a result of over pre-incubation. Inhibition activity of verapamil and cyclosporine A against BCRP have seen improved than previous results but there was some lag observed. It indicates that verapamil and cyclosporine A needs more exposure time to inhibit BCRP protein. While galaxolide gave high fluorescence at both the concentrations (1μM and 5μM). Galaxolide at 1μM concentration given better inhibition activity than 5μM concentration, though the difference was not too high. An improved activity of verapamil and cyclosporine A against MRP1 protein was observed, however these inhibitors still needs time to show their activity against MRP1. This could be stated by observing the slight lag of lower fluorescence intensity with these inhibitors. In reverse of these inhibitors, galaxolide shown better inhibition activity against all these efflux proteins, even with modified protocol. It did not show any big difference in fluorescence even after over incubation as it already shown higher fluorescence intensity from the beginning of assay. It means galaxolide has ability to inhibit these efflux proteins as immediately as its exposure to these efflux proteins.

This assay was further modified to observe further improvement in inhibition activity of verapamil and cyclosporine A against BCRP and MRP1 proteins.

**A)**

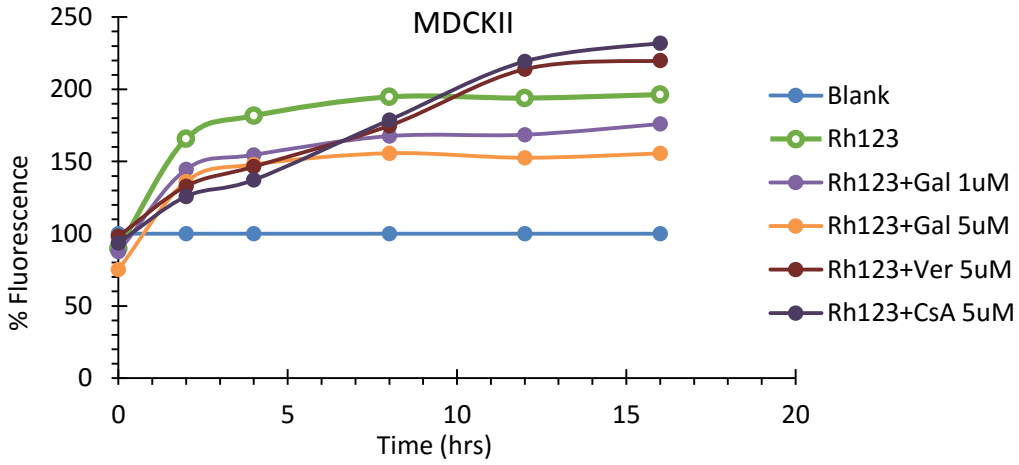
MDCKII
% Fluorescence
Time (hrs)
Blank
Rh123
Rh123+Gal 1uM
Rh123+Gal 5uM
Rh123+Ver 5uM
Rh123+CsA 5uM

**B)**

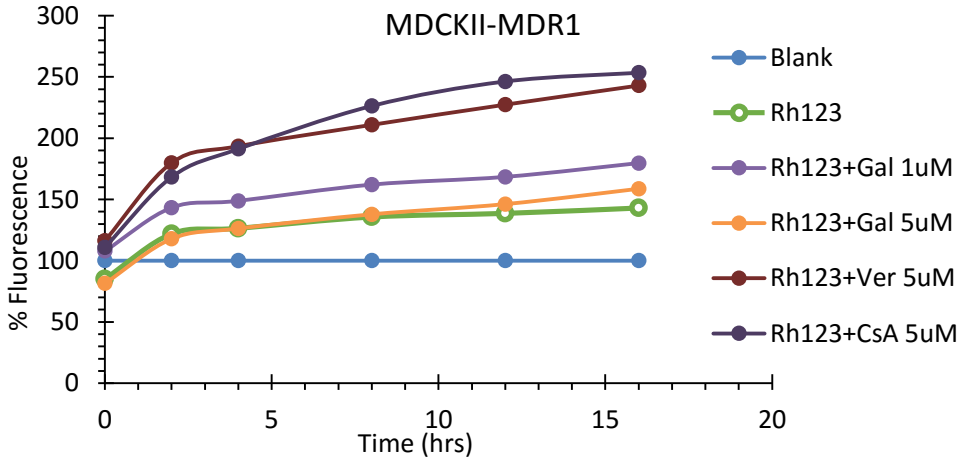
MDCKII-MDR1
% Fluorescence
Time (hrs)
Blank
Rh123
Rh123+Gal 1uM
Rh123+Gal 5uM
Rh123+Ver 5uM
Rh123+CsA 5uM

**C)**

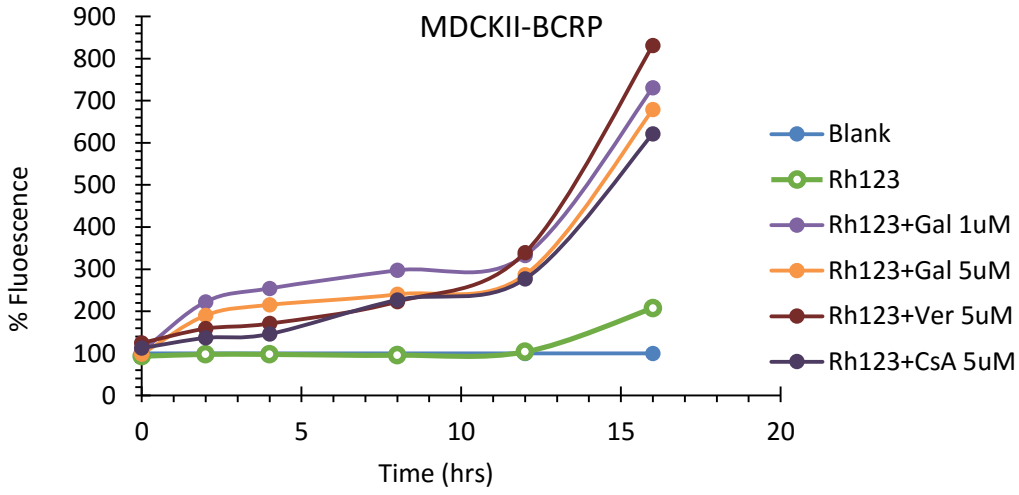
MDCKII-BCRP
% Fluoescence
Time (hrs)
Blank
Rh123
Rh123+Gal 1uM
Rh123+Gal 5uM
Rh123+Ver 5uM
Rh123+CsA 5uM

**D)**

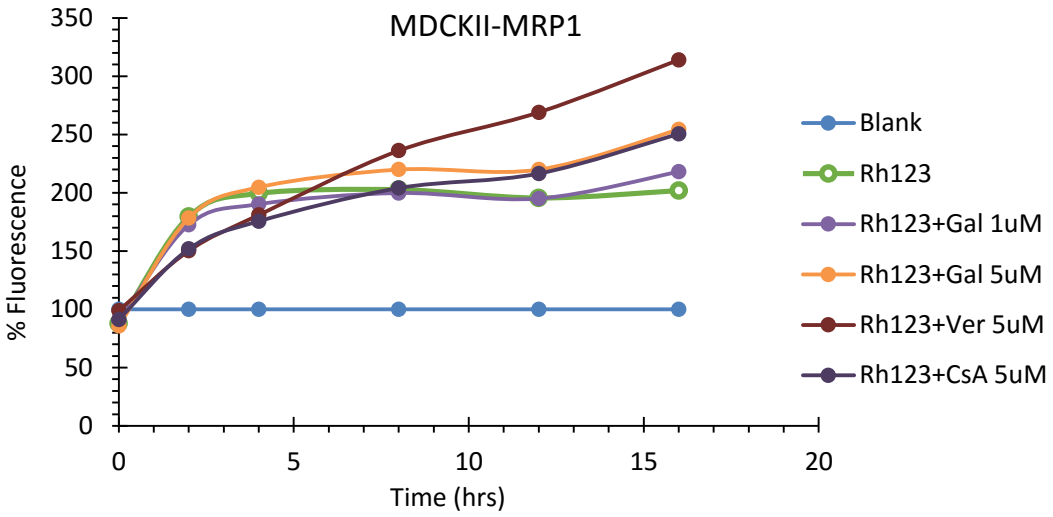


***Figure 5.24: % Fluorescence in Rh123 assay with different inhibitors***

*A)MDCKII, B) MDCKII-MDR1, C) MDCKII-BCRP and D) MDCKII-MRP1 cells (4.6,4)*

Results for assay was observed in Figure 5.24 (A, B, C and D) and these were achieved with further modification of assay procedure explained in methods section (4.6, 4). The fluorescence pattern for verapamil and cyclosporine A seemed similar like last experiment and there was no any promising change observed even after further pre-incubation of cells in presence of respective inhibitors. As like earlier results, these two known inhibitors shown strong inhibition activity only against MDR1 proteins, while it shown comparatively poor activity against BCRP and MRP1 proteins. In BCRP overexpressing cells, the activity after 12 hrs seemed to increasing rapidly. This sudden incline observed even in control samples where we did not applied any inhibitor which could stop the decay of fluorescence and show high intensity. This was unacceptable observation as compared to other graphs and mechanism of

assay. So it seems that it might be false reading observed by the plate reading as a result of some unknown factors.

From all results observed above, rh123 assay gives clear picture on the inhibition of efflux proteins. As seen in all our different procedures, Galaxolide gives better inhibition activity than other known inhibitors. Galaxolide shown better activity at 1µM concentration than 5µM and unlike verapamil and cyclosporine A it had strong inhibition activity against all three efflux proteins; MDR1, BCRP and MRP1. In reverse of this Verapamil and cyclosporine A had strong inhibition action only against MDR1 while these two compounds shown poor activity against BCRP and MRP1. So here from obtained results it could be clear that, galaxolide could be a novel efflux transport inhibitor molecule which has broad range of activity against all three major efflux proteins.

### 5.6 Summary

The objective of this study was to evaluate galaxolide as a novel efflux transport inhibitor and use this characteristics for the improvement of drug therapies against diseases in which cell confers MDR and does not respond to chemotherapy. This characteristic of galaxolide could also be used to pass the drug molecules through biological membranes which expresses efflux proteins and creates a major hurdle for the drug penetration and eventually affects drug treatment.

Before going further it was necessary to study the toxicity of galaxolide on various cell lines, so cell toxicity assays like MTT assay was performed. The assay provides us information that galaxolide was not toxic to normal cells as it shows much higher $IC_{50}$ values than the concentrations actually used for our

studies. Various cell lines were used for this study including some cancer cells as well. Galaxolide shows less toxicity for all those cells and in fact very minute toxicity at the concentrations was used to perform other experiments. Once safe concentration of galaxolide was determined, it was necessary to study the P-gp expression in cells which were planned to use in experiments. So P-gp expression was studied using two well-known methods like western blot and flow cytometry. Both studies were carried using two different antibodies used for P-gp detection. But as we seen antibody C219 gives positive results in western blot as we clearly see the bands, while other antibody anti-ABCB1 gives good results with flow cytometry. Expression of P-gp was observed in two cell lines Caco-2 and MDCK. Other technique, immunohistochemistry was also used to study P-gp expression, but due to some technical reasons and time limitations further optimization of the method was not done and no any results were mentioned. In later section of this chapter P-gp inhibition study was performed, in which rh123 efflux assay was used to study P-gp inhibition or efflux transporter inhibition. Several protocols were used with slight differences to carry this study. And finally it was found that galaxolide unlike other known inhibitors; verapamil and cyclosporine A; had better activity against all three major efflux proteins; MDR1, BCRP and MRP1. So it proves that the galaxolide is better efflux transporter inhibitor than verapamil and cyclosporine A, as it has immediate inhibitory action against these proteins.

# 6 : Permeability Study

## 6.1 Introduction

In this chapter permeability of curcumin through various cell membranes was explored as well as the development of HPLC methods for the quantification of curcumin is also studied.

## 6.2 Cell based Permeability study

Cell based permeation studies involve a transwell cell culture setup, in which the cells were grown on a permeable filter membrane inserts. Dense cell layers polarize on this filter layer to apical and basolateral sides (basolateral side facing to the solid filter growth support). The test compounds can be applied on either side of the cell layer (to the cell insert or the culture plate medium), which allows study of the permeation / transport form apical to basolateral (AB) and basolateral to apical (BA) directions. Here in this study permeation was performed only in one direction; apical to basolateral (AB) direction as per the requirement of our studies.

Typically the study involves sampling of the test compounds on both sides at given time points, followed by analysis of the test item concentration by HPLC method. Based on the measured concentrations, apparent permeation coefficient is calculated (Papp). We also check the cell layer was intact in each well by a TEER (trans-epithelial electrical resistance) measurement before the experiment.

The cell based permeation models have some active drug transporter systems, including P-glycoprotein efflux transporter (P-gp, also known as multidrug resistance protein 1, MDR1, a member of the ABC transporters). The

involvement of the transporters can be estimated both in the apical-to-basolateral vs basolateral-to-apical permeability's. As seen in earlier studies, galaxolide have P-gp inhibition activity, so it was used with curcumin in permeability study to observe effect of galaxolide on the permeation of curcumin. In addition, known P-gp inhibitor was used with curcumin during permeation to assess the activity of galaxolide.

To complete successful permeation study, it was necessary to have good analytical method so that the permeation of drug accurately could be determined. Curcumin was used as a drug molecule, so it was necessary to developed HPLC analysis method for it. Several HPLC methods were developed for the curcumin detection, out which one was developed without use of internal standard while other method was developed using internal standard. Internal standard was used to minimize the error in quantification. The most common reason to use internal standard is to eliminate variations with the injection volume. Because an internal standard method uses the ratio of responses for standard and analyte, quantitation does not depend on the amount of material injected. Further modifications in HPLC method for curcumin quantification are done according to the receiver media used in the permeation study. Several different extraction methods and solvents are used and finally extraction efficiency is determined in each method and according to that data and final HPLC method was chosen for the curcumin quantification. All method details and sample preparations are explained in methods section above (4.7).

## 6.3 HPLC analysis of curcumin

HPLC methods were developed with different receiver media. Also the method developed in presence and absence of internal standards. All the results for these developed HPLC methods were described briefly here.

### 6.3.1 HPLC analysis without internal standard

The details of this method development were described in section 4.7.1. To obtain linearity curve, acetonitrile was used as solvent for curcumin. To identify peak for curcumin, blank acetonitrile was injected and analysed with HPLC, while to differentiate curcumin peak from media peak, extracted media also injected individually without curcumin in it. And later these solvents were used to prepare samples of curcumin. Following are the different samples showing peaks for the curcumin as well as blanks solvents.

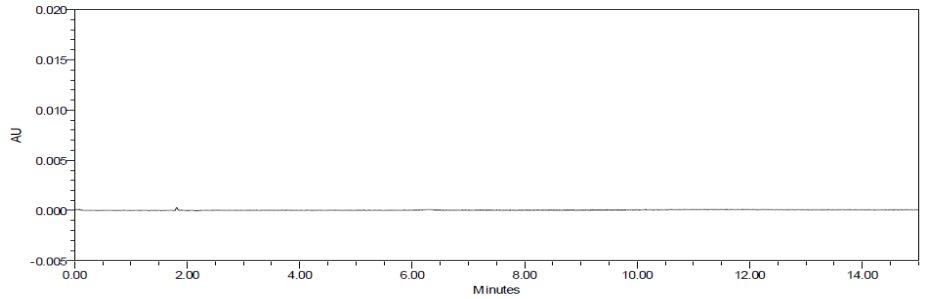


Blank ACN

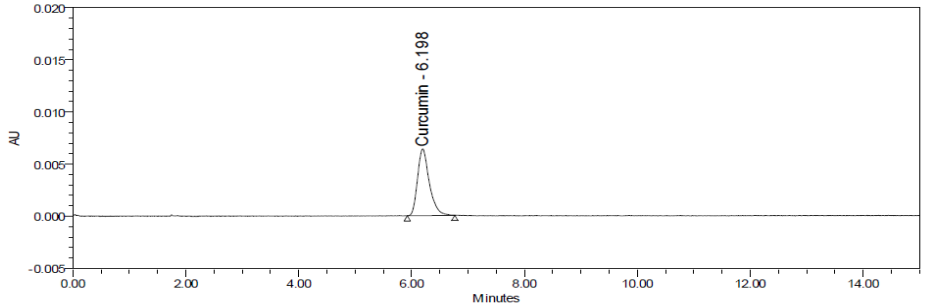


Std. Cur in ACN

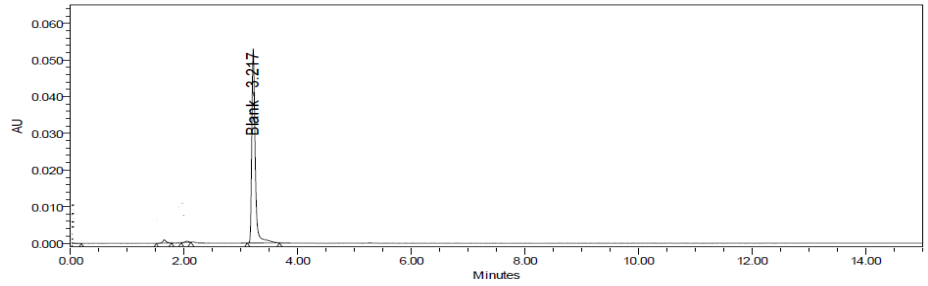


Blank Media

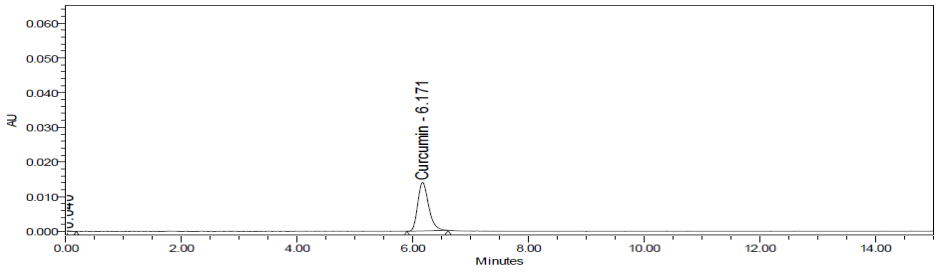


Std. Cur in Media

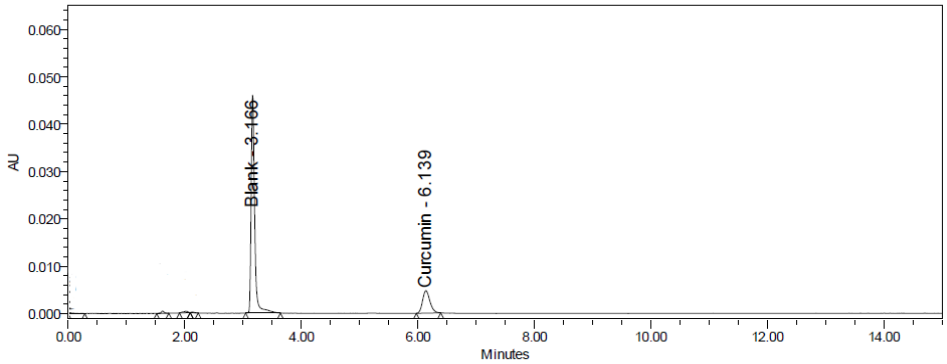


Cur in

Permeated sample

***Figure 6.1: HPLC chromatogram for curcumin (RT=6.1±0.1)***

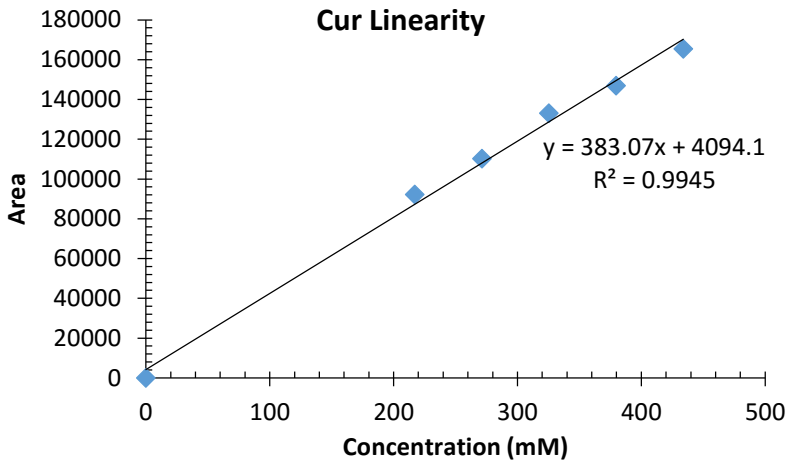


***Figure 6.2: HPLC calibration curve for curcumin***

Figure 6.1 shows the peak for curcumin and blank solvents. To identify peak for curcumin, blank samples for acetonitrile and media were injected and HPLC analysis was performed. This blank samples help to differentiate the peaks particularly observed in receiver media. From above data obtained, it clearly seems that, retention time (RT) for curcumin is 6.1±0.1 and is far away from the peak of blank media which observed around RT 3.1±0.1.The method gives fine peak for the curcumin without interference of any other peak in both solvent systems; media and acetonitrile; so this method was used to obtain calibration curve. Linearity was done using different concentrations of curcumin prepared in acetonitrile. Area obtained for different curcumin concentration was plotted against the concentration and linear calibration curve was obtained with $R^2$ value which is 0.9945 (Figure 6.2).This method of curcumin quantification was used for the analysis for initial permeation studies. Before developing further methods, studies performed to determine effect of media component and extraction method on the yield quantification of the curcumin. So serum media

and serum free media were used to examine curcumin detection in both the media.

### 6.3.2 Curcumin analysis in serum media and serum free media

During permeability study, receiver media needs to be preparing to collect the sample permeated. Receiver media plays an important role in permeation study. So it was necessary to analyse the drug of interest in possible receiver mediums. Growth media was used as receiver media and to choose effective receiver media, analysis of curcumin was done in both serum media and serum free media. So samples were prepared in these two mediums and extracted with acetonitrile by 1:1 and 1:2 extraction methods (4.7.3).

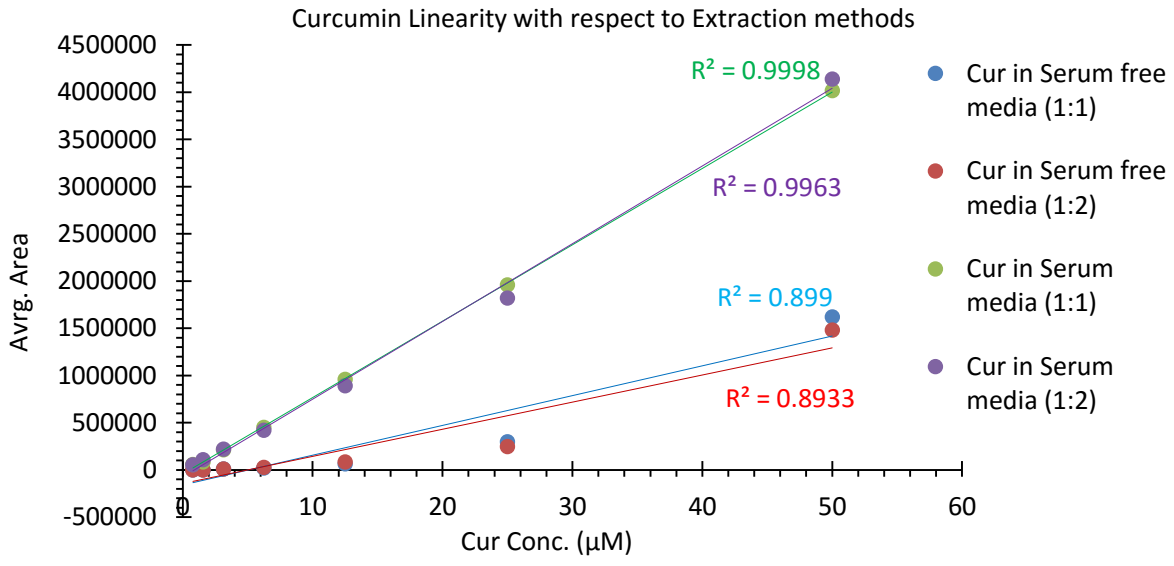


***Figure 6.3: HPLC calibration curve for Curcumin with different solvents and extraction method***

As mentioned above two different solvents were used; serum media and serum free media; and both sample sets were extracted with two different methods. Figure 6.3 gives the calibration curves for respective samples. Samples prepared in serum media gave higher yield after extraction as compared to the samples prepared in serum free media. There was no any major difference of extraction methods on the yield of curcumin. Both extraction methods (1:1 and 1:2) gave approx. similar yield in their respective samples. Extraction method did not have high impact on curcumin yield from the receiver media, but serum played important role in yield. So in all permeability studies 1:1 extraction method, and serum containing growth medium was used. To get more accurate results, new method was developed using internal standard. The internal standard used to minimize errors.

### 6.3.3 HPLC method with internal standard

The method development part was described in section 4.7.2. Emodin was used as an internal standard for curcumin. Ratio of curcumin to internal standard (IS) was used to quantify curcumin concentration in the sample. Since emodin was used as internal, standard, few changes were done in the HPLC system and are described earlier section 4.7.2. Same like previous, various individual samples were injected to perform HPLC, to differentiate peaks of blank, curcumin and internal standard.

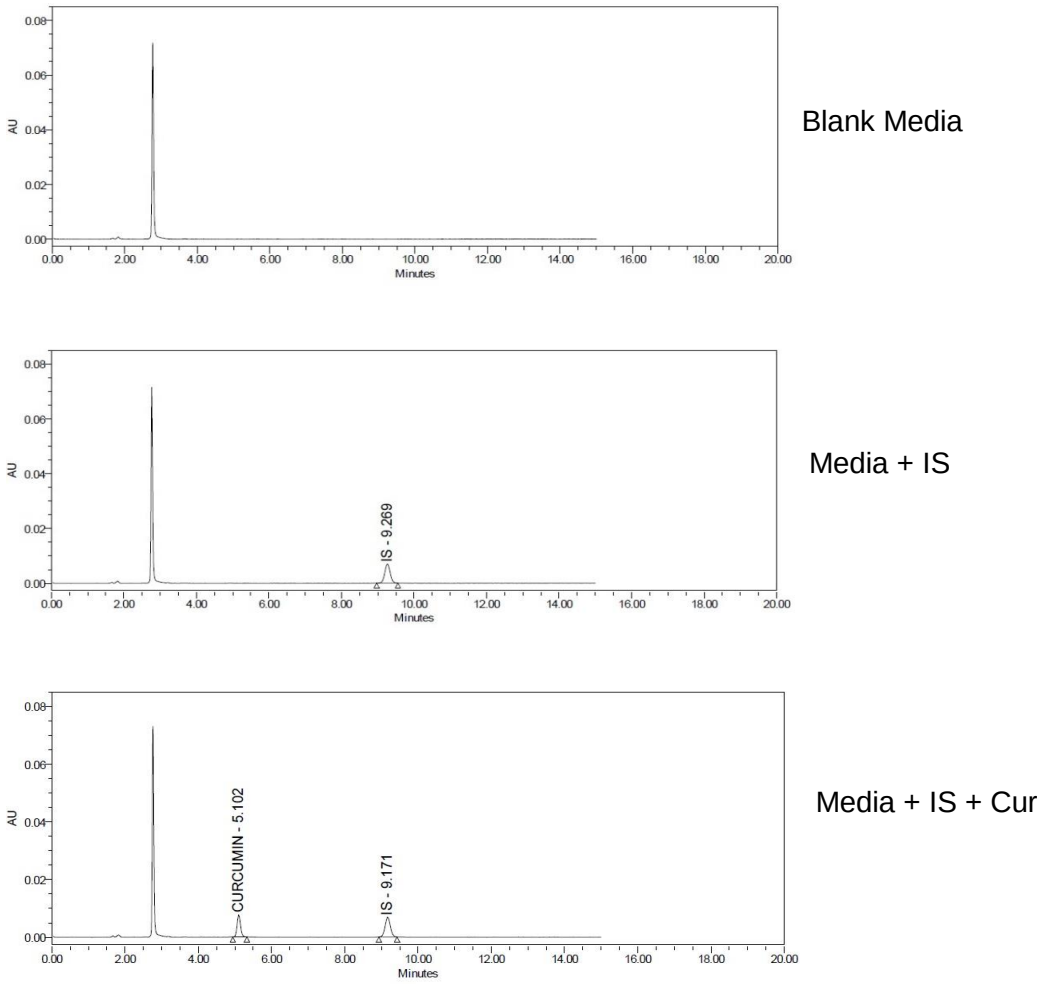


***Figure 6.4: HPLC chromatogram for curcumin (RT=5.1±0.1) with emodin (RT=9.2±0.1) as internal standard***

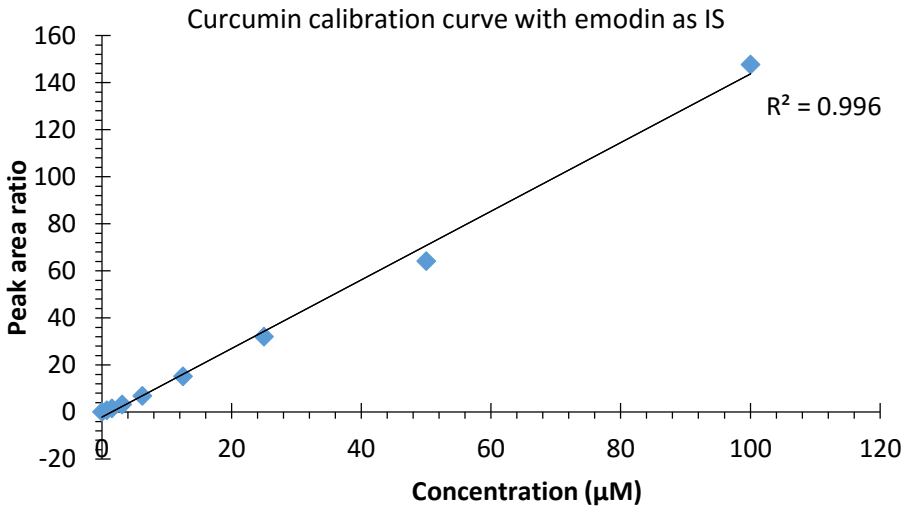


***Figure 6.5: HPLC calibration curve for Curcumin with emodin as IS***

Method for curcumin analysis was developed using internal standard. Both curcumin and IS gives sharp peaks which were completely distinct from one another. In Figure 6.4, first picture shown the peak for blank media. Only media was injected and performed HPLC, so this peak was observed and which was considered as blank peak. In next sample, addition of IS was done to the media and this mixture gives peak which was described in second picture of the same figure. The peak around RT 3 was blank peak as described in the first sample, and the other peak was observed near RT 9.2±0.1 and this peak was for internal standard. Next sample injected, had mixture of curcumin and IS in media. The third picture in above figure gave three different peaks. Out of which, peak near RT 3 and peak at RT 9.2±0.1 were the peaks for the blank and IS respectively, and third peak which is at RT 5.1±0.1 was definitely for the curcumin. So in this way HPLC method was developed for curcumin with IS. Calibration curve for curcumin with this method was determined. Graph was plotted with peak area ratio vs concentration. Linear calibration curve with $R^2$ value 0.996 is obtained (Figure 6.5).

### 6.3.4 Extraction efficiency of curcumin in serum media

All the above studies were performed to develop efficient HPLC method for curcumin analysis. Serum media was selected as a receiver media to carry out permeability study with curcumin. It is also necessary to determine exactly what percentage of curcumin is present in the extracts of the media. To study extraction efficiency, two sets of curcumin concentrations were analysed, one set is prepared in pure acetonitrile and other set is prepared in serum media. Any amount detected in acetonitrile, is considered as 100% recovery. Curcumin

recovered in serum media is calculated against curcumin recovered in acetonitrile, and percentage of recovery is determined. This percentage is then considered as extraction efficiency.

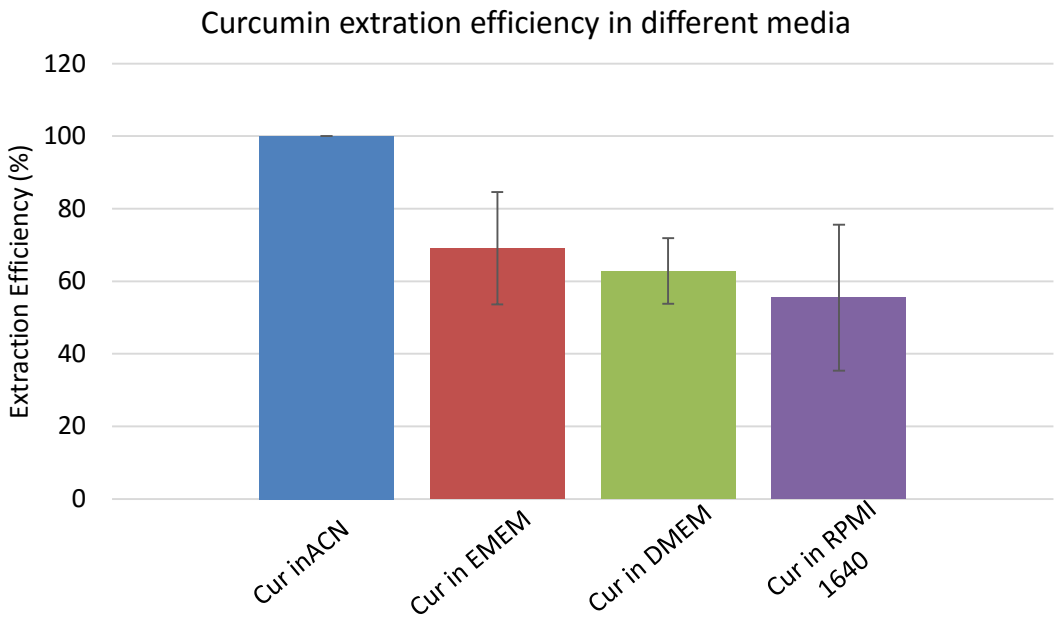


***Figure 6.6: Extraction efficiency (%) of curcumin in different media***

***Table 6.1: Extraction efficiency (%) of curcumin in different medium***

| Media | Extraction efficiency (%) ± SD (n=2) |
|---|---|
| Acetonitrile | 100 ± 0 |
| EMEM | 69.10 ± 15.47 |
| DMEM | 62.82 ± 9.06 |
| RPMI 1640 | 55.51 ± 20.13 |

Different cell lines were grown in different media, so extraction efficiency in various media was carried out. Here three different growth media were used;

EMEM, DMEM and RPMI 1640; to study extraction. EMEM media shown higher extraction as compare to other two media, though the difference was not too high. EMEM shows 69.09 ± 15.47 % of recovery of curcumin while DMEM and RPMI 1640 shows 62.82 ± 9.06 % and 55.50 ± 20.12 % of recovery as compared to the pure acetonitrile recovery. Though these media shows relatively poor extraction efficiency for curcumin recovery, these media were used further to carry permeability studies. Table 6.1 describes values of extraction efficiency for different media.

Several trials such as use of serum and serum free media or change in acetonitrile percentage during extraction were done to increase extraction efficiency using these media, but none of them were successful. So decided to use one more receiver media, which was used by some researchers to study permeation. This receiver media was HBSS with 4% BSA having pH 7.4 (Yu and Huang, 2011). The media preparation is described in section 4.7.5.

### 6.3.5 Curcumin analysis in 4% BSA media

This media was prepared with addition of 4% BSA in HBSS at pH was maintained at 7.4. 20mM HEPES buffer was added to media to maintain desired pH. This media was used to develop HPLC method with 1:1 extraction process. Similar to earlier process developed with IS, samples were prepared and analysed using HPLC.

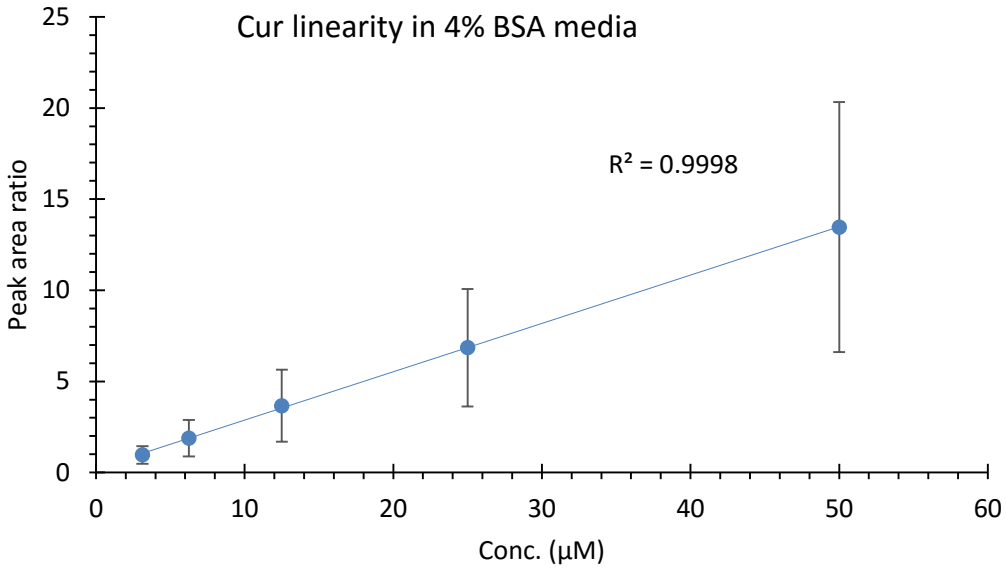


***Figure 6.7: HPLC calibration curve for curcumin in 4% BSA media***

Calibration curve was obtained with this method (Figure 6.7) with $R^2$ value 0.9998. This calibration curve was further used to quantify amount of curcumin present in unknown samples obtained after permeability study. Extraction efficiency for this media was studied to assess the curcumin recovery from the samples collected in 4% BSA receiver media.

### 6.3.6 Curcumin extraction in 4% BSA receiver media

To study extraction efficiency 4% BSA media, curcumin solutions were prepared three different solvents such as pure acetonitrile, HBSS without BSA and HBSS with 4% BSA. All these samples contains same concentration of curcumin. Samples were extracted with 1:1 extraction process, while samples prepared in 4% BSA media was extracted with both 1:1 and 1:2 extraction process. Recovery in acetonitrile considered as 100% extraction and other

solvents were compared against acetonitrile recovery to determine % extraction with respective media.

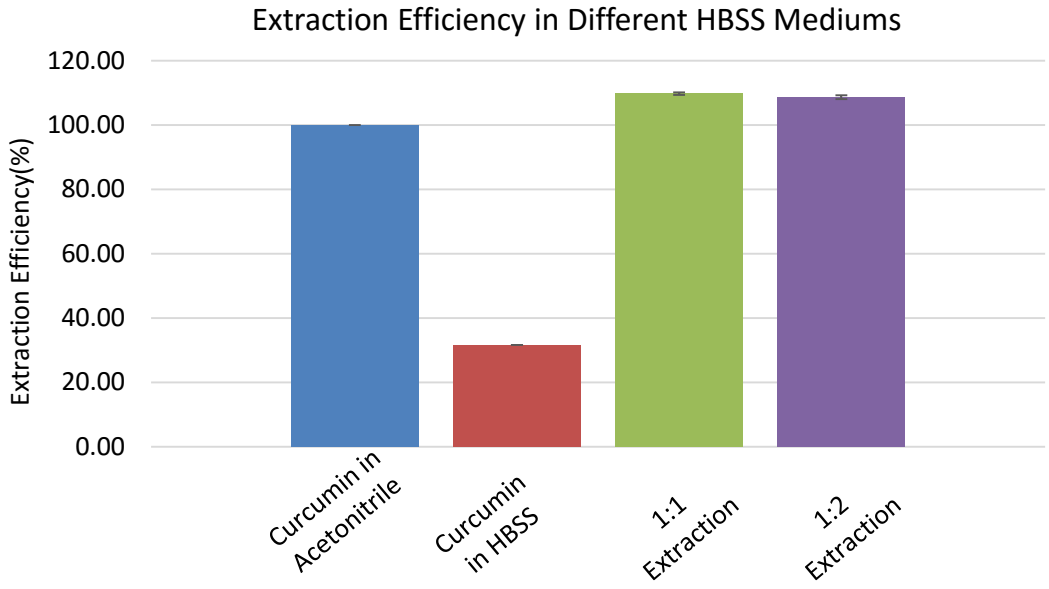


***Figure 6.8: Effect of BSA and solvent amount on extraction efficiency of curcumin from HBSS media.***

As seen in Figure 6.8, curcumin samples prepared in HBSS gave very poor yield of curcumin while samples prepared in 4% BSA media gave almost 100% recovery of curcumin. Both extraction processes 1:1 and 1:2 gave 100% recovery in 4% BSA media. So data suggested that, the 4% BSA media gave best receiver media amongst all above receiver media as it shown highest recovery of curcumin after extraction process. The values for extraction percentage for specific media are described in Table 6.2.

***Table 6.2: % extraction of curcumin in different HBSS media***

| Sample | Extraction Efficiency (%) ± SD (n=3) |
|---|---|
| Curcumin in acetonitrile | 100.00 ± 0.0 |
| Curcumin in HBSS | 31.58 ± 0.01 |
| 1:1 Extraction | 109.76 ± 0.40 |
| 1:2 Extraction | 108.62 ± 0.58 |

A HPLC method for curcumin analysis using different mediums as a solvent was developed. It was observed that, curcumin recovery was higher in serum containing media than the serum free media. And was even higher 4% BSA media. From series of experiments it was found that, any media containing protein molecules shown the higher recovery of curcumin compared to media lacking additional protein molecules. This might be due to curcumin degradation in alkaline condition in the media, while, in protein containing media, curcumin could bind proteins or BSA strongly and could reduce the chances of degradation. The binding is stronger at alkaline pH than acidic, and receiver media used in this study was alkaline (pH 7.4) (Mitra, 2015; Wahlang et al., 2011). So it is possible that the proteins or BSA present in the receiver media, protects curcumin from the degradation and eventually gives higher recovery.

## 6.4 Permeability Study

Several permeability experiments performed for curcumin with and without co-administration of galaxolide. All permeation studies were carried on day-12 from the date of plating of cells on transwell because of the trans epithelial electric resistance (TEER) value, which was higher on this day. The TEER value was measured to evaluate the confluence and integrity of cell membrane. For every permeability experiment, TEER was measured before and after permeation. Only those transwells with TEER above 300 $\Omega.cm^2$ were used for permeation studies (Wahlang et al., 2011; Yu and Huang, 2011).

### 6.4.1 Permeation study with growth media as donor and receiver media

As mentioned above, various different protocols were followed to study curcumin permeability through Caco-2. There were some minor changes in each protocols and are described here with each results.

**Permeation study-1**

In this study (Figure 6.9, Figure 6.10), growth media was used as a base for both donor and receiver media. The donor media prepared with 100 μM curcumin to carry permeation and 20μM galaxolide was used, to study its effect on permeation of curcumin and receiver media was fresh growth medium. Top chamber provided with 100 μL of donor media and bottom chamber with 600 μL receiver media. Two donor media; one had curcumin only and other had curcumin+galaxolide; were incubated separately on corresponding cell membranes and permeation was performed. Samples were collected at every 5 mins for 1hr and then continued to collect at every hour up to 6 hrs. At every

sample collection time point, both the mediums (donor and receiver media) were replaced with respective fresh media to maintain constant diffusion gradient. Each drug sample studied for permeation was done in triplets.

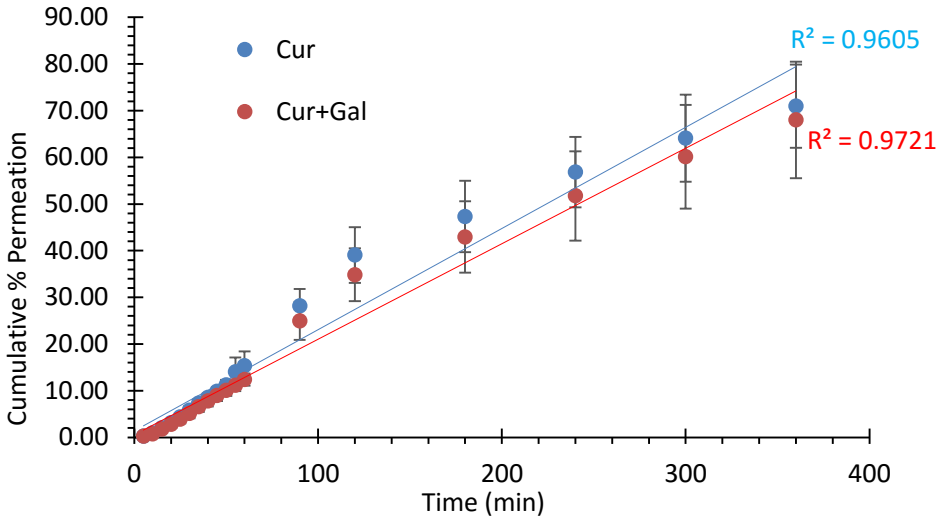


***Figure 6.9: Effect of galaxolide on permeation of curcumin through caco-2 monolayer***

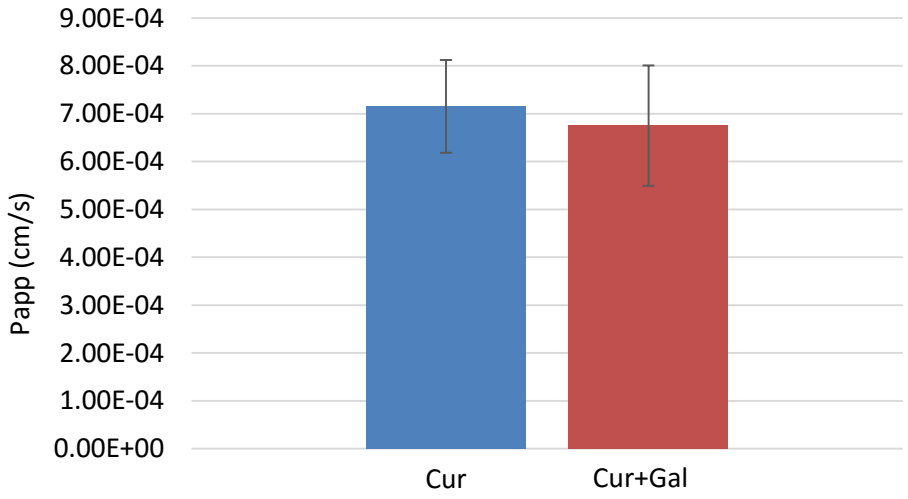


***Figure 6.10: Comparison of permeation rate of curcumin with and without galaxolide*** *(P > 0.05)*

As shown in Figure 6.9, the permeation was approx. 15% after 1 hr of permeability study, and at the end of study after 6 hrs the permeation was about 70%. The high percentage of permeation was only because, replacement of donor media every time during the sample collection with fresh donor media. That means every time there was new set of fresh curcumin concentration, which in turn gave approximately same permeation amount of curcumin every time. These permeated values then put together by taking their cumulative value and plotted on graph. And as a result of cumulative data higher permeation was observed. Same results were obtained in both the drug samples; cur and cur+gal. No promising difference in permeation percentage of curcumin was observed through Caco-2 with and without galaxolide in this study. Permeation rate ($P_{app}$) was also determined with these two drug samples through Caco-2 (Figure 6.10). The $P_{app}$ for cur and cur+gal was (7.15 ± 0.9) × $10^{-4}$ and (6.75 ± 1.2) × $10^{-4}$ respectively. This rate was considered as higher permeation rate (Yu and Huang, 2011) and as seen earlier this might be because of the permeation procedure followed as described above. Addition of galaxolide to donor media shown slightly low permeation rate and this data did not seem to be statistically significant ($P > 0.05$) using paired t-test.

## Permeation study-2

This study was repeated with similar donor and receiver media. This time unlike previous experiment, samples were collected at every 5 min up to 1hr only.

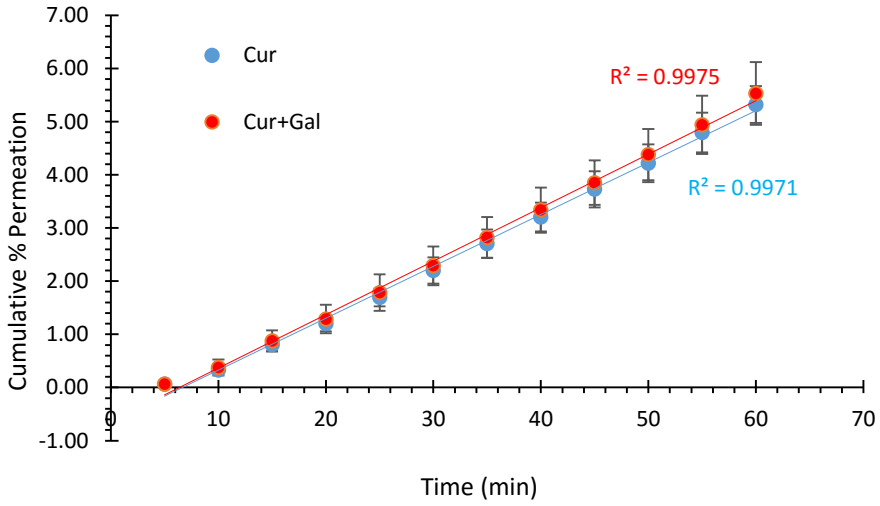


***Figure 6.11: Effect of galaxolide on permeation of curcumin through caco-2 monolayer***

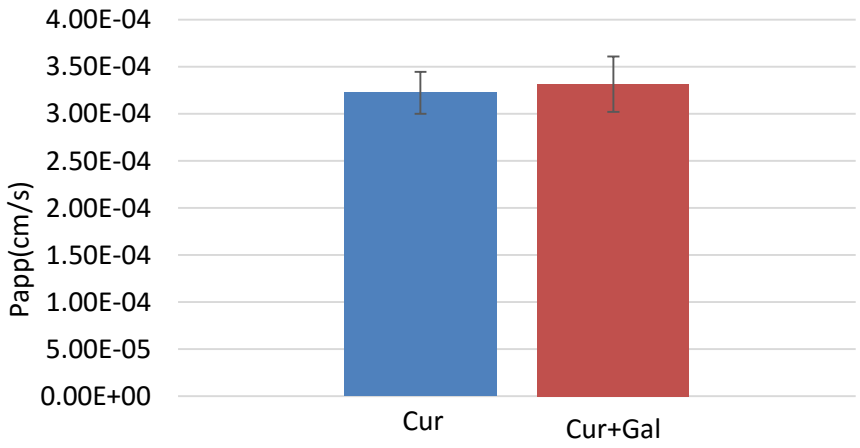


***Figure 6.12: Comparison of permeation rate of curcumin with and without galaxolide*** *(P > 0.05)*

Figure 6.11 showing approx. 5% permeation with curcumin and 5.5% permeation when galaxolide was added with curcumin and this permeation percentage investigated after 1 hr. Here also donor and receiver media were replaced with fresh mediums at the time of every sample collection point. The $P_{app}$ for the curcumin and cur+gal through Caco-2 was $(3.22 \pm 0.2) \times 10^{-4}$ and $(3.32 \pm 0.2) \times 10^{-4}$ respectively (Figure 6.12). The permeation rate seemed to be similar with no any major difference. We did not see any major effect of galaxolide on the permeation of curcumin through Caco-2. Though the permeation rate after galaxolide addition observed slightly higher than that of one without galaxolide addition, this difference was statistically insignificant ($P > 0.05$). The permeation rate was determined in this study and as mentioned above it's considered very high permeation rate, and like previous study it was possibly because of the procedure followed. Because the curcumin concentration was maintained at constant in donor media throughout study and did not allowed it to go down. So this abundance quantity of curcumin might have given higher permeation rate.

**Permeation study-3**

The permeation protocol was then further modified with no change in experimental condition. Just one thing changed that the sample collection time. Earlier samples were collected at every 5 mins and this might did not allowed enough time to permeate curcumin through the Caco-2 monolayer and because of that there might be unwanted results. So in this experiment samples were collected at every 15 mins and study was performed up to 90 mins.

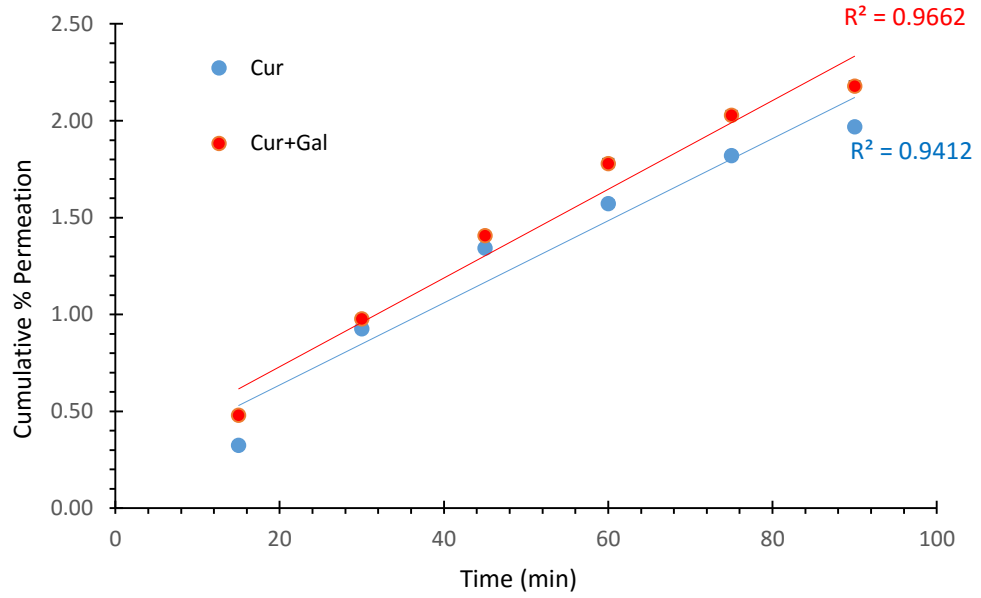


***Figure 6.13: Effect of galaxolide on permeation of curcumin through caco-2 monolayer***

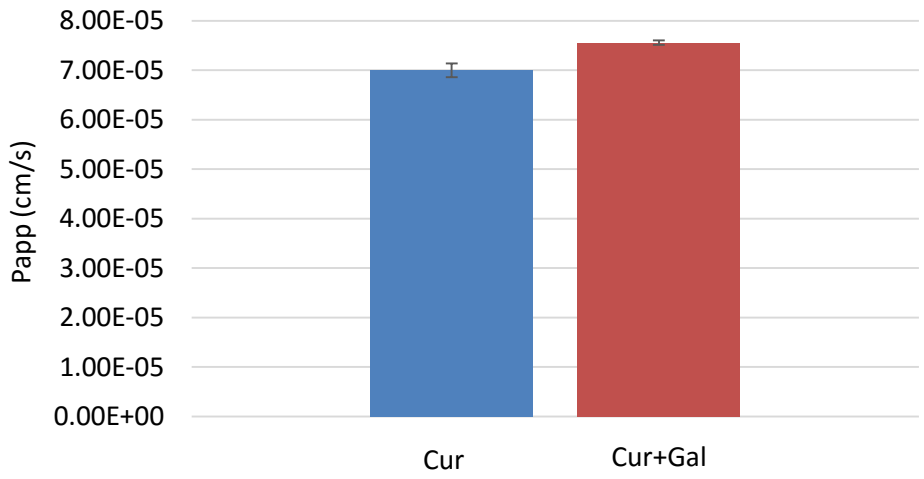


***Figure 6.14: Comparison of permeation rate of curcumin with and without galaxolide*** *(P < 0.05)*

In this study slightly different results were observed than previous experiment. As seen in Figure 6.13 less than 2% permeation of curcumin through Caco-2 monolayers was observed; while the permeation of curcumin shown more than 2% when galaxolide was added to donor media through. $P_{app}$ was also determined with both the drug samples; with and without addition of galaxolide (Figure 6.14). The permeation rate observed for curcumin was (7.00 ± 0.1) × $10^{-5}$ and the permeation rate for cur+gal was (7.56 ± 0.04) × $10^{-4}$. The permeation rate with cur+gal was significantly higher than the permeation rate with cur only ($P < 0.05$). Some enhancement was observed in curcumin permeation through the Caco-2 monolayer when galaxolide was added with curcumin in donor media (Figure 6.13). So its possibility that galaxolide could enhance the curcumin permeability. Though the permeation enhancement was observed in curcumin with galaxolide, there was no big difference in between both drug solutions permeation rate.

**Permeation study-4**

Galaxolide did not show robust effect with permeation enhancement. Galaxolide with 20 μM concentration was used, and this concentration was selected randomly. So few more concentrations of galaxolide were used except currently used 20μM and repeated permeation experiment with galaxolide concentrations such as 40μM, 60μM, 80μM and 100μM to study its effect on permeation of curcumin.

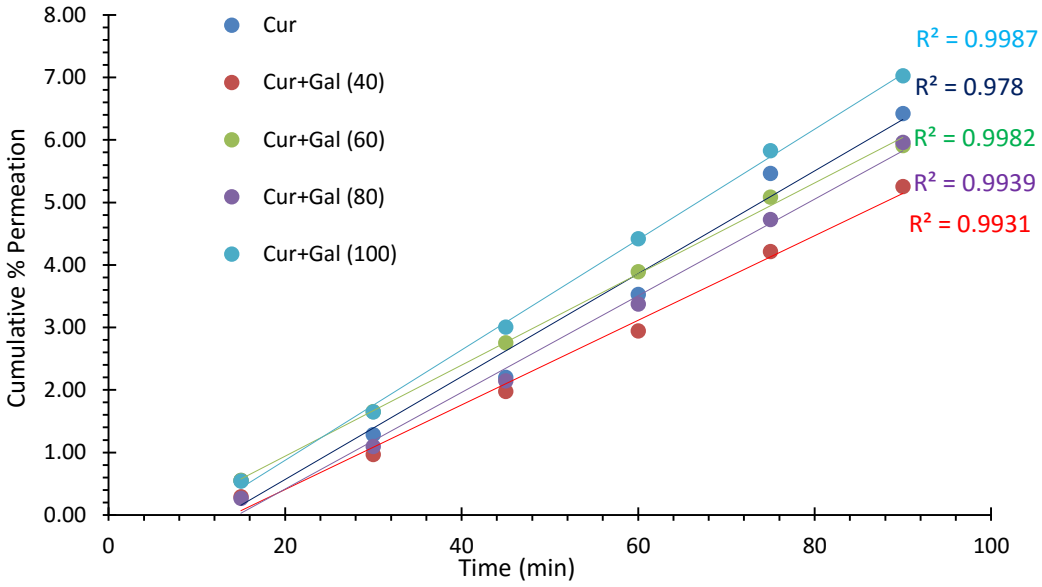


***Figure 6.15: Effect of different galaxolide concentrations on permeation of curcumin through caco-2 monolayer***

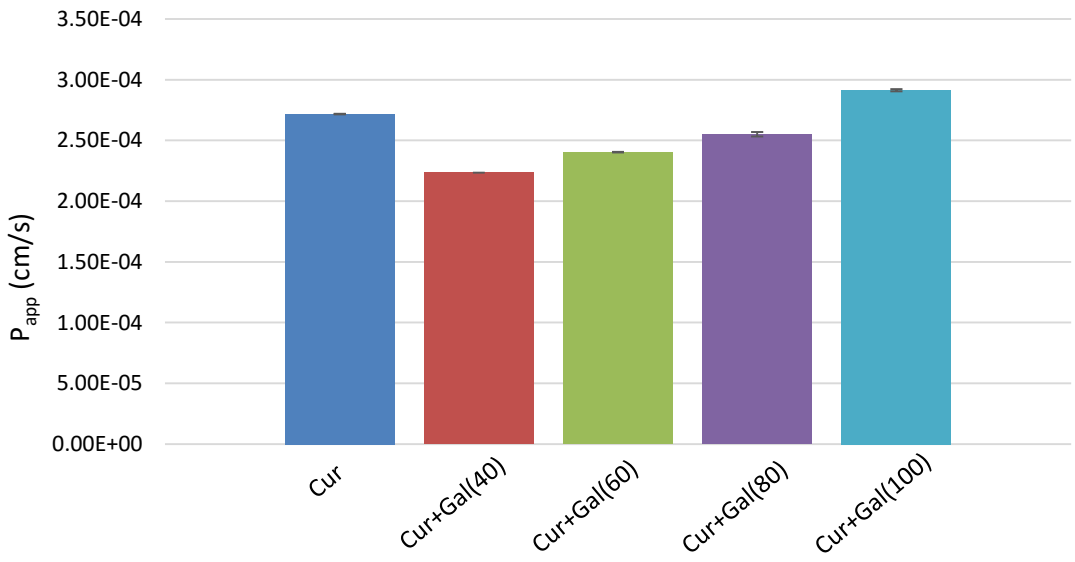


***Figure 6.16: Comparison of permeation rate of curcumin with different galaxolide concentration***

*(cur+gal 40: $P < 0.05$; cur+gal 60: $P > 0.05$; cur+gal 80: $P < 0.05$; cur+gal 100: $P < 0.05$; )*

Figure 6.15 showing the results for the permeation study with different galaxolide concentrations with curcumin as mentioned above. In this experiment as like earlier experiment, samples were collected at every 15 mins for up to 90 mins and analysed for the permeation amount. As seen in Figure 6.15, donor media with curcumin only (dark blue line) shown 6.42% permeation of curcumin after 90 mins through Caco-2 monolayer and which was better permeation percentage than other drug samples prepared with galaxolide (40 μM, 60μM and 80μM) and applied to permeate. The donor media prepared with 40μM galaxolide (red line) gave 5.25 % permeation, donor media prepared with 60μM galaxolide (green line) shown 5.91 % and donor media prepared with 80μM (purple line) galaxolide shown 5.96 % permeation of curcumin through Caco-2 monolayers. While donor media prepared with 100μM galaxolide (bright blue line) shown highest permeation percentage and which was almost 7.02 and was even higher than previously mentioned permeation study done with curcumin only samples. $P_{app}$ for each of these drug samples was calculated (Figure 6.16).Permeation rate for donor media having curcumin only (without galaxolide) was $(2.72 \pm 0.002) \times 10^{-4}$ and this rate was considered as much higher rate of permeation. Like this other curcumin combinations with various galaxolide concentration show similar values for permeation rate. Permeation rate with 40μM galaxolide was $(2.23 \pm 0.0) \times 10^{-4}$, with 60μM galaxolide was $(2.40 \pm 0.002) \times 10^{-4}$, with 80μM galaxolide was $(2.55 \pm 0.01) \times 10^{-4}$ and 100μM galaxolide was $(2.91 \pm 0.009) \times 10^{-4}$. Permeation rate was higher with 100μM galaxolide than other galaxolide concentrations. Minute differences were observed in permeation of curcumin with and without presence of galaxolide.

These differences in all galaxolide concentration were statistically significant as all have $P < 0.05$ except 60μM galaxolide which have $P > 0.05$ (0.36).

With all these permeation experiments, one common thing was seen that in all permeation procedures top chamber was supplied with fresh donor media every time samples were collected. This action have given higher permeation percentage and higher permeation rate in all experiments. Even galaxolide concentrations was changed and even sample collection time points were changed, or even there was change in duration of permeation study, same kind of results were observed. There was no any major effect of galaxolide on permeation of curcumin through the Caco-2 monolayer. In some instances data observed, where it seems some enhancement in permeation with galaxolide, while in some instances there was decrease in permeation rate with galaxolide. Though these differences was there, these enhancement and reduction in permeation did not have promising differences with their counter drug solutions studied with. So it's hard to say here that galaxolide have role in enhancement of permeation of curcumin through Caco-2. One more thing that any known control was not used along with galaxolide to study the actual effect of galaxolide on permeation of curcumin. Study performed to apply P-gp inhibitory characteristics of galaxolide to enhance permeation of curcumin by preventing efflux of curcumin. No any robust data was observed which can show enhancement of permeation of curcumin, and there was no any known P-gp inhibitors for a control was used. So it was hard to predict here anything about galaxolide effect on permeation of curcumin in all studies above.

**Permeation study-5**

To overcome these shortfalls of above experiments, permeation experiments were repeated with newly modified procedures and also with positive controls; known P-gp inhibitors verapamil and galaxolide; and negative control in which permeability was performed through blank transwells on which cells were not grown. Also different cell lines were used to study permeability of curcumin through various cells forming multi-cell layers as well. Like earlier permeation studies, growth medium was used to prepare donor and receiver media. Changes were done in curcumin concentration that, donor media was prepared with 50μM and 100μM curcumin instead of only 100μM curcumin. Lower concentration of curcumin was used to eradicate the possibility of cell to saturate with high curcumin concentration and which might eventually affect permeation. One more major change was done in galaxolide concentration. 1μM galaxolide was used to study its effect on permeation. This concentration of galaxolide was chosen from the data obtained in rh123 assay in earlier chapter (5.5.1). As per results obtained in rh123 assay, it was seen that galaxolide had highest P-gp activity at 1μM concentration and this was the reason that this concentration was selected to use with permeation study.

Some modifications in protocol was done. 100μL donor media in top chamber and 1.2 ml (1200μL) in bottom chamber was added. Donor media was not changed throughout study. It was added only once at the beginning of study and never changed until experiment finishes. While receiver media was collected every time point, and only half the receiver media was taken out and

replaced with fresh media. Samples were collected at every 15 mins up to 90 mins.

To carry this permeability study, different cell lines were used like Caco-2, MDCKII-MDR1, MDCKII-BCRP and DLD-1. DLD-1 cell line produce multi-cell layer and that iss why this cell line was used to study effect of galaxolide on curcumin permeation through multi-cell layers (DLD-1 multi cell layers are shown in histology chapter 7). Other cell lines Caco-2 and MDCKII (and derivatives of MDCKII) are the cells which are widely used cell models for the permeability studies.

These cell lines were grown in different growth media to carry out regular cell maintenance processes. So in this study these respective media were used to prepare donor and receiver media while studying permeability using these cell lines. HPLC was also performed to study calibration curve of curcumin with each media (Figure 6.17, Figure 6.18 Figure 6.19) and for every media the recovery (% extraction) of curcumin was determined after extraction process. These results for these extraction studies are explained in Figure 6.6.

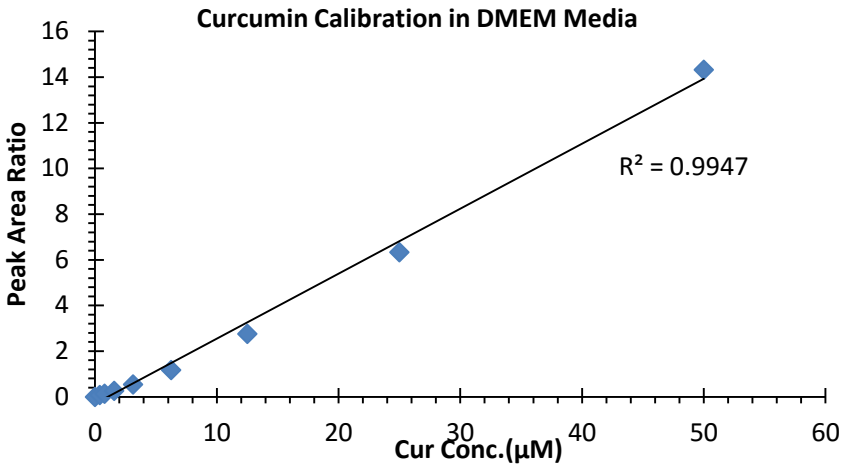


***Figure 6.17: HPLC calibration curve for curcumin in DMEM Medium***

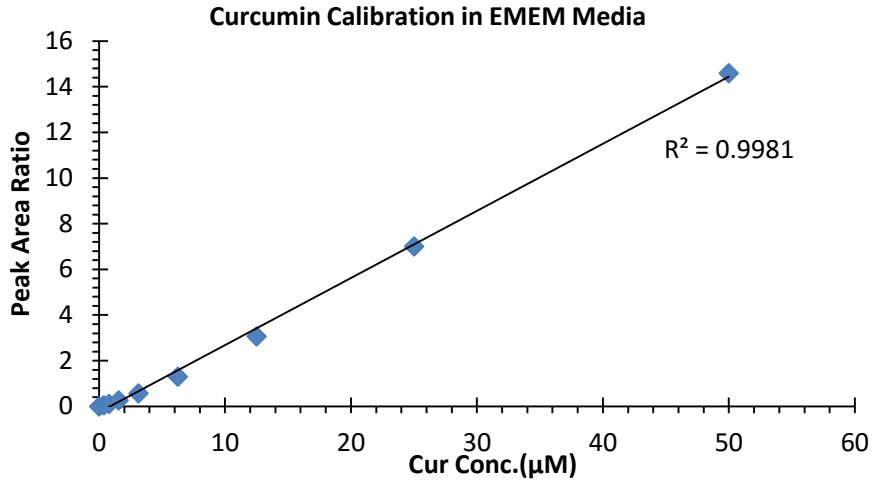


***Figure 6.18: HPLC calibration curve for curcumin in EMEM Medium***

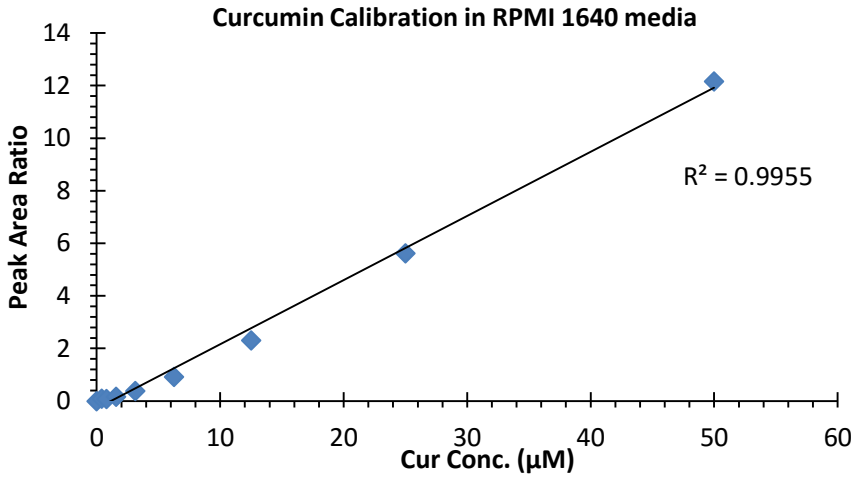


***Figure 6.19: HPLC calibration curve for curcumin in RPMI 1640 medium***

Unfortunately, with this modified method expected results were not observed. All samples for all cell lines did not shown a single peak for curcumin after permeation. Similar extraction methods were followed, and similar analysis method were used. All conditions were similar, but still failed to get permeation results. If it could say that curcumin was unable to permeate through cell membranes, it did not seen logical, because even through blank transwells permeation was not observed. This means there was something which could avoid curcumin from detection. As per new protocol followed, donor media was not replaced till the end of study, it means there was limited amount of curcumin in donor media, and as time passes the concentration of curcumin would go decreasing as permeation occurs. And whatever curcumin would permeate, could be in very little quantity. So obviously there could be very low permeation percentage as compare to the earlier studies performed. But there was no any evidence for permeation. So characteristic of curcumin was investigated to check its stability. And it was found that, curcumin readily goes under degradation and rate of degradation is higher at alkaline pH i.e. above7.0; while it has low degradation rate acidic pH i.e below 7.0. pH 7.4 shows the highest degradation of curcumin, and this pH was commonly used to transport studies (Wahlang et al., 2011). Here growth medium was used to prepare donor and receiver media. The growth medium generally has pH 7.4. As seen earlier, curcumin had highest degradation rate at this pH, so there was possibility that the curcumin used to study permeation had degraded and as a result of that its presence was not observer in samples collected during permeation study.

In earlier studies similar donor and receiver media was used, and despite of that permeation of curcumin was measured. But that time fresh donor media was used every time, and due to fresh donor media the curcumin was permeated before it gone under degradation. Here in this modified procedure, fresh donor media was not used after every sample collection time. So curcumin present in donor media have been possibly degraded during the process, or there is possibility that it had been permeated and then degraded there in receiver media before going to the analysis. Already it was possibly permeated in very low concentration, and above that it had degraded, and that is why it was possibility that, due to degradation there was no any results for this permeation study carried with various cells. Curcumin degradation could be confirmed by analysing its degradation products in receiver and donor media, but this study was not focused in that direction, so did not proceeded for this analysis.

### 6.4.2 Permeability study using 4% BSA in HBSS media

Because of unnecessary permeability values observed, donor media and receiver media were changed. New media were used; HBSS supplemented with 20mM HEPES having pH 6.5 to prepare donor media; while to achieve receiver media 4% BSA was added to HBSS supplemented with 20mM HEPES and pH is set to the 7.0. These different pH for both donor and receiver media and addition of 4% BSA to receiver media could mimic the *in vivo* condition as explained by Huang el.al.(Yu and Huang, 2011).

The permeability study with this donor and receiver media was done with two cell lines, Caco-2 and MDCKII-MDR1. Caco-2 cell line was used as intestinal

cell model while MDCKII-MDR1 was used as an *in vitro* blood-brain barrier model. Three different donor media were prepared, one having 50 µM curcumin, second with 50µM curcumin supplemented with 1µM galaxolide and third with 50µM curcumin supplemented with 5µM verapamil. Verapamil supplemented donor media was used as a positive control of the permeability study. 600µL donor media applied in top chamber and did not replaced at the time of sample collection; while 1.2 ml receiver media added to the bottom chamber and 600µL receiver media was removed during sample collection and replaced with the same volume of fresh donor media. Sample collected at every 15 mins and permeability study carried up to 90 mins. As mentioned earlier, cell membranes conferring TEER above 300 Ω.cm$^2$ were used only to study permeability.

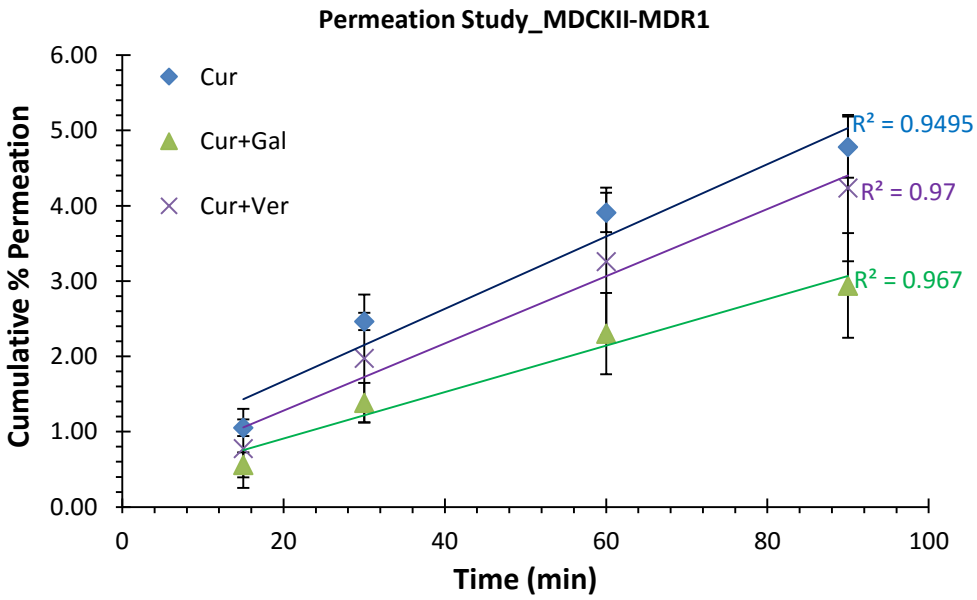


***Figure 6.20: Curcumin permeation across MDCKII-MDR1***

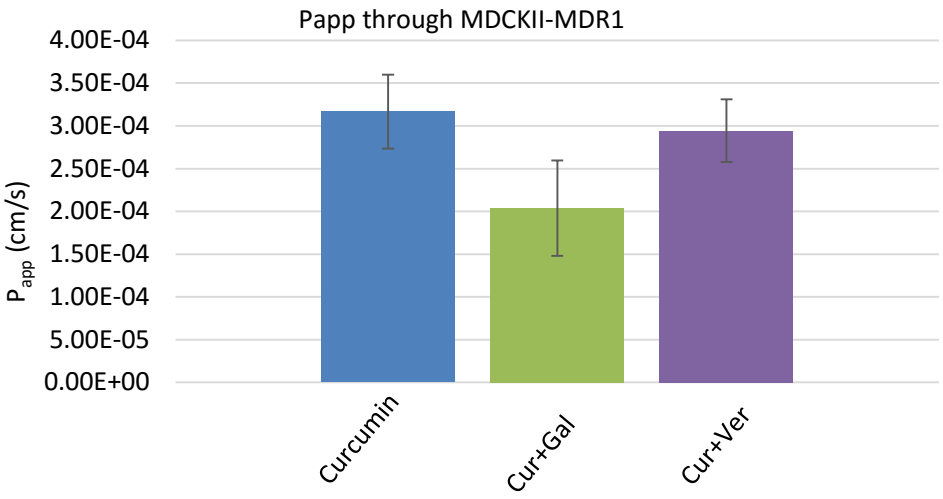


***Figure 6.21: Comparison of permeation rate of curcumin and curcumin with galaxolide and verapamil through MDCKII-MDR1***

Permeation of curcumin with newly developed donor and receiver media was observed. Donor media having curcumin (blue line in graph) shown 4.78% of curcumin permeation through the MDCKII-MDR1 cells and was the highest permeation as compare to the other two drug samples. Donor media having cur+ver (purple line in graph) shown 4.24 % permeation while donor media prepared with cur+gal (green line in graph) shown 2.94 % of curcumin permeation through the MDCKII-MDR1 cells. Cur+gal shown least permeation of curcumin as compared to other drug samples (Figure 6.20). The permeation rate for curcumin through MDCKII-MDR1 without addition of any P-gp inhibitor was $(3.17 \pm 0.4) \times 10^{-4}$ while permeation rate for cur+gal was $(2.04 \pm 0.5) \times 10^{-4}$ and for cur+ver the permeation rate was $(2.94 \pm 0.3) \times 10^{-4}$. The permeation rate for curcumin was significantly higher than the permeation rate for cur+gal ($P < 0.05$) and cur+ver ($P < 0.05$). No any enhancement was observed in permeation of curcumin with the addition of galaxolide and verapamil. Similar study was carried with Caco-2 cells.

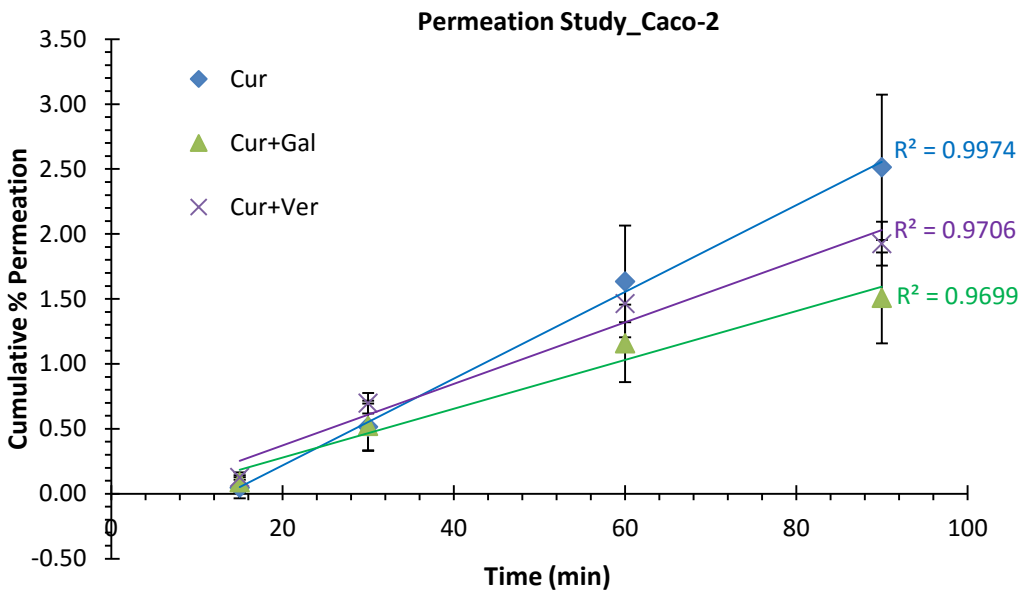


***Figure 6.22: Curcumin permeation across Caco-2***

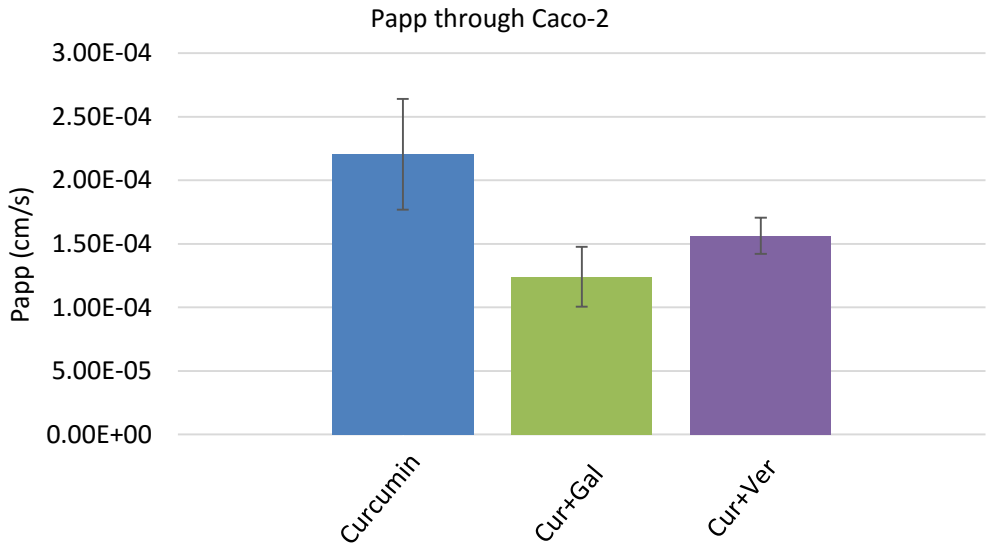


***Figure 6.23: Comparison of permeation rate of curcumin and curcumin with galaxolide and verapamil through Caco-2***

Figure 6.22 describes the permeation of curcumin through Caco-2 cell membrane. 2.51 % of curcumin permeation was observed, when donor media applied with only curcumin (blue line in graph), while cur+gal (green line in graph) shown 1.51 % curcumin permeation and cur+ver (purple line in graph) shown 1.93 % curcumin permeation across the caco-2 cells. The percentage of curcumin permeation was comparatively less through Caco-2 than MDCKII-MDR1 cells. As like results obtained with MDCKII-MDR1 cells, observation with Caco-2 permeation shown that the curcumin without addition of inhibitor molecules shown the higher permeation rate, while inhibitor addition did not show any enhancement in curcumin permeability across the cell membranes. The permeation rate through Caco-2 was determined (Figure 6.23). For donor media with curcumin only, the permeation rate was $(2.20 \pm 0.4) \times 10^{-4}$ while the permeation rate for cur+gal was $(1.24 \pm 0.2) \times 10^{-4}$ and for cur+ver the permeation rate was $(1.56 \pm 0.1) \times 10^{-4}$. The permeation rate was higher in curcumin only sample than inhibitor supplemented samples though this data was not statistically significant ($P > 0.05$).

It was observed in these studies that, permeation with addition of galaxolide and known inhibitor was less than the permeation with curcumin only. This result suggested that there was possibility that curcumin did not effluxes by the P-gp transporter or it could be the poor substrate for the P-gp. Studies also suggested that P-gp efflux did not play any role in the permeation of curcumin (Wahlang et al., 2011). And this might be the reason that there was no any enhancement of curcumin permeation with addition of galaxolide and

verapamil. The overall permeation rate of curcumin was very low, and so it could be clear that curcumin had poor permeability across the membranes.

### 6.5 Histological analysis during permeation studies.

Histology was done after the permeation study, to observe the integrity of cell monolayer during permeability study. Cell monolayers immediately after permeation were fixed and followed with histological processes.

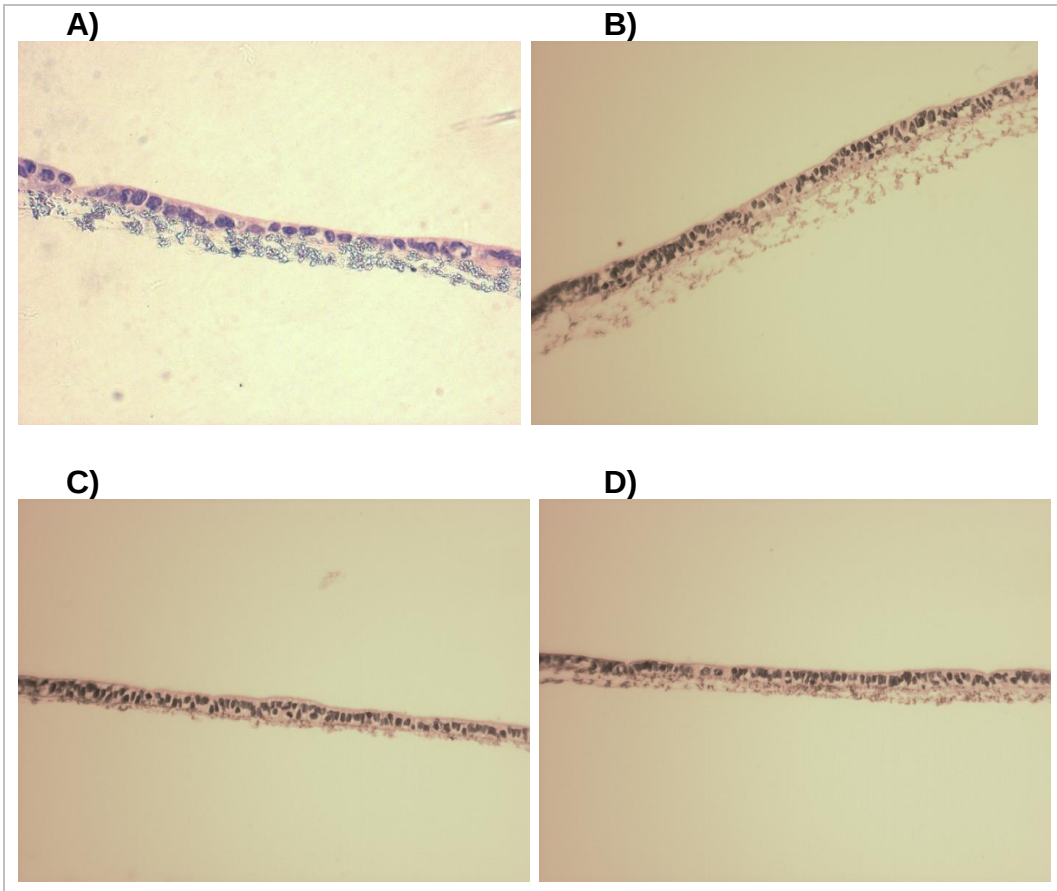


***Figure 6.24: Histology of Caco-2 cell membrane***

*before (A) and after (B,C and D) permeation study*

Figure 6.24 showing the microscopic pictures of the cell membranes before (A) permeation and after (B, C and D) permeation study. As seen in pictures, there was no any breach in the membrane after 90 mins of permeation study. All membranes were as intact even after permeation experiment as they were before the permeation experiment. So it was confirmed that, the permeation observed in our studies was not because of the breaches in the membrane.

## 6.6 Summary

This chapter was focused on the development of HPLC method for the analysis of curcumin and the permeability of curcumin through the cell membranes and effect of galaxolide on the permeation of curcumin.

In this chapter, HPLC methods for the curcumin was developed. Various methods were developed such as, initially method developed without use of internal standard. The method gave clear sharp and isolated peaks. This method was used to analyse the permeated curcumin in initial studies. Later new HPLC method was developed for curcumin analysis with internal standard application. Previous method was modified to get this new method, and internal standard was used to reduce volume dependant errors. For analysis of curcumin, curcumin was prepared in different mediums and some of which contains serum and some did not. Extraction efficiency was determined in these media and finally, found that, curcumin recovery was better in the serum containing media. Also studied the effect of different extraction methods on the recovery of curcumin and found that extraction methods (1:1 and 1:2) did not had major impact on curcumin recovery, but presence of serum had role in recovery. So serum media was selected for sample preparations and to study

curcumin calibration. Further to this, for different cell lines, curcumin calibration was performed in different serum media. Later 4% BSA media was used for the sample preparation and determined calibration and extraction efficiency in this media. The 4% BSA media gave highest extraction efficiency and which was almost 100%. All those media had protein present in it gave high recovery after extraction process. Further curcumin have high binding affinity with BSA and this binding could protect curcumin from the degradation and that's why there was high recovery in BSA containing media.

After successful development of HPLC method for analysis of curcumin, permeability of curcumin was performed. For curcumin permeability various protocols were used. In first part the protocol used, in which donor and receiver media was replaced at every time point, and as a result of which high permeation percentage and higher $P_{app}$ was observed. Both donor and receiver media were prepared in regular growth media. Further modified protocol, in which donor media was not changed every time. Just receiver media have been replaced with certain amount of volume at every sample collection point. No any results were observed in this study. Positive and negative control were also used in this study to monitor the permeation, there was no evidence of permeation in controls as well. Reason for this might be the degradation of curcumin, as curcumin has high degradation rate at alkaline pH. And the donor and receiver media had pH 7.4. So media was changed in later experiment, and this time used very controlled media. Both the donor and receiver media were set at the particular pH with the addition of HEPES buffer. The HEPES buffer helps to maintain the pH set at certain value. With these modified donor

and receiver media, the permeation of curcumin was observed through the cell membranes. But it was observed that permeation and permeation rate was higher with curcumin only samples than the samples supplemented with galaxolide as a P-gp inhibitor and verapamil. These results could say that the P-gp efflux transporter did not play any role in the curcumin permeation, and so there was no enhancement of permeation of curcumin with galaxolide. Finally histology of cell membranes were performed before and after permeations, to determine the integrity of membranes. It was observed that the cell membranes were remained intact and without any breaches within even after permeation experiment. So it could be clear that there was no any false penetration of curcumin in whatever data produced.

# 7 : Histology study

## 7.1 Introduction

Histology is the scientific study of the fine detail of biological cells and tissues using microscopes to look at specimens of tissues that have been carefully prepared using special processes called "histological techniques" or it is also defined as the study of microscopic anatomy of cells and tissues. It is commonly performed by examining cells and tissues under a light microscope or electron microscope, which have been sectioned, stained and mounted on a microscope slide. The ability to visualize or differentially identify microscopic structures is frequently enhanced through the use of histological stains.

In this study, histology tool was used to study the membrane forming ability of different cell lines. Different cell lines were used to carry permeation experiment, but before moving for permeation, it was necessary to study the integrity of cell membranes. TEER values was used to assess integrity of cell membranes, and then studied the histology of cell membranes with respect to TEER values. TEER is nothing but the electrical resistance across the cell layer. Relationship between TEER and histology was studied to see the effect of growing cells on the TEER value. TEER values should be increased as cells grows and get confluent. The TEER was used to assure the integrity of the cell layers (Yu and Huang, 2011).

## 7.2 Histology of DLD-1 cell

The cell line shown the rapid growth in flasks and transwells. Cell were grown on transwells for 6 days. TEER was measured every day after TEER measurement wells were fixed and followed with histology.

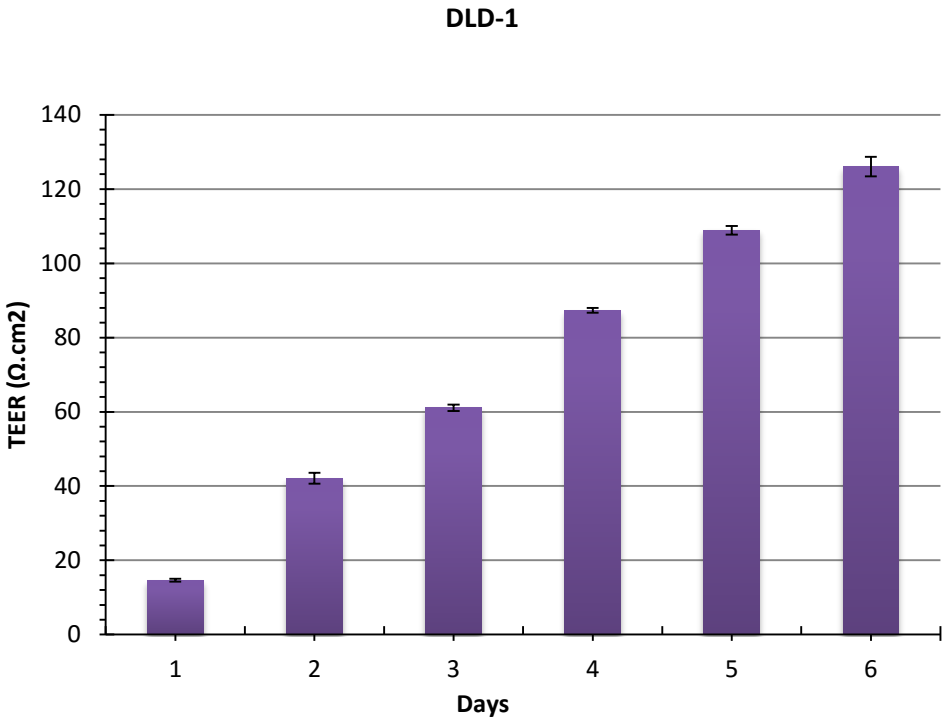


***Figure 7.1: Graphical presentation of TEER values for DLD-1 against days of incubation***

As seen in Figure 7.1, the DLD-1 cells shown gradual increase in TEER values from 14.63Ω.cm$^2$ to the 126.06 Ω.cm$^2$, as cells grows and forms membrane on the transwells. The increase in TEER values shown that, the DLD-1 forms more confluent cell membrane on Day-6 as compare to day-1. TEER was lower on day-1 possibly because the cells were not attached to each other so tightly, and as a result of which applied current passed through the gaps present in between cells and displayed low TEER readings; in reverse of this, as incubation time

goes increasing, cells started to form firm attachment, which did not allowed applied current to pass easily and confers high resistance, and that is why the TEER was higher as incubation time increases. This is the possible reason, for observed higher TEER on day-6. To assess the confluence of the cell layers, the transwells were fixed and followed for histology study. The Histological sections gave the clear idea about the confluence of cell layers.

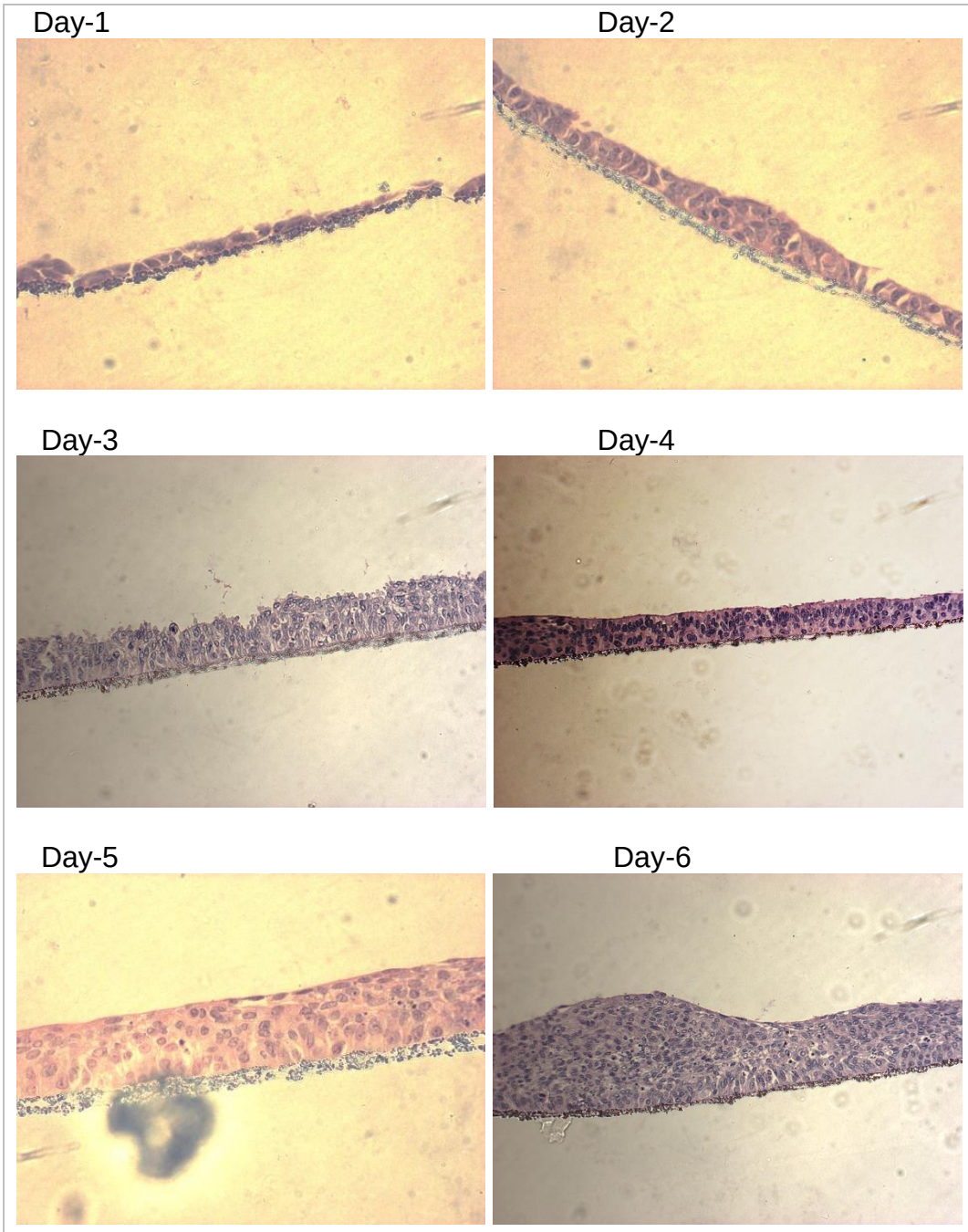


***Figure 7.2: Histology images of DLD-1 membranes formed on different days***

Figure 7.2 showing histology images of DLD-1 cell membranes on different days. As seen in images, on day-1, the section shows very thin cell layer, which was the reason for the low TEER value; while as incubation period increased

up to Day-6 the thickness of cell layers goes on increasing and as a result of which TEER goes higher. Besides the thin cell layer, there were some intercellular spaces, which might also the reason for the lowered TEER, and these intracellular spaces could be seen in images from day-1 to day-3. From day-4, these intracellular spaces reduced and seen comparatively intact cell membranes on day-4 to day-6. So from these pictures it was clear that, though cells are forming complete cell membranes, but there were some gaps present in cells, which might be responsible for the low TEER. These gaps can produce the leaky membranes, and as those spaces were filled by cellular components during the period of time, membrane becomes more confluent. And this confluence and integrity was assessed with the help of TEER. Histology pictures also clarify that, DLD-1 cells were forming multi-cell layer membranes, and multi-cell layers were increasing with the incubation time.

## 7.3 Histology of PANC-1 cells

PANC-1 cells were also grown on transwells and TEER was measured for 6 days. PANC-1 cells shown the slow growth as compare to the DLD-1, and also shown the least elevation in the TEER values at the end of Day-6.

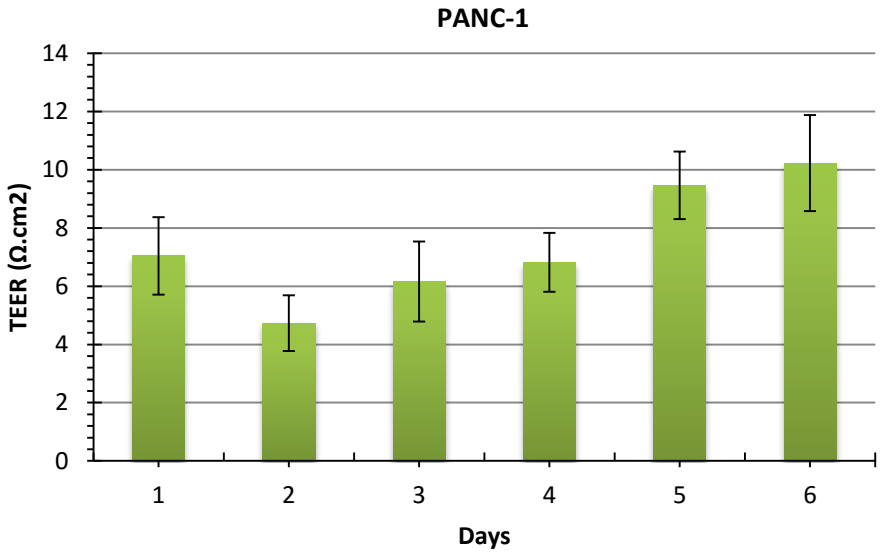


***Figure 7.3: Graphical presentation of TEER values for PANC-1 against days of incubation***

The TEER was increased from 7.04Ω.cm$^2$to 10.23Ω.cm$^2$ after 6 days incubation (Figure 7.3). PANC-1 did not show significant elevation in TEER, even after increasing incubation. Cells were seems to grow on the transwells, but were unable to give higher TEER values. There was very little increase in TEER, from the day-1 to day-2. These cell membranes were followed to study histology and the reason for this low TEER was assessed by histology sections.

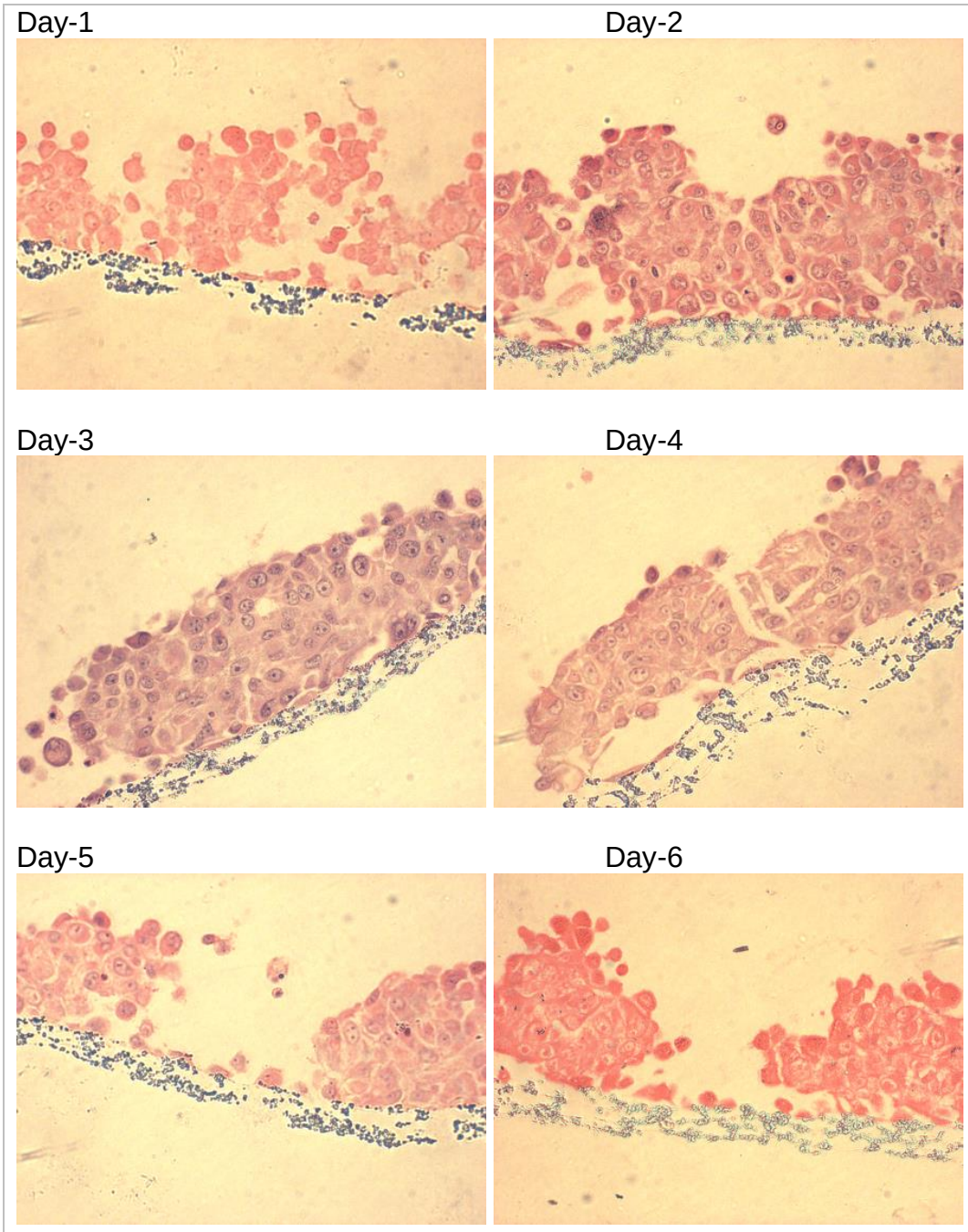


***Figure 7.4: Histology images of membranes formed by PANC-1 cells***

Figure 7.4 shows that the PANC-1 was grown in multilayer, but the layers formed by this cell line were not in uniform membrane structure. The cells seem to be loosely attached to each other, forming intracellular spaces. Also these image shown that the cells were growing in clumps and there were gaps

between two clumps. And all these intercellular spaces and the gaps between cell clumps were responsible for the low TEER values in PANC-1 even after cells were grown in enough number. The cell lines was unable to grow in uniform layers, and have ability to form clumps. This clumps forming ability of PANC-1 allowed to form very leaky membrane and this was the reason there was very low TEER through the PANC-1.

## 7.4 Histology of SiHa cells

As like DLD-1 and PANC-1; SiHa cells were cultured on transwells and allowed them to grow to form membranes. Cells were grown for 6 days and TEER was measured every day. Same wells after TEER measurement were fixed and used for histology study.

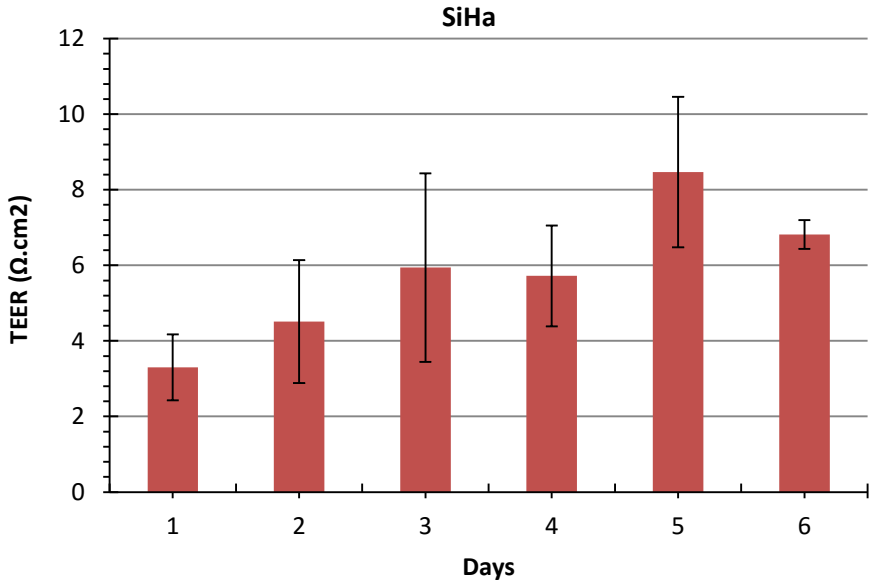


***Figure 7.5: Graphical presentation of TEER values for SiHa against days of incubation***

SiHa cells also shown the low TEER values, with little elevation from 3.30Ω.cm$^2$ to the 6.82 Ω.cm$^2$ on day-6 (Figure 7.5). The SiHa cells have shown faster growth than PANC-1 but were unable to give higher TEER values. To find the reason behind low TEER, histological study was performed for these cell membranes.

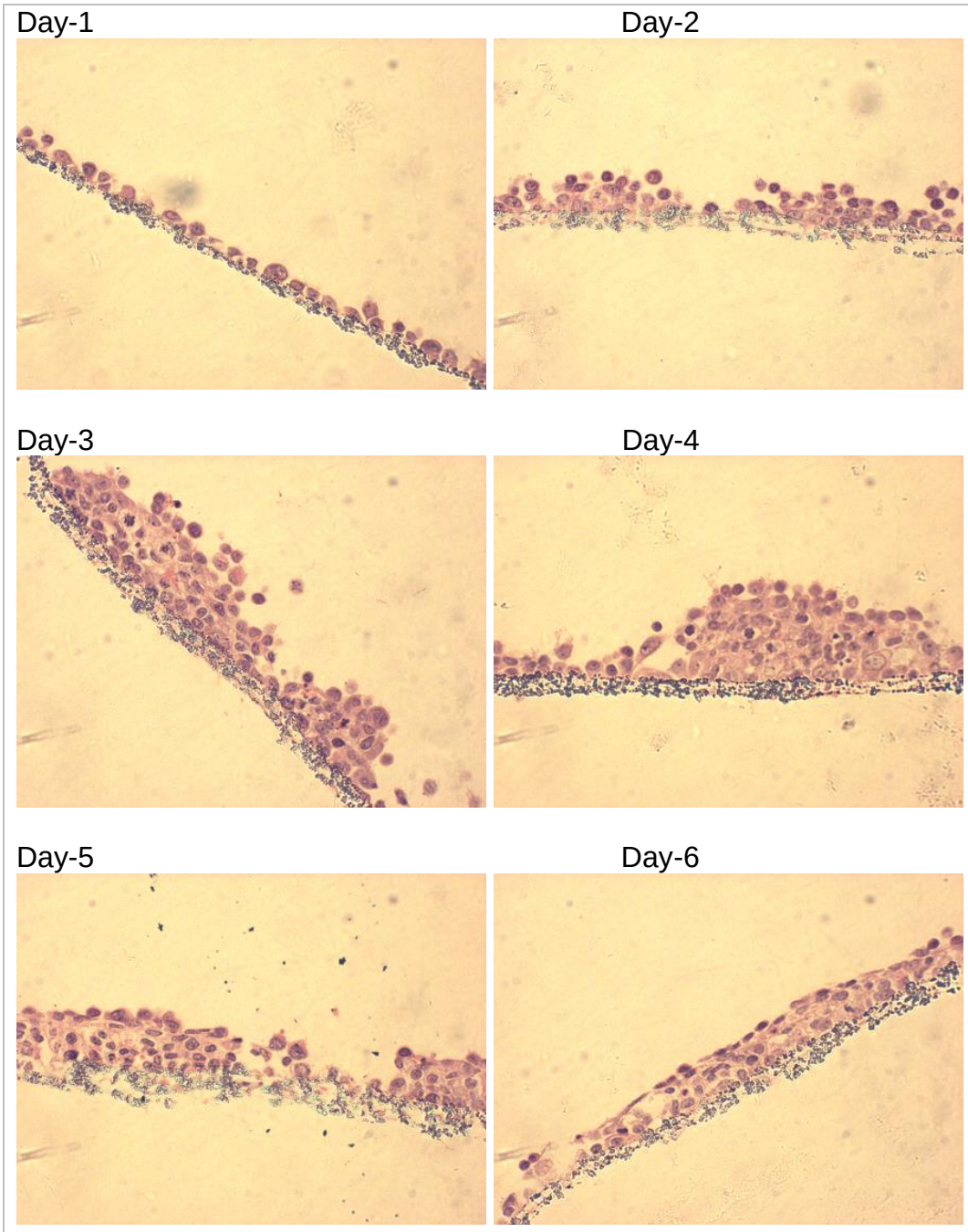


***Figure 7.6: Histology images of membranes formed by SiHa cells***

The histology images of SiHa (Figure 7.6) shows the multi-cell layer growth. On Day-1 there was monolayer of cells with spaces between the cells. The multi-cell layer starts to form from the Day-2, and the cells were grown in dome shaped structure. The images shown the breaches between the cells, which

might provide the space to pass current through it, which results in the low TEER values. The low TEER value indicates the loose intercellular associations, which might highly favours passive paracellular diffusion (Wang et al., 2005).

Histological study was performed for these three cell lines, to study their membrane forming ability, so these cells could be used to perform permeation and to study drug permeability through multi-cell layers. But, only DLD-1 cell shown the formation of confluent cell membranes.

## 7.5 Histology of Caco-2 cell lines

Caco-2 cells were grown on transwells and media was changed on every three days and the TEER was measured on every three days till the 21 days.

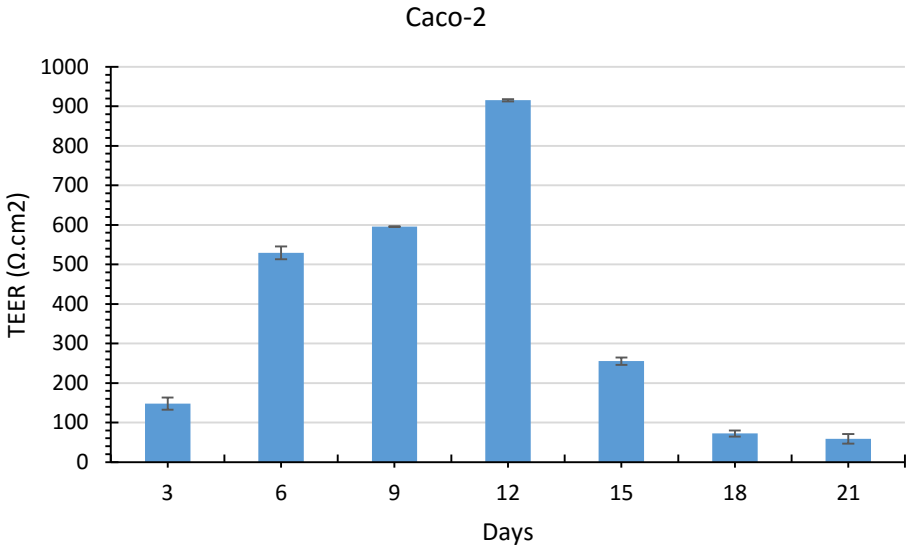


***Figure 7.7: Graphical presentation of TEER values for Caco-2 against days of incubation***

Figure 7.7 showing the TEER values obtained for the Caco-2 cells on different days. The TEER was increasing with incubation time and the highest TEER value was observed on the day-12 and which was almost 915.31 $\Omega.cm^2$. After the day-12 the TEER started decreasing and on day-21 it dropped to the 58.96 $\Omega.cm^2$ which was a lowest TEER observed. To study reason behind this rise and fall of TEER, the histology study was performed for these cell membranes.

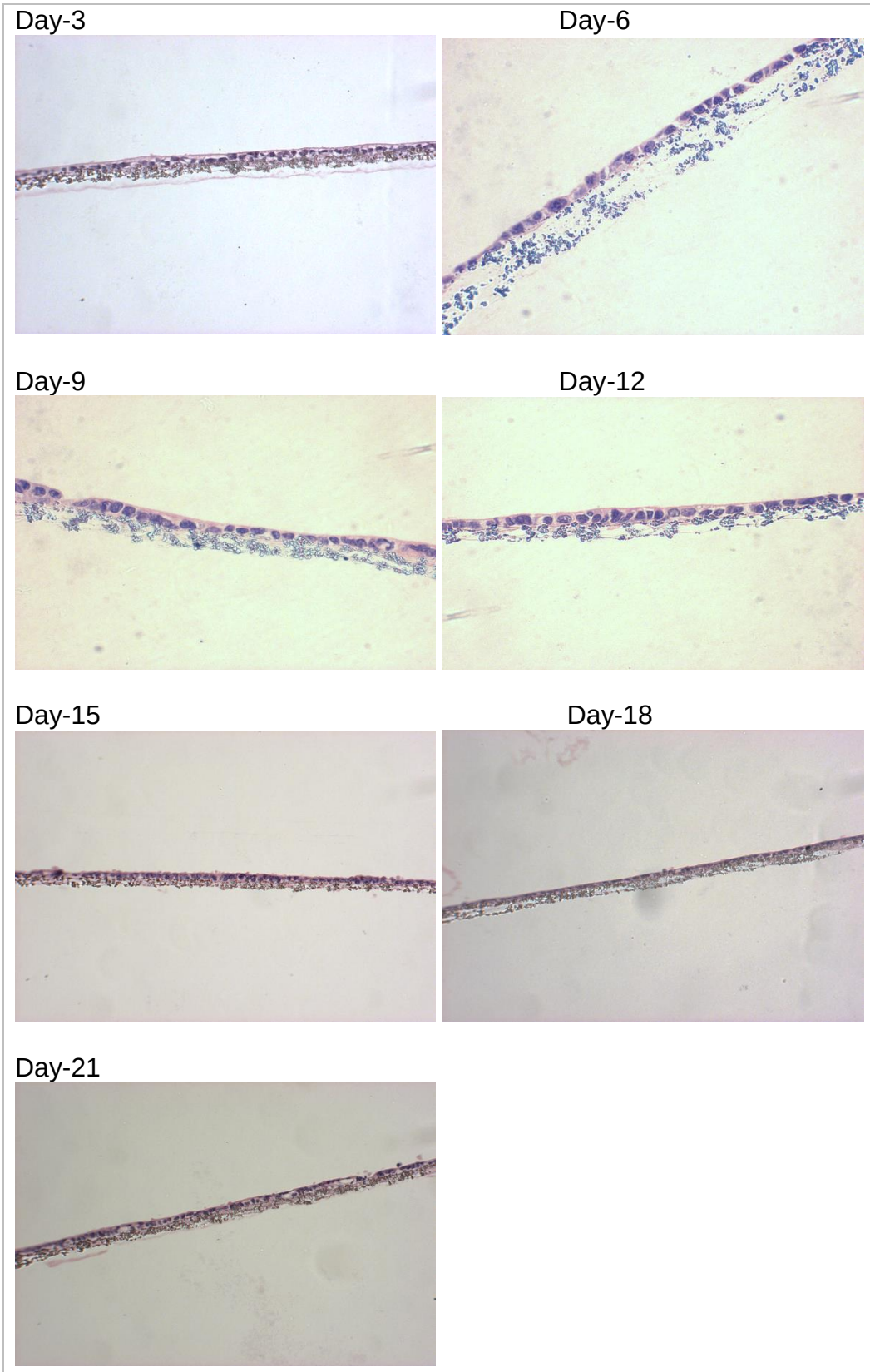


***Figure 7.8: Histology of membranes formed by Caco-2 cells***

Figure 7.8 showing the pictures for the membranes formed by the Caco-2 cell lines. The Caco-2 cells form monolayer and the single cells were aligned to form cell membrane. On day-12 where the highest TEER was observed, the cell membrane was healthier than the cell membranes observed on other days and was also confluent without any intracellular spaces. After day-12, the cell membrane observed to be shrunken and unhealthy, which might be then did not able to maintain its integrity and as a result of which, drop in TEER after day-12 was observed. This might be happen, because there was limited supply of nutrients in the transwells and this supply was not enough to feed all cells. And due to insufficient supply of nutrients, cells started dying and the membrane lose its integrity. And this was the possible reason that there was the decline in TEER after highest TEER on day-12.

## 7.6 Histology of MDCKII Cells

MDCKII cells were cultured on the transwells and every 3 days media was changed to maintain cells in healthy condition. TEER was measured on every 5 days, from day-1 to day-20.

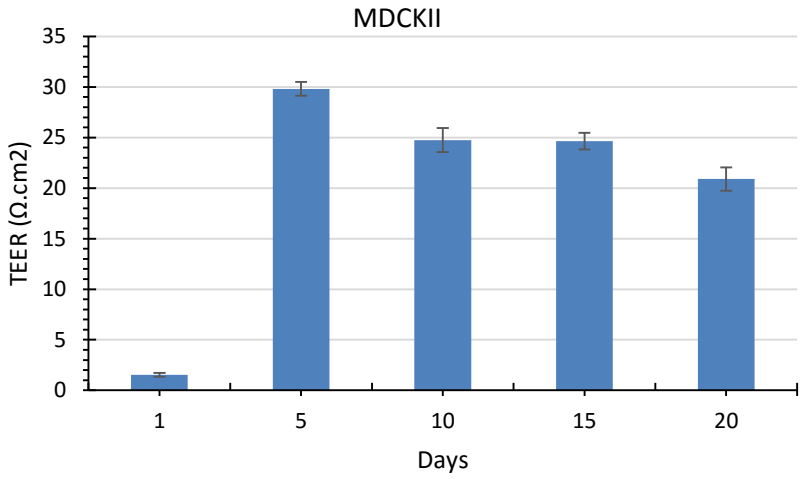


***Figure 7.9: Graphical presentation of TEER values for MDCKII cells against days of incubation***

As seen in Figure 7.9, TEER was very low at day-1 and was only 1.54 $\Omega.cm^2$. From Day-5 the TEER was increased at high level and it was observed 29.81$\Omega.cm^2$ while on day-10, 15 and 20 the TEER values were 24.75$\Omega.cm^2$, 24.64$\Omega.cm^2$ and 20.9$\Omega.cm^2$ respectively. The TEER observed consistence between day 10 and day 15 and on day 20 it shown some decline. These transwells were fixed on above mentioned time points and performed histology study.

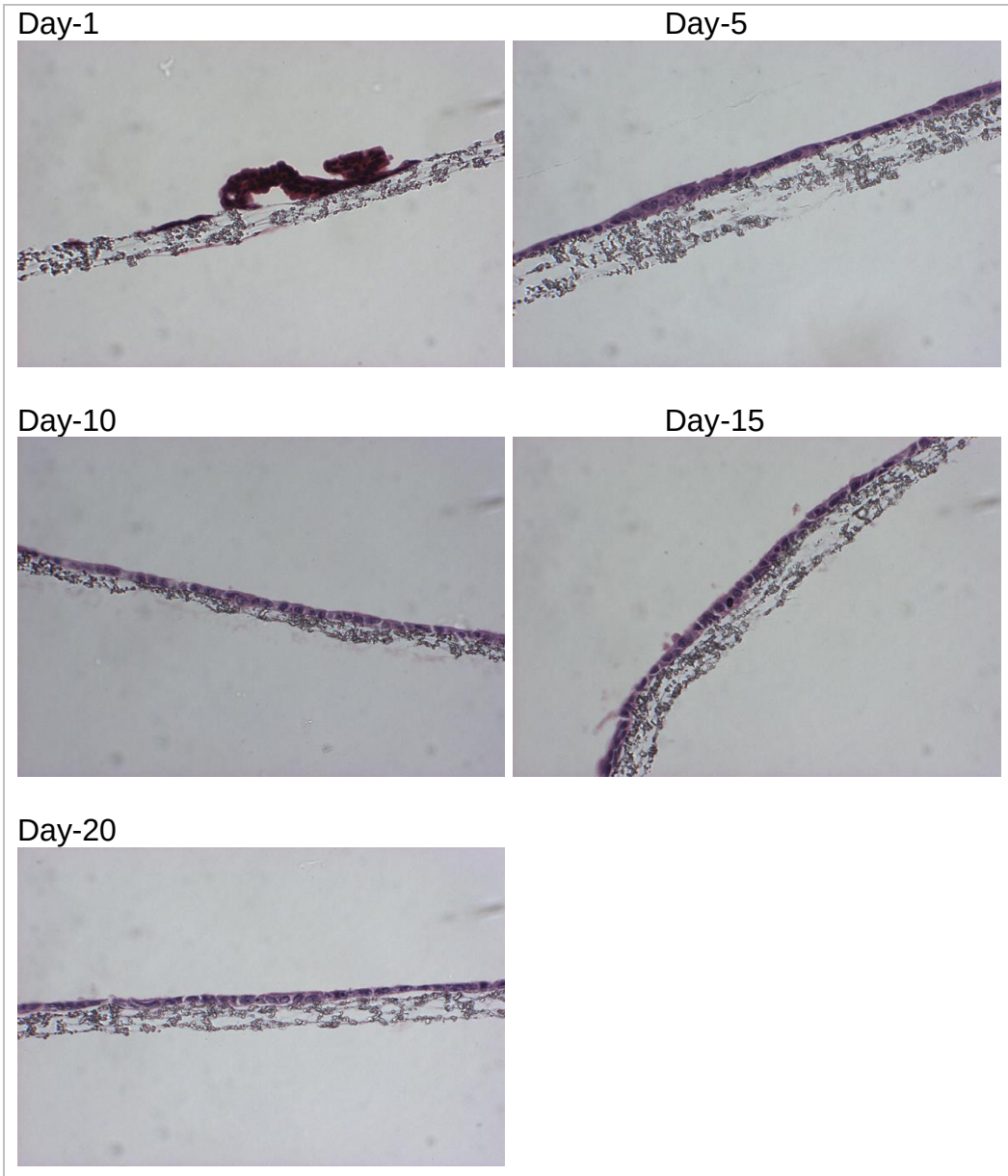


***Figure 7.10: Histology of membranes formed by MDCKII cells***

Figure 7.10 shows histology images of membranes formed by MDCKII cells with respect to different incubation time period. On day-1 very few cells on transwell membranes was observed. Cells did not observed grown completely and it was because, cells did not get enough time to grow since inoculation on transwells. But on the other hand, images for transwells incubated for day-5 to day-20 shown complete membrane of MDCKII cells over the transwells. The

MDCKII cell lines formed monolayer, and as seen in picture intact monolayer was observed except on day-1. And this was the reason very low TEER was recorded on day-1 while on others days comparatively higher TEER values were observed.

## 7.7 Histology of MDCKII-MDR1 cells

MDCKII-MDR1 cell line was a derivative of MDCKII cell line having ability to over express P-gp/MDR-1 proteins. Same like MDCKII, MDR1 cells were maintained in similar experimental conditions and performed TEER measurement.

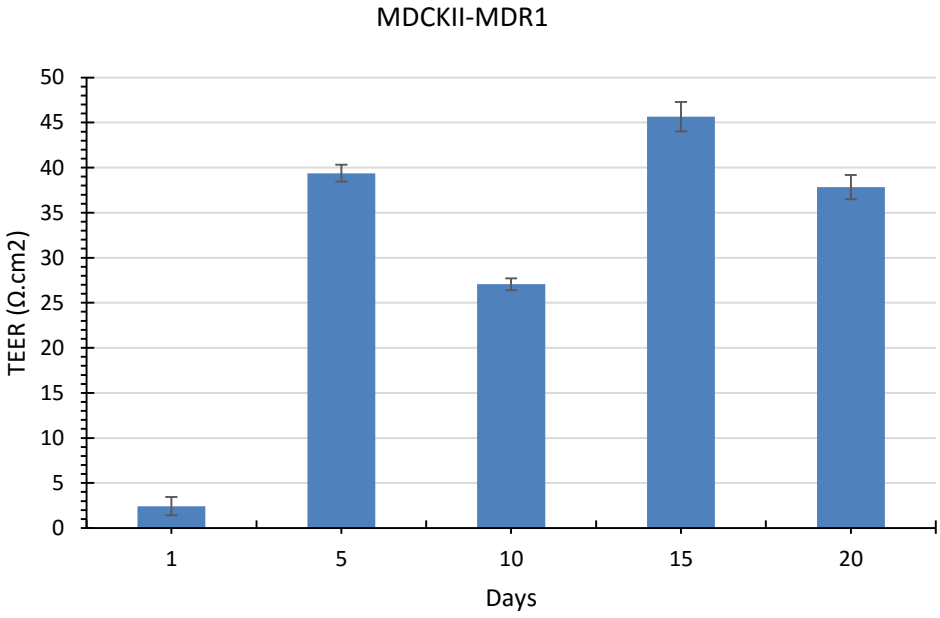


***Figure 7.11: Graphical presentation of TEER values for MDCKII-MDR1 against days of incubation***

TEER was very low on day-1 while from day 5 to day 20 the TEER was increased comparatively at high level. On day 14 the highest TEER value was observed and was about 45.65Ω.cm$^2$ and as mentioned earlier it was very high

as compared to the day 1 TEER which was just 2.42Ω.cm$^2$. Except day 1, TEER value for all other days observed higher with some differences as seen in Figure 7.11.

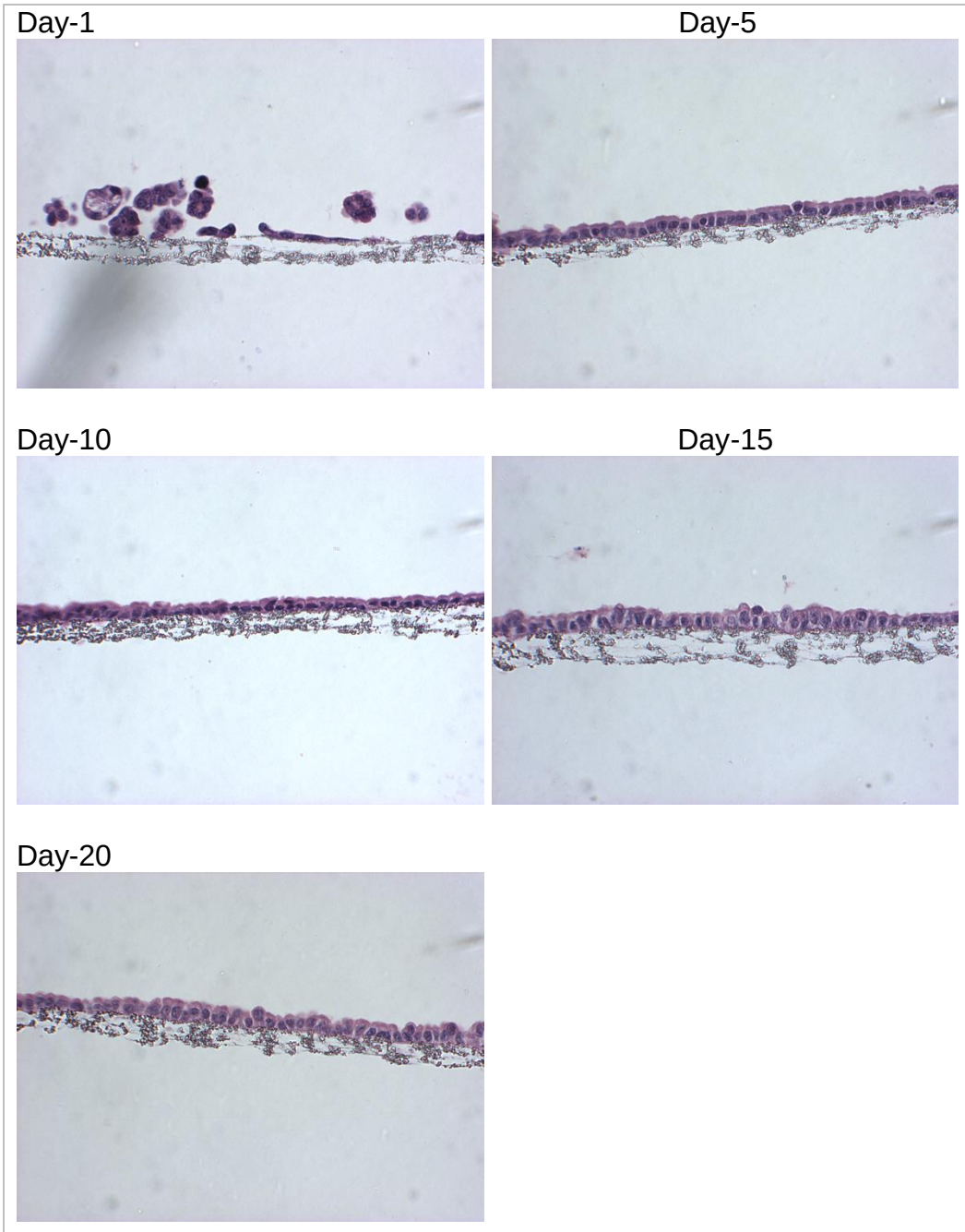


***Figure 7.12: Histology of membranes formed by MDCKII-MDR1 cells***

The Figure 7.12 shows the histology images for membraned formed by MDCKII-MDR1 cells. As seen in day 1 image, that cells were not firmly attached to the transwell membranes. Cells observed distinct and separated from one another, having huge spaces between them. Also there were very few number of cells, and this was because inappropriate incubation time. And this was the reason that low TEER was observed on day 1. Except day 1, all other images on different day's shown uniform monolayer formed on the transwell membranes, and due to this intact membrane, higher TEER compared to the day 1 was observed. Also there was low TEER on day 10 as compared to the day 5 even after long incubation time. As seen in picture on day 10, that the membrane shrunken and unhealthy unlike other membranes. This might be the reason behind decreased TEER on day 10. On day 15 highest TEER was observed and as seen in histology images, the membrane formed on day 15 observed more intact than other. Cells appeared healthier, and because of that cells might have formed the strong binding between them. And as a result of which high TEER was observed.

## 7.8 Histology of MDCKII-BCRP cells

MDCKII-BCRP was also derivative of MDCKII cell line which overexpresses BCRP proteins. Like MDR1, similar experimental conditions for this cell line to grow and form cell membranes were used.

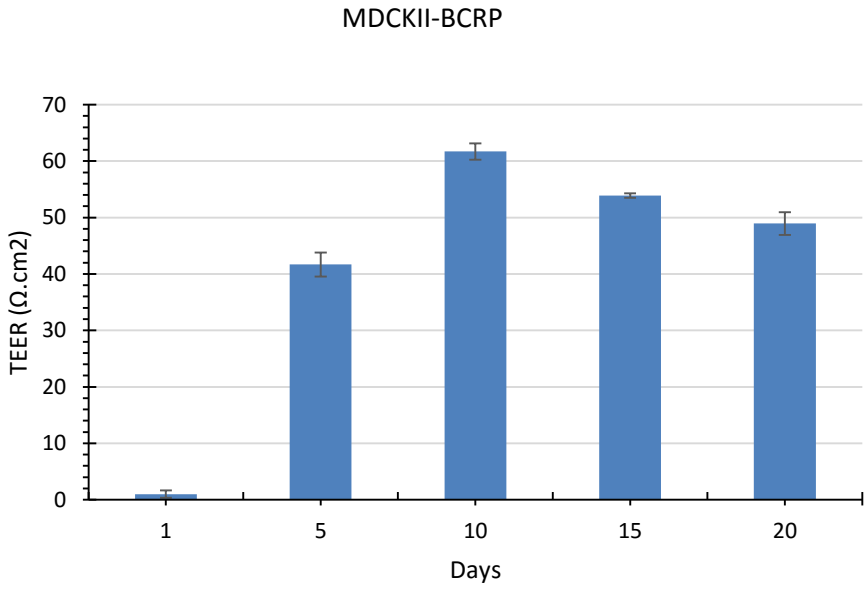


***Figure 7.13: Graphical presentation of TEER values for MDCKII-BCRP against days of incubation***

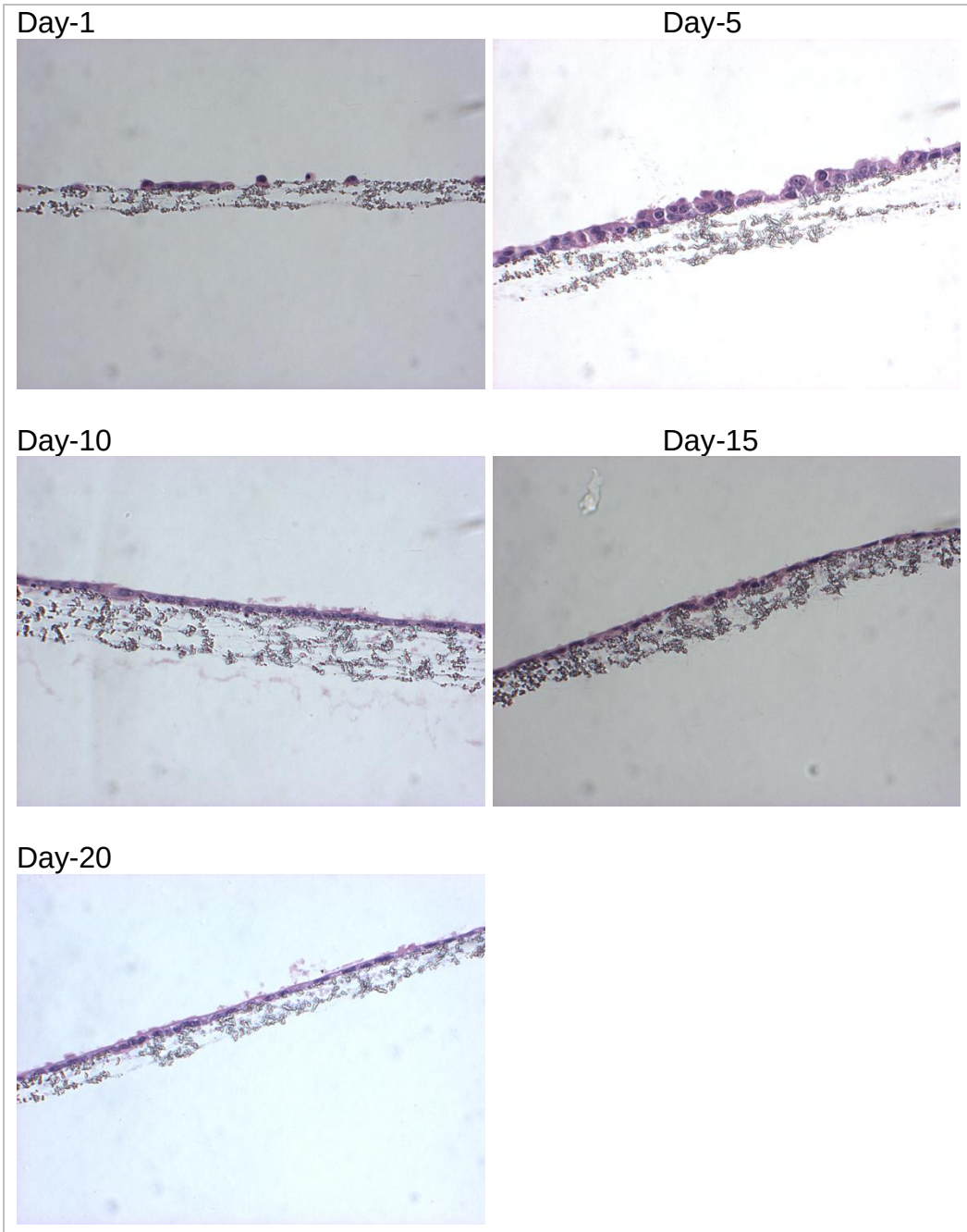


***Figure 7.14: Histology of membranes formed by MDCKII-BCRP cells***

The BCRP cell line as well shows very low TEER at day-1 and from day 5 to day 20 higher TEER was observed. On day 10 highest TEER was observed which was almost 61.71 $\Omega.cm^2$ and very high as compare to the TEER observed on day 1 and which was just 0.99$\Omega.cm^2$ (Figure 7.13).

Histology study explored the membranes formed by the MDCKII-BCRP cells (Figure 7.14).Images explored the reason behind low TEER on day 1 and high TEER on other days except day 1. Image for day 1 membrane shown the membrane which was not completely formed and have gaps between cells. Also the image explores the insufficient number if cells present on the transwell membrane to form the intact membrane. The less number of cells were because of the short incubation time. Other images than day1 images shown completely formed membrane of MDCKII-BCRP cells. And the membrane was intact and this intact structure was responsible for the high TEER which was not seen in day 1 image.

## 7.9 Histology of MDCKII-MRP1 cells

MDCKII-MRP1 was also a derivative of MDCKII cell line which over expresses MRP1 protein. As like other derivatives, MRP1 cell line was also maintained using similar experimental conditions.

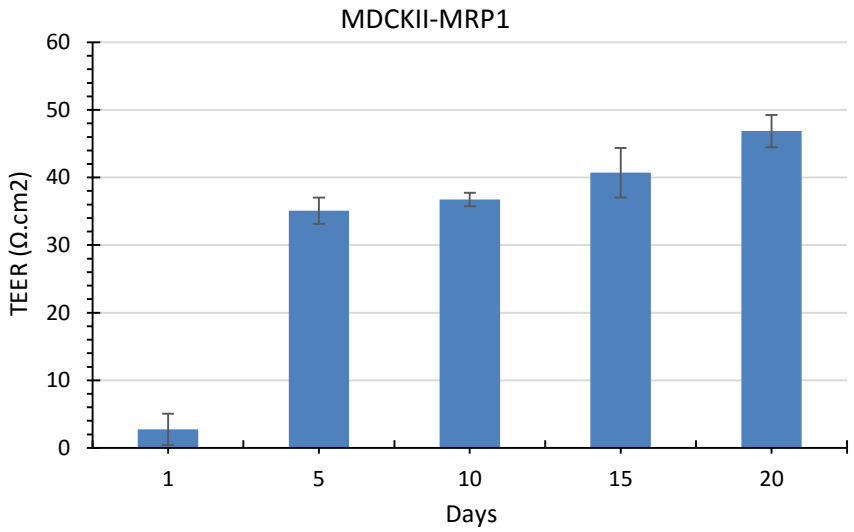


***Figure 7.15: Graphical presentation of TEER values for MDCKII-MRP1 against days of incubation***

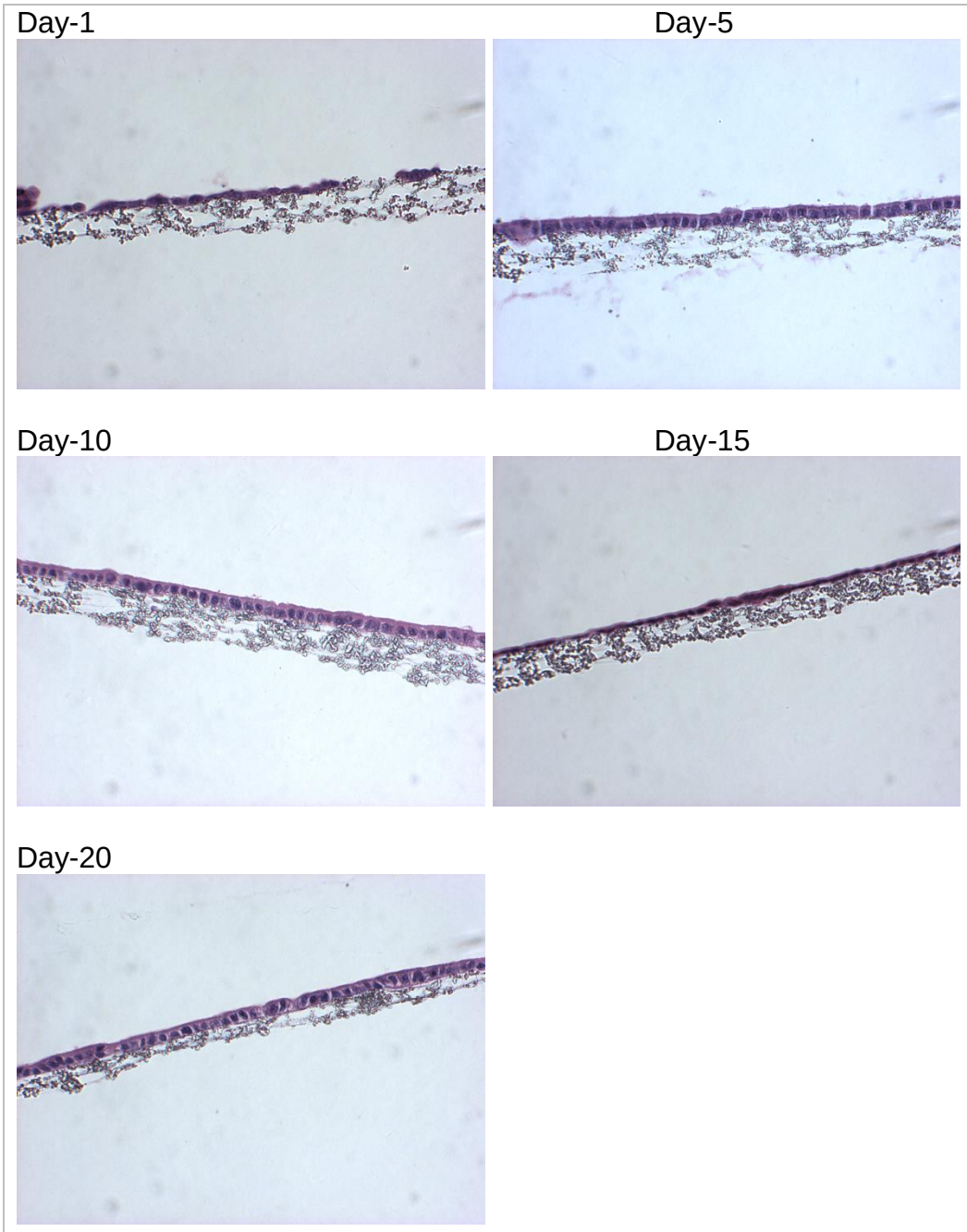


***Figure 7.16: Histology of membranes formed by MDCKII-MRP1 cells***

The MRP1 also delivered the similar set of results as the lower TEER on day 1 was observed and the TEER seems to be increased from day 5 to day 20 (Figure 7.15). The highest TEER for MRP1 was observed at day 20 and was about 46.86 $\Omega.cm^2$. Other TEER values on day 5 to day 15 were nearly similar

to each other and did not show big differences between them. The TEER seems to be gradually increasing till day 20.

Histological study for these transwells was done to observe the membranes formed by these cells (Figure 7.16). The images obtained after histology, shown the leaky membranes on day 1 and from day 5 the membrane seems intact and uniform. As mentioned earlier, the leaky membrane on day 1 was responsible for the low TEER value.

As seen above that, different cell lines were forming membranes on the transwell inserts. TEER was determined for every cell lines to assess the integrity of membranes formed by these cell lines. DLD-1 PANC-1 and SiHa cell lines had an ability to form multi-cell layers. Though these cells form multi-cell layer membranes on transwells, only DLD-1 was able to form intact and uniform cell membranes. Other cell lines PANC-1 and SiHa were not able to form intact membranes. Instead these cell lines forming clumps of growth on the transwell membranes. These structures of these cell membranes were not able to confer uniform and intact cell layer. These cells form membranes having breaches and intracellular spaces in between them. And these breaches were responsible for the low TEER values. The low TEER directly informs us about the breaches present in cell membranes. This was the reason that TEER was used to check the integrity of cell membranes. Histology for Caco-2 cells, MDCKII cells and derivatives of MDCKII cells was also studied. All these cells including Caco-2 and MDCKII with its all derivatives formed the monolayers on transwells. These monolayers were giving intact cell membranes, and these

membranes could be seen in images above with different TEER values with different incubation time.

A PANC-1 and SiHa cell did not able to form intact cell membranes. There was breaches in membranes formed by these cells. To overcome this issue with membrane forming ability of these cell lines, matrigel was applied to the cell suspension during inoculation. These cells then used to perform the histology to study effect of matrigel on membrane forming ability of cells.

### 7.10 Effect of matrigel on TEER and histology

Matrigel matrix is a reconstituted basement membrane preparation that was extracted from the Engelbreth-Holm-Swarm (EHS) mouse sarcoma, a tumour rich in extracellular matrix proteins. This material contains approximately 60%laminin, 30% collagen IV, and 8% entactin. Entactin is a bridging molecule that interacts with laminin and collagen IV, and contributes to the structural organization of these extracellular matrix molecules. Matrigel matrix also contains heparin sulfate proteoglycan (perlecan), TGF-β, epidermal growth factor, insulin-like growth factor, fibroblast growth factor, tissue plasminogen activator, and other growth factors which occur naturally in the EHS tumour. Matrigel have activity to enhance the tumour growth and is also supports an optimal growth of cell cultures (Bao et al., 1994; Fridman et al., 1991; Hughes et al., 2010; Kleinman and Martin, 2005). This growth promoting characteristics of matrigel was used to enhance the membranes forming ability of cells. Different concentrations of matrigel were used to study its effect on growth of membranes.

### 7.10.1 Application of 50% (500µl/ml) matrigel

In this experiment, 50% of matrigel was applied to the media. Cell suspension with desired cell number was prepared and centrifuges to get pellet. And this pellet was then dissolved to the media which contained 50% matrigel. All matrigel concentrations were prepared with similar dilutions. The cells with and without matrigel were cultured on transwells and incubated for 6 days. TEER was measured on day 1 and day 6 only and the same transwells after TEER measurements were used to study histology.

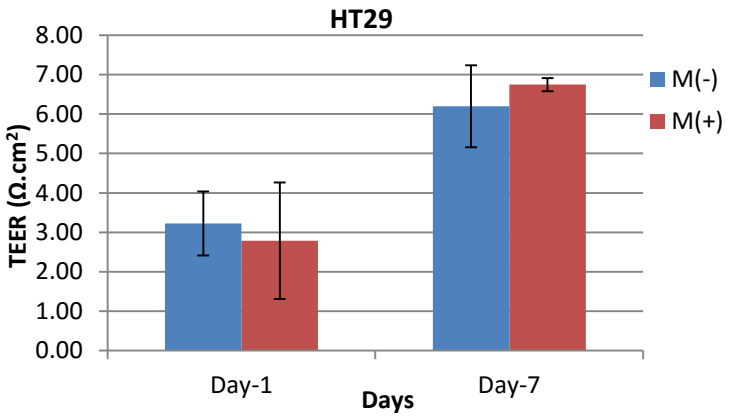


***Figure 7.17: Application of 50 % matrigel to HT29 cells***

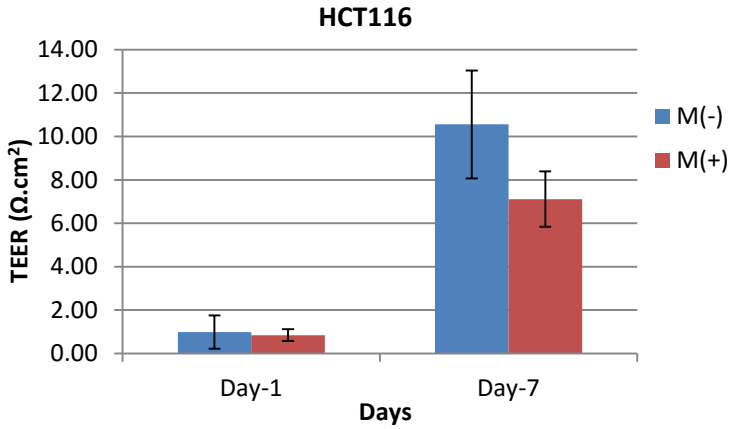


***Figure 7.18: Application of 50 % matrigel to HCT 116 cells***

Graphs in above figures shows the different between TEER values with and without application of matrigel. The HT29 cells (Figure 7.17) shown no difference in TEER values with and without application of matrigel on day-1 and day-6 as well. TEER values observed nearly similar in both the cases. The cell membrane without matrigel shown TEER increase from 3.23 $\Omega.cm^2$ to 6.20$\Omega.cm^2$, while cell membrane with addition of 50% matrigel shown TEER values 2.79$\Omega.cm^2$ and 6.75$\Omega.cm^2$ on days 1 and 6 respectively. If both the TEER values were compared with respect to matrigel addition, there was no any enhancement in TEER with HT29 cells. Application of 50% matrigel to HCT 116 cells (Figure 7.18) shown big differences in TEER values between two samples on day 6, while on day 1, there was nearly similar TEER which was very low; 0.99$\Omega.cm^2$ and 0.84$\Omega.cm^2$ for cell without addition of matrigel and with matrigel respectively. On day 6 we observed TEER value (10.56$\Omega.cm^2$) without addition of matrigel higher than TEER value (7.11$\Omega.cm^2$) with matrigel. Histology for both the cell lines mentioned above was performed.

**Without Matrigel (M-)**

Day-1 Day-6

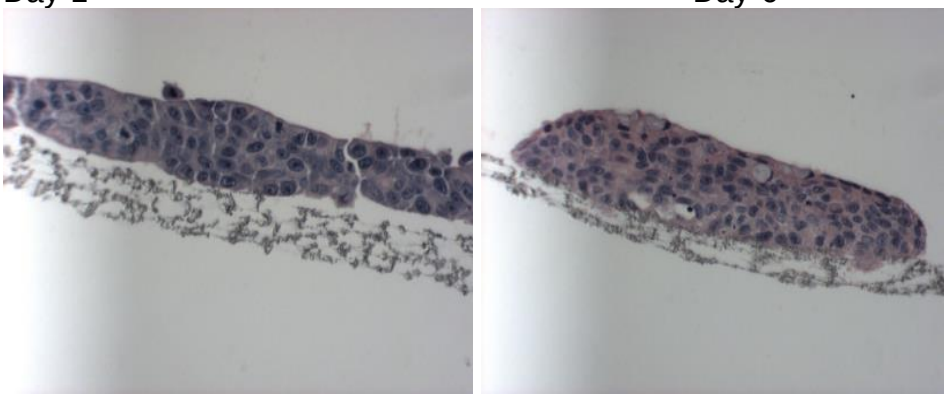

**With Matrigel (M+)**

Day-1 Day-6

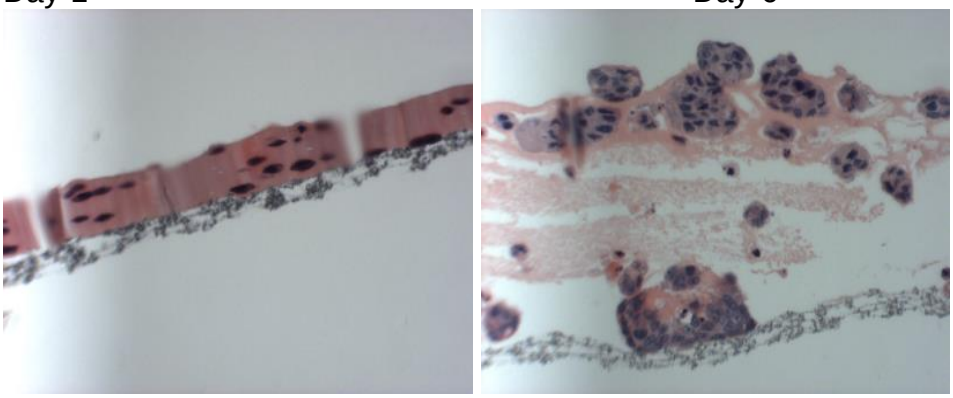

***Figure 7.19: Effect of 50 % matrigel on membrane forming ability of HT29 cells***

Histology study provided the images for the cell membranes treated with 50% matrigel. Figure 7.19 shows the membranes formed by HT 29 cells and also observed that the HT29 cells were growing in multi-layers. In image, without addition of matrigel HT29 cell on day 6 forms good multilayer, but the multi-layer membrane did not formed in continuous manner. The membrane looks to be grown in patches. Other image with addition of 50% matrigel shown the presence of matrigel around the cells and cells looks like to be trapped within the matrigel. It observed that, matrigel did not allowed cells to grow freely. There

was clear difference between cell densities present in membranes with and without matrigel application.

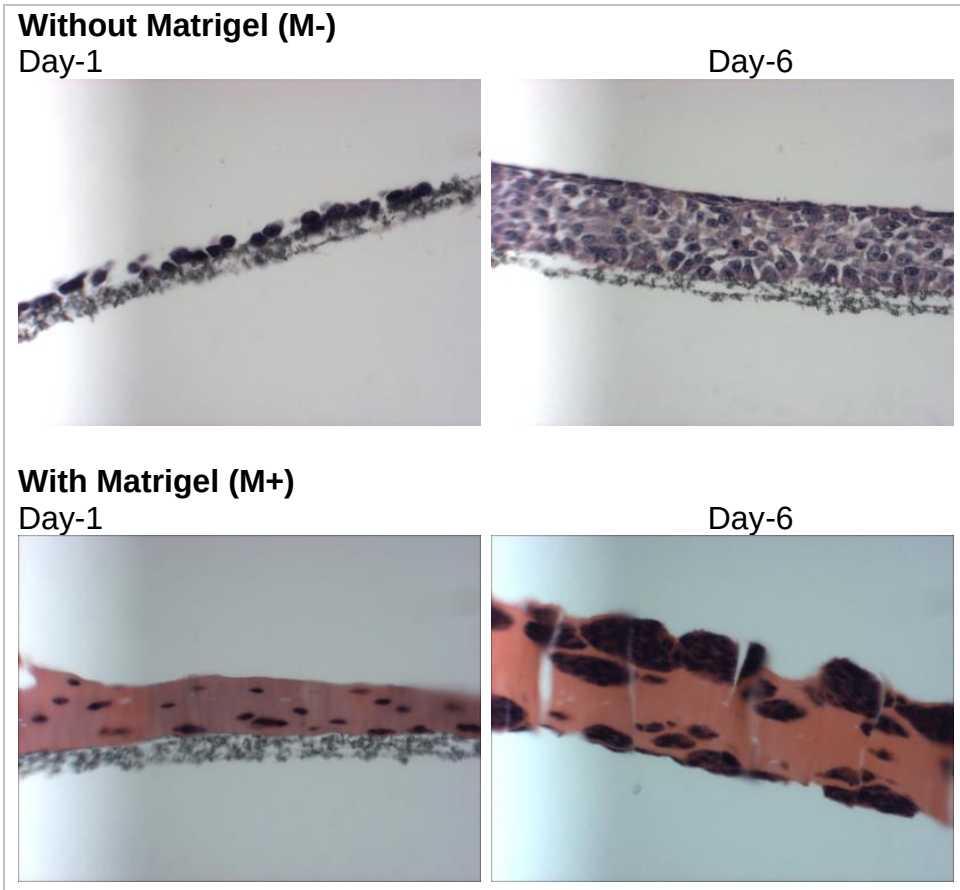


***Figure 7.20: Effect of 50 % matrigel on membrane forming ability of HCT 116 cells***

Figure 7.20 shows the membranes formed by the HCT 116, and same like HT29, the membranes formed by cells where matrigel was added, shows less cell density, while cells without matrigel shown better growth. HCT 116 without matrigel shown multi-cell layer membrane formed. The membrane had intracellular spaces and loses cell-cell attachments. This might be the reason that high TEER was not observed. With matrigel TEER was lower on day 6, and it was possibly because the low cell density present in membrane. Both the

cell lines with application of matrigel shown less growth of cells. Though there was membrane formed, but this was just matrigel overlaid not the cells. So this higher concentration of matrigel did not allowed cell growth.

As seen earlier, high concentration of matrigel was suppressing cell growth, so these experiments were repeated with lower matrigel concentrations.

### 7.10.2 Application of 2.5% (25µl/ml) matrigel

In previous experiment, it was seen that 50 % matrigel have restricted cell growth at some extent and that is why intact cell membranes were unable to grow. So lower concentrations of matrigel was used to support growth of cells and to form uniform membranes. And 2.5 % matrigel was used this time and added to cell suspension at the time of culturing cells on transwells.

(A)

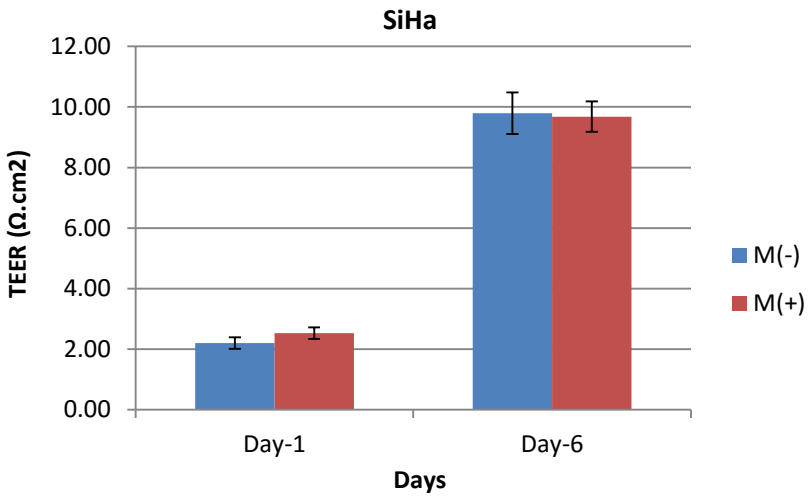
SiHa
12.00
10.00
8.00
6.00
4.00
2.00
0.00
TEER (Ω.cm2)
Day-1
Day-6
Days
M(-)
M(+)

(B)

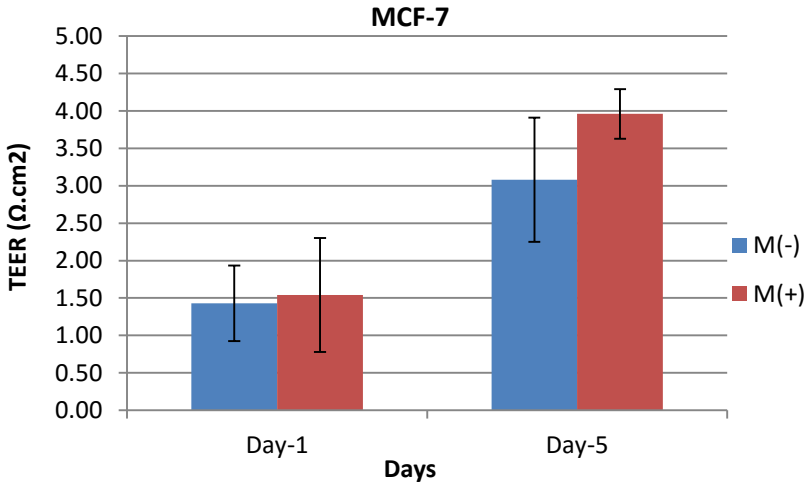
MCF-7
5.00
4.50
4.00
3.50
3.00
2.50
2.00
1.50
1.00
0.50
0.00
TEER (Ω.cm2)
Day-1
Day-5
Days
M(-)
M(+)

(C)

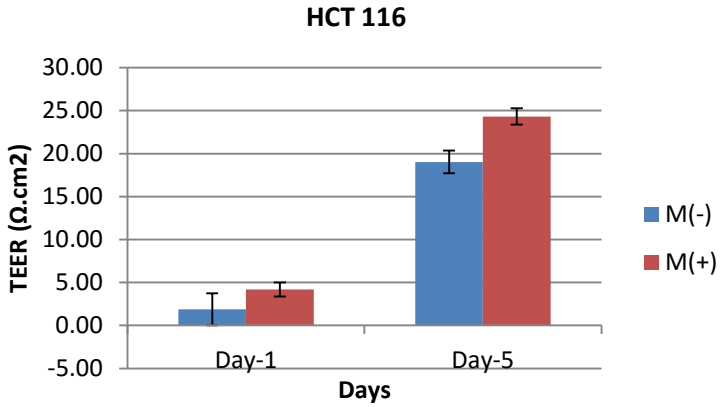
HCT 116
30.00
25.00
20.00
15.00
10.00
5.00
0.00
-5.00
TEER (Ω.cm2)
Day-1
Day-5
Days
M(-)
M(+)

**(D)**

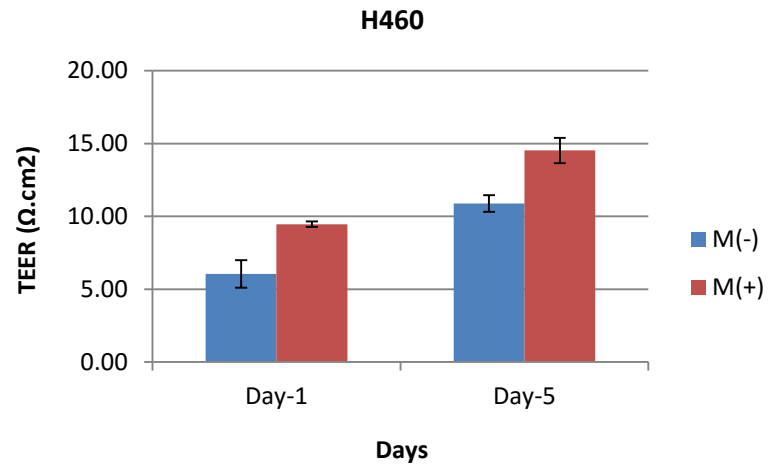


**(E)**

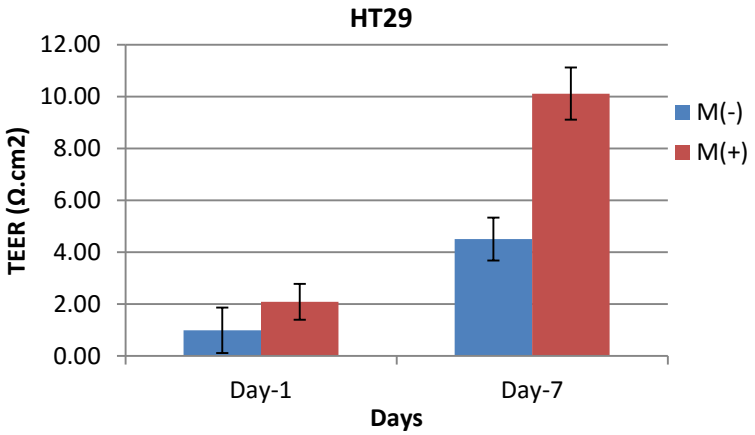


***Figure 7.21: Application of 2.5% matrigel cells***

*A) SiHa, B) MCF-7, C) HCT 116, D) H460 and E) HT29*

Various cell lines were used such as SiHa, MCF-7, HCT 116. H470 and HT29 cells. TEER for all cell lines were determined on day 1 and day 6. Cells were cultured on transwells with and without matrigel. Figure 7.21 shown the graphs obtained for TEER values for different cell lines in presence of matrigel and without matrigel.

A SiHa cell line did not show major difference in TEER values between both the cell samples. TEER was nearly equal through SiHa cell membranes even after application of 2.5% matrigel to the cells. For SiHa cells without application of matrigel TEER across membrane was 2.20 $\Omega.cm^2$ on day 1 and 9.79$\Omega.cm^2$ on day 6. While with application of matrigel TEER across SiHa membrane was 2.53$\Omega.cm^2$ on day 1 and on day 6 TEER was 9.68$\Omega.cm^2$. MCF-7 was next cell line used to study membrane forming ability with matrigel. The MCF-7 was a slow growing cell line, so it shown very low TEER on day 1 with both cell samples. Without matrigel addition TEER was 1.43 $\Omega.cm^2$ while with matrigel TEER value across MCF-7 cell membrane was 1.54 $\Omega.cm^2$ on day 1. Both TEER values were nearly similar. On day 6 slight higher TEER across MCF-7 cells grown with matrigel than those grown without matrigel was observed. But TEER with MCF-7 membranes was too low even on day 6. And this low TEER might be possibly because, MCF-7 is slowly growing cell line and because of that it did not have formed membrane on transwells and as a result of which higher TEER was not observed across MCF-7 cell membrane. HCT 116 cells shown comparatively high TEER across its membrane formed by cells grown in presence of matrigel. TEER across HCT 116 grown with matrigel was 4.18$\Omega.cm^2$ on day 1 and 24.31$\Omega.cm^2$ on day 6. These TEER values were higher than TEER obtained by cells without matrigel application. Here with HCT 116 the difference in TEER values was observed and TEER seems to be increased with addition of matrigel. Similar study performed with H460 cells and like HCT116, TEER values observed higher across the cell membrane grown in presence of matrigel. TEER across matrigel applied cell membrane was 9.46$\Omega.cm^2$ on day 1 and 14.52$\Omega.cm^2$ on day 6, while TEER across cell

membrane grown in absence of matrigel was 6.05Ω.cm$^2$ on day 1 and 10.89Ω.cm$^2$ on day 6. Next cell line used was HT29. The cell line shows increased TEER across cell membranes in presence of matrigel as compared to the cell membranes grown without matrigel. TEER across matrigel applied cell membrane was 2.09Ω.cm$^2$ and 10.12Ω.cm$^2$ on days 1 and 6 respectively. While TEER across cell membranes grown in absence of matrigel was 0.99Ω.cm$^2$ and 4.51Ω.cm$^2$ on days 1 and 6 respectively.

Here in this study, with application of 2.5 % (25µl/ml) matrigel, cell growth seems to be enhanced and it could be stated from the increasing TEER across the matrigel applied cell membranes. To support this statement, these membranes further used to perform histology study, which would give robust idea about the membrane structures.

**Without Matrigel (M-)**

Day-1 Day-6

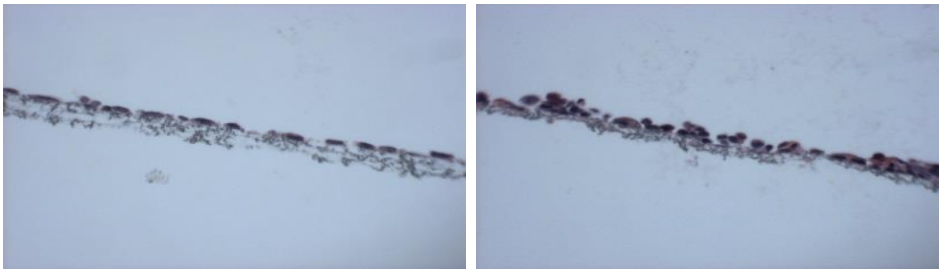

**With Matrigel (M+)**

Day-1 Day-6

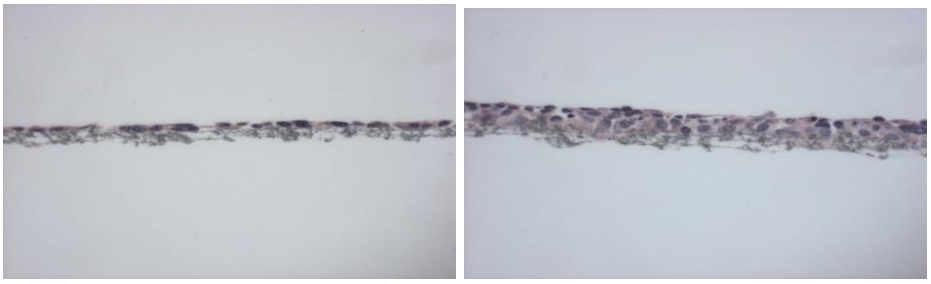

***Figure 7.22: Effect of 2.5 % matrigel on membrane forming ability of SiHa cells***

**Without Matrigel (M-)**

Day-1 Day-6

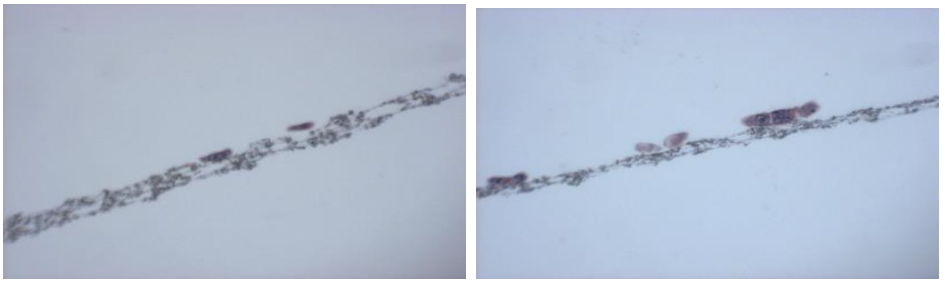

**With Matrigel (M+)**

Day-1 Day-6

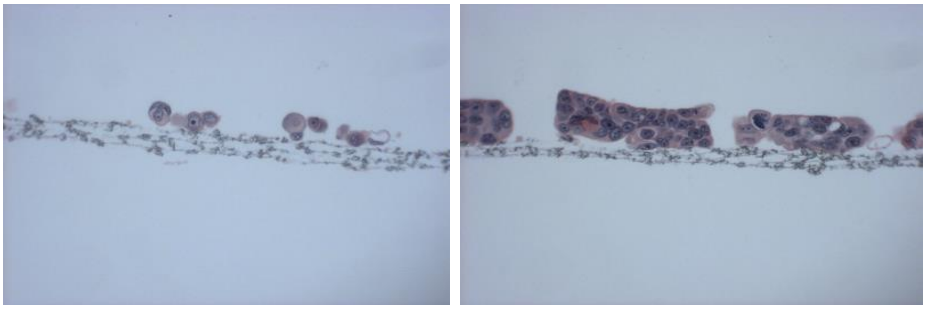

***Figure 7.23: Effect of 2.5 % matrigel on membrane forming ability of MCF-7 cells***

**Without Matrigel (M-)**

Day-1 Day-6

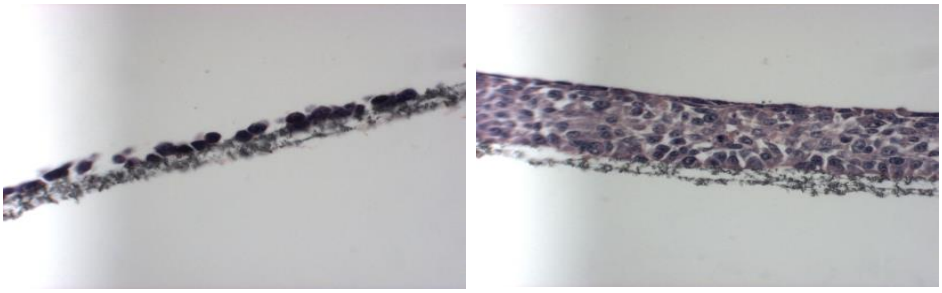

**With Matrigel (M+)**

Day-1 Day-6

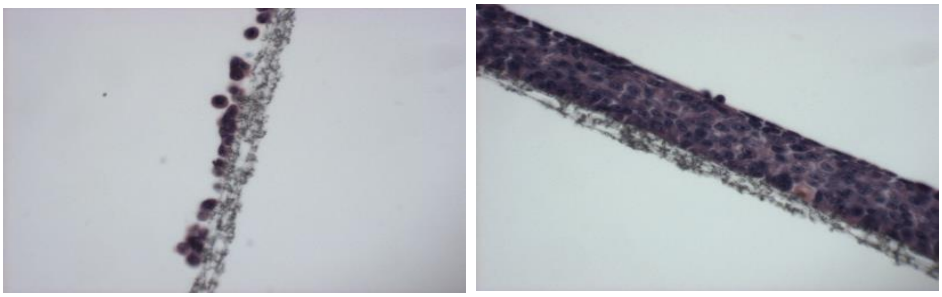

***Figure 7.24: Effect of 2.5 % matrigel on membrane forming ability of HCT116 cells***

**Without Matrigel (M-)**

Day-1 Day-6

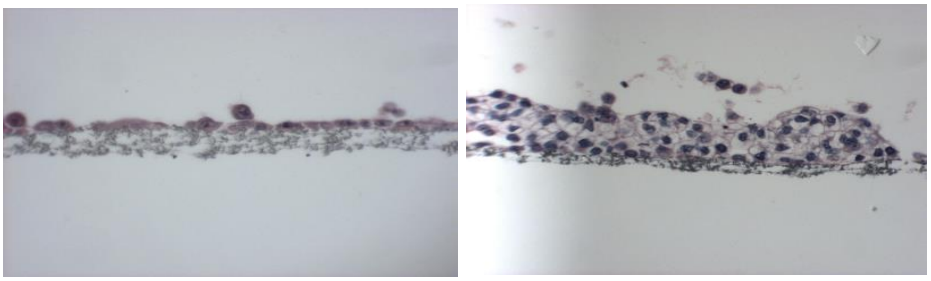

**With Matrigel (M+)**

Day-1 Day-6

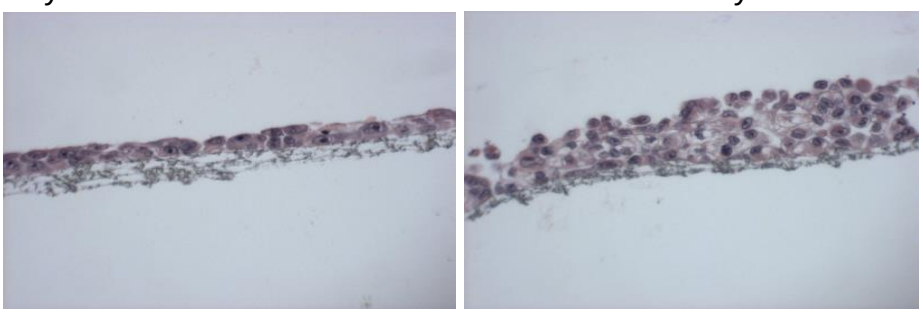

***Figure 7.25: Effect of 2.5 % matrigel on membrane forming ability of H460 cells***

**Without Matrigel (M-)**

Day-1 Day-6

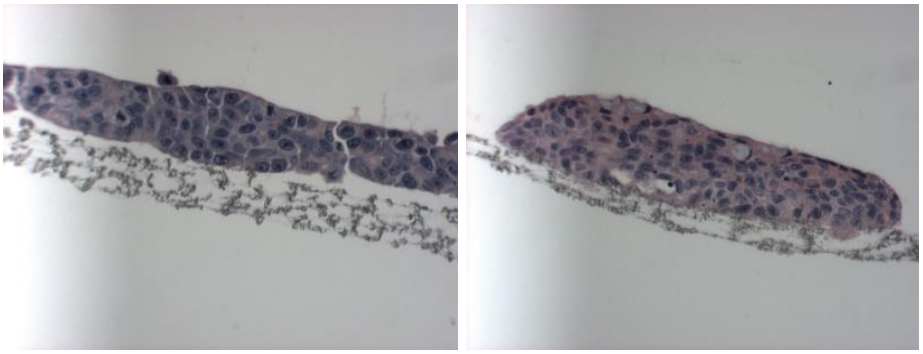

**With Matrigel (M+)**

Day-1 Day-6

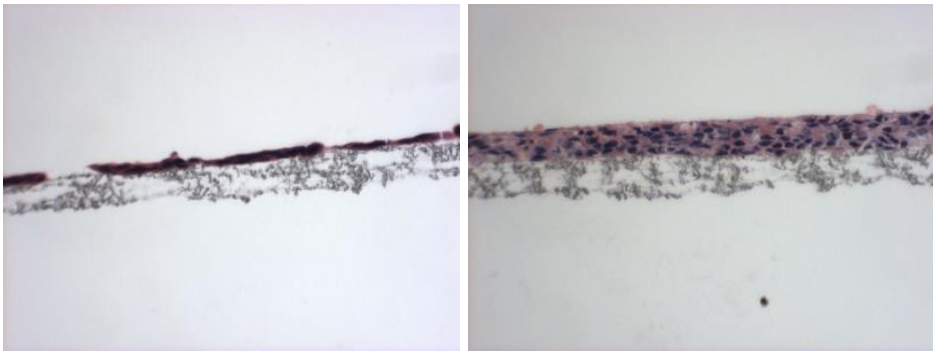

***Figure 7.26: Effect of 2.5 % matrigel on membrane forming ability of HT29 cells***

Figure 7.22, Figure 7.23, Figure 7.24, Figure 7.25 and Figure 7.26 shows histology images for cell lines forming membranes on transwells with and without application of matrigel. As seen here, the SiHa cells did not show major difference in TEER values on day 1 and 6. On day 1 images of SiHa cell grown in presence of matrigel shown higher density of cells present on transwells. Though the cell number was high, they have not formed intact membrane on day 1. Cells did not seems to be attached to each other and this might be the reason that there was no difference in TEER values on day 1. On day 6 cell

membrane grown without matrigel seems very week and with low cell density, while cells grown in presence of matrigel shows nice growth forming membrane with high cell density. Also the cells were grown in multi-layers. So it was confirmed that matrigel supports the growth of cells and that is why more cells observed in membrane. But even though the membrane was thick and multi-layered, the images shown inter cellular spaces and cells with lose attachments within the membrane. So these cells provide leaky membrane and this was the possible reason that there was no increased TEER with matrigel addition despite observing thick membrane. Very low TEER with MCF-7 cells was observed and it was stated that the low TEER might be because of the slow growth of cells. Histology images explored the exact reason for low TEER. There were very few cells were present on transwell and this was most possibly because slower growth of cells. But the high cell density was observed on day 6 in presence of matrigel as compare to the cells grown without matrigel. Though this enhanced cell number was not to form membrane, but still there was enhanced growth in presence of matrigel.

Images of HCT 116 cells shown formation of nice intact membrane on day 6. On day 1 both cell samples; with and without matrigel; shown uniform alignment of cells on membrane and on day 6 these cells have delivered an intact cell membranes developed in multi-cell layers. Both cell samples grown in presence of matrigel and without matrigel gave a uniform cell membrane. But cell membrane grown without matrigel shown cells with lose binding with each other. There was also intra cellular spaces in this membrane. Such breaches in membrane could form leaky membrane and this was the reason low TEER was

observed across this membrane grown without matrigel. On the other hand cell membrane formed by cells treated with matrigel formed a membrane which observed more intact. Still there were few intercellular spaces but these were less in number as compare to the membrane grown without matrigel. Cells in this membrane observed to be attaches firmly with one another and these tight attachments were responsible for the high TEER values observed. Similar kind of results were observed with the H460 cells. Growth of cells seems to be enhanced by the presence of matrigel in culture and which was resulted in the generation of uniform cell membrane. HT29 cells, in absence of matrigel shows growth in the form of cell clumps on the transwell membrane. While cells grown in presence of matrigel did not show clumps of cells, instead observed that the cells grown uniformly over the transwell forming multi-cell layer membrane which was more intact. In all above one thing was seen in common that application of matrigel was responsible to boost the growth of cells. Also matrigel helped cells to distribute uniformly over the transwells and because of uniform distribution the cells grown without clumps. Matrigel provided a strong basement membrane for the cells to attach and to grow.

## 7.11 Summary

TEER measurement and histology study for various cell lines was performed. The study was performed to assess the membrane forming ability of cells as well as to study the integrity of cell membranes.

In first section of this chapter the histology of various cell lines were studied including DLD-1, PANC-1, SiHa, Caco-2, MDCKII and its derivatives. It was observed that DLD-1, PANC-1 and Siha were forming multi-cell layers. Despite of multilayers, only DLD-1 gave uniform and intact membrane while other two cell lines were grown in patches on the transwells. These cells forms the cell clumps and so shown the breaches in membrane and were not delivering ideal cell membrane. There was also the lower TEER with PANC-1 and SiHa while DLD-1 cells gave higher TEER values and TEER kept increasing over the incubation time. The Caco-2, MDCKII and its derivatives were forming monolayer on the transwells. These cells gave higher TEER around the days 12-15 and so these cells were used to perform permeability study on those days. These cells form ideal cell membranes to perform drug permeability studies.

As seen that PANC-1 and SiHa were not growing in uniform membrane, and so matrigel was used in culture to promote the membrane forming ability of such cells. Initially higher concentration of matrigel was used in culture and which was almost 50 % of the total cell suspension. This high concentration resulted in the suppression of cellular growth. The matrigel turns in to solid gel above $4^0$C and this higher concentration at incubation temperature might have formed the thick gel in transwells. So this gel formation have been not allowed the cells

to grow freely as this matrigel had trapped the cells inside it. Eventually there was no membranes observed with application of such higher concentration of matrigel. Same experiment was repeated with lower concentration of matrigel (2.5 %). This concentration of matrigel supported the cell growth and enhanced the membrane forming abilities of cells. But still there was no big differences in TEER across these membranes. Even though some cells did not shown the formation of intact membranes, but still enhanced growth with matrigel was observed. To achieve more intact membranes with higher TEER across them, cells need to grow for longer duration. The higher incubation time might give good cell membranes with higher TEER.

# 8 : Conclusion and Future Work

## 8.1 Conclusion

This study was performed to develop novel efflux inhibitor molecule and to evaluate it for improvement in drug delivery. So to achieve this goal several experiments were designed, and from the research done here following conclusions can be drawn:

- The novel compound galaxolide have been tested for its toxicity against the various cell lines. From the data observed through these experiments it was confirmed that galaxolide is non-toxic for the cells. It does not have any harmful effects on both normal cells as well as cancer cells. So galaxolide can be used with other drugs without interfering the toxicity of co-drug. The experiment determining effect of galaxolide on the toxicity of other drugs was also performed. Study was unable to find any enhancement in toxicity of drug with addition of galaxolide. Actually the drug used is curcumin, and as it is seen that curcumin is not active substrate for efflux proteins and that is why galaxolide addition to this formulation does not show enhanced toxic activity against cells.

  P-gp expression and inhibition studies were also performed. To study P-gp expression two techniques were used; western blot and FACS. These studies were determined the expression of P-glycoprotein in Caco-2 and MDCK cell lines with both the methods. The P-gp inhibition studied with Rh123 assay and it is observed that galaxolide have P-gp inhibition activity. Even galaxolide shows inhibition activity against other efflux proteins like BCRP and MRP1. So it is clear that galaxolide is a potent

efflux protein inhibitor molecule and is more effective than verapamil and cyclosporine A.

- To study effect of galaxolide on drug permeability, first of all HPLC method with various receiver media was developed. Study determined that, receiver media having protein molecules present in it, gives the higher recovery of curcumin after extraction as compared to the receiver media without protein molecules. Reason for this was explained in results section. Also the pH is very critical factor for the curcumin recovery as curcumin has higher degradation at alkaline pH than acidic pH. So the preparation of donor and receiver media were done accordingly in later parts of experiments. Permeation study with curcumin done with various donor and receiver media and observed different results depending on the permeation duration and content of receiver media. But there was no any enhancement in permeation of curcumin with addition of galaxolide in any of these experiments. And as explained earlier, this is because curcumin is not active P-gp substrate. But still galaxolide can be useful to enhance the treatment of drugs which are active P-gp substrates.
- The histology studies are performed to assess the membrane forming abilities of various cell lines, so that they are useful to carry permeation study. It is observed that Caco-2, and MDCKII along with its derivatives, form nice monolayers on transwells. These membranes show higher TEER across them and are developed to be ideal cell membranes for permeability study. DLD-1 as well forms multi-cell layer membrane, which intact and gives high TEER values across it. So DLD-1 cells can

be used to study permeability of drugs across multi-cell layers. Other cells which did not form uniform membranes, so the matrigel was applied to those cells. And it is observed that the matrigel enhances the cell growth and also helps cells to form uniform membranes. Though there was no any results showing higher TEER with matrigel, but if cells were incubated for longer duration, definitely there would be generation of good membranes with matrigel. So matrigel could be the efficient tool to form cell membranes.

## 8.2 Future Work

The current findings in this research can highlight the following aspects for future studies:

- Effect of galaxolide on drug toxicity of P-gp active drugs
- Use of P-gp active substrates to study the effect of galaxolide on permeation enhancement.
- Permeation study through the multi-cell layer membranes
- Immunohistochemistry study of cell membranes to study expression of P-gp in membranes
- Use of dyes such as calcein AM and DiOC2(3) along with rh123 to study the efflux protein inhibition assays to study inhibition action of galaxolide. Also the use of FACS for analysis of data instead of plate reader only.
- Use of Matrigel to develop more efficient cell membranes conferring high TEER across them.

## 9 : References


Abbott, N. J., Dolman, D. E. and Patabendige, A. K. (2008) Assays to predict drug permeation across the blood-brain barrier, and distribution to brain. *Curr Drug Metab,* 9 (9)**,** 901-10.

Adams, J. M. and Cory, S. (2007) The Bcl-2 apoptotic switch in cancer development and therapy. *Oncogene,* 26 (9)**,** 1324-37.

Aggarwal, B. B. and Harikumar, K. B. (2009) Potential therapeutic effects of curcumin, the anti-inflammatory agent, against neurodegenerative, cardiovascular, pulmonary, metabolic, autoimmune and neoplastic diseases. *International Journal of Biochemistry & Cell Biology,* 41 (1)**,** 40-59.

Aller, S. G., Yu, J., Ward, A., Weng, Y., Chittaboina, S., Zhuo, R., Harrell, P. M., Trinh, Y. T., Zhang, Q., Urbatsch, I. L. and Chang, G. (2009) Structure of P-glycoprotein reveals a molecular basis for poly-specific drug binding. *Science,* 323 (5922)**,** 1718-22.

Altenberg, G. A., Vanoye, C. G., Horton, J. K. and Reuss, L. (1994) Unidirectional fluxes of rhodamine 123 in multidrug-resistant cells: evidence against direct drug extrusion from the plasma membrane. *Proc Natl Acad Sci U S A,* 91 (11)**,** 4654-57.

Ambudkar, S. V., Kim, I. W. and Sauna, Z. E. (2006) The power of the pump: Mechanisms of action of P-glycoprotein (ABCB1). *European Journal of Pharmaceutical Sciences,* 27 (5)**,** 392-400.

Anand, R., Gill, K. D. and Mahdi, A. A. (2014) Therapeutics of Alzheimer's disease: Past, present and future. *Neuropharmacology,* 76, Part A**,** 27-50.

Artandi, S. E. and DePinho, R. A. (2010) Telomeres and telomerase in cancer. *Carcinogenesis,* 31 (1)**,** 9-18.

Aschele, C., Debernardis, D., Bandelloni, R., Cascinu, S., Catalano, V., Giordani, P., Barni, S., Turci, D., Drudi, G., Lonardi, S., Gallo, L., Maley, F. and Monfardini, S. (2002) Thymidylate synthase protein expression in colorectal cancer metastases predicts for clinical outcome to leucovorin-modulated bolus or infusional 5-fluorouracil but not methotrexate-modulated bolus 5-fluorouracil. *Annals of Oncology,* 13 (12)**,** 1882-1892.

Ballabh, P., Braun, A. and Nedergaard, M. (2004) The blood-brain barrier: an overview - Structure, regulation, and clinical implications. *Neurobiology of Disease,* 16 (1)**,** 1-13.

Bao, L., Matsumura, Y., Baban, D., Sun, Y. and Tarin, D. (1994) Effects of inoculation site and Matrigel on growth and metastasis of human breast cancer cells. *Br J Cancer,* 70 (2)**,** 228-32.

Bardeesy, N. and Sharpless, N. E. (2006) RAS unplugged: negative feedback and oncogene-induced senescence. *Cancer Cell,* 10 (6)**,** 451-53.

Beaulieu, E., Demeule, M., Ghitescu, L. and Beliveau, R. (1997) P-glycoprotein is strongly expressed in the luminal membranes of the endothelium of blood vessels in the brain. *Biochemical Journal,* 326**,** 539-544.

Beck, W. T., Grogan, T. M., Willman, C. L., Cordon-Cardo, C., Parham, D. M., Kuttesch, J. F., Andreeff, M., Bates, S. E., Berard, C. W., Boyett, J. M., Brophy, N. A., Broxterman, H. J., Chan, H. S., Dalton, W. S., Dietel, M., Fojo, A. T., Gascoyne, R. D., Head, D., Houghton, P. J., Srivastava, D. K., Lehnert, M., Leith, C. P., Paietta, E., Pavelic, Z. P. and Weinstein, R. (1996) Methods to detect P-glycoprotein-associated multidrug resistance in patients' tumors: consensus recommendations. *Cancer Res,* 56 (13)**,** 3010-20.

Behl, C. and Moosmann, B. (2002) Antioxidant neuroprotection in Alzheimer's disease as preventive and therapeutic approach. *Free Radical Biology and Medicine,* 33 (2)**,** 182-191.

Bergers, G. and Benjamin, L. E. (2003) Tumorigenesis and the angiogenic switch. *Nat Rev Cancer,* 3 (6)**,** 401-10.

Bhowmick, N. A., Neilson, E. G. and Moses, H. L. (2004) Stromal fibroblasts in cancer initiation and progression. *Nature,* 432 (7015)**,** 332-37.

Bradfield, P. F., Nourshargh, S., Aurrand-Lions, M. and Imhof, B. A. (2007) JAM family and related proteins in leukocyte migration (Vestweber series). *Arteriosclerosis Thrombosis and Vascular Biology,* 27 (10)**,** 2104-2112.

Callaghan, R., Ford, R. C. and Kerr, I. D. (2006) The translocation mechanism of P-glycoprotein. *Febs Letters,* 580 (4)**,** 1056-1063.

Cheng, N., Chytil, A., Shyr, Y., Joly, A. and Moses, H. L. (2008) Transforming growth factor-beta signaling-deficient fibroblasts enhance hepatocyte growth factor signaling in mammary carcinoma cells to promote scattering and invasion. *Mol Cancer Res,* 6 (10)**,** 1521-33.

Childs, S., Yeh, R. L., Georges, E. and Ling, V. (1995) Identification of a sister gene to P-glycoprotein. *Cancer Res,* 55 (10)**,** 2029-34.

Croop, J. M., Raymond, M., Haber, D., Devault, A., Arceci, R. J., Gros, P. and Housman, D. E. (1989) THE 3 MOUSE MULTIDRUG RESISTANCE (MDR) GENES ARE EXPRESSED IN A TISSUE-SPECIFIC MANNER IN NORMAL MOUSE-TISSUES. *Molecular and Cellular Biology,* 9 (3)**,** 1346-1350.

Cummings, J. L. (2004) Alzheimer's disease. *N Engl J Med,* 351 (1)**,** 56-67.

David R. Hipfner[1,] R. G. D., Susan P.C. Cole[*] (1999) Structural, mechanistic and clinical aspects of MRP1. *Biochimica et Biophysica Acta*, 359-376.

Dean, M. and Annilo, T. (2005) Evolution of the ATP-binding cassette (ABC) transporter superfamily in vertebrates. *Annual Review of Genomics and Human Genetics,* 6, 123-142.

Dean, M., Hamon, Y. and Chimini, G. (2001) The human ATP-binding cassette (ABC) transporter superfamily. *Journal of Lipid Research,* 42 (7), 1007-1017.

DeBerardinis, R. J., Lum, J. J., Hatzivassiliou, G. and Thompson, C. B. (2008) The biology of cancer: metabolic reprogramming fuels cell growth and proliferation. *Cell Metab,* 7 (1), 11-20.

Deli, M. A., Abraham, C. S., Kataoka, Y. and Niwa, M. (2005) Permeability studies on in vitro blood-brain barrier models: physiology, pathology, and pharmacology. *Cell Mol Neurobiol,* 25 (1), 59-127.

DeNardo, D. G., Andreu, P. and Coussens, L. M. (2010) Interactions between lymphocytes and myeloid cells regulate pro- versus anti-tumor immunity. *Cancer Metastasis Rev,* 29 (2), 309-16.

Dvorak, H. F. (1986) Tumors: wounds that do not heal. Similarities between tumor stroma generation and wound healing. *N Engl J Med,* 315 (26), 1650-59.

Ebnet, K., Schulz, C. U., Brickwedde, M., Pendl, G. G. and Vestweber, D. (2000) Junctional adhesion molecule interacts with the PDZ domain-containing proteins AF-6 and ZO-1. *Journal of Biological Chemistry,* 275 (36), 27979-27988.

Edwards, J. E., Alcorn, J., Savolainen, J., Anderson, B. D. and McNamara, P. J. (2005) Role of P-glycoprotein in distribution of nelfinavir across the blood-mammary tissue barrier and blood-brain barrier. *Antimicrobial Agents and Chemotherapy,* 49 (4)**,** 1626-1628.

El-Readi, M. Z., Hamdan, D., Farrag, N., El-Shazly, A. and Wink, M. (2010) Inhibition of P-glycoprotein activity by limonin and other secondary metabolites from Citrus species in human colon and leukaemia cell lines. *European Journal of Pharmacology,* 626 (2-3)**,** 139-145.

Epel, D. (1998) Use of multidrug transporters as first lines of defense against toxins in aquatic organisms. *Comparative Biochemistry and Physiology a-Molecular and Integrative Physiology,* 120 (1)**,** 23-28.

Feldman, G. J., Mullin, J. M. and Ryan, M. P. (2005) Occludin: Structure, function and regulation. *Advanced Drug Delivery Reviews,* 57 (6)**,** 883-917.

Fidler, I. J. (2003) The pathogenesis of cancer metastasis: the 'seed and soil' hypothesis revisited. *Nat Rev Cancer,* 3 (6)**,** 453-58.

Forster, S., Thumser, A. E., Hood, S. R. and Plant, N. (2012) Characterization of rhodamine-123 as a tracer dye for use in in vitro drug transport assays. *PLoS One,* 7 (3)**,** e33253.

Fridman, R., Kibbey, M. C., Royce, L. S., Zain, M., Sweeney, M., Jicha, D. L., Yannelli, J. R., Martin, G. R. and Kleinman, H. K. (1991) Enhanced tumor growth of both primary and established human and murine tumor cells in athymic mice after coinjection with Matrigel. *J Natl Cancer Inst,* 83 (11)**,** 769-74.

Gerloff, T., Stieger, B., Hagenbuch, B., Madon, J., Landmann, L., Roth, J., Hofmann, A. F. and Meier, P. J. (1998) The Sister of P-glycoprotein Represents the Canalicular Bile Salt Export Pump of Mammalian Liver. *Journal of Biological Chemistry,* 273 (16)**,** 10046-10050.

Gonzalez-Mariscal, L., Betanzos, A., Nava, P. and Jaramillo, B. E. (2003) Tight junction proteins. *Progress in Biophysics & Molecular Biology,* 81 (1)**,** 1-44.

Gottesman, M. M., Fojo, T. and Bates, S. E. (2002) Multidrug resistance in cancer: role of ATP-dependent transporters. *Nat Rev Cancer,* 2 (1)**,** 48-58.

Grivennikov, S. I., Greten, F. R. and Karin, M. (2010) Immunity, inflammation, and cancer. *Cell,* 140 (6)**,** 883-99.

Gumbleton, M. and Audus, K. L. (2001) Progress and limitations in the use of in vitro cell cultures to serve as a permeability screen for the blood-brain barrier. *J Pharm Sci,* 90 (11)**,** 1681-98.

Hanahan, D. and Weinberg, R. A. (2000) The hallmarks of cancer. *Cell,* 100 (1)**,** 57-70.

Hanahan, D. and Weinberg, R. A. (2011) Hallmarks of Cancer: The Next Generation. *Cell,* 144 (5)**,** 646-674.

Hanekop, N., Zaitseva, J., Jenewein, S., Holland, I. B. and Schmitt, L. (2006) Molecular insights into the mechanism of ATP-hydrolysis by the NBD of the ABC-transporter HlyB. *Febs Letters,* 580 (4)**,** 1036-1041.

Hasima, N. and Aggarwal, B. B. (2012) Cancer-linked targets modulated by curcumin. *International journal of biochemistry and molecular biology,* 3 (4)**,** 328-51.

Haskins, J., Gu, L. J., Wittchen, E. S., Hibbard, J. and Stevenson, B. R. (1998) ZO-3, a novel member of the MAGUK protein family found at the tight junction, interacts with ZO-1 and occludin. *Journal of Cell Biology,* 141 (1)**,** 199-208.

Hawkins, B. T. and Davis, T. P. (2005) The blood-brain barrier/neurovascular unit in health and disease. *Pharmacological Reviews,* 57 (2)**,** 173-185.

Hicklin, D. J. and Ellis, L. M. (2005) Role of the vascular endothelial growth factor pathway in tumor growth and angiogenesis. *J Clin Oncol,* 23 (5)**,** 1011-27.

Hirtz, D., Thurman, D. J., Gwinn-Hardy, K., Mohamed, M., Chaudhuri, A. R. and Zalutsky, R. (2007) How common are the "common" neurologic disorders? *Neurology,* 68 (5)**,** 326-37.

Hsu, P. P. and Sabatini, D. M. (2008) Cancer cell metabolism: Warburg and beyond. *Cell,* 134 (5)**,** 703-7.

Huang, C., Xu, D., Xia, Q., Wang, P., Rong, C. and Su, Y. (2012) Reversal of P-glycoprotein-mediated multidrug resistance of human hepatic cancer cells by Astragaloside II. *Journal of Pharmacy and Pharmacology,* 64 (12)**,** 1741-1750.

Huang, Y. and Mucke, L. (2012) Alzheimer mechanisms and therapeutic strategies. *Cell,* 148 (6)**,** 1204-22.

Huber, J. D., Egleton, R. D. and Davis, T. P. (2001) Molecular physiology and pathophysiology of tight junctions in the blood-brain barrier. *Trends in Neurosciences,* 24 (12)**,** 719-725.

Hughes, C. S., Postovit, L. M. and Lajoie, G. A. (2010) Matrigel: a complex protein mixture required for optimal growth of cell culture. *Proteomics,* 10 (9)**,** 1886-90.

Iqbal, K., Alonso Adel, C., Chen, S., Chohan, M. O., El-Akkad, E., Gong, C. X., Khatoon, S., Li, B., Liu, F., Rahman, A., Tanimukai, H. and Grundke-Iqbal, I. (2005) Tau pathology in Alzheimer disease and other tauopathies. *Biochim Biophys Acta,* 1739 (2-3)**,** 198-210.

Ira, M. M. G. a. and Pastan, I. (1988) The Multidrug Transporter, a double edged sword. *The journalof biological chemistry,* Vol. 263, (Issue of September 5)**,** 12163-12166.

Itoh, M., Furuse, M., Morita, K., Kubota, K., Saitou, M. and Tsukita, S. (1999) Direct binding of three tight junction-associated MAGUKs, ZO-1, ZO-2 and ZO-3, with the COOH termini of claudins. *Journal of Cell Biology,* 147 (6)**,** 1351-1363.

Janas, E., Hofacker, M., Chen, M., Gompf, S., van der Does, C. and Tampe, R. (2003) The ATP hydrolysis cycle of the nucleotide-binding domain of the mitochondrial ATP-binding cassette transporter Mdl1p. *Journal of Biological Chemistry,* 278 (29)**,** 26862-26869.

Jiang, B. H. and Liu, L. Z. (2009) PI3K/PTEN signaling in angiogenesis and tumorigenesis. *Adv Cancer Res,* 102**,** 19-65.

Johan W. Jonker, J. W. S., Remco F. Brinkhuis, Marc Maliepaard, Jos H. and Beijnen, J. H. M. S., Alfred H. Schinkel (2000) Role of Breast Cancer Resistance Protein in the bioavailability and fetal penetration of topotecan. *Journal of the National Cancer Institute,* Vol. 92.

Johnson, J. J. and Mukhtar, H. (2007) Curcumin for chemoprevention of colon cancer. *Cancer Letters,* 255 (2)**,** 170-181.

Jones, R. G. and Thompson, C. B. (2009) Tumor suppressors and cell metabolism: a recipe for cancer growth. *Genes Dev,* 23 (5)**,** 537-48.

Kang, H. J., Choi, Y. S., Hong, S. B., Kim, K. W., Woo, R. S., Won, S. J., Kim, E. J., Jeon, H. K., Jo, S. Y., Kim, T. K., Bachoo, R., Reynolds, I. J., Gwag, B. J. and Lee, H. W. (2004) Ectopic expression of the catalytic subunit of telomerase protects against brain injury resulting from ischemia and NMDA-induced neurotoxicity. *J Neurosci,* 24 (6)**,** 1280-87.

Kannan, K., Reiner, J. L., Yun, S. H., Perrotta, E. E., Tao, L., Johnson-Restrepo, B. and Rodan, B. D. (2005) Polycyclic musk compounds in higher trophic level aquatic organisms and humans from the United States. *Chemosphere,* 61 (5)**,** 693-700.

Kawai, K., Kusano, I., Ido, M., Sakurai, M., Shiraishi, T. and Yatani, R. (1994) Identification of a P-glycoprotein-related protein (mini-P-glycoprotein) which is overexpressed in multidrug resistant cells. *Biochem Biophys Res Commun,* 198 (2)**,** 804-10.

Khlistunova, I., Biernat, J., Wang, Y., Pickhardt, M., von Bergen, M., Gazova, Z., Mandelkow, E. and Mandelkow, E. M. (2006) Inducible expression of Tau repeat domain in cell models of tauopathy: aggregation is toxic to cells but can be reversed by inhibitor drugs. *J Biol Chem,* 281 (2)**,** 1205-14.

Kimura, Y., Aoki, J., Kohno, M., Ooka, H., Tsuruo, T. and Nakanishi, O. (2002) P-glycoprotein inhibition by the multidrug resistance-reversing agent MS-209 enhances bioavailability and antitumor efficacy of orally administered paclitaxel. *Cancer Chemother Pharmacol,* 49 (4)**,** 322-28.

Kinzler, K. W. and Vogelstein, B. (1997) Cancer-susceptibility genes. Gatekeepers and caretakers. *Nature,* 386 (6627)**,** 761-763.

Kleinman, H. K. and Martin, G. R. (2005) Matrigel: basement membrane matrix with biological activity. *Semin Cancer Biol,* 15 (5)**,** 378-86.

Kong, Q., Beel, J. A. and Lillehei, K. O. (2000) A threshold concept for cancer therapy. *Medical Hypotheses,* 55 (1)**,** 29-35.

Krishna, R. and Mayer, L. D. (2000) Multidrug resistance (MDR) in cancer - Mechanisms, reversal using modulators of MDR and the role of MDR modulators in influencing the pharmacokinetics of anticancer drugs. *European Journal of Pharmaceutical Sciences,* 11 (4)**,** 265-283.

Kruijtzer, C. M., Beijnen, J. H., Rosing, H., ten Bokkel Huinink, W. W., Schot, M., Jewell, R. C., Paul, E. M. and Schellens, J. H. (2002) Increased oral bioavailability of topotecan in combination with the breast cancer resistance protein and P-glycoprotein inhibitor GF120918. *J Clin Oncol,* 20 (13)**,** 2943-50.

Lam, F. C., Liu, R. H., Lu, P. H., Shapiro, A. B., Renoir, J. M., Sharom, F. J. and Reiner, P. B. (2001) beta-Amyloid efflux mediated by p-glycoprotein. *Journal of Neurochemistry,* 76 (4)**,** 1121-1128.

Langford, D., Hurford, R., Hashimoto, M., Digicaylioglu, M. and Masliah, E. (2005) Signalling crosstalk in FGF2-mediated protection of endothelial cells from HIV-gp120. *BMC Neurosci,* 6-8.

Lee, V. M., Goedert, M. and Trojanowski, J. Q. (2001) Neurodegenerative tauopathies. *Annu Rev Neurosci,* 24**,** 1121-59.

Letai, A. G. (2008) Diagnosing and exploiting cancer's addiction to blocks in apoptosis. *Nat Rev Cancer,* 8 (2)**,** 121-32.

Li, J., Jiang, Y., Wen, J., Fan, G., Wu, Y. and Zhang, C. (2009) A rapid and simple HPLC method for the determination of curcumin in rat plasma: assay development, validation and application to a pharmacokinetic study of curcumin liposome. *Biomed Chromatogr,* 23 (11)**,** 1201-7.

Liu, W.-Y., Wang, Z.-B., Zhang, L.-C., Wei, X. and Li, L. (2012) Tight Junction in Blood-Brain Barrier: An Overview of Structure, Regulation, and Regulator Substances. *Cns Neuroscience & Therapeutics,* 18 (8)**,** 609-615.

Loo, T. W., Bartlett, M. C., Detty, M. R. and Clarke, D. M. (2012) The ATPase Activity of the P-glycoprotein Drug Pump Is Highly Activated When the N-terminal and Central Regions of the Nucleotide-binding Domains Are Linked Closely Together. *Journal of Biological Chemistry,* 287 (32)**,** 26806-26816.

Luckenbach, T. and Epel, D. (2005) Nitromusk and polycyclic musk compounds as long-term inhibitors of cellular xenobiotic defense systems mediated by multidrug transporters. *Environmental Health Perspectives,* 113 (1)**,** 17-24.

Lundquist, S., Renftel, M., Brillault, J., Fenart, L., Cecchelli, R. and Dehouck, M.-P. (2002) Prediction of Drug Transport Through the Blood-Brain Barrier in Vivo: A Comparison Between Two in Vitro Cell Models. *Pharmaceutical Research,* 19 (7)**,** 976-981.

Maida, Y., Yasukawa, M., Furuuchi, M., Lassmann, T., Possemato, R., Okamoto, N., Kasim, V., Hayashizaki, Y., Hahn, W. C. and Masutomi, K. (2009) An RNA-dependent RNA polymerase formed by TERT and the RMRP RNA. *Nature,* 461 (7261)**,** 230-35.

Mandell, K. J. and Parkos, C. A. (2005) The JAM family of proteins. *Advanced Drug Delivery Reviews,* 57 (6)**,** 857-867.

Marie, S. K. and Shinjo, S. M. (2011) Metabolism and brain cancer. *Clinics (Sao Paulo),* 66 Suppl 1**,** 33-43.

Martin-Padura, I., Lostaglio, S., Schneemann, M., Williams, L., Romano, M., Fruscella, P., Panzeri, C., Stoppacciaro, A., Ruco, L., Villa, A., Simmons, D. and Dejana, E. (1998) Junctional adhesion molecule, a novel member of the immunoglobulin superfamily that distributes at intercellular junctions and modulates monocyte transmigration. *Journal of Cell Biology,* 142 (1)**,** 117-127.

Masutomi, K., Possemato, R., Wong, J. M., Currier, J. L., Tothova, Z., Manola, J. B., Ganesan, S., Lansdorp, P. M., Collins, K. and Hahn, W. C. (2005) The telomerase reverse transcriptase regulates chromatin state and DNA damage responses. *Proc Natl Acad Sci U S A,* 102 (23)**,** 8222-27.

Mayer, U., Wagenaar, E., Dorobek, B., Beijnen, J. H., Borst, P. and Schinkel, A. H. (1997) Full blockade of intestinal P-glycoprotein and extensive inhibition of blood-brain barrier P-glycoprotein by oral treatment of mice with PSC833. *Journal of Clinical Investigation,* 100 (10)**,** 2430-2436.

Melaine, N., Lienard, M. O., Dorval, I., Le Goascogne, C., Lejeune, H. and Jegou, B. (2002) Multidrug resistance genes and P-glycoprotein in the testis of the rat, mouse, guinea pig, and human. *Biology of Reproduction,* 67 (6)**,** 1699-1707.

Mitic, L. L., van Itallie, C. M. and Anderson, J. M. (2000) Molecular Physiology and Pathophysiology of Tight Junctions - I. Tight junction structure and function: lessons from mutant animals and proteins. *American Journal of Physiology-Gastrointestinal and Liver Physiology,* 279 (2)**,** G250-G254.

Mitra, S. P. (2015) Binding and Stability of Curcumin in Presence of Bovine Serum Albumin.*J. Surface Sci. Technol ., Vol. 23, No. 3-4, 91-110*

Mosmann, T. (1983) Rapid colorimetric assay for cellular growth and survival: Application to proliferation and cytotoxicity assays. *Journal of Immunological Methods,* 65 (1)**,** 55-63.

Nicolazzo, J. A., Charman, S. A. and Charman, W. N. (2006) Methods to assess drug permeability across the blood-brain barrier. *Journal of Pharmacy and Pharmacology,* 58 (3)**,** 281-293.

Ono, K., Hasegawa, K., Naiki, H. and Yamada, M. (2004) Curcumin has potent anti-amyloidogenic effects for Alzheimer's beta-amyloid fibrils in vitro. *Journal of Neuroscience Research,* 75 (6)**,** 742-750.

Pardridge, W. M. (1999) Blood-brain barrier biology and methodology. *Journal of Neurovirology,* 5 (6)**,** 556-569.

Park, J. I., Venteicher, A. S., Hong, J. Y., Choi, J., Jun, S., Shkreli, M., Chang, W., Meng, Z., Cheung, P., Ji, H., McLaughlin, M., Veenstra, T. D., Nusse, R., McCrea, P. D. and Artandi, S. E. (2009) Telomerase modulates Wnt signalling by association with target gene chromatin. *Nature,* 460 (7251)**,** 66-72.

Pastan, M. M. G. a. I. (1993) biochemistry of multidrug resistance mediated by the multidrug transporters. *Annu. Rev. Biochem.***,** 385-427.

Prendergast, G. C. (2008) Immune escape as a fundamental trait of cancer: focus on IDO. *Oncogene,* 27 (28)**,** 3889-900.

Qian, B. Z. and Pollard, J. W. (2010) Macrophage diversity enhances tumor progression and metastasis. *Cell,* 141 (1)**,** 39-51.

Querfurth, H. W. and LaFerla, F. M. (2010) Alzheimer's Disease. *New England Journal of Medicine,* 362 (4)**,** 329-344.

Ramachandra, M., Ambudkar, S. V., Chen, D., Hrycyna, C. A., Dey, S., Gottesman, M. M. and Pastan, I. (1998) Human P-glycoprotein exhibits reduced affinity for substrates during a catalytic transition state. *Biochemistry,* 37 (14)**,** 5010-5019.

Raviv, Y., Pollard, H. B., Bruggemann, E. P., Pastan, I. and Gottesman, M. M. (1990) photosensitized labeling of a functional multidrug transporter in living drug-resistant tumor-cells. *Journal of Biological Chemistry,* 265 (7)**,** 3975-3980.

Raza, A., Franklin, M. J. and Dudek, A. Z. (2010) Pericytes and vessel maturation during tumor angiogenesis and metastasis. *Am J Hematol,* 85 (8)**,** 593-98.

Reichel, A., Begley, D. and Abbott, N. J. (2003) An Overview of In Vitro Techniques for Blood-Brain Barrier Studies. In: Nag, S. (Ed.) *The Blood-Brain Barrier.* (Methods in Molecular Medicine™) Vol. 89. Humana Press, pp. 307-324.

Rimkus, G. G. (1999) Polycyclic musk fragrances in the aquatic environment. *Toxicology Letters,* 111 (1-2)**,** 37-56.

Rimkus, G. G. and Wolf, M. (1996) Polycyclic musk fragrances in human adipose tissue and human milk. *Chemosphere,* 33 (10)**,** 2033-2043.

Ringshausen, I., Peschel, C. and Decker, T. (2006) Cell cycle inhibition in malignant lymphoma: disease control by attacking the cellular proliferation machinery. *Curr Drug Targets,* 7 (10)**,** 1349-59.

Robert, J. and Jarry, C. (2003) Multidrug resistance reversal agents. *Journal of Medicinal Chemistry,* 46 (23)**,** 4805-4817.

Roe, M., Folkes, A., Ashworth, P., Brumwell, J., Chima, L., Hunjan, S., Pretswell, I., Dangerfield, W., Ryder, H. and Charlton, P. (1999) Reversal of P-glycoprotein mediated multidrug resistance by novel anthranilamide derivatives. *Bioorganic & Medicinal Chemistry Letters,* 9 (4)**,** 595-600.

Romanitan, M. O., Popescu, B. O., Spulber, S., Bajenaru, O., Popescu, L. M., Winblad, B. and Bogdanovic, N. (2010) Altered expression of claudin family proteins in Alzheimer's disease and vascular dementia brains. *Journal of Cellular and Molecular Medicine,* 14 (5)**,** 1088-1100.

Roux, F., Durieu-Trautmann, O., Chaverot, N., Claire, M., Mailly, P., Bourre, J. M., Strosberg, A. D. and Couraud, P. O. (1994) Regulation of gamma-glutamyl transpeptidase and alkaline phosphatase activities in immortalized rat brain microvessel endothelial cells. *J Cell Physiol,* 159 (1)**,** 101-13.

Saito, T., Zhang, Z. J., Tsuzuki, H., Ohtsubo, T., Yamada, T., Yamamoto, T. and Saito, H. (1997) Expression of P-glycoprotein in inner ear capillary endothelial cells of the guinea pig with special reference to blood-inner ear barrier. *Brain Research,* 767 (2)**,** 388-392.

Sandoval, K. E. and Witt, K. A. (2008) Blood-brain barrier tight junction permeability and ischemic stroke. *Neurobiology of Disease,* 32 (2)**,** 200-219.

Santacruz, K., Lewis, J., Spires, T., Paulson, J., Kotilinek, L., Ingelsson, M., Guimaraes, A., DeTure, M., Ramsden, M., McGowan, E., Forster, C., Yue, M., Orne, J., Janus, C., Mariash, A., Kuskowski, M., Hyman, B., Hutton, M. and Ashe, K. H. (2005) Tau suppression in a neurodegenerative mouse model improves memory function. *Science,* 309 (5733)**,** 476-81.

Selkoe, D. J. (2001) Alzheimer's disease: Genes, proteins, and therapy. *Physiological Reviews,* 81 (2)**,** 741-766.

Senior, A. E., AlShawi, M. K. and Urbatsch, I. L. (1995) The catalytic cycle of P-glycoprotein. *Febs Letters,* 377 (3)**,** 285-289.

Sharom, F. J. (2008) ABC multidrug transporters: structure, function and role in chemoresistance. *Pharmacogenomics,* 9 (1)**,** 105-127.

Sherr, C. J. (2004) Principles of tumor suppression. *Cell,* 116 (2)**,** 235-46.

Sikic, B. I., Fisher, G. A., Lum, B. L., Halsey, J., BeketicOreskovic, L. and Chen, G. (1997) Modulation and prevention of multidrug resistance by inhibitors of P-glycoprotein. *Cancer Chemotherapy and Pharmacology,* 40**,** S13-S19.

Sloan, C. D. K., Nandi, P., Linz, T. H., Aldrich, J. V., Audus, K. L. and Lunte, S. M. (2012) Analytical and Biological Methods for Probing the Blood-Brain Barrier. *Annual Review of Analytical Chemistry, Vol 5,* 5**,** 505-531.

Smith, P. C., Karpowich, N., Millen, L., Moody, J. E., Rosen, J., Thomas, P. J. and Hunt, J. F. (2002) ATP binding to the motor domain from an ABC transporter drives formation of a nucleotide sandwich dimer. *Molecular Cell,* 10 (1)**,** 139-149.

Sui, H., Fan, Z. Z. and Li, Q. (2012) Signal Transduction Pathways and Transcriptional Mechanisms of ABCB1/Pgp-mediated Multiple Drug Resistance in Human Cancer Cells. *Journal of International Medical Research,* 40 (2)**,** 426-435.

T. Litmana,*, T. E. D., , W. D. S. and Batesd, a. S. E. (2001) From MDR to MXR-new understanding of multidrug resistance system, their properties and clinical significance. *CMLS Cellular and Molecular Life Sciences***,** 931–959.

Talmadge, J. E. and Fidler, I. J. (2010) AACR centennial series: the biology of cancer metastasis: historical perspective. *Cancer Res,* 70 (14)**,** 5649-69.

Tam, S. J. and Watts, R. J. (2010) Connecting Vascular and Nervous System Development: Angiogenesis and the Blood-Brain Barrier. *Annual Review of Neuroscience, Vol 33,* 33**,** 379-408.

Teng, M. W., Swann, J. B., Koebel, C. M., Schreiber, R. D. and Smyth, M. J. (2008) Immune-mediated dormancy: an equilibrium with cancer. *J Leukoc Biol,* 84 (4)**,** 988-93.

Terasaki, T., Ohtsuki, S., Hori, S., Takanaga, H., Nakashima, E. and Hosoya, K. (2003) New approaches to in vitro models of blood-brain barrier drug transport. *Drug Discovery Today,* 8 (20)**,** 944-954.

Thiebaut, F., Tsuruo, T., Hamada, H., Gottesman, M. M., Pastan, I. and Willingham, M. C. (1987) cellular-localization of the multidrug-resistance gene-product p-glycoprotein in normal human-tissues. *Proceedings of the National Academy of Sciences of the United States of America,* 84 (21)**,** 7735-7738.

Thomas, H. and Coley, H. M. (2003) Overcoming multidrug resistance in cancer: an update on the clinical strategy of inhibiting p-glycoprotein. *Cancer control : journal of the Moffitt Cancer Center,* 10 (2)**,** 159-65.

Trambas, C., Wang, Z., Cianfriglia, M. and Woods, G. (2001) Evidence that natural killer cells express mini P-glycoproteins but not classic 170 kDa P-glycoprotein. *Br J Haematol,* 114 (1)**,** 177-84.

Tsukita, S., Furuse, M. and Itoh, M. (2001) Multifunctional strands in tight junctions. *Nat Rev Mol Cell Biol,* 2 (4)**,** 285-293.

Valton, E., Amblard, C., Desmolles, F., Combourieu, B., Penault-Llorca, F. and Bamdad, M. (2015) Mini-P-gp and P-gp Co-Expression in Brown Trout Erythrocytes: A Prospective Blood Biomarker of Aquatic Pollution. *Diagnostics,* 5 (1)**,** 10-26.

Vogelstein, B. and Kinzler, K. W. (2004) Cancer genes and the pathways they control. *Nature Medicine,* 10 (8)**,** 789-799.

Wahlang, B., Pawar, Y. B. and Bansal, A. K. (2011) Identification of permeability-related hurdles in oral delivery of curcumin using the Caco-2 cell model. *Eur J Pharm Biopharm,* 77 (2)**,** 275-82.

Wang, Q., Rager, J. D., Weinstein, K., Kardos, P. S., Dobson, G. L., Li, J. and Hidalgo, I. J. (2005) Evaluation of the MDR-MDCK cell line as a permeability screen for the blood-brain barrier. *Int J Pharm,* 288 (2)**,** 349-59.

Weidenfeller, C., Svendsen, C. N. and Shusta, E. V. (2007) Differentiating embryonic neural progenitor cells induce blood-brain barrier properties. *J Neurochem,* 101 (2)**,** 555-65.

Weksler, B. B., Subileau, E. A., Perriere, N., Charneau, P., Holloway, K., Leveque, M., Tricoire-Leignel, H., Nicotra, A., Bourdoulous, S., Turowski, P., Male, D. K., Roux, F., Greenwood, J., Romero, I. A. and Couraud, P. O. (2005) Blood-brain barrier-specific properties of a human adult brain endothelial cell line. *Faseb j,* 19 (13)**,** 1872-4.

Wilhelm, I., Fazakas, C. and Krizbai, I. A. (2011) In vitro models of the blood-brain barrier. *Acta Neurobiologiae Experimentalis,* 71 (1)**,** 113-128.

Wright, W. E., Pereira-Smith, O. M. and Shay, J. W. (1989) Reversible cellular senescence: implications for immortalization of normal human diploid fibroblasts. *Mol Cell Biol,* 9 (7)**,** 3088-92.

Yu, H. and Huang, Q. (2011) Investigation of the absorption mechanism of solubilized curcumin using Caco-2 cell monolayers. *J Agric Food Chem,* 59 (17)**,** 9120-9126.

Yuan, T. L. and Cantley, L. C. (2008) PI3K pathway alterations in cancer: variations on a theme. *Oncogene,* 27 (41)**,** 5497-510.